STRINGQFT

String-Theoretic Construction
of Quantum Field Theory

VOLUME XVII

Protected Structures and Further M5 Compactifications

Xingyang Yu

StringQFT v1.0 / Source build candidate

Drafted with AI assistance under the supervision of the author.
Manuscript free to read. All rights reserved.

Contents

XVII.1 BPS particles and spectral networks **1**
XVII.1.1 M2 boundaries and central charges 1
XVII.1.2 Finite WKB trajectories 3
XVII.1.3 The two-particle AD chamber 5
XVII.1.4 Crossing the wall and the pentagon 7
XVII.1.5 What higher rank adds 11

XVII.2 The Omega background and instanton sums **16**
XVII.2.1 Rotations, fixed points and the ADHM complex 16
XVII.2.2 From monomial ideals to Young diagrams 18
XVII.2.3 Matter factors and the mass lift 20
XVII.2.4 Which partition function is being expanded? 23
XVII.2.5 The connected logarithm and the undeformed limit 25

XVII.3 An AGT example from states to correlators **31**
XVII.3.1 Virasoro states and sewing 31
XVII.3.2 The dimensionful parameter dictionary 34
XVII.3.3 Two independent expansions 37
XVII.3.4 From a block to a correlator 39
XVII.3.5 Crossing and duality 41

XVII.4 Higher rank, defects and quantum Hitchin equations **47**
XVII.4.1 From Virasoro to the spin-three current 47
XVII.4.2 A controlled higher-rank block 50
XVII.4.3 A surface defect and the BPZ equation 52
XVII.4.4 Keeping one equivariant parameter 55
XVII.4.5 Monodromy and an analytic endpoint problem 58

XVII.5 The Schur index and curve gluing **64**
XVII.5.1 The Schur trace and its letters 64
XVII.5.2 Gauging as a singlet projection 67
XVII.5.3 The T2 trinion and its wavefunctions 69
XVII.5.4 Two ways to glue four punctures 71
XVII.5.5 The diagonal sewing algebra 73

XVII.6 Schur operators and vertex operator algebras **79**
XVII.6.1 Cohomology and a holomorphic plane . . . 79
XVII.6.2 Stress tensors, currents and anomalies . . . 82
XVII.6.3 Free fields and conformal gauging . . . 84
XVII.6.4 The so8 algebra of four-flavor SU2 . . . 86
XVII.6.5 T3 and the E6 comparison . . . 89

XVII.7 Four supercharges from a wrapped curve **95**
XVII.7.1 Rotations in the two normal planes . . . 95
XVII.7.2 Constructing the two holomorphic line bundles . . . 98
XVII.7.3 Choosing R symmetry and flavor . . . 100
XVII.7.4 The eight-supercharge limit . . . 102
XVII.7.5 Colored local boundary conditions . . . 104

XVII.8 Colored gluing, anomalies and mass deformations **110**
XVII.8.1 Colored blocks and their couplings . . . 110
XVII.8.2 A closed genus-two theory . . . 113
XVII.8.3 The same anomalies from six dimensions . . . 115
XVII.8.4 An adjoint mass deformation . . . 118
XVII.8.5 Changed colors, unitarity and bundle data . . . 121
Exercises . . . 123
Take-home result and exit check . . . 125
Sources and scope . . . 125

XVII.9 M5-branes on three-manifolds **127**
XVII.9.1 A diagonal twist preserving four real supercharges . . . 127
XVII.9.2 Boundary holonomies and a polarization . . . 130
XVII.9.3 A complex connection and two different equations . . . 132
XVII.9.4 A figure-eight vacuum chart computed in two ways . . . 135
XVII.9.5 Branches, singular limits and integration cycles . . . 138
XVII.9.6 Exercises . . . 140
XVII.9.7 Take-home result and exit check . . . 141

XVII.10 From tetrahedra to three-dimensional theories **143**
XVII.10.1 A chiral multiplet for an ideal tetrahedron . . . 143
XVII.10.2 Gluing, gauging and edge interactions . . . 146
XVII.10.3 The figure-eight complement in six tetrahedra . . . 148
XVII.10.4 A two-to-three move and SQED/XYZ . . . 150
XVII.10.5 Protected factors and their analytic domains . . . 153
XVII.10.6 Exercises . . . 156

XVII.11 Boundaries, duality walls and filling **159**
XVII.11.1 Polarization and boundary states . . . 159
XVII.11.2 Mapping cylinders and Abelian wall operations . . . 161
XVII.11.3 Dehn filling conditions . . . 163
XVII.11.4 Flat sectors after filling . . . 165

XVII.11.5 Protected integrals and global limits 167

XVII.12 Strings from M5-branes on divisors **173**
XVII.12.1 A smooth divisor becomes a string 173
XVII.12.2 Integrating the M5 anomaly 176
XVII.12.3 Two ways to compute the central charges 178
XVII.12.4 The quintic and its first two divisor degrees 180
XVII.12.5 The modified genus, spectral flow and the Cardy window . . . 182

XVII.13 An atlas of wrapped-M5 constructions **189**
XVII.13.1 Choose the protected question before the tool 189
XVII.13.2 One four-dimensional theory, several protected structures . . . 191
XVII.13.3 Change the geometry and retain its premises 194
XVII.13.4 Recompute a witness and expose what it forgets 196
XVII.13.5 Carry the observable into the next construction 197

Chapter XVII.1

BPS particles and spectral networks

A Seiberg–Witten curve determines the central charge of an electromagnetic charge. To determine whether a particle carries that charge, we need a further physical construction. In the M5 description, a particle can arise from a membrane whose boundary lies on the spectral curve. Its projection to the base is a finite path or web. The phase of the differential selects the allowed directions of that projection.

We will follow this construction in the simplest interacting Argyres–Douglas example. Two finite paths give periods that we can evaluate exactly at a symmetric point. Moving the Coulomb parameter then rotates those periods through a wall of marginal stability. A two-node quiver explains which bound representation becomes stable, while an explicit identity of rational transformations describes the corresponding wall-crossing product. Finally, a rank-three example shows why paths need sheet labels and why composable paths generate a third path at a joint.

We use the spectral differential and period convention of XVI.4, the Argyres–Douglas scaling geometry of XVI.9, and the distinction between particle and line charges in XVI.11. The local vanishing-cycle picture of XII.4 is useful, but a vanishing cycle alone will not determine particle existence. The physical identifications of finite saddles and stable representations with BPS states are additional inputs. Keeping that distinction visible lets us calculate the geometry without assigning a state to every available period.

XVII.1.1 M2 boundaries and central charges

Why does the boundary of a membrane carry a four-dimensional charge? The M5 wraps a spectral cover $\pi\colon \Sigma \to C$. Away from ramification, a point of the base has several lifts. In a local coordinate z, the differential on sheet i is $\lambda_i = x_i(z)\,dz$. A membrane strip stretched between sheets i and j projects to an oriented path p in C. Its two boundary

components have opposite orientations. Consequently its boundary class and period are

$$\gamma = p_i - p_j, \qquad \int_\gamma \lambda_{\mathrm{geom}} = \int_p (\lambda_i - \lambda_j), \qquad Z_\gamma = c_{\mathrm{SW}} \int_\gamma \lambda_{\mathrm{geom}}. \tag{XVII.1.1}$$

Here c_{SW} is a fixed nonzero complex normalization. We keep its magnitude and phase unspecified. The strip closes when its endpoints reach branch points where the two sheets coincide. Figure XVII.1.1 displays this closure. For the compact rank-two charge sector used below, these closed lifted paths are particle charges. In a general class-S theory the physical charge lattice requires additional restrictions or quotients, as discussed in XVI.11.

The membrane description supplies a useful local mass functional. Let s be arclength along its projected path. The effective tension along that path and the integrated mass are

$$T_{ij}(s) = |c_{\mathrm{SW}}| \, \big|(\lambda_i - \lambda_j)(\partial_s)\big|, \qquad M[p] = |c_{\mathrm{SW}}| \int_p |\lambda_i - \lambda_j|. \tag{XVII.1.2}$$

The triangle inequality now compares a sum of local positive contributions with the complex period,

$$M[p] \;\geq\; |c_{\mathrm{SW}}| \left| \int_p (\lambda_i - \lambda_j) \right| = |Z_\gamma|. \tag{XVII.1.3}$$

Equality requires all nonzero infinitesimal contributions to have the same phase. If that geometric phase is θ, the local condition is

$$e^{-i\theta}(\lambda_i - \lambda_j)(\partial_s) \in \mathbb{R}_{>0}, \qquad \arg Z_\gamma = \theta + \arg c_{\mathrm{SW}}. \tag{XVII.1.4}$$

Thus the mass bound becomes a direction field on the base. It is a condition on a candidate membrane. The existence and quantization of a finite solution remain physical questions.

We can check orientations before solving that direction field. Reversing p changes the sign of both its boundary charge and its period. Exchanging the sheet labels does the same. Performing both operations leaves the represented boundary unchanged,

$$\gamma[-p; i, j] = -\gamma[p; i, j], \qquad \gamma[p; j, i] = -\gamma[p; i, j], \qquad \gamma[-p; j, i] = \gamma[p; i, j]. \tag{XVII.1.5}$$

A single reversal describes the opposite charge. It does not change the mass, because $|-Z| = |Z|$. These orientation conventions will fix both the intersection pairing and the wall-crossing signs.

Our recurring curve is the deformed (A_1, A_2) Argyres–Douglas scaling family,

$$x^2 = P(z), \qquad P(z) = z^3 - 3\Lambda^2 z + u, \qquad \lambda_{\mathrm{geom}} = x\, dz, \qquad \Lambda > 0. \tag{XVII.1.6}$$

The discriminant follows by eliminating a common root of P and P'. Since $P' = 3(z^2 - \Lambda^2)$, a repeated root is $z = \pm\Lambda$. Substitution gives the singular parameters,

$$P(\Lambda) = u - 2\Lambda^3, \qquad P(-\Lambda) = u + 2\Lambda^3, \qquad \mathrm{Disc}_z\, P = 27(4\Lambda^6 - u^2). \tag{XVII.1.7}$$

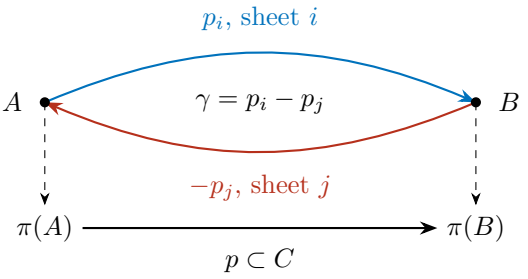


Figure XVII.1.1: A closed two-sheet lift of an interval between two branch points. The upper boundary runs from A to B on sheet i, while the lower boundary returns from B to A on sheet j. The base path has the orientation $A \to B$. The separation of the two drawn sheets is schematic. Their meeting at each endpoint closes the membrane boundary $p_i - p_j$.

We work away from those values. In this irregular scaling chart z is dimensionful. Requiring the two sides of $x^2 = z^3 + \cdots$ to have equal weight and requiring the differential to have mass dimension one yields

$$2[x] = 3[z], \qquad [x] + [z] = 1, \qquad [z] = [\Lambda] = \frac{2}{5}, \quad [x] = \frac{3}{5}, \quad [u] = \frac{6}{5}. \tag{XVII.1.8}$$

These are scaling dimensions of the irregular chart, rather than the dimensionless regular coordinate used elsewhere on C.

For example, the outgoing and returning portions of a two-sheet lift contribute equally. On return the sheet value and the path orientation both change sign. For the left interval at $u = 0$, with $a = \sqrt{3}\Lambda$, this gives

$$\int_{\gamma_2} \lambda_{\text{geom}} = \int_{-a}^{0} \sqrt{P(z)}\, dz + \int_{0}^{-a} (-\sqrt{P(z)})\, dz = 2\int_{-a}^{0} \sqrt{P(z)}\, dz. \tag{XVII.1.9}$$

A one-sheet integral would miss a factor of two in the charge period. The next section evaluates both finite intervals and determines their geometric phases.

XVII.1.2 Finite WKB trajectories

The local phase condition now has a concrete differential equation. For a two-sheet curve, $x_i - x_j = 2\sqrt{P(z)}$. Rescaling the positive path parameter from arclength to τ absorbs the magnitude of this difference. Equation (XVII.1.4) becomes

$$2\sqrt{P(z)}\,\frac{dz}{d\tau} = e^{i\theta}, \qquad \frac{dz}{d\tau} = \frac{e^{i\theta}}{2\sqrt{P(z)}}. \tag{XVII.1.10}$$

The rescaled parameter is convenient for the direction field; it is not arclength. An integral curve is called a WKB trajectory. A finite trajectory joining turning points is the candidate saddle relevant here.

Near a simple turning point z_0, put $\delta = z - z_0$ and $p_1 = P'(z_0) \neq 0$. The leading differential and its primitive are

$$2\sqrt{P(z)}\,dz = 2\sqrt{p_1}\,\delta^{1/2}d\delta + O(\delta^{3/2}d\delta), \qquad w = \frac{4}{3}\sqrt{p_1}\,\delta^{3/2} + O(\delta^{5/2}). \quad \text{(XVII.1.11)}$$

A trajectory has $e^{-i\theta}w$ real. On an outgoing sheet one chooses it positive. Squaring that relation removes the sheet choice and gives the three projected directions,

$$\arg\delta = \frac{2\theta - \arg p_1 + 2\pi k}{3}, \qquad k = 0, 1, 2 \pmod 3. \quad \text{(XVII.1.12)}$$

Changing the sheet can reverse the oriented lift without changing the projected ray. The three rays are separated by $2\pi/3$, rather than the four directions that a naive treatment of the square root as a regular linear coordinate would suggest.

At $u = 0$, the turning points are $-a, 0, a$. On the two real intervals, the polynomial has opposite signs. The outgoing branches and geometric phases are

$$\begin{aligned} -a < z < 0\colon &\quad x = +\sqrt{z^3 - 3\Lambda^2 z}, \quad \theta_2 = 0, \\ 0 < z < a\colon &\quad x = +i\sqrt{3\Lambda^2 z - z^3}, \quad \theta_1 = \frac{\pi}{2}. \end{aligned} \quad \text{(XVII.1.13)}$$

With $dz > 0$, multiplying $2x\,dz$ by the corresponding $e^{-i\theta}$ gives a positive real number throughout either interval. These are actual finite WKB saddles of the cubic. They are drawn in Figure XVII.1.2.

The left period can be evaluated by two substitutions. First write $z = -as$, reversing the limits, and use $a^2 = 3\Lambda^2$. Then put $t = s^2$,

$$\begin{aligned} \mathcal{Z}_2 \equiv \int_{\gamma_2} \lambda_{\text{geom}} &= 2a^{5/2}\int_0^1 s^{1/2}(1-s^2)^{1/2}ds \\ &= a^{5/2}\int_0^1 t^{-1/4}(1-t)^{1/2}dt = 3^{5/4}\Lambda^{5/2}B\left(\frac{3}{4},\frac{3}{2}\right). \end{aligned} \quad \text{(XVII.1.14)}$$

The symbol $\mathcal{Z}$ denotes a geometric period, so the physical central charge is $Z = c_{\text{SW}}\mathcal{Z}$. The right outgoing branch contributes an extra factor i, while its real positive integral is the same. Defining $\mathcal{B}$ as the positive beta-function value gives

$$\mathcal{B} = 3^{5/4}\Lambda^{5/2}B\left(\frac{3}{4},\frac{3}{2}\right), \qquad (\mathcal{Z}_1, \mathcal{Z}_2) = (i\mathcal{B}, \mathcal{B}), \qquad \mathcal{B}\big|_{\Lambda=1} = 3.78441894434\ldots. \quad \text{(XVII.1.15)}$$

The two candidate masses agree at this point, although their central-charge phases differ by $\pi/2$. Equality of masses is therefore quite different from marginal alignment.

Scaling the curve supplies another useful check. At fixed $\widehat{u} = u/\Lambda^3$, put $z = \Lambda\widehat{z}$ and $x = \Lambda^{3/2}\widehat{x}$. The curve and differential reduce to

$$\widehat{x}^2 = \widehat{z}^3 - 3\widehat{z} + \widehat{u}, \qquad \lambda_{\text{geom}} = \Lambda^{5/2}\widehat{x}\,d\widehat{z}, \qquad \mathcal{Z}_\gamma = \Lambda^{5/2}\widehat{\mathcal{Z}}_\gamma. \quad \text{(XVII.1.16)}$$

In particular, doubling Λ multiplies the symmetric periods by $2^{5/2}$, not by four. The exponent has mass dimension $(5/2)(2/5) = 1$. It supplies no calibration of $|c_{\text{SW}}|$.

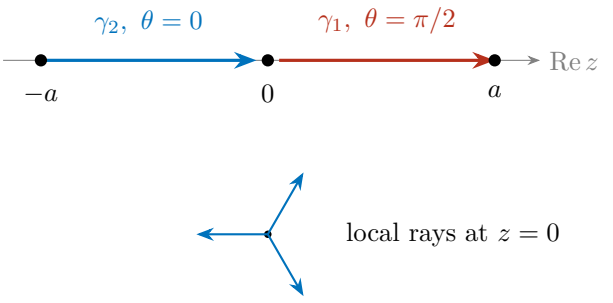


Figure XVII.1.2: The cubic at $u = 0$ has turning points $-a, 0, a$, with $a = \sqrt{3}\Lambda$. The left interval is the outgoing part of γ_2 at geometric phase zero; the right interval is the outgoing part of γ_1 at phase $\pi/2$. Arrows follow increasing z. The inset shows the three projected rays near the central turning point for $\theta = 0$; since $P'(0) < 0$, their angles are $-\pi/3, \pi/3, \pi$. The intervals are actual finite trajectories, while the inset only describes their local direction rule.

A changed phase tests what the trajectory condition actually selects. Keep the left real interval fixed, but set $\theta = \pi/8$. At $\Lambda = 1, z = -1$ the differential coefficient is $2\sqrt{2}$, and hence

$$\mathrm{Im}\left(e^{-i\pi/8} 2\sqrt{2}\right) = -2\sqrt{2}\sin\frac{\pi}{8} \neq 0. \tag{XVII.1.17}$$

The same projected interval is no longer a trajectory of that phase. Conversely, satisfying the phase equation on a short segment is insufficient for a finite particle. It must close appropriately at its endpoints, and the isolated-saddle quantization that supplies a hypermultiplet is a physical input. We now combine that input with the two finite saddles.

XVII.1.3 The two-particle AD chamber

The two saddles supply two candidate charges. To compare them as electromagnetic charges, we must orient their intersection on the cover, rather than intersect their projections on the base. Near the common branch point $z = 0$, a nonsingular cover coordinate is $t = \sqrt{z}$. At $\Lambda = 1$ the curve has the local form

$$z = t^2, \qquad x = i\sqrt{3}\, t + O(t^5). \tag{XVII.1.18}$$

The closed lift of the right interval passes through the branch point along the positive real t direction. The left lift passes along the positive imaginary direction. Using the complex orientation $(\mathrm{Re}\, t, \mathrm{Im}\, t)$ gives

$$v_1 = (1, 0), \qquad v_2 = (0, 1), \qquad \langle \gamma_1, \gamma_2 \rangle = \det(v_1, v_2) = +1. \tag{XVII.1.19}$$

This is the compact rank-two odd lattice in this example. Reversing just one lifted orientation reverses the pairing and changes the arrow convention accordingly.

The physical identification of this Argyres–Douglas chamber states that the two isolated finite saddles give its complete particle spectrum in a chosen half-plane. We use a geometric particle half-plane that contains both rays strictly,

$$-\frac{\pi}{4} < \arg \mathcal{Z} < \frac{3\pi}{4}, \qquad \Omega(\gamma_1) = \Omega(\gamma_2) = 1. \tag{XVII.1.20}$$

The physical half-plane is rotated by $\arg c_{\mathrm{SW}}$. The index convention assigns $+1$ to a hypermultiplet. CPT-conjugate antiparticles occupy the opposite half-plane. The statement of completeness in this chamber is sourced physics, beyond our evaluation of the two periods.

The quiver gives a second way to organize the stability question. Our arrow convention assigns $j \to i$ to a positive $\langle \gamma_i, \gamma_j \rangle$. Thus the quiver and a representation of dimension vector $(1, 1)$ are

$$2 \longrightarrow 1, \qquad V_1 = \mathbb{C}, \quad V_2 = \mathbb{C}, \qquad B \colon V_2 \longrightarrow V_1. \tag{XVII.1.21}$$

The node order is part of the convention. Exchanging labels relative to another presentation must exchange the central charges as well. Figure XVII.1.3 relates the local intersection to this arrow.

A subrepresentation consists of subspaces $S_i \subset V_i$ satisfying $B(S_2) \subset S_1$. Since each V_i has dimension one, every subspace is either zero or the whole node space. For a nonzero arrow, B is invertible. The only nonzero proper allowed dimension vector is therefore

$$B \neq 0 \quad \Longrightarrow \quad (\dim S_1, \dim S_2) = (1, 0), \qquad (0, 1) \text{ is excluded by } B(V_2) \not\subset 0. \tag{XVII.1.22}$$

For $B = 0$, that obstruction disappears,

$$B = 0 \quad \Longrightarrow \quad (\dim S_1, \dim S_2) \in \{(1, 0), (0, 1)\}. \tag{XVII.1.23}$$

The zero-arrow representation is the direct sum of the two simple representations. The nonzero arrows are all isomorphic, because independent changes of basis at the two nodes can set any nonzero scalar B to one.

With all phases in the chosen half-plane, the stability prescription is a strict inequality for every nonzero proper subrepresentation,

$$\arg Z(S) < \arg Z(R), \qquad Z(R) = Z_1 + Z_2, \qquad Z(S) = n_1 Z_1 + n_2 Z_2. \tag{XVII.1.24}$$

The common factor c_{SW} rotates all these arguments together and does not change the comparison. For $B \neq 0$, equation (XVII.1.22) reduces the whole stability calculation to one inequality,

$$\arg \mathcal{Z}_1 < \arg(\mathcal{Z}_1 + \mathcal{Z}_2). \tag{XVII.1.25}$$

At the symmetric point we have $\arg \mathcal{Z}_1 = \pi/2$ and $\arg(\mathcal{Z}_1 + \mathcal{Z}_2) = \pi/4$. The inequality fails. The additive central charge certainly exists,

$$\mathcal{Z}_{\gamma_1+\gamma_2} = (1 + i)\mathcal{B}, \qquad |Z_{\gamma_1+\gamma_2}| = \sqrt{2}\,|c_{\mathrm{SW}}|\mathcal{B}, \qquad \frac{\pi}{2} \not< \frac{\pi}{4}. \tag{XVII.1.26}$$

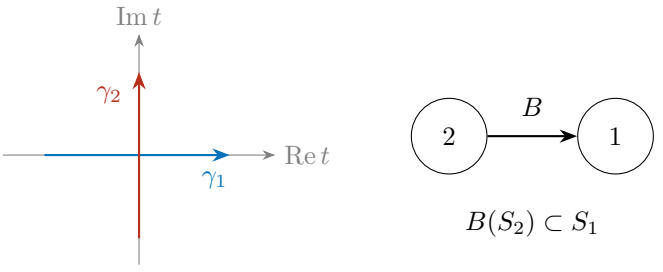


Figure XVII.1.3: On the left, the two oriented tangents on the smooth t-plane intersect with determinant $+1$. Labels are attached to the corresponding cycles, rather than to their base projections. On the right, the adopted arrow convention converts $\langle \gamma_1, \gamma_2 \rangle = +1$ into $B\colon V_2 \to V_1$. For $B \neq 0$, the node-one simple is a subrepresentation; the node-two simple is not.

It does not label a stable bound state in this chamber. The formal value of a central charge should never be mistaken for a list of occupied charges.

For the zero arrow, both simple subrepresentations would have to have phase below the phase of their sum. In a half-plane of width π, the sum lies strictly between two unequal phases. One of the two inequalities must fail. When the phases coincide, the strict inequality fails for both. Thus the zero arrow is never a stable $(1,1)$ representation in these circumstances. The physical prescription relating stable quiver representations to BPS states is imported; the subspace enumeration itself is elementary linear algebra. Varying the periods will now show precisely when the nonzero arrow becomes stable.

XVII.1.4 Crossing the wall and the pentagon

A wall of marginal stability occurs when the central charges of possible constituents align positively. We will locate a wall by actually varying the Coulomb parameter. Set $\Lambda = 1$ and move along $u = iv$, with $0 \le v \le 3$. This path encounters neither discriminant point $u = \pm 2$. The roots can be written without solving a new cubic at every value of v. Substituting $z = ih$ gives

$$h^3 + 3h = v, \qquad h = 2\sinh\left(\frac{1}{3}\operatorname{arsinh}\frac{v}{2}\right), \qquad A = \sqrt{3 + \frac{3h^2}{4}}. \tag{XVII.1.27}$$

Indeed, $h = 2\sinh t$ gives $h^3 + 3h = 2\sinh 3t$. Factoring out $z - ih$ yields the three continuously labeled roots,

$$P(z) = (z - ih)(z^2 + ihz - 3 - h^2), \qquad r_- = -A - \frac{ih}{2}, \quad r_0 = ih, \quad r_+ = A - \frac{ih}{2}. \tag{XVII.1.28}$$

At $v = 0$ these recover $-\sqrt{3}, 0, \sqrt{3}$. They provide integration representatives for the transported left and right cycles.

For adjacent roots a, b and the remaining root c, use the straight segment $z = a + (b-a)t$. Put $d = b - a$ and $m = (a+b)/2$. Endpoint factorization gives

$$\begin{aligned} P(a+dt) &= -d^2 t(1-t)(a+dt-c), \\ \mathcal{I}(a,b;c) &= 2d\sqrt{-d^2(m-c)}\int_0^1 \sqrt{t(1-t)}\sqrt{\frac{a+dt-c}{m-c}}\,dt. \end{aligned} \tag{XVII.1.29}$$

The square roots are continued from the outgoing sheets at $v = 0$. The left and right periods are then

$$\mathcal{Z}_2(v) = \mathcal{I}(r_-, r_0; r_+), \qquad \mathcal{Z}_1(v) = \mathcal{I}(r_0, r_+; r_-). \tag{XVII.1.30}$$

These straight segments represent transported cycles. Away from $v = 0$, we have not shown that they obey the WKB direction equation. Period integration and trajectory construction are distinct operations.

The square-root continuation in equation (XVII.1.29) can be followed explicitly. For the left interval, $d = A + 3ih/2$ and $m - c = -3A/2 + 3ih/4$; for the right interval their values are $A - 3ih/2$ and $3A/2 + 3ih/4$. Using $A^2 = 3 + 3h^2/4$ gives

$$\begin{aligned} -d_L^2(m_L - c_L) &= \frac{9A}{2} + i\left(\frac{45h}{4} + \frac{9h^3}{2}\right), \\ -d_R^2(m_R - c_R) &= -\frac{9A}{2} + i\left(\frac{45h}{4} + \frac{9h^3}{2}\right). \end{aligned} \tag{XVII.1.31}$$

The left radicand stays to the right of the imaginary axis. The right stays in the upper half-plane, starting on the negative real axis with the prescribed positive imaginary square root. The normalized ratios under the integral also have positive real part. This follows because $m - c$ and each $a + dt - c$ have real parts of the same fixed sign and nonnegative imaginary parts. Thus their scalar product has positive real part. The principal-root expression continues the original sheets along this path.

Reflection of the root configuration gives a useful relation between the periods. Write $\mathcal{Z}_1 = a_1 + ib_1$ with real a_1, b_1. The continued sheets give

$$\mathcal{Z}_1 = i\overline{\mathcal{Z}_2}, \qquad \mathcal{Z}_2 = b_1 + ia_1, \qquad \mathcal{Z}_1\overline{\mathcal{Z}_2} = 2a_1b_1 + i(b_1^2 - a_1^2). \tag{XVII.1.32}$$

The equivalent relation is $\mathcal{Z}_2 = i\overline{\mathcal{Z}_1}$. In particular it agrees with $(i\mathcal{B}, \mathcal{B})$ at $v = 0$.

Quadrature of the transported periods gives the following representative values. The entries refer to the geometric differential at $\Lambda = 1$, rather than absolute physical masses,

v	$\mathcal{Z}_1$	$\mathcal{Z}_2$	$\mathrm{Im}(\mathcal{Z}_1\overline{\mathcal{Z}_2})$
1	$1.981595 + 3.721383i$	$3.721383 + 1.981595i$	9.921974
2	$3.912025 + 3.555878i$	$3.555878 + 3.912025i$	−2.659673
3	$5.776036 + 3.327226i$	$3.327226 + 5.776036i$	−22.292160

(XVII.1.33)

The phase order reverses between $v = 1$ and $v = 2$. At $v = 3$ the charges remain in the declared particle half-plane, and the same reversed order persists. Numerically the positively aligned solution on this interval is

$$v_* \simeq 1.830440607764, \qquad \mathcal{Z}_1(v_*) = \mathcal{Z}_2(v_*) \simeq 3.589348833914(1+i). \tag{XVII.1.34}$$

Endpoint-regularized quadrature and direct quadrature of the unfactored polynomial with independently determined roots agree at the selected sample points. These numerical comparisons have no certified error enclosure and establish no global uniqueness theorem for walls. The quoted digits describe a numerical solution.

Positive alignment needs a second condition beyond the vanishing imaginary part,

$$\operatorname{Im}(Z_1\overline{Z_2}) = 0, \qquad \operatorname{Re}(Z_1\overline{Z_2}) > 0, \qquad |Z_1 + Z_2| = |Z_1| + |Z_2|. \tag{XVII.1.35}$$

Replacing Z_2 by $-Z_2$ also makes the imaginary part vanish at the same point, but makes the real part negative. That is anti-alignment. It does not give the positive constituent mass equality. The common normalization c_{SW} multiplies $Z_1\overline{Z_2}$ by $|c_{\mathrm{SW}}|^2$, so it does not move the alignment condition.

The stability calculation of the previous section now becomes quantitative. Reflection fixes the phase of $\mathcal{Z}_1 + \mathcal{Z}_2$ to $\pi/4$ on this path. The sample phases are

$$\begin{aligned} &v = 1\colon \quad \arg \mathcal{Z}_1 \simeq 1.0815 > \pi/4, \quad B \neq 0 \text{ unstable},\\ &v = 2\colon \quad \arg \mathcal{Z}_1 \simeq 0.7377 < \pi/4, \quad B \neq 0 \text{ stable},\\ &v = 3\colon \quad \arg \mathcal{Z}_1 \simeq 0.5226 < \pi/4, \quad B \neq 0 \text{ stable}. \end{aligned} \tag{XVII.1.36}$$

At the wall the strict inequality becomes equality, so the representation is semistable. The sourced Argyres–Douglas spectrum in the adjacent three-particle chamber is

$$\Omega(\gamma_1) = \Omega(\gamma_2) = \Omega(\gamma_1 + \gamma_2) = 1. \tag{XVII.1.37}$$

The period calculation locates an alignment and the representation calculation explains the stability change. Completeness of these two- and three-state spectra is additional physical input. Figure XVII.1.4 shows the changed order of the geometric rays.

We next compute the classical wall-crossing product exactly. Introduce commutative torus coordinates and a quadratic refinement,

$$X_{(a,b)} = x^a y^b, \qquad \langle (a,b),(c,d)\rangle = ad - bc, \qquad \sigma(a,b) = (-1)^{a+b+ab}. \tag{XVII.1.38}$$

Modulo two, the cross term in $(a+c)(b+d)$ is $ad + bc = ad - bc$. Therefore this sign obeys

$$\sigma(\gamma+\eta) = (-1)^{\langle\gamma,\eta\rangle}\sigma(\gamma)\sigma(\eta), \qquad \sigma(1,0) = \sigma(0,1) = \sigma(1,1) = -1. \tag{XVII.1.39}$$

The minus sign of the composite charge is essential even though its coordinate is the ordinary product xy.

For a hypermultiplet, define the classical Kontsevich–Soibelman transformation by

$$K_\gamma(X_\eta) = X_\eta(1 - \sigma(\gamma)X_\gamma)^{\langle\eta,\gamma\rangle}. \tag{XVII.1.40}$$

Applying the pairing to $\eta = \gamma_1$ and $\eta = \gamma_2$ gives three explicit rational maps,

$$\begin{aligned} A = K_1 = \left(x, \frac{y}{1+x}\right), \qquad B = K_2 = \big(x(1+y), y\big),\\ C = K_{12} = \left(x(1+xy), \frac{y}{1+xy}\right). \end{aligned} \tag{XVII.1.41}$$

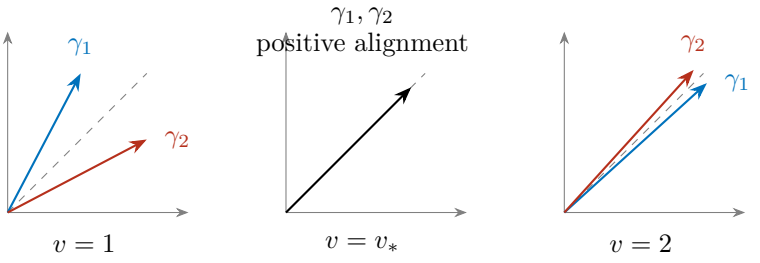


Figure XVII.1.4: Geometric period rays at $v = 1$, at the numerical wall v_*, and at $v = 2$. Only directions are shown; lengths are rescaled for readability. The diagonal is the ray of $\gamma_1 + \gamma_2$. Before the wall, the node-one subrepresentation has larger phase than the sum. After the wall, it has smaller phase and the nonzero-arrow representation is stable. At the wall, the two constituent rays coincide positively. The physical rays undergo a common rotation by $\arg c_{\mathrm{SW}}$.

We use composition of coordinate maps, so $F \circ G$ means substitute the pair $G(x, y)$ into F. The left product is immediately

$$(A \circ B)(x, y) = \left(x(1 + y), \frac{y}{1 + x(1 + y)} \right). \tag{XVII.1.42}$$

To compare with three factors, first apply A and then C. Put $D = 1 + x + xy$. Direct substitution gives

$$(C \circ A)(x, y) = \left(\frac{xD}{1 + x}, \frac{y}{D} \right), \qquad (B \circ C \circ A)(x, y) = \left(\frac{x(D + y)}{1 + x}, \frac{y}{D} \right). \tag{XVII.1.43}$$

Since $D + y = (1 + x)(1 + y)$, the result agrees with equation (XVII.1.42). We have derived the exact classical pentagon identity,

$$A \circ B = B \circ C \circ A, \qquad (x, y) \longmapsto \left(x(1 + y), \frac{y}{1 + x + xy} \right). \tag{XVII.1.44}$$

This is an identity of rational maps on their common domain, away from the denominator divisors. Its exactness is algebraic. Applying it to physical wall crossing still uses the sourced BPS spectrum and wall-crossing prescription.

Omitting the composite factor gives a different map,

$$(B \circ A)(x, y) = \left(\frac{x(1 + x + y)}{1 + x}, \frac{y}{1 + x} \right). \tag{XVII.1.45}$$

At $x = y = 1$, the correct product gives $(2, 1/3)$, whereas this product gives $(3/2, 1/2)$. This small example makes the role of the bound factor explicit. The coordinates commute throughout. We have neither introduced a quantum torus parameter nor proved a quantum-dilogarithm identity.

XVII.1.5 What higher rank adds

For a double cover, the difference of the two sheets determines a single local trajectory field at fixed phase. With three or more sheets, each ordered pair determines a different field. A path can change its sheet type at a joint, so a projected curve without sheet labels no longer carries enough information to recover its lift.

A concrete rank-three spectral chart is

$$x^3 + 3\Lambda^2 x + z^2 + u = 0, \qquad \lambda_i = x_i\, dz. \tag{XVII.1.46}$$

In the positive-ϕ convention of XVI.4, where $x^3 - \phi_2 x - \phi_3 = 0$ in a local trivialization, this means

$$\phi_2 = -3\Lambda^2 dz^2, \qquad \phi_3 = -(z^2{+}u)dz^3, \qquad \mathrm{Disc}_x = -27\big((z^2{+}u)^2{+}4\Lambda^6\big). \tag{XVII.1.47}$$

This is a separate spectral presentation. It does not identify its z, x coordinates with those of the rank-two scaling family. The discriminant identifies where two sheets collide, but we will use a regular point where all sheets are distinct.

Take $\Lambda = 1, z = 1, u = 0$, so that the sheets solve $x^3 + 3x + 1 = 0$. Order their labels by increasing imaginary part,

$$\begin{aligned} x_1 &\simeq 0.1610926773 - 1.7543809598i, \\ x_2 &\simeq -0.3221853546, \\ x_3 &\simeq 0.1610926773 + 1.7543809598i. \end{aligned} \tag{XVII.1.48}$$

Their sum vanishes, as required by the missing quadratic coefficient. The three cyclic sheet differences are

$$\begin{aligned} d_{12} &\simeq 0.4832780319 - 1.7543809598i, \\ d_{23} &\simeq -0.4832780319 - 1.7543809598i, \\ d_{31} &\simeq 3.5087619196i, \qquad d_{12} + d_{23} + d_{31} = 0. \end{aligned} \tag{XVII.1.49}$$

They determine the local directions directly. With a positive rescaling of the path parameter, the trajectory condition is

$$\frac{dz_{ij}}{d\tau} = \frac{e^{i\theta}}{d_{ij}}, \qquad e^{-i\theta}(\lambda_i - \lambda_j)(\partial_\tau) = 1. \tag{XVII.1.50}$$

At $\theta = 0$, for example, the first two directions have positive imaginary parts and opposite real parts. They are transverse. The third cyclic direction is negative imaginary. This computes possible local tangent directions at the specified point. It does not construct three globally arriving streets.

The direction equation also explains the local balance of tensions. The unit tangent and the corresponding force vector, up to a common positive normalization, are

$$\widehat{t}_{ij} = e^{i\theta}\frac{\overline{d_{ij}}}{|d_{ij}|}, \qquad T_{ij} = |c_{\mathrm{SW}}|\,|d_{ij}|, \qquad F_{ij} = T_{ij}\widehat{t}_{ij} = |c_{\mathrm{SW}}|e^{i\theta}\overline{d_{ij}}. \tag{XVII.1.51}$$

The cyclic sheet differences sum to zero, so the three outward cyclic forces can balance,

$$F_{12} + F_{23} + F_{31} = 0, \qquad d_{13} = d_{12} + d_{23} = -d_{31}. \tag{XVII.1.52}$$

The second equality is the composability rule for a child path of type 13. Its orientation is opposite to the cyclic outward 31 leg. This distinction prevents a sheet-label error when translating a balanced drawing into path multiplication.

At a local joint, a lifted 12 path followed by a lifted 23 path can compose to a 13 path. Matrix units encode just the endpoint labels. With E_{ij} the matrix having a single one in row i, column j, multiplication gives

$$E_{ij}E_{kl} = \delta_{jk}E_{il}, \qquad E_{12}E_{23} = E_{13}, \qquad E_{23}E_{12} = 0. \tag{XVII.1.53}$$

Thus reversing the order changes the possible lifted path, rather than merely changing the sign of a scalar. Let a, b denote the local soliton coefficients of the two parents. One ordering of their contributions gives

$$(I + aE_{12})(I + bE_{23}) = I + aE_{12} + bE_{23} + abE_{13}. \tag{XVII.1.54}$$

The other route around the joint has the reversed parent order and a child contribution c. Its product is

$$(I + bE_{23})(I + cE_{13})(I + aE_{12}) = I + aE_{12} + bE_{23} + cE_{13}. \tag{XVII.1.55}$$

Equality of the two local path transports requires $c = ab$. Figure XVII.1.5 depicts this local composition rule. The coefficients count local soliton data; they are not the bulk hypermultiplet indices Ω used in the pentagon.

Relative winding introduces a sign in the formal composite generator. If w is the relative winding number, write

$$X_c = (-1)^w E_{13}, \qquad \Delta\mu_{13} = (-1)^w ab, \qquad \Delta\mu_{13}X_c = abE_{13}. \tag{XVII.1.56}$$

Both signs are required. For example, $a = 2, b = 3$ gives $\Delta\mu_{13} = 6$ at $w = 0$ and -6 at $w = 1$, while the actual coefficient multiplying E_{13} remains six. Using the odd-winding coefficient with the unsigned generator would reverse that matrix coefficient and spoil equality of the two products.

The local rule is powerful because it tells us which additional path must occur when two composable types meet. A full spectral network additionally requires branch-point initial data, trajectories integrated on the whole base, their global incidence and lifted homotopy classes, and the appropriate soliton data. Those data are absent from a single matrix identity. The next use of networks must supply them before extracting a global BPS spectrum.

Take-home message

The membrane boundary converts a finite sheet-labeled path into a particle charge, while constant differential phase saturates its mass bound. In the cubic Argyres–Douglas example the two real saddles have exactly calculable beta-function periods.

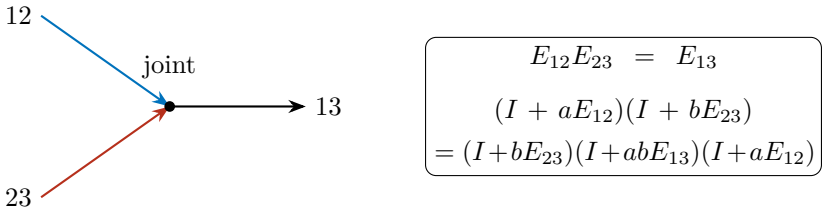


Figure XVII.1.5: A local schematic $12, 23 \to 13$ joint. The two incoming labels share the intermediate sheet 2, so their ordered lifts compose. The child has endpoints on sheets 1 and 3. The left panel records path composition; the right panel compares the two ordered local transport products. It does not assert a global network for the rank-three curve or the existence of three streets reaching the illustrated point.

Their transported periods positively align as $u = iv$ varies, and the nonzero $2 \to 1$ representation becomes stable when their phase order reverses. The exact classical pentagon relates the two- and three-factor products appropriate to the sourced adjacent spectra. At higher rank, sheet composability and a winding sign already matter locally. Physical state existence, chamber completeness and global network reconstruction each require more than the corresponding period or local algebra.

Exercises

1. Set $\Lambda = 1, u = 0$. Compute the outgoing, returning and full left period numerically, and the full period after reversing its charge. Give the sign of the period after reversing both the projected path and the sheet labels. Derive the equality of the outgoing and returning contributions, and explain why the double reversal preserves the represented membrane boundary.

2. At a simple turning point with $P'(z_0) = 1$ and $\theta = 0$, determine the three projected ray angles in $[0, 2\pi)$. At $z = -1$ on the actual cubic, compute the imaginary part in equation (XVII.1.17). Derive the fractional-power primitive and explain why these local rays alone do not establish a finite BPS particle.

3. Derive the beta-function period through both substitutions in equation (XVII.1.14). Compute its scaling exponent and the ratio of periods at $\Lambda = 2$ and $\Lambda = 1$, holding u/Λ^3 fixed. Explain how the weighted dimensions restore mass dimension one, and which normalization is still missing from an absolute BPS mass.

4. Use the continued periods at $v = 1, 2, 3$ to compute $\mathrm{Im}(\mathcal{Z}_1\overline{\mathcal{Z}_2})$. Determine whether the nonzero and zero $(1, 1)$ arrows are stable at each sample. At the wall, also compute the sign of the real part after replacing $\mathcal{Z}_2$ by $-\mathcal{Z}_2$. Derive the subrepresentation condition and distinguish the sourced physical stability prescription from the finite representation calculation.

5. Derive both sides of the classical pentagon by substitution. Evaluate the correct product and the product omitting C at $x = y = 1$. Give $\sigma(1, 1)$ and explain why treating it as $\sigma(1, 0)\sigma(0, 1)$ would change the composite map. State the domain restrictions and the distinction from a quantum or full-spectrum identity.

6. Set the parent joint coefficients to $a = 2, b = 3$. For $w = 0$ and $w = 1$, find the child coefficient and its signed generator, and give the coefficient of E_{13} in each full product. Compute the reversed matrix-unit product $E_{23}E_{12}$. Derive the local transport equality and list the global data needed before this becomes a network calculation.

For benchmark submissions, see `benchmark/PROTOCOL.md`. Equivalent numerical and symbolic forms are accepted. Include the requested written derivations and explanations.

Sources and scope

Section 1.1. The M2 boundary, sheet-difference tension and BPS interpretation are sourced [GEO-E] and [BPS:1/2|idx] input, following Gaiotto et al. 2013b, arXiv v2, pp. 22–24, §3.1.3, eqs. (3.8)–(3.11); the general charge-lattice qualification is in Gaiotto et al. 2013a, arXiv v2, pp. 9–11, §§2–3.1. The half fraction refers to the eight supercharges of the four-dimensional theory. The boundary integral, triangle inequality, orientation algebra, discriminant and scaling dimensions are explicit calculations. The common uncalibrated c_{SW} follows XVI.4. The oriented cycles and the irregular scaling coordinates are specified above.

Section 1.2. The WKB direction rule and three turning-point rays follow Gaiotto et al. 2013b, arXiv v2, pp. 76–78, §§6.1–6.3, eq. (6.3). The actual AD family is its eqs. (9.7), (9.29), pp. 105–106, 112–114. The two real saddles, beta integral and scaling are explicit [MATH] calculations. The isolated-saddle-to-hypermultiplet identification is sourced physical input, not a consequence of the numerical period alone.

Section 1.3. The rank-two pairing and complete two-particle chamber are sourced [BPS:1/2|idx] statements in Gaiotto et al. 2013b, arXiv v2, §9.4.4, eqs. (9.29)–(9.32), Figs. 46–48. The arrow convention and phase-stability prescription follow Alim et al. 2014, arXiv v1, p. 7, §2.1.1, pp. 13–16, eqs. (2.14)–(2.24). The source interchanges the labels of the two nodes relative to those used here. The determinant and subrepresentation enumeration are finite calculations. The physical correspondence between stable representations and BPS states remains an input.

Section 1.4. Root continuation, geometric periods, positive-alignment diagnostics and rank-one stability are explicit calculations; numerical values lack certified interval bounds or a global wall-uniqueness theorem. The two- and three-state physical spectra are sourced from Gaiotto et al. 2013b, arXiv v2, pp. 112–114, §9.4.4 and Alim et al. 2014, arXiv v1, pp. 15–17, §2.3.1. The classical wall-crossing premise and KS rule follow Gaiotto et al. 2013b, arXiv v2, p. 16, eq. (2.6), pp. 17–18, eqs. (2.10)–(2.11). The displayed rational-map identity is exact [MATH]; it is not independently a proof of the physical spectra, and no quantum refinement is claimed.

Section 1.5. The rank-three chart is Gaiotto et al. 2013a, arXiv v2, p. 46, §8.1, eq. (8.3). Its coefficient signs reuse XVI.4. Local soliton composition and relative winding follow Gaiotto et al. 2013a, arXiv v2, pp. 21–23, §5.2, eqs. (5.5)–(5.9). The sheet roots, directions, force sum and signed matrix products are explicit local calculations. They do not reconstruct globally arriving streets or a bulk spectrum. These finite geometry and algebra calculations do not certify the physical premises.

References

Alim, M. et al. (2014). "N=2 Quantum Field Theories and Their BPS Quivers". In: *Adv. Theor. Math. Phys.* 18.1, pp. 27–127. DOI: 10.4310/ATMP.2014.v18.n1.a2. arXiv: 1112.3984 [hep-th].

Gaiotto, D., G. W. Moore, and A. Neitzke (2013a). "Spectral networks". In: *Annales Henri Poincare* 14, pp. 1643–1731. DOI: 10.1007/s00023-013-0239-7. arXiv: 1204.4824 [hep-th].

Gaiotto, D., G. W. Moore, and A. Neitzke (2013b). "Wall-crossing, Hitchin Systems, and the WKB Approximation". In: *Adv. Math.* 234, pp. 239–403. DOI: 10.1016/j.aim.2012.09.027. arXiv: 0907.3987 [hep-th].

Chapter XVII.2

The Omega background and instanton sums

Instantons contribute holomorphic terms to the low-energy action of a four-dimensional $\mathcal{N} = 2$ gauge theory. Their position, size and gauge orientation make a direct integral over instantons difficult. The Omega background replaces this integral by an equivariant integral. Rotations of the two complex planes resolve the calculation into isolated configurations. The answer is a sum of rational functions, one for each pair of Young diagrams.

Our aim is to compute that sum through two instantons for the four-flavor $SU(2)$ frame introduced in XVI.3. The first task is to determine the weights of the fluctuations around an instanton. The second is to attach the matter weights with the correct mass convention. Only then can we extract the connected logarithm and compare it with an undeformed holomorphic quantity. A complete calculation involves just two one-instanton configurations and five two-instanton configurations, but already distinguishes several physically different normalizations.

We assume familiarity with complex quotients, supersymmetric localization and the Coulomb branch. The localization prescription, its resolved framed instanton space and its low-energy interpretation are physical inputs. We will derive the finite equivariant weights and coefficients that follow from them. Throughout, $(a_1, a_2) = (a, -a)$ with $a \neq 0$. These are parameters in the localization convention. Their relation to the geometric periods of XVI.4 requires a further normalization choice. The auxiliary $U(2)$ presentation used here also requires an abelian normalization before it supplies the series needed in XVII.3.

XVII.2.1 Rotations, fixed points and the ADHM complex

How can a continuous space of instantons reduce to a finite calculation at fixed instanton number? Write Euclidean space as $\mathbb{C}^2$ with coordinates z_1, z_2. The two rotation

parameters ϵ_1, ϵ_2 enter the equivariant action through

$$(z_1, z_2) \longmapsto (e^{t\epsilon_1} z_1, e^{t\epsilon_2} z_2), \qquad \epsilon_+ = \epsilon_1 + \epsilon_2, \qquad p = \epsilon_1 \epsilon_2. \tag{XVII.2.1}$$

Here t is a formal group parameter. The ϵ_i, a and all masses have mass dimension one. The supersymmetry used for localization squares to a combination of the rotation generators J_i and a gauge transformation,

$$Q_\Omega^2 = \epsilon_1 J_1 + \epsilon_2 J_2 + \delta_{\text{gauge}}(a). \tag{XVII.2.2}$$

This equivariant algebra is sufficient for the calculation below. It does not specify a complete curved-space metric. The instanton sector is a protected sector of the underlying theory; a generic deformation need not preserve four untwisted supercharges.

The ADHM description uses a complex vector space V_0 of dimension k and a framing space W_0 of dimension N. Two maps B_1, B_2 lie in $\operatorname{End} V_0$, while $I\colon W_0 \to V_0$ and $J\colon V_0 \to W_0$. The complex equation and complexified gauge quotient are

$$[B_1, B_2] + IJ = 0, \qquad (B_1, B_2, I, J)/GL(V_0). \tag{XVII.2.3}$$

A stability condition and a resolved, or noncommutative, regulator give the smooth framed space to which localization is applied. At a stable point, the deformation complex removes one gauge variation and one complex relation for each element of $\operatorname{End} V_0$. Thus

$$\dim_{\mathbb{C}} T = 2k^2 + 2kN - k^2 - k^2 = 2kN = 4k \quad (N = 2). \tag{XVII.2.4}$$

The subtraction of the moment-map relation matters. Dropping it would leave k^2 extra directions. At $k = 2, N = 2$ the resulting count would be 12 instead of 8. A quotient of singular, unstable data need not admit this tangent-space interpretation.

To determine each fluctuation weight, let $t_i = e^{\epsilon_i}$ and introduce dual characters V, W. The actual ADHM spaces carry characters $V_0 = V^*$ and $W_0 = W^*$. At a fixed point labeled by two diagrams Y_1, Y_2, define

$$W = e^a + e^{-a}, \qquad V = \sum_{\alpha=1}^{2} \sum_{(i,j)\in Y_\alpha} e^{a_\alpha + (i-1)\epsilon_1 + (j-1)\epsilon_2}. \tag{XVII.2.5}$$

The dual convention fixes the orientation of the framing maps. In particular I has character V^*W, and J has character $t_1 t_2 W^* V$. The two B maps, gauge quotient and complex relation then give

$$\begin{aligned} T &= V^*W + t_1 t_2 W^* V + (t_1 + t_2 - 1 - t_1 t_2) V^* V, \\ &= V^*W + t_1 t_2 W^* V - (1 - t_1)(1 - t_2) V^* V. \end{aligned} \tag{XVII.2.6}$$

A character is a signed sum before cancellation. After cancellation at the resolved fixed points considered here it becomes a sum of $4k$ positive multiplicities. An exponential e^w denotes a tangent direction of additive weight w.

For one box in the first color, $V = e^{a}$ and $V^{*}V = 1$. We can see every cancellation explicitly,

$$V^{*}W = 1 + e^{-2a}, \qquad t_1 t_2 W^{*}V = t_1 t_2 (1 + e^{2a}), \tag{XVII.2.7}$$

$$\begin{aligned} T_{(\square,\varnothing)} &= 1 + e^{-2a} + t_1 t_2 (1 + e^{2a}) - 1 + t_1 + t_2 - t_1 t_2 \\ &= t_1 + t_2 + e^{-2a} + e^{2a+\epsilon_+}. \end{aligned} \tag{XVII.2.8}$$

The four weights are $\epsilon_1, \epsilon_2, -2a, 2a + \epsilon_+$. Their product is the equivariant Euler class,

$$D_{(\square,\varnothing)} = -p(2a)(2a + \epsilon_+). \tag{XVII.2.9}$$

There is no absolute value in this expression. Localization uses a complex oriented Euler class, so its signs affect the answer. Replacing a by $-a$ gives the second one-box configuration. The weights occur in pairs $w, \epsilon_+ - w$, reflecting the equivariant symplectic form.

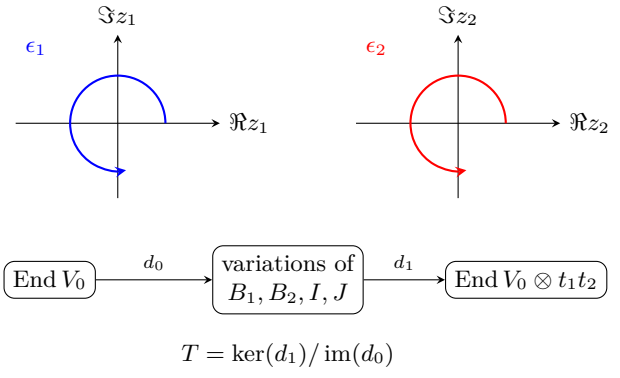


Figure XVII.2.1: The rotation torus acts on the two coordinate planes. Below it, the ADHM deformation complex subtracts gauge directions and the complex moment-map relation from the variations of B_1, B_2, I, J. Its middle cohomology supplies the tangent weights.

The framing character remembers the Coulomb parameters even after all positions have been localized to the origin. Figure XVII.2.1 separates the spacetime action from this internal deformation complex. In the next section the same tangent character will become a product over boxes. This is the step that lets us compute the instanton expansion needed for the protected structures of XVII.3.

XVII.2.2 From monomial ideals to Young diagrams

The character calculation is finite, but repeated expansion becomes cumbersome. We want a product formula that retains its individual weights. A torus-fixed monomial ideal leaves a downward-closed set of monomials in the quotient. If $z_1^{i-1} z_2^{j-1}$ remains,

every divisor remains. Such a set is a Young diagram. Write a partition as $Y = (Y_1 \geq Y_2 \geq \cdots)$, with box coordinates satisfying $1 \leq j \leq Y_i$. For a box $s = (i, j)$ define

$$A_Y(s) = Y_i - j, \qquad L_W(s) = W_j^T - i, \qquad \phi_\alpha(s) = a_\alpha + (i-1)\epsilon_1 + (j-1)\epsilon_2. \tag{XVII.2.10}$$

Here $W_j^T = \#\{i \mid W_i \geq j\}$ is the height of column j of W, equivalently the length of row j of W^T. The leg is measured in the other diagram and may be negative. For example, a box in row $i = 1$ compared with the empty diagram has $L_\varnothing = -1$. Setting that leg to zero changes the off-diagonal weights.

The product form of the tangent character assigns two weights for every ordered pair of colors and every occupied box,

$$E_{\alpha\beta}(s) = a_\alpha - a_\beta - \epsilon_1 L_{Y_\beta}(s) + \epsilon_2\big(A_{Y_\alpha}(s) + 1\big), \tag{XVII.2.11}$$

$$D_{Y_1,Y_2} = \prod_{\alpha,\beta=1}^{2} \prod_{s \in Y_\alpha} E_{\alpha\beta}(s)\big(\epsilon_+ - E_{\alpha\beta}(s)\big), \qquad z_{\text{vec}} = D_{Y_1,Y_2}^{-1}. \tag{XVII.2.12}$$

For one occupied box in the first color the same-color pair is ϵ_2, ϵ_1. Against the empty second diagram it is $2a + \epsilon_+, -2a$. Thus this formula reproduces (XVII.2.9), including its sign.

At total size two the two boxes can occupy one color as a row or a column, or occupy both colors separately. The complete list is

$$((2), \varnothing), \quad ((1,1), \varnothing), \quad ((1), (1)), \quad (\varnothing, (2)), \quad (\varnothing, (1,1)). \tag{XVII.2.13}$$

Figure XVII.2.2 depicts these five configurations. Our horizontal displacement is ϵ_2, and our vertical displacement is ϵ_1. This assignment follows the algebraic box coordinates in (XVII.2.10).

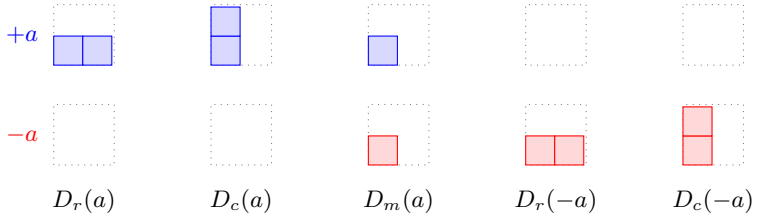


Figure XVII.2.2: The five colored fixed points at instanton number two. Blue boxes carry Coulomb parameter $+a$, red boxes carry $-a$. The empty small frames mark the unoccupied color. A row advances in the ϵ_2 direction and a column advances in the ϵ_1 direction.

For the first row diagram the boxes are $(1,1)$ and $(1,2)$. Their arms are $1, 0$, their same-color legs vanish, and both legs against the empty diagram equal -1. The resulting weights are

$$\begin{aligned} \mathcal{W}_{((2),\varnothing)} = \{&2\epsilon_2, \epsilon_1 - \epsilon_2, \epsilon_2, \epsilon_1, \\ &2a + \epsilon_1 + 2\epsilon_2, -2a - \epsilon_2, 2a + \epsilon_+, -2a\}. \end{aligned} \tag{XVII.2.14}$$

They can also be obtained directly from the ADHM complex. Substituting $V = e^a(1+t_2)$ gives $V^*V = 2 + t_2 + t_2^{-1}$ and

$$\begin{aligned} T_r &= (1+t_2^{-1})(1+e^{-2a}) + t_1t_2(1+t_2)(1+e^{2a}) \\ &\quad - (1-t_1)(1-t_2)(2+t_2+t_2^{-1}) && \text{(XVII.2.15)} \\ &= t_2^2 + t_1t_2^{-1} + t_2 + t_1 + e^{2a}t_1t_2^2 + e^{-2a}t_2^{-1} + e^{2a}t_1t_2 + e^{-2a}. && \text{(XVII.2.16)} \end{aligned}$$

The same-color t_2^{-1} terms cancel, whereas the off-diagonal term $e^{-2a}t_2^{-1}$ remains. Reading the additive exponents gives precisely (XVII.2.14). All multiplicities are now positive, even though some additive weights can be negative. This calculation relates the monomial description directly to the eight tangent directions.

For later use, set $b = 2a$ and denote the row, column and mixed denominators by D_r, D_c, D_m. Multiplying the displayed weights gives all five denominators in a compact form,

$$D_r(a) = 2bp\epsilon_2(b+\epsilon_2)(\epsilon_1-\epsilon_2)(b+\epsilon_+)(b+\epsilon_1+2\epsilon_2), \quad \text{(XVII.2.17)}$$

$$D_c(a) = -2bp\epsilon_1(b+\epsilon_1)(\epsilon_1-\epsilon_2)(b+\epsilon_+)(b+2\epsilon_1+\epsilon_2), \quad \text{(XVII.2.18)}$$

$$D_m(a) = p^2(b^2-\epsilon_1^2)(b^2-\epsilon_2^2), \quad \text{(XVII.2.19)}$$

$$D_{\varnothing,(2)} = D_r(-a), \qquad D_{\varnothing,(1,1)} = D_c(-a). \quad \text{(XVII.2.20)}$$

The mixed denominator deserves a separate calculation. Both boxes now have arm and leg zero against either occupied diagram. Its eight weights are

$$\mathcal{W}_{(\square,\square)} = \{\epsilon_2, \epsilon_1, b+\epsilon_2, -b+\epsilon_1, \epsilon_2, \epsilon_1, -b+\epsilon_2, b+\epsilon_1\}. \quad \text{(XVII.2.21)}$$

Their product gives (XVII.2.19). In particular the mixed configuration cannot be recovered by doubling a same-color term. It includes interactions between the two occupied colors.

Transposing a diagram exchanges rows and columns. Exchanging the two rotation planes at the same time gives

$$D_r(a;\epsilon_1,\epsilon_2) = D_c(a;\epsilon_2,\epsilon_1), \qquad D_m(a;\epsilon_1,\epsilon_2) = D_m(a;\epsilon_2,\epsilon_1). \quad \text{(XVII.2.22)}$$

Individual row and column expressions have poles at $\epsilon_1 = \epsilon_2$. When a combined coefficient has a removable singularity, it must be combined before taking that limit. Throughout our examples parameters avoid the denominator hyperplanes. The box product now supplies the vector contribution. Matter will turn these denominators into the rational functions that enter the instanton sum.

XVII.2.3 Matter factors and the mass lift

A hypermultiplet changes the numerator of each fixed-point contribution. Its equivariant mass depends on how flavor rotations combine with the supersymmetry used in localization. We must therefore distinguish that parameter from a physical mass before asking for a massless theory.

Use two anti-fundamentals of equivariant masses μ_1, μ_2 and two fundamentals of masses μ_3, μ_4. For a box of weight ϕ, their combined matter polynomial is

$$P(\phi) = (\phi + \mu_1)(\phi + \mu_2)(\phi - \mu_3 + \epsilon_+)(\phi - \mu_4 + \epsilon_+). \tag{XVII.2.23}$$

The first two factors have the opposite representation orientation from the last two. The centered supersymmetric mass convention is

$$\mu_f = m_f + \frac{\epsilon_+}{2}, \qquad P(\phi) = \prod_{f=1}^{2} \left(\phi + m_f + \frac{\epsilon_+}{2}\right) \prod_{f=3}^{4} \left(\phi - m_f + \frac{\epsilon_+}{2}\right). \tag{XVII.2.24}$$

This half-epsilon lift is a sourced physical convention, rather than a conclusion from the finite combinatorial sum. It also occurs in the one-loop hypermultiplet determinants. In this convention representation conjugation acts as

$$\mu \longmapsto \epsilon_+ - \mu, \qquad m \longmapsto -m, \qquad \phi - (\epsilon_+ - \mu) + \epsilon_+ = \phi + \mu. \tag{XVII.2.25}$$

Figure XVII.2.3 shows the center of this reflection. At nonzero ϵ_+, physical massless matter has $\mu = \epsilon_+/2$. Taking $\mu = 0$ instead gives physical mass $-\epsilon_+/2$.

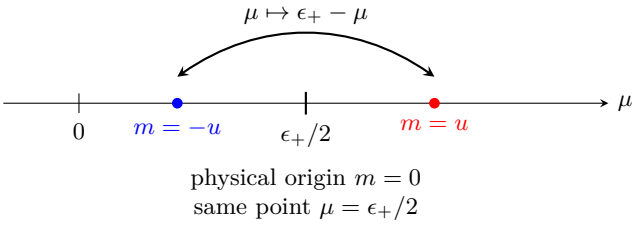


Figure XVII.2.3: The affine equivariant mass line and its centered physical coordinate. The arbitrary displacement u from the physical mass origin labels the pair $m = \pm u$. Conjugation reflects around $\mu = \epsilon_+/2$. The drawing represents the algebraic translation and reflection of complex parameters, rather than an ordering of real energies.

Let Z_k denote the sum at instanton number k and set $Z_0 = 1$. Each occupied box contributes one P factor, so

$$Z_k = \sum_{|Y_1|+|Y_2|=k} \frac{\prod_{\alpha,s\in Y_\alpha} P(\phi_\alpha(s))}{D_{Y_1,Y_2}}, \qquad Z_{\text{inst}}^{U(2)} = 1 + qZ_1 + q^2 Z_2 + O(q^3). \tag{XVII.2.26}$$

The two one-box terms give a useful closed expression valid for generic masses,

$$Z_1 = -\frac{P(a)}{p(2a)(2a+\epsilon_+)} - \frac{P(-a)}{p(-2a)(-2a+\epsilon_+)}. \tag{XVII.2.27}$$

The five terms at the next order are equally explicit once the denominators are known,

$$\begin{aligned} Z_2 = {} & \frac{P(a)P(a+\epsilon_2)}{D_r(a)} + \frac{P(a)P(a+\epsilon_1)}{D_c(a)} + \frac{P(a)P(-a)}{D_m(a)} \\ & + \frac{P(-a)P(-a+\epsilon_2)}{D_r(-a)} + \frac{P(-a)P(-a+\epsilon_1)}{D_c(-a)}. \end{aligned} \tag{XVII.2.28}$$

Each numerator has dimension $4k$, canceling the dimension of the tangent denominator. Thus Z_k and the four-flavor counting coordinate q are dimensionless.

We can now perform an asymmetric exact example, which tests more than a symmetric mass assignment. Choose

$$a=\frac{7}{3},\qquad (\epsilon_1,\epsilon_2)=(2,3),\qquad (m_1,m_2,m_3,m_4)=\left(\frac{1}{3},\frac{2}{5},-\frac{4}{7},\frac{3}{2}\right), \tag{XVII.2.29}$$

$$(\mu_1,\mu_2,\mu_3,\mu_4)=\left(\frac{17}{6},\frac{29}{10},\frac{27}{14},4\right), \tag{XVII.2.30}$$

$$P(x)=\left(x+\frac{17}{6}\right)\left(x+\frac{29}{10}\right)\left(x+\frac{43}{14}\right)(x+1). \tag{XVII.2.31}$$

For the one-box configurations the elementary products are

$$P(a)=\frac{1104809}{2268},\qquad D_{\square,\varnothing}=-\frac{812}{3}, \tag{XVII.2.32}$$

$$P(-a)=-\frac{527}{1890},\qquad D_{\varnothing,\square}=\frac{28}{3}. \tag{XVII.2.33}$$

Their quotient sum yields $Z_1=-114607/62640$. At the next order it is useful to keep the five contributions visible,

(Y_1,Y_2)	contribution to Z_2
$(\varnothing,(2))$	8853073/127008000
$(\varnothing,(1,1))$	−133331/9483264
$((1),(1))$	−582234343/35054208000
$((2),\varnothing)$	−96329401519/8713474560
$((1,1),\varnothing)$	458012933467/38673936000

(XVII.2.34)

For example, the first entry follows from

$$D_r(-a)=-\frac{2800}{9},\qquad P(-a)P(-a+3)=-\frac{8853073}{408240}. \tag{XVII.2.35}$$

Dividing gives the stated positive contribution. Summing all five gives

$$Z_1=-\frac{114607}{62640},\qquad Z_2=\frac{95920869631}{116021808000}. \tag{XVII.2.36}$$

Omitting the mixed-color term would change Z_2 by 582234343/35054208000. This is a finite way to detect an incomplete enumeration.

A second example changes both masses and the rotation ray,

$$a=\frac{11}{4},\quad (\epsilon_1,\epsilon_2)=\left(\frac{3}{2},-\frac{2}{3}\right),\quad m=\left(2,-3,\frac{4}{5},\frac{1}{7}\right), \tag{XVII.2.37}$$

$$\mu=\left(\frac{29}{12},-\frac{31}{12},\frac{73}{60},\frac{47}{84}\right),\quad (Z_1,Z_2)=\left(\frac{26601}{37240},\frac{526266553}{980156800}\right). \tag{XVII.2.38}$$

We can also hold the rotations at $(2,3)$ and compare two meanings of massless. Setting all physical masses to zero gives $\mu_f = 5/2$, while setting all equivariant masses to zero omits the centered shift. The changed numerators and one-instanton coefficients are

$$P_{m=0}(a) = \left(\frac{29}{6}\right)^4 = \frac{707281}{1296}, \qquad Z_1\big|_{m=0} = -\frac{871}{432}, \tag{XVII.2.39}$$

$$P_{\mu=0}(a) = a^2(a+5)^2 = \frac{23716}{81}, \qquad Z_1\big|_{\mu=0} = \frac{2401}{783}. \tag{XVII.2.40}$$

These are different finite-background assignments, even though their mass difference vanishes in the undeformed limit. Negative equivariant parameters cause no difficulty away from poles. Replacing a by $-a$ permutes the colors, while exchanging ϵ_1, ϵ_2 transposes the diagrams. Both changes preserve the two summed coefficients in these examples. These finite sums prepare the normalization problem, but do not by themselves identify a conformal block.

XVII.2.4 Which partition function is being expanded?

The instanton sum is only one part of a fixed-Coulomb-parameter partition function. Before comparing it with another protected object we must state which factors are included. In the source convention used here,

$$Z_{\text{full}} = Z_{\text{classical}} Z_{\text{1loop}} Z_{\text{inst}}^{U(2)}, \qquad Z_{\text{classical}} = q^{-a^2/p}, \qquad q = e^{2\pi i \tau_{\text{UV}}}. \tag{XVII.2.41}$$

This specifies the instanton coordinate in a gauge-theory scheme. Its relation to a marked-curve coordinate in XVI.3 is an additional dictionary. We also keep fixed a throughout; no Coulomb integral or sphere partition function is being evaluated.

For clarity, we record the determinant convention needed for the mass lift. Write the regularized Barnes function as

$$\gamma_\epsilon(x) = \log \Gamma_2(x + \epsilon_+ \mid \epsilon_1, \epsilon_2). \tag{XVII.2.42}$$

The sourced one-loop factors in this convention are

$$Z_{\text{1loop}}^{\text{vec}} = \exp[-\gamma_\epsilon(2a - \epsilon_1) - \gamma_\epsilon(2a - \epsilon_2)], \tag{XVII.2.43}$$

$$Z_{\text{1loop}}^{\text{anti}}(\mu) = \prod_{\sigma=\pm 1} \exp \gamma_\epsilon(-\sigma a + \mu - \epsilon_+), \tag{XVII.2.44}$$

$$Z_{\text{1loop}}^{\text{fund}}(\mu) = \prod_{\sigma=\pm 1} \exp \gamma_\epsilon(\sigma a - \mu). \tag{XVII.2.45}$$

Substituting $\mu = m + \epsilon_+/2$ centers both hypermultiplet arguments at a half-epsilon shift. The regularization and the allowed local counterterms are part of these formulas. A finite rational sum does not derive the infinite determinant.

One elementary part of the undeformed determinant can be checked directly. On a chosen logarithm branch take

$$g(x) = \frac{x^2}{2}\log x - \frac{3x^2}{4}, \qquad g'(x) = x \log x - x, \tag{XVII.2.46}$$

$$g''(x) = \log x. \tag{XVII.2.47}$$

The quadratic subtraction removes the extra 3/2 that would appear on twice differentiating $x^2 \log x/2$ alone. This local primitive is consistent with a logarithmic coupling; it fixes neither the full determinant nor its polynomial ambiguities.

There is a separate abelian normalization in the four-flavor instanton series. Define paired mass coordinates and its exponent by

$$m_0 = \frac{\mu_1 + \mu_2}{2}, \quad \widetilde{m}_0 = \frac{\mu_1 - \mu_2}{2}, \quad m_1 = \frac{\mu_3 + \mu_4}{2}, \quad \widetilde{m}_1 = \frac{\mu_3 - \mu_4}{2}, \tag{XVII.2.48}$$

$$\eta = \frac{2m_0(\epsilon_+ - m_1)}{p}, \qquad Z_{U(1)} = (1-q)^{\eta}, \qquad Z_{\text{red}} = (1-q)^{-\eta} Z_{\text{inst}}^{U(2)}. \tag{XVII.2.49}$$

The symbols m_0, m_1 here are paired equivariant coordinates, distinct from the four signed physical masses m_f of the previous section. The factor has no a dependence. Its removal is a choice of normalization in the AGT presentation, rather than a proof of a freely propagating decoupled $U(1)$ sector. In particular it is not the six-dimensional center discussed in XVI.1 or the neutral hypermultiplet of XVI.3.

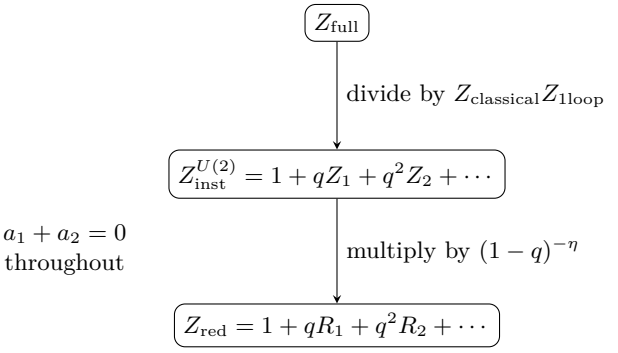


Figure XVII.2.4: The fixed-Coulomb partition function and the two different separations used here. Removing classical and one-loop factors isolates the instanton series. Dividing its particular abelian factor gives Z_{red}, the series whose comparison with a conformal block requires an independent calculation in XVII.3.

The binomial expansion makes the first two normalization changes completely explicit,

$$(1-q)^{-\eta} = 1 + \eta q + \frac{\eta(\eta+1)}{2} q^2 + O(q^3), \tag{XVII.2.50}$$

$$Z_{\text{red}} = 1 + qR_1 + q^2 R_2 + O(q^3), \qquad R_1 = Z_1 + \eta, \tag{XVII.2.51}$$

$$R_2 = Z_2 + \eta Z_1 + \frac{\eta(\eta+1)}{2}. \tag{XVII.2.52}$$

For (XVII.2.29), $\eta = 817/420$. Substituting (XVII.2.36) yields

$$R_1 = \frac{50699}{438480}, \qquad R_2 = \frac{15350739781}{116021808000}. \tag{XVII.2.53}$$

This is a convolution, so subtracting a constant from Z_2 alone cannot remove the factor. For the second example $\eta = -23/2520$ and the same operation gives

$$R_1 = \frac{23635}{33516}, \qquad R_2 = \frac{20875493677}{39696350400}. \tag{XVII.2.54}$$

The sign of the exponent is visible already at order q.

A useful flavor test reflects $m_0 \mapsto \epsilon_+ - m_0$ while holding $\widetilde{m}_0, m_1, \widetilde{m}_1$ fixed. In the first example the original pair and the reflected pair are

$$(\mu_1, \mu_2) = \left(\frac{17}{6}, \frac{29}{10}\right) \longmapsto \left(\frac{21}{10}, \frac{13}{6}\right). \tag{XVII.2.55}$$

The raw coefficient changes from $-114607/62640$ to $-584053/438480$. Applying the corresponding exponent to each series gives instead

$$(R_1', R_2') = (R_1, R_2) = \left(\frac{50699}{438480}, \frac{15350739781}{116021808000}\right). \tag{XVII.2.56}$$

The same comparison holds at the second example. Thus traceless Coulomb parameters alone have not supplied the desired flavor symmetry. Figure XVII.2.4 displays the required extra step. The proposed identification of the resulting series with a Virasoro block is a source correspondence. The independent block calculation belongs to XVII.3.

XVII.2.5 The connected logarithm and the undeformed limit

Why does the low-energy holomorphic quantity involve $\log Z$, rather than Z? Disconnected instanton contributions exponentiate. At two instantons their product contains the square of the one-instanton pole. Expanding the logarithm removes precisely this contribution,

$$\log(1+x) = x - \frac{x^2}{2} + O(x^3), \qquad x = qZ_1 + q^2 Z_2, \tag{XVII.2.57}$$

$$\log Z_{\mathrm{inst}} = qZ_1 + q^2 C_2 + O(q^3), \qquad C_2 = Z_2 - \frac{Z_1^2}{2}. \tag{XVII.2.58}$$

We choose the local convention

$$\mathcal{F}_{\mathrm{loc,inst}} = -\lim_{\epsilon_1, \epsilon_2 \to 0} p \log Z_{\mathrm{inst}}, \tag{XVII.2.59}$$

with limits taken coefficientwise in q. The sourced low-energy interpretation attaches to this undeformed protected quantity. We will compute two coefficients along two nonsingular rays, at fixed $a \neq 0$ and fixed physical masses. This does not assert a uniform all-order limit.

First take physical massless four-flavor matter on the ray $(\epsilon_1, \epsilon_2) = (h, -h)$. Here $\epsilon_+ = 0$, so $\mu_f = 0$ and $P(x) = x^4$. The one-instanton expression reduces to

$$Z_1 = \frac{a^2}{2h^2}, \qquad C_2 = \frac{a^2(26a^4 - 13a^2h^2 + 2h^4)}{8h^2(4a^2 - h^2)^2}. \tag{XVII.2.60}$$

Multiplying by $-p = h^2$ now gives finite coefficients,

$$h^2 Z_1 = \frac{a^2}{2}, \qquad \lim_{h\to 0} h^2 C_2 = \frac{26a^6}{8\cdot 16a^4} = \frac{13a^2}{64}. \tag{XVII.2.61}$$

The cancellation can also be read as a Laurent expansion,

$$Z_2 = \frac{a^4}{8h^4} + \frac{13a^2}{64h^2} + O(1), \qquad \frac{Z_1^2}{2} = \frac{a^4}{8h^4}. \tag{XVII.2.62}$$

Taking $h^2 Z_2$ would retain a divergent $a^4/(8h^2)$. Subtracting Z_1^2 instead of $Z_1^2/2$ would also leave a pole, with the opposite leading sign.

We next change the ray to $(h, 2h)$. Keeping physical masses zero now requires $\mu_f = 3h/2$, not $\mu_f = 0$. The one-instanton coefficient and the leading connected terms become

$$Z_1 = -\frac{a^2}{4h^2} - \frac{27}{16}, \qquad \frac{Z_1^2}{2} = \frac{a^4}{32h^4} + \frac{27a^2}{64h^2} + O(1), \tag{XVII.2.63}$$

$$Z_2 = \frac{a^4}{32h^4} + \frac{41a^2}{128h^2} + O(1), \qquad C_2 = -\frac{13a^2}{128h^2} + O(1). \tag{XVII.2.64}$$

Multiplication by $-p = -2h^2$ reproduces the same answer,

$$\mathcal{F}^{N_f=4,m=0}_{\text{loc,inst}} = a^2\left(\frac{q}{2} + \frac{13q^2}{64}\right) + O(q^3). \tag{XVII.2.65}$$

The two rays illustrate why the mass lift must precede the limit. They also distinguish the connected finite part from a cancellation special to $\epsilon_+ = 0$.

There is an independent elliptic-series comparison in the source coupling chart. The source uses the nome $Q = e^{2\pi i \tau_{\text{IR}}}$ and the modular relation $q = \lambda(2\tau_{\text{IR}})$. Write $\lambda_{\text{nome}}(Q)$ for this function expressed in the nome. The theta ratio supplies the relation

$$\begin{aligned} q = \lambda_{\text{nome}}(Q) &= 16Q\frac{(1+Q^2+O(Q^6))^4}{(1+2Q+O(Q^4))^4} \\ &= 16Q - 128Q^2 + 704Q^3 + O(Q^4). \end{aligned} \tag{XVII.2.66}$$

To invert it, write $Q = c_1 q + c_2 q^2 + c_3 q^3 + O(q^4)$. Comparing successive coefficients gives

$$16c_1 = 1, \qquad 16c_2 - 128c_1^2 = 0, \tag{XVII.2.67}$$

$$16c_3 - 256c_1c_2 + 704c_1^3 = 0, \qquad Q = \frac{q}{16} + \frac{q^2}{32} + \frac{21q^3}{1024} + O(q^4). \tag{XVII.2.68}$$

The logarithm then gives

$$\log\frac{16Q}{q} = \log\left(1 + \frac{q}{2} + \frac{21q^2}{64} + O(q^3)\right) = \frac{q}{2} + \frac{13q^2}{64} + O(q^3). \tag{XVII.2.69}$$

The coefficient $13/64$ follows from $21/64 - (1/2)^2/2$. This reproduces the two numbers in (XVII.2.65) by series reversion. Interpreting this elliptic chart as the massless infrared

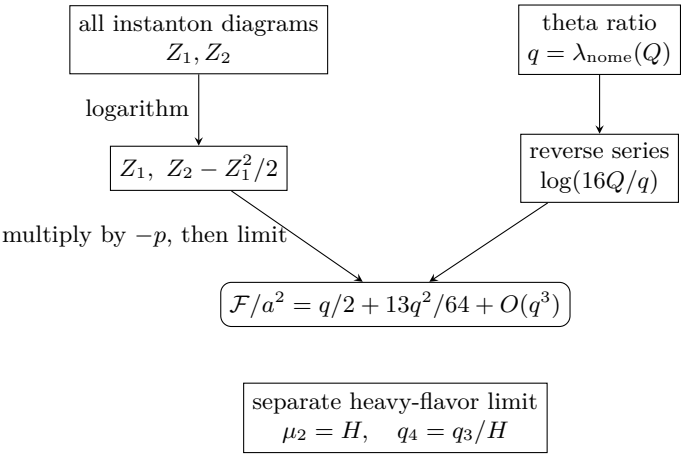


Figure XVII.2.5: Two finite calculations yield the massless coefficients $1/2, 13/64$. The instanton route combines all diagrams and removes disconnected contributions before taking the rotation limit. The elliptic route reverses the specified theta-series chart. The heavy-flavor limit is a separate coefficientwise operation at fixed equivariant parameters.

coupling uses the source relation $q = \lambda(2\tau_{\mathrm{IR}})$. It does not identify our a with an absolutely normalized period of XVI.4.

Changing the matter content provides another useful comparison. For the pure sum every box has numerator one, and the counting parameter q_{pure} has mass dimension four. On $(h, -h)$ the first connected coefficients are

$$Z_1^{\mathrm{pure}} = \frac{1}{2a^2h^2}, \qquad C_2^{\mathrm{pure}} = \frac{10a^2 - h^2}{8a^4h^2(4a^2 - h^2)^2}. \tag{XVII.2.70}$$

The same logarithmic limit, also reproduced on $(h, 2h)$, gives

$$\mathcal{F}_{\mathrm{loc,inst}}^{\mathrm{pure}} = \frac{q_{\mathrm{pure}}}{2a^2} + \frac{5q_{\mathrm{pure}}^2}{64a^6} + O(q_{\mathrm{pure}}^3). \tag{XVII.2.71}$$

Both terms have mass dimension two. A separate rational-residue formula lets us recover the two coefficients without the Young-diagram sum. Define $S_\pm(x) = (x \pm 2a)^{-2}$. Then

$$S_\pm(0) = \frac{1}{4a^2}, \qquad S_\pm''(0) = \frac{3}{8a^4}, \qquad \mathcal{F}_1^{\mathrm{pure}} = S_+(0) + S_-(0) = \frac{1}{2a^2}, \tag{XVII.2.72}$$

$$\begin{aligned} \mathcal{F}_2^{\mathrm{pure}} &= \frac{1}{4}\sum_{\sigma=\pm} S_\sigma(0)S_\sigma''(0) + \frac{2S_+(0)S_-(0)}{(2a)^2} \\ &= \frac{3}{64a^6} + \frac{1}{32a^6} = \frac{5}{64a^6}. \end{aligned} \tag{XVII.2.73}$$

The residue formula is a sourced independent route to these finite coefficients. It does not determine the absolute physical prepotential or the normalization of a_D.

Finally remove a heavy flavor at fixed nonzero rotation parameters. Set the second anti-fundamental mass to $\mu_2 = H$. Every occupied box contributes $\phi + H$, and hence a k-box configuration has leading growth H^k. To retain a finite three-flavor coefficient choose

$$P_H(x) = (x+\mu_1)(x+H)(x-\mu_3+\epsilon_+)(x-\mu_4+\epsilon_+), \tag{XVII.2.74}$$

$$q_4 = \frac{q_3}{H}, \qquad \lim_{H\to\infty} q_4^k Z_k^{(4)} = q_3^k \lim_{H\to\infty} H^{-k} Z_k^{(4)} = q_3^k Z_k^{(3)}. \tag{XVII.2.75}$$

This limit leaves one anti-fundamental and two fundamental factors. For the light parameters of (XVII.2.31), we can derive the first coefficient using the cubic polynomial

$$P_3(x) = \left(x+\frac{17}{6}\right)\left(x+\frac{43}{14}\right)(x+1), \qquad Z_1^{(3)} = \frac{P_3(a)}{-812/3} + \frac{P_3(-a)}{28/3} = -\frac{5797}{14616}. \tag{XVII.2.76}$$

At order two the same five denominators in (XVII.2.28), now with P_3 in each numerator, give

$$Z_2^{(3)} = \frac{136263011}{1804783680} = \lim_{H\to\infty} H^{-2} Z_2^{(4)}. \tag{XVII.2.77}$$

The coefficients $Z_k^{(3)}$ have dimension $-k$, so q_3 has dimension one. Using $q_4 = q_3/H^2$ instead would send both nonzero-instanton coefficients to zero. Figure XVII.2.5 keeps this threshold operation separate from the undeformed limit. It establishes coefficient-wise decoupling through order two in the protected sum. A full finite-scale decoupling statement, or a relation to the geometric scale in XVI.9, needs further physical information.

Take-home message

The instanton sum is determined by tangent Euler classes and matter weights. The dual ADHM character fixes their signs, while the five two-box configurations make the second coefficient complete. Physical massless matter requires the centered equivariant lift. An abelian convolution and a connected logarithm perform different operations on the resulting series. Keeping them distinct yields a usable normalization for XVII.3 and finite undeformed coefficients that can be compared with elliptic and rational-residue calculations.

Before continuing, the reader should be able to reconstruct the four one-box weights, evaluate the row and mixed two-box terms, translate m_f to μ_f, and derive both convolution coefficients. The coefficient 13/64 should be recoverable from the connected instanton limit and from the inverse theta series. The finite Omega background will also provide the starting point for the different, one-parameter limit studied in XVII.4.

Exercises

Each exercise has finite algebraic outputs and a separately assessed written argument. Use complex equivariant parameters away from denominator hyperplanes.

For benchmark submissions, see `benchmark/PROTOCOL.md`. Use the variable names `a,e1,e2,u,v,n,q,Q` specified by the exercise fields. The heavy mass H occurs in the limiting argument, while the required finite answers contain no H. Algebraically equivalent rational expressions are accepted.

1. Starting with $V = e^a$ and $W = e^a + e^{-a}$, expand the tangent character and list its four additive weights. Give its complex dimension and the dimension obtained by dropping the complex moment-map relation at $k = 2, N = 2$. Expand the row character with $V = e^a(1 + t_2)$ and explain the cancellation of negative multiplicities. In writing, state why stability and resolution are needed before calling this a tangent space.

2. Enumerate all five colored pairs at total size two. Derive the mixed-color denominator and the row denominator in the first color. Give the two box weights entering the row matter numerator and express it in terms of $P(a)$ and $P(a + \epsilon_2)$. Explain in writing why a single two-box diagram cannot stand for the full two-instanton coefficient, and how transposition exchanges the two rotation parameters.

3. At $a = 7/3$, $(\epsilon_1, \epsilon_2) = (2, 3)$ and physical masses $(1/3, 2/5, -4/7, 3/2)$, give the four equivariant masses, $P(a)$ and $P(-a)$, and the physical mass conjugate to $m_1 = 1/3$. At the changed assignment of physical massless matter with the same rotations, give $P(a)$ both for the correct lift and for the choice $\mu_f = 0$. Explain in writing why these differ.

4. For the first massive example compute η, R_1, R_2 and the reflected pair (μ_1', μ_2'). Repeat the convolution at symbolic $Z_1 = u, Z_2 = v$ and exponent $\eta = n$. In writing, distinguish an abelian normalization from a dynamical factorization statement, and explain why $a_1 + a_2 = 0$ does not perform the convolution.

5. Given a series $1 + qu + q^2 v$, compute its connected coefficient at order two. Reverse $q = 16Q - 128Q^2 + 704Q^3 + O(Q^4)$ through order q^3 and give the two coefficients of $\log(16Q/q)$. Give the two massless and two pure coefficients of $\mathcal{F}_{\mathrm{loc}}$. In writing, diagnose the divergence caused by omitting the logarithm and explain what remains unspecified about physical period normalization.

6. Remove $\mu_2 = H$ at fixed light parameters of the first massive example. Give the required power s in $q_4 = q_3/H^s$, the first two three-flavor coefficients, and the mass dimension of q_3. State the limits of $H^{-1}Z_1^{(4)}$ and $H^{-2}Z_1^{(4)}$. In writing, explain why the per-box leading factor establishes a coefficientwise statement and does not alone prove a full QFT decoupling theorem.

Sources and scope

§1. The protected instanton contribution has status BPS:1/2|holo, referring to the underlying instanton/F-term sector. Localization, framed boundary conditions, stability and the resolved regulator are sourced premises. The finite character and dimension calculations have status MATH at every $k \leq 2$ fixed point used here. Sources are

Nekrasov 2003, arXiv:hep-th/0206161v1, pp. 2–5, (1.3)–(1.15), pp. 8–18, (2.2), (2.10)–(2.13), (3.1)–(3.19), with the explicit dual-character translation stated in the text. No general singular-quotient theorem is derived.

§2–3. The enumeration, Euler products and per-box polynomial are MATH. The generic one-instanton expression and weight identities are exact; the two massive rational examples verify finite coefficients, rather than an all-mass or all-order physical identity. The physical mass lift is a source premise. Alday et al. 2010, arXiv:0906.3219v2, pp. 24–25, (B.3)–(B.11), supplies the vector and oriented matter convention; pp. 26–27, (B.22), (B.23), (B.27), (B.28), supplies the centered physical translation. These masses are not identified with geometric residues of XVI.4.

§4. The abelian convolution and the stated finite reflection comparisons are MATH. The proposed correspondence with a Virasoro block has status CONJ+ as imported from Alday et al. 2010, pp. 8–9, (3.8)–(3.13), and p. 28, (C.1). No block coefficient is independently computed here. Classical and Barnes determinants, including regularization and counterterms, are source inputs from pp. 25–27, (B.14)–(B.28). Only the elementary primitive is differentiated here. No Coulomb measure or full correlator has been evaluated.

§5. The connected limits along two rays, theta reversion, pure residue comparison and heavy threshold through order two have status MATH. Their low-energy F-term interpretation is sourced and has status BPS:1/2|holo. Sources are Alday et al. 2010, p. 7, (3.2), pp. 27–28, (B.29)–(B.31), for the massless source scheme, and Nekrasov 2003, pp. 19–20, (3.22)–(3.24), for the pure residue formula. The coefficientwise heavy-flavor argument uses the per-box matter factor, with the scale interpretation motivated by pp. 3–4, (1.7)–(1.8), of the latter source. We choose $\mathcal{F}_{\mathrm{loc}} = -p \log Z$ before the limit[1]. No absolute house prepotential, a_D or c_{SW} normalization is fixed. No full AGT correspondence, all-order limit or finite-scale decoupling theorem follows from these finite calculations.

References

Alday, L. F., D. Gaiotto, and Y. Tachikawa (2010). "Liouville Correlation Functions from Four-dimensional Gauge Theories". In: *Lett. Math. Phys.* 91. Version 2, 9 February 2010, pp. 167–197. DOI: 10.1007/s11005-010-0369-5. arXiv: 0906.3219 [hep-th].

Nekrasov, N. A. (2003). "Seiberg-Witten Prepotential from Instanton Counting". In: *Adv. Theor. Math. Phys.* 7. Version 1, 18 June 2002, pp. 831–864. DOI: 10.4310/ATMP.2003.v7.n5.a4. arXiv: hep-th/0206161.

[1] For the same Z, (3.2) of arXiv:0906.3219v2 gives $+h^2 \log Z$ on $(h, -h)$, while (B.15) prints $+\epsilon_1\epsilon_2 \log Z = -h^2 \log Z$. These are opposite signs. We use the former, compatible with (B.16) and the positive instanton coefficients in (B.29). A quantity defined with $+p \log Z$ for this same series is $-\mathcal{F}_{\mathrm{loc}}$. Translating another source also requires its coupling and period conventions.

Chapter XVII.3

An AGT example from states to correlators

A four-punctured sphere gives an $SU(2)$ theory with four hypermultiplets. In the previous chapter its protected instanton contribution became a sum over pairs of Young diagrams. The same sphere also supports a two-dimensional conformal field theory. Cutting it into two three-punctured spheres suggests a second expansion, obtained by propagating conformal states through the connecting tube. Why should these two expansions agree, and which normalization makes the comparison meaningful?

We answer the computational part of this question through two instanton orders. The conformal calculation starts with the Virasoro algebra, builds the inner products of descendants, and uses them to sew two three-point functions. The gauge calculation starts with the localized fixed-point weights of Chapter 2. The AGT dictionary relates their parameters and removes an abelian factor. A chiral block is only one ingredient of a full Liouville correlator. Three-point constants, an intermediate-momentum integral, and an external power of the cross ratio enter when we pass to that observable.

The prerequisites are the pants decompositions of XVI.3, the distinction between a protected coordinate and a low-energy period in XVI.4, and the mass and instanton conventions of XVII.2. We recall the needed conformal Ward identity below. The physical AGT identification and the analytic Liouville sewing and crossing results are source inputs. The explicit algebra will determine what can be tested with a finite expansion.

XVII.3.1 Virasoro states and sewing

How does the tube of XVI.3 propagate conformal states when those states are not orthogonal? Radial quantization assigns a state to a circle around the pair of punctures at q and 0. A highest-weight state $|h\rangle$ and its descendants describe the intermediate

channel. We use the contravariant pairing

$$[L_m, L_n] = (m-n)L_{m+n} + \frac{c}{12}(m^3 - m)\delta_{m+n,0}, \qquad L_0|h\rangle = h|h\rangle, \qquad L_{n>0}|h\rangle = 0. \tag{XVII.3.1}$$

The normalization is $\langle h|h\rangle = 1$ and the algebraic adjoint is $L_n^\dagger = L_{-n}$. For complex weights this specifies a bilinear form, without implying positivity. At levels one and two choose the ordered bases

$$\mathcal{B}_1 = (L_{-1}|h\rangle), \qquad \mathcal{B}_2 = (L_{-2}|h\rangle, L_{-1}^2|h\rangle). \tag{XVII.3.2}$$

The Gram matrix is the matrix of pairings in this basis. The central term first contributes at level two. Commuting positive modes to the right gives

$$\langle h|L_1 L_{-1}|h\rangle = 2h, \tag{XVII.3.3}$$

$$\langle h|L_2 L_{-2}|h\rangle = 4h + c/2, \tag{XVII.3.4}$$

$$\langle h|L_2 L_{-1}^2|h\rangle = 3\langle h|L_1 L_{-1}|h\rangle = 6h, \tag{XVII.3.5}$$

$$L_1 L_{-1}^2|h\rangle = 2(2h+1)L_{-1}|h\rangle. \tag{XVII.3.6}$$

The last relation uses $L_0 L_{-1}|h\rangle = (h+1)L_{-1}|h\rangle$. A second L_1 therefore gives the remaining diagonal entry. The result and determinant are

$$\begin{aligned} G_1 &= (2h), \\ G_2 &= \begin{pmatrix} 4h + c/2 & 6h \\ 6h & 4h(2h+1) \end{pmatrix}, \\ D_2 &= \det G_2 = 2h\big[16h^2 + 2(c-5)h + c\big]. \end{aligned} \tag{XVII.3.7}$$

The off-diagonal entry measures the overlap between two ways of producing a level-two state. Retaining only the diagonal would count overlapping states as independent orthogonal states.

For a nonsingular Gram matrix, the projector onto level n must act as the identity on every state at that level. This fixes its coefficients rather than leaving an arbitrary choice of normalization,

$$\begin{aligned} \Pi_n &= \sum_{Y,Y' \in \mathcal{B}_n} |Y\rangle (G_n^{-1})_{YY'} \langle Y'|, \\ \Pi_n|Z\rangle &= \sum_{Y,Y'} |Y\rangle (G_n^{-1})_{YY'} (G_n)_{Y'Z} = |Z\rangle. \end{aligned} \tag{XVII.3.8}$$

In particular,

$$G_2^{-1} = \frac{1}{D_2} \begin{pmatrix} 4h(2h+1) & -6h \\ -6h & 4h + c/2 \end{pmatrix}. \tag{XVII.3.9}$$

This inverse is defined away from $h = 0$ and the zeros of the bracket in (XVII.3.7). Figure XVII.3.1 depicts its role between the two three-point functions.

To determine the three-point couplings, normalize a primary vertex by

$$\begin{aligned} f(z) &= \langle H_L|V_D(z)|H_R\rangle = z^k, \qquad k = H_L - H_R - D, \\ [L_n, V_D(z)] &= \mathcal{D}_n V_D(z), \quad \mathcal{D}_n = z^n(z\partial_z + (n+1)D). \end{aligned} \tag{XVII.3.10}$$

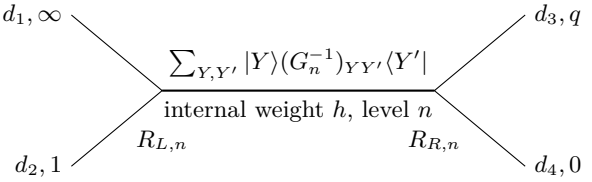


Figure XVII.3.1: Two three-point functions joined through the internal weight h. The two indices on G_n^{-1} belong to the two descendant bases. The contraction compensates their nonorthogonality. The outer punctures have the fixed order $(\infty, 1, q, 0)$.

A negative mode moved from the ket across the vertex gives a minus sign. Thus

$$\langle H_L | V_D(z) L_{-n} | H_R \rangle = -\mathcal{D}_{-n} f(z) = -(k + (1-n)D) z^{k-n}. \tag{XVII.3.11}$$

Repeated L_{-1} action differentiates again, with the exponent lowered after each step. For external weights (d_1, d_2, d_3, d_4) at $(\infty, 1, q, 0)$ define $A = h + d_2 - d_1$ and $B = h + d_3 - d_4$. The two coupling vectors become

$$R_{L,1} = A, \quad R_{R,1} = B, \qquad R_{L,2} = \begin{pmatrix} h + 2d_2 - d_1 \\ A(A+1) \end{pmatrix}, \quad R_{R,2} = \begin{pmatrix} h + 2d_3 - d_4 \\ B(B+1) \end{pmatrix}. \tag{XVII.3.12}$$

Here the left vertex has $(H_L, D, H_R) = (d_1, d_2, h)$ and the right vertex has (h, d_3, d_4). Moving a positive bra mode gives $+\mathcal{D}_n$ and also its action on the ket. That second contribution matters for mixed descendant couplings.

We can reconstruct the entire two-sided trinion through level two without tabulating sixteen long polynomials. Order both legs as $(1, L_{-1}, L_{-2}, L_{-1}^2)$ and form the row of ket matrix elements

$$v(z) = \big(z^k, -k z^{k-1}, -(k-D) z^{k-2}, k(k-1) z^{k-2} \big). \tag{XVII.3.13}$$

The actions of L_1, L_2 on the ket basis are the matrices

$$T_1 = \begin{pmatrix} 0 & 2H_R & 0 & 0 \\ 0 & 0 & 3 & 2(2H_R+1) \\ 0 & 0 & 0 & 0 \\ 0 & 0 & 0 & 0 \end{pmatrix}, \qquad T_2 = \begin{pmatrix} 0 & 0 & 4H_R + c/2 & 6H_R \\ 0 & 0 & 0 & 0 \\ 0 & 0 & 0 & 0 \\ 0 & 0 & 0 & 0 \end{pmatrix}. \tag{XVII.3.14}$$

Each column is the action on one ket. Apply $\mathcal{D}_n$ component by component. The four bra rows of the mixed matrix are then

$$M(z) = \begin{pmatrix} v \\ \mathcal{D}_1 v + v T_1 \\ \mathcal{D}_2 v + v T_2 \\ \mathcal{D}_1(\mathcal{D}_1 v + v T_1) + (\mathcal{D}_1 v + v T_1) T_1 \end{pmatrix}, \qquad M = M(1). \tag{XVII.3.15}$$

For example, the entries with a mode on each side are

$$M_{1,1} = -k(k - 1 + 2D) + 2H_R, \tag{XVII.3.16}$$

$$M_{2,2} = -(k-D)(k - 2 + 3D) + 4H_R + c/2. \tag{XVII.3.17}$$

At $D = 0$ and $H_L = H_R = h$, the level-one and level-two equal-level submatrices give precisely G_1, G_2. An identity vertex therefore reproduces state propagation. This is also a useful way to detect a missing ket-action term.

Insert the projector into the four-point function. Separating the leading operator-product power defines the normalized block,

$$\mathcal{F}_h(q) = 1 + B_1 q + B_2 q^2 + \cdots, \qquad \mathcal{V}_h(q) = q^{h-d_3-d_4}\mathcal{F}_h(q), \qquad B_n = R_{L,n}^{\mathsf{T}} G_n^{-1} R_{R,n}. \tag{XVII.3.18}$$

Let $U = h + 2d_2 - d_1$, $V = h + 2d_3 - d_4$, $A_2 = A(A+1)$ and $B_2' = B(B+1)$. The first two coefficients are explicitly

$$B_1 = \frac{AB}{2h}, \qquad B_2 = \frac{4h(2h+1)UV - 6h(UB_2' + A_2 V) + (4h + c/2)A_2 B_2'}{D_2}. \tag{XVII.3.19}$$

The prime distinguishes the vertex polynomial B_2' from the block coefficient. As $c \to \infty$ at fixed nonsingular h, the L_{-2} contribution is suppressed and this reduces to $A(A+1)B(B+1)/[4h(2h+1)]$, the global conformal descendant contribution.

A singular Gram matrix requires a representation choice. With $c = 1 + 6Q^2$, $Q = b + b^{-1}$, its level-two zeros have the form

$$h_{r,s} = \frac{Q^2 - (rb + s/b)^2}{4}, \qquad D_2 = 32h(h - h_{2,1})(h - h_{1,2}). \tag{XVII.3.20}$$

For $b = 2$ we have $c = 77/2$, $h_{2,1} = -7/2$. Direct multiplication gives

$$G_2 = \begin{pmatrix} 21/4 & -21 \\ -21 & 84 \end{pmatrix}, \qquad G_2 \begin{pmatrix} 1 \\ 1/4 \end{pmatrix} = 0, \qquad |\chi\rangle = (L_{-2} + \tfrac{1}{4}L_{-1}^2)|h\rangle. \tag{XVII.3.21}$$

For $(d_3, d_4) = (3, 5)$ its right-vertex coupling is

$$\langle\chi|V_3(1)|5\rangle = h + 6 - 5 + \frac{1}{4}(h + 3 - 5)(h + 3 - 5 + 1) = \frac{59}{16}. \tag{XVII.3.22}$$

A generic block consequently has a meromorphic pole there. Choosing $d_3 = h, d_4 = 0$ instead makes that coupling zero. Defining a quotient block still requires the left vertex to annihilate the null submodule as well, and requires a specified quotient or limiting prescription. Substituting the singular weight into G_2^{-1} does not perform that operation.

The identity module is a separate instructive case. At $h = 0$, with $d_1 = d_2$, $d_3 = d_4$, quotient by $L_{-1}|0\rangle$ while keeping $L_{-2}|0\rangle$. Its norm and two couplings give

$$\langle 0|L_2 L_{-2}|0\rangle = c/2, \qquad B_1^{\mathrm{vac}} = 0, \qquad B_2^{\mathrm{vac}} = \frac{d_2 d_3}{c/2} = \frac{2d_2 d_3}{c}, \quad c \neq 0. \tag{XVII.3.23}$$

The stress tensor propagates even though the level-one vacuum descendant vanishes. This distinction will matter whenever a degeneration selects the identity channel.

XVII.3.2 The dimensionful parameter dictionary

Which conformal weights should be used for the gauge theory of Chapter 2? The correspondence assigns the Coulomb parameter to the internal momentum and the

four masses to puncture momenta. Conformal momenta are dimensionless, whereas localization parameters have mass dimension one. Restoring that difference first prevents an implicit choice of units from changing the answer.

Let a, ϵ_1, ϵ_2 and μ_f have mass dimension one. Keep the centered equivariant mass convention of XVII.2,

$$p = \epsilon_1\epsilon_2 \neq 0, \qquad E = \epsilon_1 + \epsilon_2, \qquad s_0^2 = p, \qquad \mu_f = m_f + E/2. \tag{XVII.3.24}$$

Here m_f are signed centered physical masses in that localization convention. These are not an identification with geometric residues used in another normalization. Choose a square root s_0 and set

$$\begin{gathered} b = \epsilon_1/s_0, \quad b^{-1} = \epsilon_2/s_0, \quad Q = E/s_0, \\ a_c = a/s_0, \quad \alpha = Q/2 + a_c, \\ \Delta(\beta) = \beta(Q-\beta), \quad c = 1 + 6Q^2. \end{gathered} \tag{XVII.3.25}$$

The product of the two quantities denoted b and b^{-1} is one because $s_0^2 = p$. The internal weight is therefore

$$h = \Delta(\alpha) = \frac{E^2/4 - a^2}{p}. \tag{XVII.3.26}$$

For the two pairs of external masses introduce the dimensionless variables

$$t_0 = \frac{\mu_1 - \mu_2}{2s_0}, \quad M_0 = \frac{\mu_1 + \mu_2}{2s_0}, \qquad t_1 = \frac{\mu_3 - \mu_4}{2s_0}, \quad M_1 = \frac{\mu_3 + \mu_4}{2s_0}. \tag{XVII.3.27}$$

The puncture assignment is ordered, as shown in Figure XVII.3.2,

$$\begin{gathered} (\beta_1, \beta_2, \beta_3, \beta_4) = (\alpha_0, M_0, M_1, \alpha_1), \\ \alpha_0 = Q/2 + t_0, \quad \alpha_1 = Q/2 + t_1, \\ (z_1, z_2, z_3, z_4) = (\infty, 1, q, 0). \end{gathered} \tag{XVII.3.28}$$

Consequently $d_i = \Delta(\beta_i)$ can be evaluated with rational operations alone,

$$d_1 = \frac{E^2 - (\mu_1 - \mu_2)^2}{4p}, \tag{XVII.3.29}$$

$$d_2 = \frac{(\mu_1 + \mu_2)(2E - \mu_1 - \mu_2)}{4p}, \tag{XVII.3.30}$$

$$d_3 = \frac{(\mu_3 + \mu_4)(2E - \mu_3 - \mu_4)}{4p}, \tag{XVII.3.31}$$

$$d_4 = \frac{E^2 - (\mu_3 - \mu_4)^2}{4p}. \tag{XVII.3.32}$$

All these weights are invariant under a common nonzero rescaling of every dimensionful parameter. Reversing the square root changes the signs of Q, all momenta and b, leaving the weights unchanged. The elementary reflections are

$$a \mapsto -a \implies \alpha \mapsto Q - \alpha, \qquad \mu_1 \leftrightarrow \mu_2 \implies \alpha_0 \mapsto Q - \alpha_0. \tag{XVII.3.33}$$

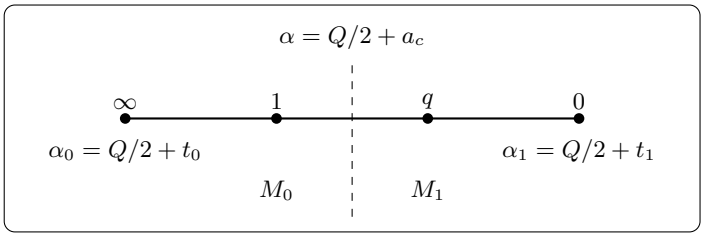


Figure XVII.3.2: The ordered puncture dictionary for the channel joining q and 0. Mass sums determine M_0, M_1 while differences determine t_0, t_1. The internal momentum depends on a_c. Exchanging two marked positions changes the channel assignment as well as the ordering of external weights.

Both preserve the indicated weights. A general exchange of external weights at fixed q instead changes the ordered four-point block.

The instanton sum in XVII.2 uses two antifundamental masses μ_1, μ_2 and two fundamental masses μ_3, μ_4. This orientation fixes the abelian factor. Define dimensionful mass sums $\mathfrak{m}_0 = (\mu_1 + \mu_2)/2$, $\mathfrak{m}_1 = (\mu_3 + \mu_4)/2$ and set

$$\eta = \frac{2\mathfrak{m}_0(E - \mathfrak{m}_1)}{p} = 2M_0(Q - M_1), \qquad Z_{\mathrm{inst}}^{U(2)} = (1-q)^{\eta} Z_{\mathrm{red}}. \tag{XVII.3.34}$$

This factor is a normalization of the selected chiral quantity. It does not assert the existence of an additional dynamical neutral hypermultiplet. The source scheme identifies

$$q = q_{\mathrm{inst}} = e^{2\pi i \tau_{\mathrm{UV}}} \tag{XVII.3.35}$$

with the sewing cross ratio. This is a specified ultraviolet coordinate dictionary. It does not identify q with an infrared elliptic nome or determine an absolute Seiberg–Witten period normalization.

For a concrete example take $a = 7/3$, $(\epsilon_1, \epsilon_2) = (2, 3)$ and

$$(m_1, m_2, m_3, m_4) = (1/3, 2/5, -4/7, 3/2), \qquad (\mu_1, \mu_2, \mu_3, \mu_4) = (17/6, 29/10, 27/14, 4). \tag{XVII.3.36}$$

Since $p = 6$ and $E = 5$, direct substitution gives

$$c = 26, \quad h = \frac{29}{216}, \qquad (d_1, d_2, d_3, d_4) = \left(\frac{703}{675}, \frac{688}{675}, \frac{1577}{1568}, \frac{1353}{1568}\right), \qquad \eta = \frac{817}{420}. \tag{XVII.3.37}$$

For instance, $\mu_1 - \mu_2 = -1/15$ gives $d_1 = (25 - 1/225)/24 = 703/675$. Multiplying all dimensionful parameters by $7/3$ reproduces every number in (XVII.3.37). The scaling test uses the restored p explicitly.

XVII.3.3 Two independent expansions

Do the conformal descendants reproduce the instanton coefficients after the stated normalization? We now keep the two computations separate until their final coefficients. The conformal route uses (XVII.3.19). The gauge route uses the fixed-point products of XVII.2, recalled here with their orientation intact.

For a box $s = (i, j)$ of a partition Y, define its arm and leg by $A_Y(s) = Y_i - j$, $L_Y(s) = Y_j^{\mathsf{T}} - i$. A leg relative to another partition can be negative. For Coulomb parameters $(a_1, a_2) = (a, -a)$ the tangent weights are

$$E_{uv}(s) = a_u - a_v - \epsilon_1 L_{Y_v}(s) + \epsilon_2(A_{Y_u}(s) + 1), \qquad \phi_u(s) = a_u + (i-1)\epsilon_1 + (j-1)\epsilon_2. \tag{XVII.3.38}$$

With the matter polynomial

$$P(\phi) = (\phi + \mu_1)(\phi + \mu_2)(\phi - \mu_3 + E)(\phi - \mu_4 + E), \tag{XVII.3.39}$$

the contribution of a pair of partitions is

$$Z_{\boldsymbol{Y}} = \frac{\displaystyle\prod_{u=1}^{2} \prod_{s \in Y_u} P(\phi_u(s))}{\displaystyle\prod_{u,v=1}^{2} \prod_{s \in Y_u} E_{uv}(s)(E - E_{uv}(s))}, \qquad Z_k = \sum_{|Y_1|+|Y_2|=k} Z_{\boldsymbol{Y}}. \tag{XVII.3.40}$$

The two one-box and five two-box configurations, seven in total, are

$$([1], \varnothing), (\varnothing, [1]); \qquad ([2], \varnothing), ([1,1], \varnothing), (\varnothing, [2]), (\varnothing, [1,1]), ([1], [1]). \tag{XVII.3.41}$$

For one box of color u, the empty other partition has leg -1. Thus $E_{uv} = a_u - a_v + E$ for $v \neq u$, and its partner is $-(a_u - a_v)$. The result is

$$Z_1 = -\frac{P(a)}{p\, 2a(2a + E)} - \frac{P(-a)}{p\, 2a(2a - E)}. \tag{XVII.3.42}$$

Both terms are needed for Coulomb Weyl invariance.

As a second-order example, put both boxes into the row $Y_1 = [2]$. Their contents are $a, a + \epsilon_2$, their self-color tangent product is $2p\epsilon_2(\epsilon_1 - \epsilon_2)$, and their other-color product is $2a(2a + \epsilon_2)(2a + E)(2a + E + \epsilon_2)$. Hence

$$Z_{([2],\varnothing)} = \frac{P(a)P(a + \epsilon_2)}{2p\epsilon_2(\epsilon_1 - \epsilon_2)\, 2a(2a + \epsilon_2)(2a + E)(2a + E + \epsilon_2)}. \tag{XVII.3.43}$$

Transposing the row exchanges ϵ_1, ϵ_2 in this expression; changing its color sends $a \mapsto -a$. The mixed-color configuration has the denominator

$$Z_{([1],[1])} = \frac{P(a)P(-a)}{p^2(\epsilon_1^2 - 4a^2)(\epsilon_2^2 - 4a^2)}. \tag{XVII.3.44}$$

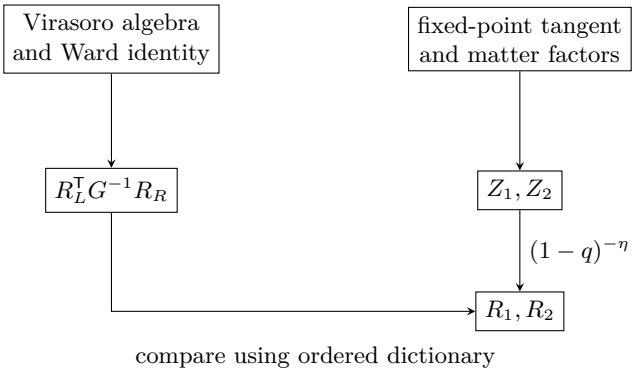


Figure XVII.3.3: The two coefficient calculations. The conformal route uses Virasoro norms and three-point Ward identities. The gauge route sums all colored fixed points and then divides by the abelian factor. Agreement is a comparison of the resulting coefficients, after applying the ordered parameter dictionary.

These operations give all five summands. The level-two conformal states and the five fixed points are not identified one by one. It is their full weighted sums that the correspondence compares.

Expand the inverse abelian factor using its binomial series,

$$(1-q)^{-\eta} = 1 + \eta q + \tfrac{1}{2}\eta(\eta+1)q^2 + O(q^3). \tag{XVII.3.45}$$

Multiplication by $Z_{\text{inst}}^{U(2)} = 1 + Z_1 q + Z_2 q^2 + \cdots$ gives

$$R_1 = Z_1 + \eta, \qquad R_2 = Z_2 + \eta Z_1 + \tfrac{1}{2}\eta(\eta+1), \qquad Z_{\text{red}} = 1 + R_1 q + R_2 q^2 + \cdots . \tag{XVII.3.46}$$

The plus sign in R_1 follows from dividing by $(1-q)^{\eta}$. Reversing that division changes the result already at first order. The first-order equality can be reduced to a single rational identity. Substituting (XVII.3.32) yields

$$A = \frac{E^2/4 - a^2 + (\mu_1+\mu_2)E/2 - \mu_1\mu_2 - E^2/4}{p} \tag{XVII.3.47}$$

$$= \frac{-a^2 + E(\mu_1+\mu_2)/2 - \mu_1\mu_2}{p}, \tag{XVII.3.48}$$

$$B = \frac{-a^2 + E(\mu_3+\mu_4)/2 - \mu_3\mu_4}{p}. \tag{XVII.3.49}$$

For A, the cancellation uses $d_2 - d_1 = [E(\mu_1+\mu_2)/2 - \mu_1\mu_2 - E^2/4]/p$; the right pair works identically. Combining the two fractions in (XVII.3.42) and adding η gives

$$Z_1 + \eta = \frac{[-a^2 + E(\mu_1+\mu_2)/2 - \mu_1\mu_2][-a^2 + E(\mu_3+\mu_4)/2 - \mu_3\mu_4]}{2p(E^2/4 - a^2)} = \frac{AB}{2h}. \tag{XVII.3.50}$$

This equality holds as a rational identity away from its singular denominators. The comparison at second order below evaluates the independently obtained rational expressions at two generic points.

At the input (XVII.3.36), the conformal computation uses

$$A = \frac{29}{216} - \frac{1}{45}, \qquad B = \frac{29}{216} + \frac{1}{7}, \qquad U = h + 2d_2 - d_1, \qquad V = h + 2d_3 - d_4. \tag{XVII.3.51}$$

The $1/7$ follows from $(1577 - 1353)/1568$. Inserting these values into (XVII.3.19), and independently summing (XVII.3.40), gives the first row of the comparison table. For a changed input take

$$a = 11/4, \quad (\epsilon_1, \epsilon_2) = (3/2, -2/3), \qquad (\mu_1, \mu_2, \mu_3, \mu_4) = (29/12, -31/12, 73/60, 47/84). \tag{XVII.3.52}$$

Here $p = -1$, $c = -19/6$, $h = 133/18$, $\eta = -23/2520$, and

$$(d_1, d_2, d_3, d_4) = (875/144, 11/144, 8579/176400, -11581/176400). \tag{XVII.3.53}$$

These are meromorphic algebraic examples. In particular the second is not a test on the unitary Liouville integration contour.

Input	k	Z_k	$R_k = B_k$
First	1	$-114607/62640$	$50699/438480$
First	2	$95920869631/116021808000$	$15350739781/116021808000$
Second	1	$26601/37240$	$23635/33516$
Second	2	$526266553/980156800$	$20875493677/39696350400$

The respective level-two determinants are

$$D_2^{(1)} = \frac{674975}{78732}, \qquad D_2^{(2)} = \frac{8076292}{729}. \tag{XVII.3.54}$$

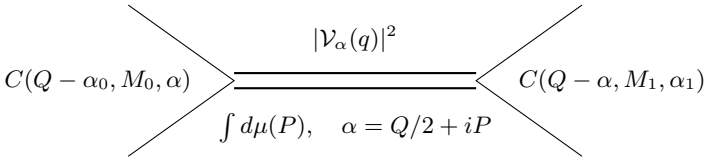
Both have $h \neq 0$ and $D_2 \neq 0$, so the inverse-Gram computation is legitimate. The numerical differences between Z_k and B_k expose the normalization rather than an error in sewing. The generic first-order identity and these two second-order matches test the AGT dictionary. Finite coefficients do not establish its all-order physical assertion.

XVII.3.4 From a block to a correlator

How does the block comparison with XVII.2 enter a physical four-point function? A chiral block propagates one specified representation. A Liouville correlator sews left and right movers, includes the three-point structure constants, and integrates the continuous internal spectrum. We use the direct unitary regime $b > 0$ and external principal-series momenta. Its internal contour is

$$\alpha = Q/2 + iP, \quad P \in \mathbb{R}, \qquad h = Q^2/4 + P^2, \qquad a_c = iP. \tag{XVII.3.55}$$

Reflection identifies P and $-P$. One may integrate over $P \geq 0$ and absorb the associated constant into the normalization. Analytic continuation of external momenta can move poles across the contour and require deformations and discrete residues.



internal numerator $\longrightarrow$ $4P^2$ on the contour

Figure XVII.3.4: Full sewing integrates the intermediate principal-series momentum. Each vertex carries a DOZZ constant, and the tube carries both the holomorphic block and its antiholomorphic partner. Reflection pairs the two internal momentum labels. The measure arises together with the internal factors of the constants.

In the reflected-bra convention, the sewn correlator has the form

$$G_s(q,\bar{q}) = \int_{Q/2+i\mathbb{R}} \frac{d\alpha}{2\pi}\, C(Q-\alpha_0, M_0, \alpha) C(Q-\alpha, M_1, \alpha_1) \left| q^{h-d_3-d_4} \mathcal{F}_h(q) \right|^2 . \tag{XVII.3.56}$$

For a principal-series external momentum, $Q-\alpha_0$ is the conjugate momentum. Contour orientation and an overall reflection normalization are part of the analytic convention. Equation (XVII.3.56) imports the Liouville spectrum and three-point constants. It is not obtained by summing the two coefficients just computed. The finite arguments of those constants explain the matter dictionary. Write

$$\Upsilon(x) = \frac{1}{\Gamma_2(x|b,b^{-1})\Gamma_2(Q-x|b,b^{-1})}, \qquad \Upsilon(Q-x) = \Upsilon(x). \tag{XVII.3.57}$$

Up to a conventional cosmological prefactor, the DOZZ expression for a triple (x,y,z) is

$$C(x,y,z) = \Lambda_b^{(Q-x-y-z)/b} \frac{\Upsilon'(0)\Upsilon(2x)\Upsilon(2y)\Upsilon(2z)}{\Upsilon(x+y+z-Q)\Upsilon(x+y-z)\Upsilon(x-y+z)\Upsilon(-x+y+z)}. \tag{XVII.3.58}$$

Here Λ_b is the conventional Liouville cosmological normalization. The definition and regularization of the double Gamma function and this three-point formula are analytic source inputs. We can nevertheless derive their finite argument matching explicitly.

For the left triple $(Q-\alpha_0, M_0, \alpha)$ the four denominator arguments are

$$(M_0 + a_c - t_0,\ M_0 - a_c - t_0,\ Q + a_c - M_0 - t_0,\ M_0 + a_c + t_0). \tag{XVII.3.59}$$

Reflect the third argument using $\Upsilon(x) = \Upsilon(Q-x)$. The multiset becomes $\{M_0 \pm t_0 \pm a_c\}$. The right triple similarly gives

$$(M_1 - a_c + t_1,\ M_1 - a_c - t_1,\ Q - a_c - M_1 + t_1,\ M_1 + a_c + t_1) \ \longrightarrow\ \{M_1 \pm t_1 \pm a_c\}. \tag{XVII.3.60}$$

The signs in each multiset are independent. Since $M_0 \pm t_0 = \mu_{1,2}/s_0$ and $M_1 \pm t_1 = \mu_{3,4}/s_0$, these are the eight mass and Coulomb combinations required by the chosen

matter orientation, after the reflected arguments are expressed in double Gamma functions. For example $M_0 = 3, t_0 = 1, a_c = 1/2$ gives the four arguments $9/2, 7/2, 5/2, 3/2$. Their order is immaterial inside a product. Establishing the equality of the regularized infinite products with the localization determinant also uses the sourced conjugation and regularization prescriptions.

The internal numerator supplies the vector measure. Denote $\Gamma_2(x|b, b^{-1})$ by $g(x)$. Its sourced shift relation is

$$g(x+b)g(x+b^{-1}) = xg(x)g(x+Q). \tag{XVII.3.61}$$

Put $x = 2a_c$ and use $2\alpha = Q + x$. Reflection and (XVII.3.57) give

$$\Upsilon(2\alpha)\Upsilon(2Q-2\alpha) = \frac{1}{g(Q+x)g(-x)g(Q-x)g(x)}. \tag{XVII.3.62}$$

Apply the shift relation at x and $-x$. Their polynomial factors multiply to $x(-x) = -x^2$, giving

$$\Upsilon(2\alpha)\Upsilon(2Q-2\alpha) = \frac{-4a_c^2}{\prod_{\sigma=\pm 1}\prod_{j=1}^{2}\Gamma_2(2\sigma a_c + \epsilon_j/s_0|b, b^{-1})}. \tag{XVII.3.63}$$

This derivation is conditional on the analytic shift relation. Multiplying x and $-x$ verifies the finite measure factor, rather than deriving the infinite products from a polynomial. On the principal contour $-4a_c^2 = 4P^2$. Restoring dimensionful variables supplies a constant scale through $a_c^2 da_c = a^2 da/s_0^3$, together with contour orientation. It does not prescribe a positive real $a^2 da$ on every complex contour.

Finally the classical factor and the block's leading power differ. In this convention

$$Z_{\rm cl} = q^{-a^2/p}, \qquad q^{h-d_3-d_4} = q^{\kappa} Z_{\rm cl}, \qquad \kappa = Q^2/4 - d_3 - d_4. \tag{XVII.3.64}$$

For example at the first rational input the exponent is $25/24 - 1577/1568 - 1353/1568$, independent of a. That independence allows it to leave the Coulomb integral, but does not make it independent of q. In the source rewriting the structure is

$$G_s = \mathcal{N}(b, \beta_i)\, |q^{\kappa}|^2 \int_{\mathcal{C}_a} a^2 da\, |Z_{\rm cl} Z_{\rm 1loop} Z_{\rm red}|^2. \tag{XVII.3.65}$$

The constant scale and orientation are included in $\mathcal{N}$ and $\mathcal{C}_a$. External leg normalizations retain the displayed q-dependent prefactor. Replacing $Z_{\rm red}$ by the raw $U(2)$ sum would also change the observable. The round-S^4 interpretation is source-supported at $b = 1$. This argument supplies neither an arbitrary-b ellipsoid derivation nor an evaluation of the full integral.

XVII.3.5 Crossing and duality

A different pants decomposition gives a different weakly coupled gauge description. On the conformal side it gives a different channel expansion of the same full correlator. To

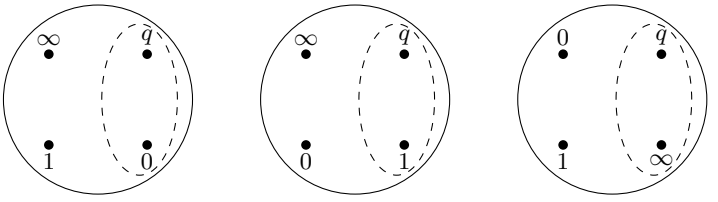


Figure XVII.3.5: Three degenerations of the marked four-punctured sphere. A circle encloses the colliding pair in each panel. The corresponding local coordinates are q, $1-q$, and $1/q$. Channel changes transport external labels and change the internal representation being integrated.

distinguish channel coordinates from the much stronger crossing assertion, begin with the marked cross ratio

$$r(z_1,z_2,z_3,z_4)=\frac{(z_1-z_2)(z_3-z_4)}{(z_1-z_3)(z_2-z_4)},\qquad r(\infty,1,q,0)=q. \tag{XVII.3.66}$$

For a Möbius map $f(z)=(Az+B)/(Cz+D)$, each difference is

$$f(z_i)-f(z_j)=\frac{(AD-BC)(z_i-z_j)}{(Cz_i+D)(Cz_j+D)},\qquad r(f(z_1),\dots,f(z_4))=r(z_1,\dots,z_4). \tag{XVII.3.67}$$

The denominator factors and determinant cancel between numerator and denominator. Relabeling marked punctures is a different operation. Direct substitution gives

$$r(z_1,z_3,z_2,z_4)=1/r,\qquad r(z_1,z_4,z_3,z_2)=1-r. \tag{XVII.3.68}$$

The three degeneration coordinates can thus be chosen as

$$s=q\to 0,\qquad t=1-q\to 0,\qquad u=1/q\to 0. \tag{XVII.3.69}$$

These describe collisions of $(q,0)$, $(q,1)$, and (q,∞) respectively. The topological pants move of XVI.3 has acquired an analytic local coordinate in each channel. For the t chart use $w=1-z$ and then order the punctures again as $(\infty,1,t,0)$. Their old labels are $(1,4,3,2)$, so

$$\begin{aligned}(d_1',d_2',d_3',d_4')&=(d_1,d_4,d_3,d_2),\\ \mathcal{V}^{(s)}_{h_s}&=q^{h_s-d_3-d_4}(1+O(q)),\\ \mathcal{V}^{(t)}_{h_t}&=t^{h_t-d_2-d_3}(1+O(t)).\end{aligned} \tag{XVII.3.70}$$

The changed leading exponent comes from fusing a different pair. Even if the same numerical internal weight were inserted, the two local series would describe different expansions. At the concrete configuration $(z_1,z_2,z_3,z_4)=(4,3,2,0)$ one finds $r=1/3$; exchanging labels $2,3$ gives 3 and exchanging $2,4$ gives $2/3$. This example checks the marked-coordinate algebra without using dynamics.

The sourced fusion transformation concerns full chiral blocks with their normalization and continuation conventions,

$$\mathcal{V}^{(s)}_{\alpha_s}(q) = \int_{\mathbb{S}} d\mu(\alpha_t)\, F_{\alpha_s\alpha_t}[\beta_i]\, \mathcal{V}^{(t)}_{\alpha_t}(1-q). \tag{XVII.3.71}$$

Here $\mathbb{S} = Q/2 + i\mathbb{R}_{\geq 0}$, F is the fusion kernel, and $d\mu$ includes the chosen reflection normalization. A single intermediate representation in one channel generally expands into a continuum in the other. This is why a fixed-momentum equality between two truncated series would not express crossing.

The role of the DOZZ factors can be seen by substituting (XVII.3.71) into the full sewing integral. Let W_s denote the product of three-point constants in the s channel, and use an analogous W_t for the transported labels. Schematically the resulting double integral over t momenta contains

$$K(\alpha_t, \alpha'_t) = \int_{\mathbb{S}} d\mu(\alpha_s)\, W_s(\alpha_s) F_{\alpha_s\alpha_t} \overline{F_{\alpha_s\alpha'_t}}. \tag{XVII.3.72}$$

In the source normalization the DOZZ-weighted orthogonality relation has the distributional form

$$K(\alpha_t, \alpha'_t) = W_t(\alpha_t)\, \delta_\mu(\alpha_t, \alpha'_t), \qquad \int d\mu(\alpha'_t) \delta_\mu(\alpha_t, \alpha'_t) f(\alpha'_t) = f(\alpha_t). \tag{XVII.3.73}$$

Using this relation removes one integration and yields the t-channel sewing. This step is analytic Liouville input, including its spectrum, kernel and normalization. The finite cross-ratio manipulations establish the coordinate and label changes; they do not establish this orthogonality relation. We use the direct $b > 0$ principal-series setting. Continuation outside it can change the contour and add residues rather than preserving the same displayed integral unchanged.

With the corresponding kinematic factors attached, crossing identifies the two full correlator expressions,

$$G_s(q, \bar{q}; \beta_1, \beta_2, \beta_3, \beta_4) = G_t(1-q, 1-\bar{q}; \beta_1, \beta_4, \beta_3, \beta_2). \tag{XVII.3.74}$$

Through the sourced AGT correspondence this is the protected-observable expression of the change between gauge descriptions. Both the DOZZ measure and the external q factors of Section XVII.3.4 belong to that assertion. The low-order agreement of Section XVII.3.3 gives explicit local evidence for the block dictionary. An all-order identification, a construction of the fusion kernel and the global form of the line-operator theory require additional input.

Exercises

Each exercise has a finite calculation and a written explanation. For benchmark submissions, see `benchmark/PROTOCOL.md`. Algebraically equivalent expressions are accepted. The written arguments require separate assessment.

1. At $h = 2, c = 3$, calculate G_1, G_2, G_2^{-1}, and the two block coefficients for $(d_1, d_2, d_3, d_4) = (1, 2, 3, 4)$. Derive the central term and the off-diagonal entry from commutators. Explain why the inverse Gram matrix is required even without a positive inner product.

2. At $b = 2$, find the null vector at $h = -7/2$ normalized to have L_{-2} coefficient one. Evaluate its right coupling for $(d_3, d_4) = (3, 5)$ and $(h, 0)$. For the identity quotient with $c = 26, d_2 = 2/3, d_3 = 4/5$, compute B_1, B_2. Explain the two-vertex compatibility condition and why the vacuum still propagates a stress tensor.

3. Use $a = 2$, $(\epsilon_1, \epsilon_2) = (1, 2)$ and $(\mu_1, \mu_2, \mu_3, \mu_4) = (1/3, 4/5, 7/6, -2/3)$. Find c, h, d_i, η and the centered physical masses. Repeat after a common factor of three rescaling. Explain the square-root choice, the fixed puncture order and the ultraviolet meaning of q.

4. Reproduce both rows of second-order comparisons using the weights and raw Z_1, Z_2 displayed in Section XVII.3.3. Submit both sewn pairs and reduced pairs. Quantify why omitting the Gram off-diagonal or multiplying by the abelian factor gives a different answer. State the exact scope of a two-coefficient match.

5. Derive the two reflected DOZZ argument multisets as polynomials in M_0, M_1, t_0, t_1 and a_c. Submit their polynomial product, the internal measure polynomial, its value at $a_c = iP$, and the classical offset. Explain which analytic premises enter the shift argument, which contour is used, and why the external q power survives.

6. Derive the two cross-ratio permutations, the external labels under $z \mapsto 1 - z$, and the two leading block exponents. Submit their symbolic forms. Explain how inserting a fusion integral into the correlator requires the orthogonality relation weighted by the DOZZ constants, and why marked-coordinate algebra alone does not prove crossing.

Take-home result and exit checklist

The inverse Gram matrix converts descendant couplings into a correctly sewn block. In the ordered mass dictionary that block agrees with the reduced instanton expansion at generic first order and at the two explicit second-order inputs. A full correlator also requires the DOZZ constants, a continuous internal spectrum and the retained external q factor. Its crossing relation therefore has analytic content beyond matching a finite series.

A reader should now be able to reconstruct the mixed trinion through level two, diagnose a null-state obstruction before inversion, convert dimensionful masses into puncture weights, strip the abelian factor in the correct direction, and explain which extra ingredients turn a block comparison into a statement about a duality-invariant observable.

Sources and scope

§1. [**MATH**] The Gram matrices, mixed trinion reconstruction, inverse-Gram contraction, level-two determinant, non-vacuum null overlap and identity quotient are derived in this section. The source conventions are arXiv:0906.3219v2, printed pp. 20–21, (A.1)–(A.5), and p. 15, (5.2), together with arXiv:hep-th/0104158v3, p. 60, §17.1, (209)–(211). The finite reconstruction includes all sixteen mixed entries through level two on both legs. Singular representation quotients require the conditions stated locally. Sources are Alday et al. 2009; Teschner 2001.

§2. [**CONJ+**] The physical AGT parameter and ultraviolet-coordinate dictionary is taken from arXiv:0906.3219v2, pp. 8–9, (3.5)–(3.13), with its scheme in (B.1). [**MATH**] Restoration of $\sqrt{\epsilon_1\epsilon_2}$, the weight formulas, scaling and reflection tests are finite algebra in that dictionary. The centered mass convention is the one used in XVII.2, following the same source's Appendix B. No absolute-period or global-line normalization follows. Sources are Alday et al. 2009.

§3. [**MATH**] The generic first-order rational equality and two nonsingular second-order comparisons use independently sewn Virasoro coefficients and the actual fixed-point sum of XVII.2. The source fixed-point products and orientations are arXiv:0906.3219v2, pp. 24–27, (B.3)–(B.11), (B.14), (B.16), (B.21)–(B.28). The physical all-order identification remains [**CONJ+**] at the inspected source strength. The examples are meromorphic evaluations, not principal-contour correlator tests. Sources are Alday et al. 2009.

§4. [**MATH**] The eight denominator arguments, conditional shift reduction of the measure polynomial, and classical exponent offset are derived here. [**GEO-E**] The analytic DOZZ formula, double-Gamma shift, contour spectrum and regularized one-loop interpretation are source premises, arXiv:0906.3219v2, pp. 12–13, (4.1)–(4.7), p. 15, (4.12)–(4.14), and pp. 22–23, (A.14), (A.16)–(A.20). The source supports the round-S^4 interpretation at $b = 1$. The complete integral and infinite products have not been evaluated in this chapter. Sources are Alday et al. 2009.

§5. [**MATH**] Cross-ratio transformations, transported labels and leading powers follow by finite algebra. [**MATH**] Fusion and DOZZ-weighted crossing are imported in the stated regime from arXiv:hep-th/0104158v3, p. 64, §18.3, (231)–(232), and pp. 69–70, §19.6, (249)–(252). Remark 10 treats continuation and §19.7 discusses limitations of the strong-coupling argument. The protected S-duality interpretation uses [**CONJ+**] AGT input. No unrestricted continuation theorem or fixed-momentum block equality is inferred. Sources are Teschner 2001; Alday et al. 2009.

References

Alday, L. F., D. Gaiotto, and Y. Tachikawa (2009). “Liouville Correlation Functions from Four-dimensional Gauge Theories”. In: Version 2, 9 February 2010; inspected version. arXiv: 0906.3219 [hep-th].

Teschner, J. (2001). “Liouville theory revisited”. In: Version 3, 9 November 2001; inspected version. arXiv: hep-th/0104158.

Chapter XVII.4

Higher rank, defects and quantum Hitchin equations

A differential equation for a defect observable is only part of a spectral problem. The equation specifies local propagation. A spectrum also requires a domain, an endpoint or monodromy condition, and a parameter that the condition can select. This distinction matters when conformal blocks are used to describe quantum Hitchin systems. A null state can produce a differential equation without selecting any of its solutions as physical states.

We develop this distinction through two calculations. A restricted A_2 Toda block shows how an extra conserved current changes the Ward identities, and why a special external insertion is needed to close them. A rank-one block then supplies an exactly soluble differential equation. We retain its coordinate powers, compute its connection matrix, and finally impose a precise analytic endpoint condition. The discrete values selected by that last condition belong to the stated mathematical boundary problem.

The prerequisites are the Virasoro states and sewing of Chapter 3, the equivariant parameters of Chapter 2, and the geometric quadratic differential of XVI.4. The higher-rank AGT proposal and the identification of a degenerate insertion with a surface defect enter as physical source premises. In the Nekrasov–Shatashvili limit we will also require a differentiable factorization of a selected block. The algebra derived from that assumption determines the quantum operator, while its accessory function and a gauge-theory Hilbert-space domain remain additional inputs.

XVII.4.1 From Virasoro to the spin-three current

What changes when the marked sphere describes a higher-rank theory? The Virasoro stress tensor measures a quadratic invariant of momentum. For W_3 symmetry, the independent cubic invariant requires a spin-three current. A pair of bosons makes both invariants visible before we attempt to sew any states.

Use the traceless plane in $\mathbb{R}^3$, with Euclidean pairing and roots of squared length

two. Write

$$\alpha_1^{\rm root} = e_1 - e_2, \quad \alpha_2^{\rm root} = e_2 - e_3, \quad h_j = e_j - \tfrac{1}{3}(e_1+e_2+e_3), \\ \omega_1 = h_1, \quad \omega_2 = -h_3, \quad \rho = (1,0,-1). \tag{XVII.4.1}$$

The three h_j are weights of the defining representation, rather than three independent coordinates. In particular

$$\sum_j h_j = 0, \qquad (h_i,h_j) = \delta_{ij} - \tfrac{1}{3}, \qquad (\rho,\rho) = 2, \qquad (\omega_i, \alpha_j^{\rm root}) = \delta_{ij}. \tag{XVII.4.2}$$

Figure XVII.4.1 depicts the plane on which the momentum lives. Weyl transformations permute its three components.

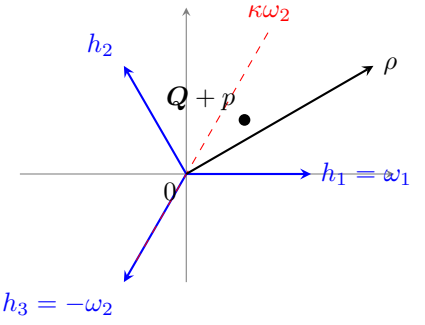


Figure XVII.4.1: The traceless weight plane. The three defining weights sum to zero. The background direction is $\rho = \omega_1 + \omega_2$, the semi-degenerate family lies on $\kappa\omega_2$, and a generic momentum is displaced from the background by p. The axes are schematic coordinates in this plane.

For bosons with $\phi_a(z)\phi_b(w) \sim -\delta_{ab}\log(z-w)$, take the improved stress tensor and the background vector to be

$$T = -\tfrac{1}{2}{:}(\partial\phi,\partial\phi){:} + (\boldsymbol{Q},\partial^2\phi), \qquad \boldsymbol{Q} = Q\rho, \qquad Q = b + b^{-1}. \tag{XVII.4.3}$$

There are two free-boson contributions to the fourth-order pole of TT. The improvement contributes $6(\boldsymbol{Q},\boldsymbol{Q})$ to that pole, since $\partial_z^2\partial_w^2[-\log(z-w)] = 6/(z-w)^4$. Comparing its coefficient with $c/2$ gives

$$\frac{c}{2} = 1 + 6(\boldsymbol{Q},\boldsymbol{Q}), \qquad c = 2 + 24Q^2. \tag{XVII.4.4}$$

Contracting T with $V_\alpha = \exp(\alpha,\phi)$ similarly gives

$$\Delta(\alpha) = \frac{(\alpha, 2\boldsymbol{Q}-\alpha)}{2}, \qquad \alpha = \boldsymbol{Q}+p \quad\Longrightarrow\quad \Delta = \frac{\boldsymbol{Q}^2 - p^2}{2}. \tag{XVII.4.5}$$

Thus permutations of the components of p preserve the dimension. They also preserve the cubic invariant

$$I_3(p) = \prod_{j=1}^{3}(p,h_j) = p_1p_2p_3, \qquad \sum_j p_j = 0. \tag{XVII.4.6}$$

For $b = 1/2$ and $p = (1/3, -1/5, -2/15)$, the numerical size of the background and the two invariants are

$$Q = \tfrac{5}{2}, \quad c = 152, \quad p^2 = \tfrac{38}{225}, \quad \Delta = \tfrac{5549}{900}, \quad I_3 = \tfrac{2}{225}. \tag{XVII.4.7}$$

These rational momenta provide meromorphic algebraic examples. They are not a choice of unitary Toda integration contour.

Normalize the additional current by

$$\begin{aligned} W(z) &= \sum_n W_n z^{-n-3}, \quad [L_m, W_n] = (2m-n)W_{m+n}, \\ w &= i\sqrt{\frac{48}{22+5c}}\, I_3(p), \quad W_0|\alpha\rangle = w|\alpha\rangle. \end{aligned} \tag{XVII.4.8}$$

The square root is positive real for real $b > 0$. The factor i is part of this analytic convention. In the ordered level-one basis $(L_{-1}|\alpha\rangle, W_{-1}|\alpha\rangle)$ the contravariant form is

$$G_1 = \begin{pmatrix} 2\Delta & 3w \\ 3w & \Delta\left[\dfrac{32(\Delta+1/5)}{22+5c} - \dfrac{1}{5}\right] \end{pmatrix}. \tag{XVII.4.9}$$

The first entry follows from $[L_1, L_{-1}] = 2L_0$, and the mixed entry from $[L_1, W_{-1}] = 3W_0$. The last entry uses the spin-three commutator in the chosen normalization. This is a bilinear algebraic form. An imaginary mixed entry does not diagnose failure of a positive physical inner product, since positivity was never imposed here.

A sign change of the current changes only the mixed entries,

$$W \longmapsto -W, \quad w \longmapsto -w, \qquad G_1 \longmapsto DG_1D, \quad D = \mathrm{diag}(1,-1). \tag{XVII.4.10}$$

In particular its determinant and both diagonal entries are invariant. This accounts for the sign translation from the defining weights used in the source normalization.

Now choose $\alpha = \kappa\omega_2$. Direct substitution into the determinant gives

$$\det G_1 = 0, \qquad G_1 \begin{pmatrix} -3w/(2\Delta) \\ 1 \end{pmatrix} = 0, \qquad \left(W_{-1} - \frac{3w}{2\Delta} L_{-1}\right)|\kappa\omega_2\rangle = 0, \quad \Delta \neq 0. \tag{XVII.4.11}$$

This is the semi-degenerate null relation. It removes one of the two independent level-one descendants. For $b = 1/2$, $\kappa = 7/5$ the actual entries are

$$\begin{aligned} \Delta_\kappa &= \frac{427}{150}, \quad w_\kappa = -\frac{20069\sqrt{2346}\, i}{2639250}, \\ G_1 &= \begin{pmatrix} 427/75 & -20069\sqrt{2346}\, i/879750 \\ -20069\sqrt{2346}\, i/879750 & -943243/4398750 \end{pmatrix}. \end{aligned} \tag{XVII.4.12}$$

The same operation at the generic momentum used above gives instead

$$\det G_1(\boldsymbol{Q} + p) = \frac{163842599921}{35629875000} \neq 0. \tag{XVII.4.13}$$

It would therefore be incorrect to impose the semi-null relation on a generic vertex.

The relation has a concrete use in a three-point amplitude. Normalize the primary amplitude at $z = 1$ and use scale covariance,

$$\langle\alpha_L|V_\kappa(z)|\alpha_R\rangle = z^{\Delta_L-\Delta_\kappa-\Delta_R}, \qquad \langle\alpha_L|(L_{-1}V_\kappa)(z)|\alpha_R\rangle = \partial_z z^{\Delta_L-\Delta_\kappa-\Delta_R}. \tag{XVII.4.14}$$

The null state then determines the one spin-three descendant amplitude,

$$\langle\alpha_L|(W_{-1}V_\kappa)(1)|\alpha_R\rangle = \frac{3w_\kappa}{2\Delta_\kappa}(\Delta_L - \Delta_\kappa - \Delta_R). \tag{XVII.4.15}$$

For the generic momenta $\alpha_L = \boldsymbol{Q} + p_1$ and $\alpha_R = \boldsymbol{Q} + p_2$ with

$$p_1 = (1/3, -1/5, -2/15), \qquad p_2 = (-1/7, 2/9, -5/63), \tag{XVII.4.16}$$

the descendant amplitude is $26984063\sqrt{2346}\,i/2327818500$. The calculation identifies precisely the extra information supplied by a semi-degenerate insertion. Virasoro derivatives alone do not determine a generic spin-three vertex. The higher-rank AGT proposal associates suitable semi-degenerate fields with simple punctures, but this finite calculation has not yet compared an $SU(3)$ instanton coefficient.

XVII.4.2 A controlled higher-rank block

Can the spin-three Ward identities produce a scalar equation for a four-point block? A fully degenerate insertion provides three possible fusion channels. A generic choice of the other three fields still leaves extra descendant amplitudes. The semi-degenerate field of the preceding section removes the needed freedom in one particular configuration,

$$\Psi(z) = \langle V_{-b\omega_1}(z)V_{\alpha_1}(0)V_{\kappa\omega_2}(1)V_{\alpha_2}(\infty)\rangle_{\text{chiral}}. \tag{XVII.4.17}$$

The resulting third-order equation is a sourced null/Ward result for this configuration. We will derive its series and exponents, rather than infer a generic Toda equation from the number of channels.

Let $p_i = \alpha_i - \boldsymbol{Q}$ and separate the coordinate factors,

$$\Psi = z^r(1-z)^s G, \qquad r = b(\alpha_1, h_1), \quad s = b\kappa/3, \qquad \theta = z\partial_z. \tag{XVII.4.18}$$

The parameters and scalar equation in this normalization are

$$A_j = \frac{b\kappa}{3} - \frac{2b^2}{3} + b(p_1, h_1) + b(p_2, h_j), \quad j = 1, 2, 3, \tag{XVII.4.19}$$

$$B_j = 1 + b(p_1, h_1 - h_{j+1}), \quad j = 1, 2. \tag{XVII.4.20}$$

$$\left[z\prod_{j=1}^{3}(\theta + A_j) - \theta(\theta + B_1 - 1)(\theta + B_2 - 1) \right] G = 0. \tag{XVII.4.21}$$

The background term $-2b^2/3$ is essential to the fusion exponents. The chiral powers r, s are half the corresponding powers in the full correlator written as absolute-value

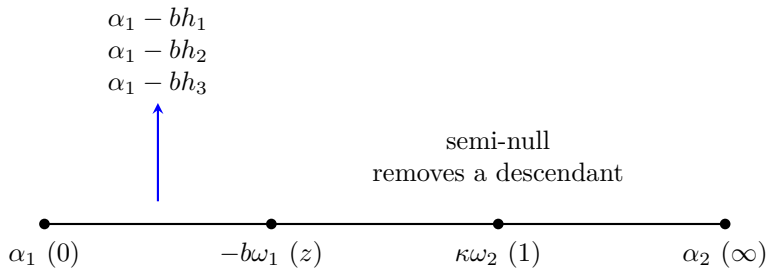


Figure XVII.4.2: The special Toda four-point block. The field at z is fully degenerate, the field at 1 is semi-degenerate, and the other two momenta are generic. The three labels on the fusion lines are the momenta permitted next to the fully degenerate insertion. Removing the semi-degenerate restriction changes the Ward problem.

factors. We are selecting a chiral solution with $G(0) = 1$, without assembling a full single-valued correlator.

To solve near zero, set $G = \sum_{n\geq 0} c_n z^n$. Since $\theta z^n = n z^n$, the two terms contribute to the same coefficient with adjacent indices,

$$\prod_{j=1}^{3}(n-1+A_j)c_{n-1} - n(n-1+B_1)(n-1+B_2)c_n = 0, \qquad n \geq 1. \tag{XVII.4.22}$$

Using the rising factorials $(a)_0 = 1$ and $(a)_n = \prod_{k=0}^{n-1}(a+k)$ gives

$$\frac{c_n}{c_{n-1}} = \frac{\prod_j (n-1+A_j)}{n(n-1+B_1)(n-1+B_2)}, \qquad c_n = \frac{(A_1)_n (A_2)_n (A_3)_n}{n!\,(B_1)_n (B_2)_n}. \tag{XVII.4.23}$$

This is ${}_3F_2(A_1, A_2, A_3; B_1, B_2; z)$. The formula specifies a local branch for $|z| < 1$. If a B_j is a nonpositive integer, the recurrence denominator vanishes and a resonant prescription is necessary. Cancellation in a specially terminating case must be analyzed before substitution.

With $b = 1/2$, $\kappa = 7/5$, and the two p_i of the previous section, the parameters are

$$(A_1, A_2, A_3) = \left(\frac{17}{105}, \frac{31}{90}, \frac{61}{315}\right), \qquad (B_1, B_2) = \left(\frac{19}{15}, \frac{37}{30}\right), \quad (r, s) = \left(\frac{17}{12}, \frac{7}{30}\right). \tag{XVII.4.24}$$

The first two steps of the recurrence retain a useful factorized form,

$$c_1 = \frac{(17/105)(31/90)(61/315)}{(19/15)(37/30)} = \frac{32147}{4650345}, \tag{XVII.4.25}$$

$$c_2 = c_1 \frac{(122/105)(121/90)(376/315)}{2(34/15)(67/30)} = \frac{2624004548}{2061056155725}. \tag{XVII.4.26}$$

For example, substituting $1 + c_1 z + c_2 z^2$ into the operator cancels the coefficients through z^2. The remaining z^3 term determines c_3 rather than invalidating the truncated calculation.

The indicial equation at zero comes from the second product in the operator. Restoring the power z^r gives three exponents,

$$\nu_j = r + \{0, 1 - B_1, 1 - B_2\}_j = \Delta(\alpha_1 - bh_j) - \Delta(\alpha_1) - \Delta(-b\omega_1). \qquad \text{(XVII.4.27)}$$

In this example they are $17/12$, $23/20$, and $71/60$. At infinity the leading first product gives $G \sim z^{-A_j}$, so the growth powers and the local exponents in $w = 1/z$ are

$$\gamma_j = r + s - A_j = \Delta(\alpha_2) - \Delta(\alpha_2 - bh_j) - \Delta(-b\omega_1), \qquad \nu_j^{(\infty)} = -\gamma_j. \quad \text{(XVII.4.28)}$$

Here $r + s = 33/20$ and hence $\gamma_j = 33/20 - A_j$. These expressions test all three channels, including the coordinate powers that a reduced series alone would conceal.

The need for the extra insertion restriction can be seen already in the Ward balance of the sourced third-order construction. The three generic contributions would have sum $9b^2$, whereas closure requires $8b^2$. The special field changes that sum,

$$3(3b^2) = 9b^2 \neq 8b^2, \qquad 2(3b^2) + 2b^2 = 8b^2. \qquad \text{(XVII.4.29)}$$

This is a diagnosis of the generic closure obstruction, not a derivation of all higher null relations from a single numerical equality. The semi-null relation identifies which independent descendant has been removed.

As a transfer calculation, keep p_1 fixed and change $b = 2/3$, $\kappa = 5/4$, $p_2 = (1/4, -1/6, -1/12)$. Repeating the same recurrence gives

$$G = 1 + \frac{2500}{874557} z + \frac{17921875}{39708326736} z^2 + \frac{5872998437500}{40705430119815591} z^3 + O(z^4). \quad \text{(XVII.4.30)}$$

Changing the momenta changes the coefficients without changing the reason the equation closes. A generic replacement of the semi-degenerate field would change the problem itself. This bounded example motivates the defect insertion below, where the rank-one equation can be derived completely and its connection problem solved exactly.

XVII.4.3 A surface defect and the BPZ equation

A surface defect preserves a two-dimensional subalgebra on a real two-dimensional submanifold of four-dimensional spacetime. In the source correspondence, a simple surface defect is represented by a degenerate Liouville insertion. Its position on the marked curve becomes a variable of the block. That identification is a physical premise. The null relation and its differential consequences can then be calculated within conformal theory.

The equivariant convention of Chapter 3 is $b^2 = \epsilon_1/\epsilon_2$. Choose the dual parameter for the insertion,

$$\beta = b^{-1}, \qquad Q = \beta + \beta^{-1}, \qquad h_d = \Delta(-\beta/2) = -\frac{1}{2} - \frac{3\beta^2}{4}, \quad \Delta(\alpha) = \alpha(Q - \alpha). \qquad \text{(XVII.4.31)}$$

In the earlier Kac convention $h_{rs} = Q^2/4 - (rb + s/b)^2/4$, this is h_{12}. The source calls the same insertion $(2, 1)$ while calling its parameter β by the name b. The state and null vector, rather than the index names, fix the equation.

Use the ordered level-two basis $(L_{-2}, L_{-1}^2)|h_d\rangle$. The matrix recalled from Chapter 3 obeys

$$G_2 = \begin{pmatrix} 4h_d + c/2 & 6h_d \\ 6h_d & 4h_d(2h_d+1) \end{pmatrix}, \quad c = 1 + 6Q^2, \qquad G_2 \begin{pmatrix} \beta^2 \\ 1 \end{pmatrix} = 0. \quad \text{(XVII.4.32)}$$

For example, its first component is $\beta^2(4h_d + c/2) + 6h_d = 0$ after inserting h_d. Its second component vanishes by the same substitution. Thus the quotient relation is

$$(L_{-1}^2 + \beta^2 L_{-2})|h_d\rangle = 0. \quad \text{(XVII.4.33)}$$

It annihilates the chosen chiral amplitude only when its three-point couplings descend to the quotient. For an external degenerate insertion the restriction is at the vertex incident to that insertion in each channel,

$$\alpha_s = \alpha_0 \pm \beta/2, \qquad \alpha_t = \alpha_1 \pm \beta/2. \quad \text{(XVII.4.34)}$$

The other generic vertex has no further degenerate fusion constraint. An internal null representation would require quotient-compatible couplings at both incident vertices. Substituting a degenerate weight in a generic inverse Gram matrix does not implement either quotient.

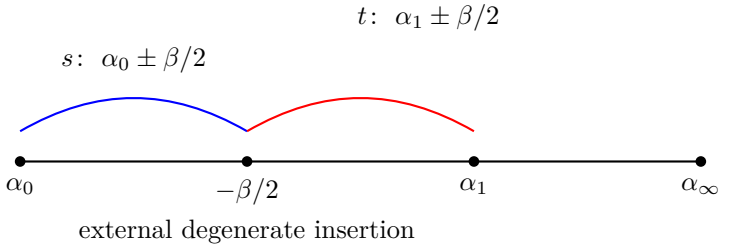


Figure XVII.4.3: The rank-one four-point block with one external degenerate field. The two channels adjacent to this field fuse with α_0 or α_1. The displayed pairs of momenta are alternative local fusion choices. A restriction is imposed at the incident vertex in the channel being used.

Let

$$F(z) = \langle V_{\alpha_\infty}(\infty) V_{\alpha_1}(1) V_{-\beta/2}(z) V_{\alpha_0}(0) \rangle. \quad \text{(XVII.4.35)}$$

The stress-tensor Ward identity replaces L_{-2} by $\sum_i [h_i/(z-z_i)^2 + \partial_{z_i}/(z-z_i)]$. To fix the positions, first eliminate derivatives of the heavy insertions using translations and dilations. Writing $K = h_0 + h_1 + h_d - h_\infty$, one obtains

$$\partial_1 F = -z\partial_z F - KF, \qquad \partial_0 F = (z-1)\partial_z F + KF. \quad \text{(XVII.4.36)}$$

It follows, retaining the constant contribution, that

$$\frac{\partial_0 F}{z} + \frac{\partial_1 F}{z-1} = \frac{1-2z}{z(z-1)} \partial_z F - \frac{K}{z(z-1)} F. \quad \text{(XVII.4.37)}$$

The reduced null equation is therefore

$$\left[\beta^{-2}\partial_z^2 + \frac{1-2z}{z(z-1)}\partial_z + \frac{h_0}{z^2} + \frac{h_1}{(z-1)^2} - \frac{h_0+h_1+h_d-h_\infty}{z(z-1)}\right] F = 0. \quad \text{(XVII.4.38)}$$

The derivative term is a consequence of fixing coordinates. It is present at finite β and cannot be dropped.

Factor the branch that fuses to $\alpha_0 - \beta/2$,

$$F = z^r(1-z)^s f, \quad r = \beta\alpha_0, \quad s = \beta\alpha_1, \qquad g = \partial_z \log[z^r(1-z)^s] = \frac{r}{z} + \frac{s}{z-1}. \quad \text{(XVII.4.39)}$$

If $P = (1-2z)/[z(z-1)]$ and V denotes the potential above, conjugation gives

$$z^{-r}(1-z)^{-s}\mathcal{D}z^r(1-z)^s = \beta^{-2}\partial_z^2 + (P + 2\beta^{-2}g)\partial_z + V + Pg + \beta^{-2}(g' + g^2). \quad \text{(XVII.4.40)}$$

The double poles cancel. Multiplication by $\beta^2 z(1-z)$ leaves

$$z(1-z)f'' + [C - (A+B+1)z]f' - ABf = 0, \quad \text{(XVII.4.41)}$$

where the full parameter map is

$$A = \beta(\alpha_0 + \alpha_1 + \alpha_\infty - Q - \beta/2), \quad \text{(XVII.4.42)}$$

$$B = \beta(\alpha_0 + \alpha_1 - \alpha_\infty - \beta/2), \qquad C = 2\beta\alpha_0 - \beta^2. \quad \text{(XVII.4.43)}$$

The two solutions and their actual coordinate powers are

$$F_1 = z^r(1-z)^s {}_2F_1(A, B; C; z), \quad \text{(XVII.4.44)}$$

$$F_2 = z^{r+1-C}(1-z)^s {}_2F_1(A-C+1, B-C+1; 2-C; z). \quad \text{(XVII.4.45)}$$

At zero their exponents are $\beta\alpha_0$ and $\beta(Q-\alpha_0)$. Direct expansion of Δ verifies

$$\Delta(\alpha_0 \mp \beta/2) - \Delta(\alpha_0) - h_d = \begin{cases} \beta\alpha_0, & - \\ \beta(Q-\alpha_0), & + . \end{cases} \quad \text{(XVII.4.46)}$$

The growth powers at infinity are $r+s-A$ and $r+s-B$. These powers will reappear in the monodromy calculation.

For the recurring example choose

$$\beta = \tfrac{1}{2}, \quad (\alpha_0, \alpha_1, \alpha_\infty) = (\tfrac{19}{12}, \tfrac{169}{420}, \tfrac{163}{140}), \quad (A, B, C) = (\tfrac{1}{5}, \tfrac{2}{7}, \tfrac{4}{3}), \quad (r, s) = (\tfrac{19}{24}, \tfrac{169}{840}). \quad \text{(XVII.4.47)}$$

All powers use real logarithms on $0 < z < 1$, followed by continuation on a slit plane. This is an analytic continuation of CFT momenta, rather than a principal-spectrum Liouville state.

The defect interpretation also distinguishes several physical objects. In the infrared source construction, a point on the spectral curve projects to z on the marked curve, while derivatives of an open-path twisted superpotential $\mathcal{W}_{\mathrm{def}}$ give Abel–Jacobi couplings,

$$t_i = \frac{\partial \mathcal{W}_{\mathrm{def}}}{\partial a_i}. \quad \text{(XVII.4.48)}$$

This does not impose a global equality $z = \exp(2\pi i t)$. A line operator is supported on a one-dimensional locus. Creation, transport and fusion of degenerate fields can define a line action on blocks in the source construction. The ordinary monodromy of the scalar equation alone is not a computed line expectation value. Next we add a bulk modulus distinct from z and ask which part of the equation survives a fixed-ϵ_1 limit.

XVII.4.4 Keeping one equivariant parameter

The four-point example has three heavy insertions and no independent bulk accessory modulus. For a four-punctured bulk sphere we must instead retain heavy fields at $0, q, 1, \infty$, together with the degenerate insertion at z. The variable q is the bulk cross ratio. The variable z specifies the insertion. Their derivatives have different physical jobs.

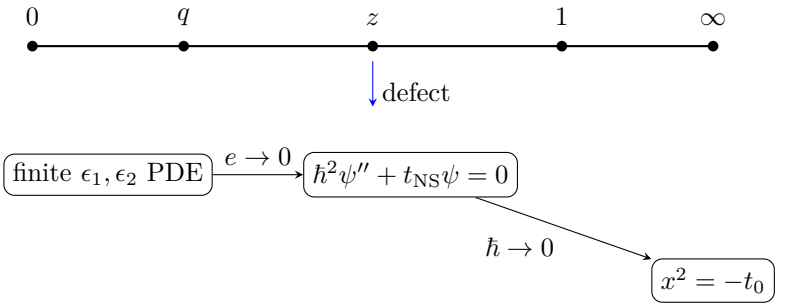


Figure XVII.4.4: The five-point block has a movable defect insertion at z and a distinct bulk modulus q. The first limit keeps $\hbar = \epsilon_1$ and produces a quantum differential equation, conditional on block factorization. The subsequent limit $\hbar \to 0$ gives an algebraic curve. Endpoint and monodromy choices are additional operations.

Let $K = h_0 + h_q + h_1 + h_d - h_\infty$. Translations and dilations now give

$$\partial_1 F = -zF_z - qF_q - KF, \qquad \partial_0 F = (z-1)F_z + (q-1)F_q + KF. \tag{XVII.4.49}$$

Combining the three heavy-field derivative terms yields the exact identity

$$\frac{\partial_0 F}{z} + \frac{\partial_q F}{z-q} + \frac{\partial_1 F}{z-1} = PF_z + A_q F_q - \frac{K}{z(z-1)}F, \tag{XVII.4.50}$$

with

$$P = \frac{1-2z}{z(z-1)}, \qquad A_q = \frac{q(q-1)}{z(z-1)(z-q)}. \tag{XVII.4.51}$$

The finite-parameter equation is a partial differential equation,

$$[\beta^{-2}\partial_z^2 + P\partial_z + A_q\partial_q + V]F = 0, \qquad V = \frac{h_0}{z^2} + \frac{h_q}{(z-q)^2} + \frac{h_1}{(z-1)^2} - \frac{K}{z(z-1)}. \tag{XVII.4.52}$$

In particular no accessory number can replace ∂_q before specifying the block and the limiting operation.

Take $\epsilon_1 = \hbar \neq 0$, $\epsilon_2 = e \to 0$, and choose one branch of $s_0^2 = \hbar e$. A mass-fixed scaling is

$$\beta^2 = \frac{e}{\hbar}, \qquad \alpha_i = \frac{Q}{2} + \frac{m_i}{s_0}, \qquad h_i = \frac{(\hbar+e)^2/4 - m_i^2}{\hbar e}. \tag{XVII.4.53}$$

The centered momenta m_i have mass dimension one. They are not yet identified with geometric residues with a fixed physical normalization or Lagrangian hypermultiplet masses. The variables z, q, α_i are dimensionless.

Assume the selected fusion-compatible block has differentiated local asymptotics

$$F(z,q) = e^{\mathcal{W}_{\mathrm{CFT}}(q)/e}[\psi(z,q) + O(e)]. \tag{XVII.4.54}$$

Here $\mathcal{W}_{\mathrm{CFT}}$ has mass dimension one. Differentiation must preserve the indicated orders locally away from punctures and turning points. Existence of such a factorization is an analytic and physical premise. The simultaneous small-parameter semiclassics of the defect source is not a proof of this fixed-$\hbar$ assumption.

The derivatives that carry the limiting equation are

$$e^{-\mathcal{W}_{\mathrm{CFT}}/e}F_{zz} = \psi_{zz} + O(e), \qquad e^{-\mathcal{W}_{\mathrm{CFT}}/e}F_q = \frac{\partial_q \mathcal{W}_{\mathrm{CFT}}}{e}\psi + \psi_q + O(1). \tag{XVII.4.55}$$

After multiplying the PDE by $\hbar e$, the kinetic term and weights have finite limits,

$$\hbar e \beta^{-2} = \hbar^2, \qquad \lim_{e\to 0} \hbar e h_i = k_i = \frac{\hbar^2}{4} - m_i^2, \qquad \lim_{e\to 0} \hbar e h_d = 0. \tag{XVII.4.56}$$

The terms $\hbar e P \psi_z$ and $\hbar e A_q \psi_q$ vanish at this order. The differentiated exponential survives in the second term and gives

$$[\hbar^2 \partial_z^2 + t_{\mathrm{NS}}(z)]\psi = 0, \qquad U = \hbar \partial_q \mathcal{W}_{\mathrm{CFT}}, \tag{XVII.4.57}$$

where

$$\begin{aligned} t_{\mathrm{NS}}(z) = {} & \frac{k_0}{z^2} + \frac{k_q}{(z-q)^2} + \frac{k_1}{(z-1)^2} - \frac{k_0 + k_q + k_1 - k_\infty}{z(z-1)} \\ & + \frac{q(q-1)U}{z(z-1)(z-q)}. \end{aligned} \tag{XVII.4.58}$$

Both terms have mass dimension two. The kinetic term fixes the orientation of the degenerate insertion for this limit. Choosing $V_{-b/2}$ would give $\hbar e b^{-2} = e^2$, losing this finite kinetic coefficient. The disappearance of the first derivative here follows from scaling the exact equation; deleting it at finite e would change the equation.

The pole and infinity conditions can be read off directly,

$$\lim_{z\to z_i} (z - z_i)^2 t_{\mathrm{NS}} = k_i, \quad z_i = 0, q, 1, \qquad \operatorname*{Res}_{z=q} t_{\mathrm{NS}} = U, \qquad \lim_{z\to\infty} z^2 t_{\mathrm{NS}} = k_\infty. \tag{XVII.4.59}$$

For completeness put $D = k_0 + k_q + k_1 - k_\infty$. The simple-pole residues at zero and one are

$$c_0 = D + (q-1)U, \qquad c_1 = -D - qU, \qquad c_q = U, \qquad c_0 + c_1 + c_q = 0. \tag{XVII.4.60}$$

Expanding the simple poles at infinity gives $k_0 + k_q + k_1 + q c_q + c_1 = k_\infty$, which explains the coefficient of the compensating rational term. These are constraints on a potential with an unspecified U. No four-heavy accessory function has been evaluated here.

A three-heavy specialization retains the Gauss parameters along a fixed mass ray,

$$A = \frac{1}{2} + \frac{m_0 + m_1 + m_\infty}{\hbar}, \qquad B = \frac{1}{2} + \frac{m_0 + m_1 - m_\infty}{\hbar}, \qquad C = 1 + \frac{2m_0}{\hbar}. \tag{XVII.4.61}$$

These parameters are in fact independent of e in the specified centered-mass scaling. The coordinate powers are not,

$$r = \frac{1}{2} + \frac{e}{2\hbar} + \frac{m_0}{\hbar}, \qquad s = \frac{1}{2} + \frac{e}{2\hbar} + \frac{m_1}{\hbar}. \tag{XVII.4.62}$$

For $(m_0, m_1, m_\infty)/\hbar = (1/6, -89/210, -3/70)$, the same $(A, B, C) = (1/5, 2/7, 4/3)$ occurs at $\beta = 1/2, 1/3, 1/5$ and in the NS limit. At $\beta = 1/2$, $e/\hbar = 1/4$ reproduces $r = 19/24$ and $s = 169/840$. Thus keeping the masses fixed is different from keeping the CFT momenta fixed.

To compare with XVI.4 define the quantum quadratic differential by

$$\phi_{2,\mathrm{quant}} = -t_{\mathrm{NS}}, \qquad [(\hbar\partial_z)^2 - \phi_{2,\mathrm{quant}}]\psi = 0, \qquad [\hbar\partial_z, z] = \hbar. \tag{XVII.4.63}$$

There is no $-i$ in this complex differential-operator convention. Substituting $\psi = \exp(S/\hbar)$ gives the exact Riccati relation

$$p = S', \qquad p^2 + \hbar p' = -t_{\mathrm{NS}}. \tag{XVII.4.64}$$

A further $\hbar \to 0$ limit, with finite prescribed mass and accessory family, yields

$$x^2 = -t_0(z), \qquad \lambda_{\mathrm{geom}} = x\,dz, \qquad S_0 = \int^z \pm\sqrt{-t_0(\zeta)}\,d\zeta. \tag{XVII.4.65}$$

The branch and integration path must avoid turning points. This is a subsequent semiclassical construction, not the NS limit itself. Near a double pole the exact local indices solve

$$\hbar^2\nu(\nu-1) + \frac{\hbar^2}{4} - m_i^2 = 0, \qquad \nu = \frac{1}{2} \pm \frac{m_i}{\hbar}. \tag{XVII.4.66}$$

The half shift is absent from the bare leading WKB exponent. Local WKB does not select a global boundary domain or supply a resummed solution.

Finally, the three twisted superpotentials encountered here have different definitions. The source gauge construction defines $\mathcal{W}_{\mathrm{gauge}} = \lim_{e\to 0} e \log Z_{\mathrm{gauge}}$ in a specified normalization. The bulk block exponent is $\mathcal{W}_{\mathrm{CFT}}$, whereas $\mathcal{W}_{\mathrm{def}}$ was an open-path quantity. Classical, external and abelian prefactors can depend on q. For example,

$$F \longmapsto e^{g(q)/e} F \quad \Longrightarrow \quad \mathcal{W}_{\mathrm{CFT}} \longmapsto \mathcal{W}_{\mathrm{CFT}} + g, \qquad U \longmapsto U + \hbar g'(q). \tag{XVII.4.67}$$

A normalization independent of q leaves U unchanged. Equality with a chosen gauge twisted superpotential requires those factors and existence of the limit. Neither this local derivation nor the geometric equation fixes an absolute Seiberg–Witten period normalization. The gauge/Bethe interpretation also requires a theory, branches and boundary conditions. We next impose one explicit analytic condition in the exactly soluble example to see how selection actually occurs.

XVII.4.5 Monodromy and an analytic endpoint problem

A local solution can be continued around a puncture without satisfying any particular endpoint condition. To separate these operations, first compute the connection between the zero and one bases for the recurring Gauss equation. Define the column $f^{(0)} = (f_1^{(0)}, f_2^{(0)})^{\mathsf{T}}$ by the two reduced solutions of Section 3 and set

$$f_1^{(1)} = {}_2F_1(A, B; A + B - C + 1; 1 - z), \tag{XVII.4.68}$$

$$f_2^{(1)} = (1 - z)^{C-A-B}{}_2F_1(C - A, C - B; C - A - B + 1; 1 - z). \tag{XVII.4.69}$$

Away from resonant differences and gamma poles, the Gauss connection theorem gives $f^{(0)} = Kf^{(1)}$. Its four entries are

$$K_{11} = \frac{\Gamma(C)\Gamma(C - A - B)}{\Gamma(C - A)\Gamma(C - B)}, \qquad K_{12} = \frac{\Gamma(C)\Gamma(A + B - C)}{\Gamma(A)\Gamma(B)}, \tag{XVII.4.70}$$

$$K_{21} = \frac{\Gamma(2 - C)\Gamma(C - A - B)}{\Gamma(1 - A)\Gamma(1 - B)}, \quad K_{22} = \frac{\Gamma(2 - C)\Gamma(A + B - C)}{\Gamma(A - C + 1)\Gamma(B - C + 1)}. \tag{XVII.4.71}$$

At resonance a limiting basis, often involving a logarithm, must replace these separate power solutions. A divergent gamma expression by itself is not a statement that the differential equation has no solution.

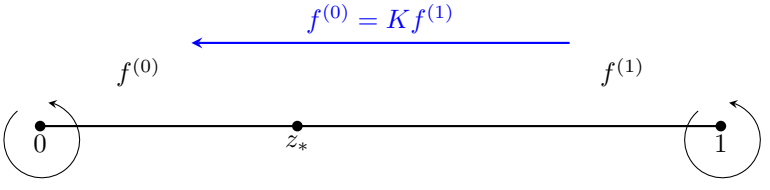


Figure XVII.4.5: The two local bases are related through a common regular point by K. Continuation around zero or one acts on the full solution column, including its coordinate powers. In the separate endpoint problem, holomorphy of the factored function selects the analytic branch at each end of the interval.

For $(A,B,C)=(1/5,2/7,4/3)$ the actual connection is

$$K \simeq \begin{pmatrix} 1.0879788984 & -0.4458256211 \\ 1.0161323189 & -0.0549269800 \end{pmatrix}. \tag{XVII.4.72}$$

It relates values and derivatives at $z_* = 37/100$,

$$f^{(0)}(z_*) = K f^{(1)}(z_*), \qquad \partial_z f^{(0)}(z_*) = K \partial_z f^{(1)}(z_*). \tag{XVII.4.73}$$

Direct 60-digit evaluations give residuals below 10^{-49} for these relations. These numerical comparisons support the transcription of the exact connection theorem. They do not supply certified numerical error bounds.

Take counterclockwise loops about the finite punctures with connecting paths in the usual slit plane. On the column of full solutions $F^{(0)} = z^r(1-z)^s f^{(0)}$, the two actions are

$$M_0 = \operatorname{diag}(e^{2\pi i r}, e^{2\pi i(r+1-C)}), \tag{XVII.4.74}$$

$$M_1 = K \operatorname{diag}(e^{2\pi i s}, e^{2\pi i(s+C-A-B)}) K^{-1}. \tag{XVII.4.75}$$

The coordinate powers therefore affect both matrices. With $r = 19/24$ and $s = 169/840$, the values are

$$M_0 \simeq \begin{pmatrix} .258819 - .965926i & 0 \\ 0 & -.965926 + .258819i \end{pmatrix}, \tag{XVII.4.76}$$

$$M_1 \simeq \begin{pmatrix} 1.052335 + .202901i & -.803501 + .803501i \\ .092456 - .092456i & .202901 + 1.052335i \end{pmatrix}. \tag{XVII.4.77}$$

These are solution-basis column actions. Acting on coefficient columns would require the corresponding transposed convention. Fix the loop-product convention by $M_\infty = (M_0 M_1)^{-1}$. Then the infinity exponents imply

$$\operatorname{tr} M_\infty = e^{2\pi i(A-r-s)} + e^{2\pi i(B-r-s)}, \qquad \det M_1 = e^{2\pi i(2s+C-A-B)}. \tag{XVII.4.78}$$

The nonzero off-diagonal entries of M_1 show how a zero-channel solution becomes a combination after continuation about one. This is ordinary scalar-equation monodromy. Its existence neither selects a boundary solution nor computes a four-dimensional Wilson-loop expectation value.

Now change the question. Fix $C = 4/3$ and $A + B = 26/15$, let $\lambda = -AB$ vary, and demand that f be holomorphic at both endpoints, with $f(0) = 1$. The equation is

$$z(1-z)f'' + \left[\frac{4}{3} - \frac{41}{15}z\right] f' + \lambda f = 0, \qquad 0 < z < 1. \tag{XVII.4.79}$$

The local exponent pairs of f are $(0, -1/3)$ at zero and $(0, -2/5)$ at one. Each endpoint consequently has exactly one normalized analytic branch. The zero-analytic solution is ${}_2F_1(A, B; 4/3; z)$; its coefficient of the nonanalytic branch at one is

$$K_{12} = \frac{\Gamma(4/3)\Gamma(2/5)}{\Gamma(A)\Gamma(B)}. \tag{XVII.4.80}$$

The numerator is finite and nonzero. Since gamma has no zeros and has poles at the nonpositive integers, this coefficient vanishes precisely when

$$A = -n \text{ or } B = -n, \qquad n \in \mathbb{Z}_{\geq 0}, \qquad \lambda_n = n\left(n + \frac{26}{15}\right). \tag{XVII.4.81}$$

At either choice the series terminates,

$$f_n(z) = {}_2F_1\left(-n, n + \frac{26}{15}; \frac{4}{3}; z\right), \tag{XVII.4.82}$$

so the analytic continuation has no nonanalytic term and is a polynomial. The gamma argument proves the selection for all n, rather than extrapolating from a finite list. The first three selected pairs are

$$(\lambda_0, f_0) = (0, 1), \tag{XVII.4.83}$$

$$(\lambda_1, f_1) = \left(\frac{41}{15}, 1 - \frac{41}{20}z\right), \tag{XVII.4.84}$$

$$(\lambda_2, f_2) = \left(\frac{112}{15}, 1 - \frac{28}{5}z + \frac{142}{25}z^2\right). \tag{XVII.4.85}$$

For $n = 2$, the constant term in the equation is $\frac{4}{3}(-28/5) + 112/15 = 0$. The linear and quadratic terms cancel as well after inserting $f_2' = -28/5 + 284z/25$ and $f_2'' = 284/25$. This checks the spectral value against the actual polynomial.

The boundary example still comes from the same BPZ mechanism. At $\beta = 1/2$ it uses $\alpha_0 = 19/12$, $\alpha_1 = 33/20$, and at $n = 2$ takes $\alpha_\infty = -269/60$. Thus

$$(A, B, C) = (-2, 56/15, 4/3), \qquad (r, s) = (19/24, 33/40). \tag{XVII.4.86}$$

For the full F, the condition selects exponents r and s. It does not demand that F itself be single-valued. Changing instead to $A = 1/7$, $B = 26/15 - 1/7$ gives

$$K_{12} \simeq 0.3389407686 \neq 0, \tag{XVII.4.87}$$

so the solution analytic at zero fails the endpoint condition at one. This failure has a specific coefficient and a specified forbidden branch.

The equation also has a weighted differential form. With

$$w = z^{1/3}(1 - z)^{2/5}, \qquad p = z^{4/3}(1 - z)^{7/5}, \qquad \mathcal{L}f = -\frac{1}{w}(pf')', \tag{XVII.4.88}$$

one has $p/w = z(1 - z)$ and $p'/w = 4/3 - 41z/15$, so $\mathcal{L}f = \lambda f$. Polynomial solutions have $pf' \to 0$ at both endpoints. We have proved the analytic endpoint selection just imposed. Identifying a self-adjoint realization, proving its completeness, or choosing a gauge-theory Hilbert domain requires further analysis and physical input.

The source gauge/Bethe construction relates suitable vacuum equations for $\mathcal{W}_{\text{gauge}}$ to a quantum integrable-system problem after its theory and domain are specified. Our explicit endpoint example demonstrates the extra selection step. It supplies neither the uncomputed four-heavy accessory function nor a general higher-rank AGT proof. The NS limit, its subsequent WKB expansion, the further classical curve, and an exact boundary problem remain distinct constructions.

Exercises

Each exercise has a finite submission and a written argument. For benchmark submissions, see `benchmark/PROTOCOL.md`. Preserve ordered momentum components, coefficient lists and matrix rows. Exact algebraic expressions may be submitted using rational arithmetic and square roots. Include the requested written arguments.

1. At $b = 1/2$, compute c, Δ and I_3 for the generic p of Section 1, and compute the two components of $G_1(-3w/(2\Delta), 1)^{\mathsf{T}}$ at $\alpha = (7/5)\omega_2$. Explain why the latter vanishing does not imply a generic null, and why this pairing has no positivity assertion.

2. Repeat the Toda recurrence at $b = 2/3$, $\kappa = 5/4$, $p_1 = (1/3, -1/5, -2/15)$ and $p_2 = (1/4, -1/6, -1/12)$. Submit c_1, c_2, the three zero exponents, and the three local infinity exponents in defining-weight order. Derive the recurrence and explain exactly which insertion restriction closes this equation.

3. For the recurring rank-one example submit h_d, the ordered null coefficients in (L_{-2}, L_{-1}^2), (A, B, C), and the ordered zero exponents. Derive the coordinate Ward elimination and explain the incident-vertex fusion condition in the s and t channels.

4. Put $\hbar = 2$, $(m_0, m_q, m_1, m_\infty) = (1/3, 1/4, -2/5, 1/7)$, $q = 2/5$, and $\partial_q \mathcal{W}_{\mathrm{CFT}} = 3/7$. Submit the retained kinetic coefficient, four k_i in that order, U, and the three-heavy (A, B, C) obtained by omitting m_q. Derive the limiting equation and distinguish all three $\mathcal{W}$'s and both successive limits.

5. Use $(A, B, C) = (1/4, 1/3, 7/6)$ and $(r, s) = (2/5, 1/7)$. Submit the four gamma connection entries as a two-row matrix, the two full exponents at zero, the two full exponents at one, and $\det M_1$ and $\operatorname{tr} M_\infty$. Numerical complex quantities use relative tolerance 10^{-10}. Specify branches and the action convention, and explain the change needed at resonance.

6. For the analytic endpoint family compute λ_3 and the ordered coefficients of f_3 beginning with the constant. Submit also the singular coefficient for $A = 1/7$ in the same family. Prove the all-n selection using the gamma theorem, and identify the additional choices needed for a gauge Hilbert-space interpretation.

Take-home message

A semi-degenerate field removes an independent spin-three descendant and makes one special higher-rank equation calculable. A rank-one external null field gives a fusion-compatible BPZ equation with nontrivial coordinate powers. Conditional NS factorization turns the five-point PDE into a quantum differential equation with a shifted mass term and an accessory function. A separate analytic endpoint condition selects discrete values in the exactly solved Gauss family.

Before proceeding, the reader should be able to recover the Toda recurrence from its Euler operator, retain the full BPZ powers in monodromy, derive the accessory residue

without assigning it a Coulomb period, and explain why a local quantum curve alone does not define a spectrum.

Sources and scope

§1. The free-boson central charge, dimensions, cubic invariant, explicit Gram matrix, its semi-null and the low descendant Ward substitution are [**MATH**] calculations in the displayed conventions. The spin-three algebra and semi-degenerate relation follow Wyllard 2009, arXiv:0907.2189v2, equations 3.2–3.19, and Fateev and Litvinov 2005, arXiv:hep-th/0505120v1, equations 2–4. The defining weights of Wyllard's equation 3.22 have the opposite sign, so $W_{\text{here}} = -W_{\text{source}}$ and only mixed Gram entries reverse sign. The higher-rank AGT and simple-puncture interpretation is a sourced [**CONJ+**] premise from Wyllard, equations 3.21–3.24 and section 3.3. No $SU(3)$ instanton match is calculated.

§2. The special third-order null/Ward equation is imported from Fateev–Litvinov, equations 8–14 and 17. The recurrence, finite coefficients and both sets of fusion exponents are [**MATH**] consequences of that equation. Its external semi-degenerate restriction is essential. The chiral solution is not the full Toda correlator.

§3. The rank-one null, coordinate Ward elimination, prefactor reduction and fusion exponents are [**MATH**] identities. The physical defect dictionary is a [**CONJ+**] source premise of Alday et al. 2009, arXiv:0909.0945v2, equation 2.12, section 3.1, and appendix B.1, printed pages 52–54. Its parameter b is our β, and its $(2,1)$ field is our h_{12}. Surface and line interpretations require the additional source constructions described there.

§4. The five-point PDE is an exact Ward calculation. Its NS operator, pole coefficients, mass shift and Riccati equation are [**MATH**] conditional on the stated differentiable factorization. Existence of that factorization and equality to a normalized gauge twisted superpotential remain [**CONJ+**] premises. Nekrasov and Shatashvili 2009, arXiv:0908.4052v1, equations 3.5–3.8, supplies the fixed-parameter physical limit. AGGTV equation 2.14 uses simultaneous semiclassics and does not prove that assumption. The four-heavy accessory function, absolute physical periods, and global WKB completion remain uncomputed.

§5. The exact Gauss connection theorem is sourced from AGGTV appendix B.1, equations B.10–B.13. Full monodromy and the analytic endpoint selection are [**MATH**] consequences in the specified nonresonant bases. The high-precision comparisons have no certified numerical error bound. The endpoint condition belongs to the factored function f; no gauge Hilbert spectrum or self-adjoint completeness is established. The wider gauge/Bethe interpretation is a [**CONJ+**] premise of Nekrasov–Shatashvili, equations 2.17–2.19, 3.7–3.8 and section 5.3.1.

References

Alday, L. F. et al. (2009). "Loop and surface operators in N=2 gauge theory and Liouville modular geometry". In: Version 2; equation 2.12, section 3.1 and appendix B.1. arXiv: 0909.0945 [hep-th].

Fateev, V. A. and A. V. Litvinov (2005). "On differential equation on four-point correlation function in the Conformal Toda Field Theory". In: Version 1; equations 8–14 and 17. arXiv: hep-th/0505120.

Nekrasov, N. A. and S. L. Shatashvili (2009). "Quantization of Integrable Systems and Four Dimensional Gauge Theories". In: Version 1; equations 2.17–2.19 and 3.5–3.8. arXiv: 0908.4052 [hep-th].

Wyllard, N. (2009). "A_{N-1} conformal Toda field theory correlation functions from conformal N=2 SU(N) quiver gauge theories". In: Version 2; source equations 3.2–3.19 and 3.21–3.24. arXiv: 0907.2189 [hep-th].

Chapter XVII.5

The Schur index and curve gluing

A class-S surface can be cut into pairs of pants in more than one way. The cuts expose different gauge groups and different elementary matter descriptions. A protected trace gives a concrete quantity to compare across those descriptions. We will construct that trace for the four-punctured A_1 sphere, keep all four puncture fugacities distinct, and carry out the singlet projection in two channels. The first nontrivial answer already knows about the enhanced flavor algebra.

The required ingredients from Volume XVI are modest. A regular maximal A_1 puncture carries an $SU(2)$ flavor group. The trinion T_2 is one half-hypermultiplet in the pseudoreal representation $(\mathbf{2},\mathbf{2},\mathbf{2})$. Gauging a common puncture of two trinions gives $SU(2)$ with four full fundamental hypermultiplets. Here we learn how those operations act on a local-operator trace. We assume the protected-trace and weak-coupling localization prescriptions, and derive their finite algebraic consequences.

The variable q_S grades Schur operators. It is independent of the instanton parameter and the ultraviolet cross-ratio used in the preceding chapters. We set $t^2 = q_S$ to make the half-integral grades of elementary scalars integral. Our central comparison keeps four independent flavor variables through $t^6 = q_S^3$. A diagonal character basis will then explain why sewing is simple, with the full trinion identity supplied by its analytic source. The finite comparison is a calculation within that framework, rather than a proof of full crossing or physical S-duality.

XVII.5.1 The Schur trace and its letters

The index counts a protected part of the radial Hilbert space on S^3, with a fermion sign. The first task is to specify which shortening conditions survive the specialization. Let E be radial energy, j_1, j_2 the Lorentz Cartan eigenvalues, R the $SU(2)_R$ Cartan, and r the abelian R-charge. We use a Cartan frame in which the two positive supercharge

anticommutators are proportional to

$$\delta_R = E - 2j_2 - 2R + r, \qquad \delta_L = E + 2j_1 - 2R - r. \tag{XVII.5.1}$$

The chosen source labels are $\widetilde{Q}_{1\dot{-}}$ and Q_{1+}. The subscripts label supercharges; the j_i in (XVII.5.1) are actual eigenvalues. Solving the two kernel conditions gives

$$E = 2R - j_1 + j_2, \qquad r = j_1 + j_2. \tag{XVII.5.2}$$

The resulting trace is

$$\mathcal{I}_S(q_S; \boldsymbol{a}) = \mathrm{Tr}_{\delta_L=\delta_R=0}(-1)^F q_S^{E-R} \prod_i a_i^{f_i}, \qquad \mathcal{I}_S(0) = 1. \tag{XVII.5.3}$$

Here F is fermion number and f_i are flavor Cartan charges. No supersymmetric Casimir-energy factor is included. In a unitary radial Hilbert space, states outside a supercharge kernel pair with opposite fermion signs and equal commuting grades. Protection under suitable supersymmetric deformations is the physical input that permits evaluation in a weakly coupled frame. A discrete graded trace and deformations preserving its definition are required. The trace is signed, so its coefficients need not be dimensions of spaces of bosonic operators.

We can now read the surviving letters directly. The four relevant charge assignments are

	E	j_1	j_2	R	r	$E-R$
h	1	0	0	$\frac{1}{2}$	0	$\frac{1}{2}$
λ_{1-}	$\frac{3}{2}$	$-\frac{1}{2}$	0	$\frac{1}{2}$	$-\frac{1}{2}$	1
$\bar{\lambda}_{1\dot{+}}$	$\frac{3}{2}$	0	$\frac{1}{2}$	$\frac{1}{2}$	$\frac{1}{2}$	1
$\partial_{-\dot{+}}$	1	$-\frac{1}{2}$	$\frac{1}{2}$	0	0	1

(XVII.5.4)

Substitution in (XVII.5.1) gives zero for every row. Each application of the retained derivative increases $E - R$ by one. Thus the scalar and the two fermions generate geometric towers,

$$f_{\frac{1}{2}H}(t) = \sum_{k\geq 0} t^{1+2k} = \frac{t}{1-t^2}, \qquad f_V(t) = -2\sum_{k\geq 0} t^{2+2k} = \frac{-2t^2}{1-t^2}. \tag{XVII.5.5}$$

A half-hyper contributes this expression once for each weight of its pseudoreal representation. There is no additional doubling for its complex conjugate. The minus sign and factor two in f_V come from the two retained gaugini.

A useful changed-input test is to keep the other angular fugacity generic before taking the Schur limit. Call the general-index R-fugacity u, so that it cannot be confused with our t. The source single-letter functions are

$$f_{\frac{1}{2}H}(p,q,u) = \frac{\sqrt{u} - pq/\sqrt{u}}{(1-p)(1-q)}, \qquad f_V(p,q,u) = -\frac{p}{1-p} - \frac{q}{1-q} + \frac{pq/u - u}{(1-p)(1-q)}. \tag{XVII.5.6}$$

Setting $u = q = q_S$, while leaving p arbitrary, gives

$$f_{\frac{1}{2}H}\big|_{u=q} = \frac{\sqrt{q}(1-p)}{(1-p)(1-q)} = \frac{\sqrt{q}}{1-q}, \qquad f_V\big|_{u=q} = -\frac{2q}{1-q}. \tag{XVII.5.7}$$

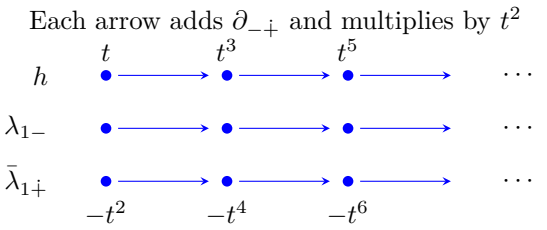


Figure XVII.5.1: The retained derivative moves along the joint kernel and raises the Schur grade by one. The scalar tower begins at t; each of the two fermionic towers begins at t^2. Their opposite signs are part of the trace. The arrows indicate applications of $\partial_{-\dot{+}}$, rather than changes of gauge or flavor weight.

For the vector, the last fraction becomes $(p-q)/((1-p)(1-q))$ and cancels the unwanted p dependence. Setting $p=q$ at the start would conceal this cancellation. As a second diagnostic, the vector scalar with $(E, j_1, j_2, R, r) = (1, 0, 0, 0, -1)$ has $\delta_R = 0$ but $\delta_L = 2$. It is absent from the joint kernel, even though it satisfies one shortening condition.

The passage from letters to multiparticle operators uses the plethystic exponential. For a signed letter character f, define

$$\mathrm{PE}[f] = \exp\left[\sum_{k\geq 1} \frac{1}{k} f(t^k, x_1^k, \ldots, x_s^k)\right]. \tag{XVII.5.8}$$

Every variable is raised to the same power. For a monomial weight x^w of grade d, the elementary identities are

$$\mathrm{PE}[t^d x^w] = (1 - t^d x^w)^{-1}, \qquad \mathrm{PE}[-t^d x^w] = 1 - t^d x^w. \tag{XVII.5.9}$$

They give symmetric bosonic occupation and signed fermionic occupation, respectively. Replacing a negative coefficient by a positive one changes the observable.

There are two practical finite expansions. Multiplying the factors in (XVII.5.9) is one. For the other, write $f = \sum_{d\geq 1} t^d f_d(\boldsymbol{x})$ and $\mathrm{PE}[f] = \sum_{n\geq 0} t^n A_n$. Logarithmic differentiation yields

$$n A_n = \sum_{k=1}^{n} B_k A_{n-k}, \qquad B_k = \sum_{d|k} d\, f_d(\boldsymbol{x}^{k/d}), \qquad A_0 = 1. \tag{XVII.5.10}$$

This triangular recursion uses only previously determined coefficients. To work through degree L, it suffices to retain letters of degree at most L. It supplies an independent route to the product expansion and will let us assemble the two gluing channels differently. The trace counts local operators in the conformal theory; the particle chambers of Chapter 1 play no role in this operation.

XVII.5.2 Gauging as a singlet projection

The letters of a weak gauge theory carry gauge weights. Physical local operators must be gauge invariant. Haar integration performs this projection representation by representation, while the vector multiplet supplies its own signed letters. Keeping these two ingredients separate prevents a common error in index sewing.

For $SU(2)$, use a torus coordinate z with fundamental weights z, z^{-1}. A representation of highest weight n has character

$$\chi_n(z) = z^n + z^{n-2} + \cdots + z^{-n}, \qquad \chi_0 = 1, \quad \chi_1 = z + z^{-1}, \quad \chi_2 = z^2 + 1 + z^{-2}. \tag{XVII.5.11}$$

Its dimension is $n+1$. The normalized Weyl integration formula is

$$\int d\mu(z)\, f(z) = \frac{1}{2} \oint_{|z|=1} \frac{dz}{2\pi i z} (1 - z^2)(1 - z^{-2}) f(z). \tag{XVII.5.12}$$

For a finite Laurent polynomial, the contour integral means extraction of the constant term, denoted CT_z. Expanding the Weyl factor gives

$$\int d\mu\, f = \mathrm{CT}_z\, f - \tfrac{1}{2}\, \mathrm{CT}_z(z^2 f + z^{-2} f), \qquad \int d\mu\, 1 = 1. \tag{XVII.5.13}$$

If $f(z) = f(z^{-1})$, the last two constant terms coincide. Only under this hypothesis may we simplify to

$$\int d\mu\, f = \mathrm{CT}_z[(1 - z^2) f]. \tag{XVII.5.14}$$

For instance $f = z^2$ has full integral $-1/2$ and reduced expression zero. This nonsymmetric example explains why the reduced rule must not be applied before checking Weyl invariance.

The projection can be derived without a contour. Every nontrivial even character has one zero weight and one weight -2, whereas an odd character has neither. Consequently

$$\int d\mu\, \chi_n = \delta_{n0}, \qquad \chi_n \chi_m = \sum_{j=0}^{\min(n,m)} \chi_{n+m-2j}. \tag{XVII.5.15}$$

Only $n = m$ allows the last sum to contain χ_0, and it occurs once. Therefore

$$\int d\mu\, \chi_n \chi_m = \delta_{nm}. \tag{XVII.5.16}$$

In contrast, a $U(1)$ constant term would retain the zero weight of every even $SU(2)$ representation. In particular it would give one for the adjoint, which has no $SU(2)$ singlet.

Two small examples distinguish different operator constructions. Four distinguishable fundamental factors give

$$\chi_1^2 = \chi_2 + \chi_0, \qquad \chi_1^4 = \chi_4 + 3\chi_2 + 2\chi_0, \qquad \int d\mu\, \chi_1^4 = 2. \tag{XVII.5.17}$$

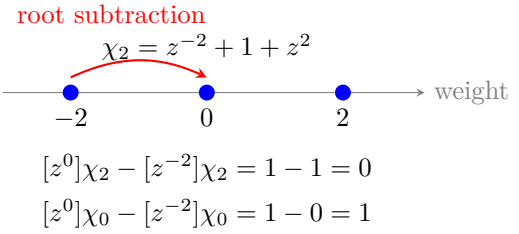


Figure XVII.5.2: The Weyl projector acts on a complete character. In the adjoint, the constant term of the weight-zero state is canceled by the root subtraction, leaving no singlet. For χ_0, the subtraction has no matching weight and the result is one. Merely retaining the central weight would instead project onto $U(1)$ neutrality.

The two singlets are independent pairwise epsilon contractions after imposing the linear relation among the three possible pairings. Now change the question to quadratic bosonic operators made from four copies of the doublet. Their single-particle character is $W(z) = 4\chi_1(z)$. The symmetric-square character is

$$\operatorname{ch}\operatorname{Sym}^2 W = \tfrac{1}{2}\big[W(z)^2 + W(z^2)\big]. \tag{XVII.5.18}$$

The second term is the two-cycle contribution, not the square of $W(z)$. Using $\chi_1(z^2) = \chi_2(z) - 1$ gives

$$\operatorname{Sym}^2(4\mathbf{2}) = 10\mathbf{3} \oplus 6\mathbf{1}, \qquad \int d\mu \operatorname{ch}\operatorname{Sym}^2 W = 6. \tag{XVII.5.19}$$

Equivalently, the antisymmetric gauge contraction forces the two flavor-copy indices to be antisymmetric, giving $\binom{4}{2} = 6$. This answer differs from two because the occupation problem differs. Checking only an unlabeled collection of doublets would lose this distinction.

For index gauging, insert the vector multiplet in the adjoint,

$$\mathcal{I}_V(t;z) = \operatorname{PE}\left[\frac{-2t^2}{1-t^2}\chi_2(z)\right], \qquad \mathcal{I}_V = 1 - 2t^2\chi_2(z) + O(t^4). \tag{XVII.5.20}$$

If $\mathcal{I}_L$ and $\mathcal{I}_R$ carry a common puncture group, the sewing prescription is

$$\mathcal{I}_{L\#R} = \int d\mu(z)\, \mathcal{I}_V(t;z)\mathcal{I}_L(t;z)\mathcal{I}_R(t;z^{-1}). \tag{XVII.5.21}$$

The inverse coordinate pairs a representation with its dual. Every $SU(2)$ character here is self-dual, so this inversion does not alter our polynomial. It is still useful to display it because complex higher-rank representations need a dual pairing. The Haar measure alone is not the vector index, and the vector index alone does not project gauge invariants.

The weak frame uses compact $SU(2)$ gauging with liftable backgrounds. No statement about an independent $SO(3)$ quotient follows from this character integral. Nor

does the integral itself derive the path-integral localization prescription. With that prescription supplied, however, every fixed-order coefficient is reduced to finite Laurent multiplication and the normalized projection above. We now have precisely the operation needed to sew the T_2 blocks of XVI.3.

XVII.5.3 The T2 trinion and its wavefunctions

The trinion is especially useful because its matter content is free. The three punctures have independent torus coordinates a, b, c. Define the eight-weight character

$$H(a,b,c) = \chi_1(a)\chi_1(b)\chi_1(c) = \sum_{\epsilon_1,\epsilon_2,\epsilon_3=\pm1} a^{\epsilon_1} b^{\epsilon_2} c^{\epsilon_3}. \tag{XVII.5.22}$$

The half-hyper assignment means one copy of each of these eight weights. The index is consequently

$$T_2(t;a,b,c) = \mathrm{PE}\left[\frac{tH(a,b,c)}{1-t^2}\right] = \prod_{k\geq 0}\prod_{\boldsymbol{\epsilon}} \frac{1}{1-t^{2k+1}a^{\epsilon_1}b^{\epsilon_2}c^{\epsilon_3}}. \tag{XVII.5.23}$$

This formula immediately distinguishes a single half-hyper from a doubled full hyper in the same representation. The latter would square the product and change the coefficient of t from H to $2H$.

Let $H_k = H(a^k, b^k, c^k)$. Expanding the logarithm through cubic degree gives

$$\log T_2 = tH + \tfrac{1}{2}t^2 H_2 + t^3(H + \tfrac{1}{3}H_3) + O(t^4). \tag{XVII.5.24}$$

Exponentiation separates symmetric occupation from descendants,

$$T_2 = 1 + tH + \frac{t^2}{2}(H^2 + H_2) + t^3\left[\frac{H^3 + 3HH_2 + 2H_3}{6} + H\right] + O(t^4). \tag{XVII.5.25}$$

The last H is one derivative acting on a scalar. It would be absent if the letter were truncated to its primary term tH. Thus the cubic coefficient is an early test of whether the derivative tower was included.

The representation decomposition makes the flavor content visible. First use

$$\chi_1(x)^2 = \chi_2(x) + 1, \qquad \chi_1(x^2) = \chi_2(x) - 1. \tag{XVII.5.26}$$

Writing $A = \chi_2(a)$, $B = \chi_2(b)$, $C = \chi_2(c)$, the quadratic coefficient becomes

$$\tfrac{1}{2}\big[(A+1)(B+1)(C+1) + (A-1)(B-1)(C-1)\big] = ABC + A + B + C. \tag{XVII.5.27}$$

The even number of minus choices selects the completely symmetric triple and the three single adjoints. At cubic degree, substitution of $\chi_1(x^3) = \chi_3(x) - \chi_1(x)$ into (XVII.5.25) gives

$$[t^3]T_2 = \chi_3(a)\chi_3(b)\chi_3(c) + H\big[\chi_2(a) + \chi_2(b) + \chi_2(c) - 1\big]. \tag{XVII.5.28}$$

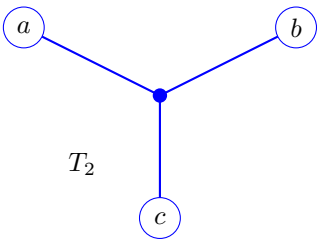


Figure XVII.5.3: A trinion has three separately labeled $SU(2)$ punctures. Its elementary scalar weights are the eight sign triples. The boundary circles label flavor groups rather than gauge integrations.

At unit fugacities the quadratic answer is $27+9=36$. The cubic answer is $64+8(9-1)=128$. Independently, eight bosons have $\binom{10}{3}=120$ symmetric cubic occupations, and the first derivative gives eight more. These counts explain both terms rather than just their total.

To diagonalize sewing, introduce a universal puncture factor and a scalar infinite product,

$$K(t;a)=\mathrm{PE}\left[\frac{t^2}{1-t^2}\chi_2(a)\right],\qquad \psi_n(t;a)=K(t;a)\chi_n(a),\qquad P(q_S)=\prod_{j\geq1}(1-q_S^j). \tag{XVII.5.29}$$

Both K and P have constant term one, while ψ_n has constant term $\chi_n(a)$. The quantum dimension in our highest-weight labeling is

$$[n+1]_{q_S}=t^{-n}\frac{1-q_S^{n+1}}{1-q_S},\qquad \mathcal{N}_{222}=\frac{P(q_S)}{1-q_S}. \tag{XVII.5.30}$$

The sourced all-order A_1 trinion identity is

$$T_2(t;a,b,c)=\sum_{n\geq0}C_n(t)\psi_n(t;a)\psi_n(t;b)\psi_n(t;c),\qquad C_n=\frac{P(q_S)t^n}{1-q_S^{n+1}}. \tag{XVII.5.31}$$

We will test its coefficients and derive its sewing consequences. Its analytic proof is not supplied by a finite expansion. A pole and residue comparison underlies the source argument.

The scalar normalization in this formula matters. For example,

$$\mathcal{N}_{222}=\prod_{j\geq2}(1-q_S^j)=1-q_S^2-q_S^3+O(q_S^4),\qquad C_0=\mathcal{N}_{222}. \tag{XVII.5.32}$$

Dropping it preserves the vacuum and even the first q_S coefficient, but changes higher orders. Another common convention uses a puncture factor K/P, obtained by adding one singlet weight inside the plethystic exponential. Its scalar prefactor is $P^4/(1-q_S)$ before the three legs are multiplied. Thus

$$\frac{P^4}{1-q_S}\left(\frac{K}{P}\right)^3=\frac{P}{1-q_S}K^3. \tag{XVII.5.33}$$

The apparent extra zero weight and its scalar compensation must be translated together.

Changing all three flavor variables to one yields the reproducible finite result

$$T_2(t;1,1,1) = 1 + 8t + 36t^2 + 128t^3 + 394t^4 + 1088t^5 + 2776t^6 + O(t^7). \quad \text{(XVII.5.34)}$$

Retaining a, b, c separately is stronger. Direct product expansion and the character sum agree as Laurent polynomials through t^6. At this order the trinion requires modes through $n = 6$, since C_n starts at t^n. Truncating the representation sum at a convenient small label without checking this valuation would discard allowed contributions. The orthogonality of the same puncture basis will turn the next four-point integral into a single mode sum.

XVII.5.4 Two ways to glue four punctures

Keep the puncture labels a, b, c, d fixed while changing the pairing. The s channel joins (a, b, z) to (z, c, d); the t channel joins (a, c, z) to (z, b, d). The class-S construction identifies these as weak descriptions of the same SCFT. We can now compare an explicit protected quantity without relabeling an answer after it has been computed.

$$\begin{aligned} \mathcal{I}_s &= \int d\mu(z)\, \mathcal{I}_V(t;z) T_2(t;a,b,z) T_2(t;z,c,d), \\ \mathcal{I}_t &= \int d\mu(z)\, \mathcal{I}_V(t;z) T_2(t;a,c,z) T_2(t;z,b,d). \end{aligned} \quad \text{(XVII.5.35)}$$

The gauge matter characters, with the gauge doublet stripped off, are

$$V_s = \chi_1(a)\chi_1(b) + \chi_1(c)\chi_1(d), \qquad V_t = \chi_1(a)\chi_1(c) + \chi_1(b)\chi_1(d). \quad \text{(XVII.5.36)}$$

Each is an eight-weight flavor representation. Multiplication by the two gauge weights gives sixteen scalar weights, which is precisely eight half-doublets or four full $SU(2)$ hypers. The total letter character for either integral is

$$f_{\text{gauge}}(t;z) = \frac{t\chi_1(z)V - 2t^2\chi_2(z)}{1 - t^2}. \quad \text{(XVII.5.37)}$$

The vector term is shared; the flavor pairings inside V change.

The first nontrivial coefficient can be calculated by hand. The linear term integrates to zero because a single doublet is not a singlet. Let V_2 denote V with all flavor fugacities squared. At quadratic degree the integrand is

$$[t^2]\,\mathrm{PE}[f_{\text{gauge}}] = \tfrac{1}{2}\big[\chi_1(z)^2 V^2 + \chi_1(z^2)V_2\big] - 2\chi_2(z). \quad \text{(XVII.5.38)}$$

The three integrals needed are

$$\int d\mu\, \chi_1^2 = 1, \qquad \int d\mu\, \chi_1(z^2) = -1, \qquad \int d\mu\, \chi_2 = 0. \quad \text{(XVII.5.39)}$$

The second value follows from $\chi_1(z^2) = \chi_2 - 1$. Hence

$$[q_S]\mathcal{I} = \tfrac{1}{2}(V^2 - V_2). \quad \text{(XVII.5.40)}$$

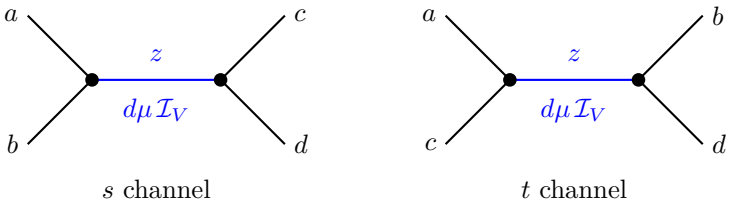


Figure XVII.5.4: The two sewing channels retain the external labels. On the left, a, b meet one trinion and c, d meet the other. On the right the pairs are a, c and b, d. Each internal edge is an $SU(2)$ gauging with the vector index and normalized Haar measure. Equality is tested with the flavor variables held fixed.

The antisymmetric flavor square is forced by the gauge epsilon tensor. For the s channel, put $A = \chi_1(a)\chi_1(b)$ and $B = \chi_1(c)\chi_1(d)$. Then

$$\tfrac{1}{2}(V_s^2 - (V_s)_2) = \tfrac{1}{2}(A^2 - A_2) + \tfrac{1}{2}(B^2 - B_2) + AB. \tag{XVII.5.41}$$

The first term is $\chi_2(a)+\chi_2(b)$, as follows by expanding $(\chi_2(a)+1)(\chi_2(b)+1)-(\chi_2(a)-1)(\chi_2(b)-1)$. The final answer is symmetric in all four labels,

$$[q_S]\mathcal{I} = \chi_2(a) + \chi_2(b) + \chi_2(c) + \chi_2(d) + \chi_1(a)\chi_1(b)\chi_1(c)\chi_1(d). \tag{XVII.5.42}$$

Repeating the same decomposition with V_t gives the same polynomial. At unit fugacities its dimension is $4 \cdot 3 + 2^4 = 28$. This is the adjoint branching compatible with the enhanced $\mathfrak{so}(8)$ flavor algebra. A Lie-algebra character by itself does not determine the global flavor group.

To extend the calculation, each coefficient can be treated as a finite Laurent polynomial. For a chosen cutoff L, multiply the Euler factors only through degree L and apply (XVII.5.14). Independently use (XVII.5.10) for the other channel. At $L = 6$ the two projected answers agree in all 820 nonzero monomials. The two assemblies use distinct puncture pairings and different expansion methods, while sharing the weight-generation rule and normalized group projector. Their agreement therefore checks the finite algebra but does not supply complete independence of physical premises or letter assignment.

There is a useful explanation of why only integer powers of q_S survive. The center $z \mapsto -z$ acts by minus one on each matter letter and trivially on vector letters. A singlet has an even number of gauge fundamentals. Derivatives change the t degree by two. Therefore

$$[t^{2k+1}]\mathcal{I}_s = [t^{2k+1}]\mathcal{I}_t = 0. \tag{XVII.5.43}$$

This condition is insensitive to many flavor errors, so it complements rather than replaces the labeled comparison.

A changed flavor input probes more structure than the number 28. Setting $(a, b, c, d) = (2, 3, 5, 7)$ in (XVII.5.42) gives

$$[q_S]\mathcal{I}(2, 3, 5, 7) = \frac{17681689}{44100}. \tag{XVII.5.44}$$

The same exact substitution can be made in each higher Laurent coefficient. The second independent choice $(3/2, 4/3, 5/4, 6/5)$ gives another unequal series with equal s and t answers. These are substitutions in finite polynomials. No assertion about a finite-q_S contour integral at these numerical fugacities is needed.

At unit fugacities the direct gauge calculation extends further,

$$\begin{aligned}\mathcal{I}(t;1,1,1,1) = 1 &+ 28q_S + 329q_S^2 + 2632q_S^3 \\ &+ 16380q_S^4 + 85764q_S^5 + O(q_S^6).\end{aligned} \tag{XVII.5.45}$$

The next section will recover these coefficients from a separate scalar sum. The two finite matches support the protected observable in these frames. They do not establish equality to all orders, the whole physical theory, or its line-operator and global-form choices. Those stronger physical identifications require the class-S construction and its source arguments.

XVII.5.5 The diagonal sewing algebra

The vector factor complicates a direct gauge integral but becomes simple in the puncture basis. Its logarithm is minus twice the logarithm of K. Thus, as formal series,

$$\mathcal{I}_V(t;z)K(t;z)^2 = 1. \tag{XVII.5.46}$$

Since K has constant term one, its inverse is defined order by order. Combining this cancellation with ordinary character orthogonality gives the metric

$$\langle \psi_n, \psi_m \rangle_V = \int d\mu(z)\, \mathcal{I}_V(t;z)\psi_n(t;z)\psi_m(t;z) = \delta_{nm}. \tag{XVII.5.47}$$

Here the scalar product is bilinear in the formal characters. In our self-dual $SU(2)$ setting the inversion on the second puncture is harmless. This is the concrete reason to dress characters by K, rather than an arbitrary change of basis.

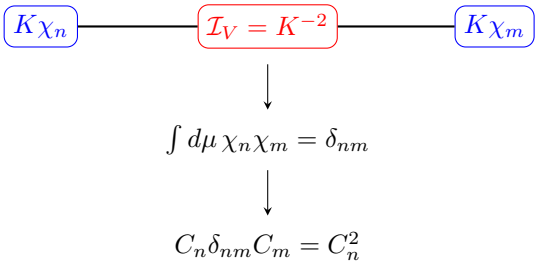


Figure XVII.5.5: Two puncture factors cancel the vector factor on an internal tube. Haar orthogonality then forces the incoming and outgoing labels to agree. Each trinion contributes C_n, so a four-punctured sphere carries C_n^2. The mode label propagates through the tube; it is a representation label rather than a spacetime excitation number.

It is possible to test diagonalization directly on the trinion before using the sourced sum. Strip the puncture factors and expand

$$F(t;a,b,c)=\frac{T_2(t;a,b,c)}{K(t;a)K(t;b)K(t;c)}. \tag{XVII.5.48}$$

For a Weyl-invariant Laurent polynomial in one variable, write $f(a)=\sum_{n\geq 0} m_n\chi_n(a)$. Every weight a^n with $n\geq 0$ occurs in $\chi_n,\chi_{n+2},\ldots$, so subtracting adjacent weights isolates a highest weight,

$$m_n=[a^n]f-[a^{n+2}]f. \tag{XVII.5.49}$$

Apply this operation separately in the three variables. At a fixed t degree, the coefficient of $\chi_n(a)\chi_m(b)\chi_\ell(c)$ is

$$m_{nm\ell}=\sum_{\epsilon_1,\epsilon_2,\epsilon_3=0}^{1}(-1)^{\epsilon_1+\epsilon_2+\epsilon_3}[a^{n+2\epsilon_1}b^{m+2\epsilon_2}c^{\ell+2\epsilon_3}]F. \tag{XVII.5.50}$$

This extraction acts on the actual product (XVII.5.23), not on an already diagonal array. For all 64 label triples $0\leq n,m,\ell\leq 3$, its expansion through t^6 is zero unless all three labels agree. The surviving series include

$$\begin{aligned} C_0&=1-t^4-t^6+O(t^8), \quad & C_1&=t-t^3+O(t^7),\\ C_2&=t^2-t^4-t^6+O(t^8), \quad & C_3&=t^3-t^5+O(t^7). \end{aligned} \tag{XVII.5.51}$$

The displayed remainders state only the retained finite orders. Separately, expanding independently assembled $\mathcal{I}_V$ and K gives the metric (XVII.5.47) through t^6 for labels zero through three. These calculations test both the dressing and the diagonal coefficient, rather than merely substituting the identity one seeks to check.

Insert (XVII.5.31) twice into the four-point sewing. The metric contracts the two internal labels,

$$\mathcal{I}_{0,4}(t;a,b,c,d)=K(a)K(b)K(c)K(d)\sum_{n\geq 0}C_n(t)^2\chi_n(a)\chi_n(b)\chi_n(c)\chi_n(d). \tag{XVII.5.52}$$

This expression treats all four external labels symmetrically. At unit fugacities, $K(t;1)=P^{-3}$, and $\chi_n(1)=n+1$. Therefore

$$\mathcal{I}_{0,4}(t;1,1,1,1)=P^{-10}\sum_{n\geq 0}\frac{(n+1)^4q_S^n}{(1-q_S^{n+1})^2}. \tag{XVII.5.53}$$

The power -10 follows from four K factors and two numerator factors P, so it also tests normalization. Expansion gives (XVII.5.45) without gauge-weight multiplication.

The same algebra organizes a stable untwisted A_1 surface with genus g and s regular maximal punctures. Let the number of pants be $p=2g-2+s>0$. Each internal metric identifies labels, yielding the sourced expression

$$\mathcal{I}_{g,s}=\sum_{n\geq 0}C_n(t)^p\prod_{i=1}^{s}\psi_n(t;a_i), \qquad p>0. \tag{XVII.5.54}$$

This is the zero-area q-deformed Yang–Mills organization of the Schur index, with the scalar normalization retained. Its puncture space has infinitely many labels. We are using an infinite-dimensional sewing algebra, rather than asserting the literal finite-dimensional Atiyah TQFT axioms. It is also a different two-dimensional structure from the Liouville theory in AGT and from the chiral algebra of the next chapter.

The formal cutoff is exact. Since $C_n = t^n$ times a series of constant term one and all K factors have nonnegative valuation,

$$\mathrm{val}_t(C_n^p) = pn, \qquad [\mathcal{I}_{g,s}]_{\le t^L} \text{ needs only } n \le \lfloor L/p \rfloor. \tag{XVII.5.55}$$

For a trinion at $L = 6$, the largest mode is six. For a four-punctured sphere it is three. The latter boundary contributes $t^6 \prod_i \chi_3(a_i)$ with nonzero leading coefficient; omitting it changes the result. Adding mode four cannot change any coefficient through t^6. If we instead raise the four-point cutoff to $L = 8$, mode four must be retained. This is a changed-input rule derived from valuation, not from numerical smallness. The unpunctured torus has $p = 0$, so this argument supplies no finite cutoff for it. Unstable caps and cylinders also require their own definitions.

Formal power series require no analytic convergence, because each retained coefficient involves finitely many modes and letter factors. To interpret the contour analytically, choose a branch $t^2 = q_S$ with $|t| < 1$, the unit gauge contour, and initially unit-modulus external fugacities. More generally put $R_i = \max(|a_i|, |a_i|^{-1})$. A sufficient common neighborhood for both four-point channels obeys

$$\begin{gathered} |t| R_i R_j < 1 \quad \text{for pairs used in either channel,} \\ |q_S| R_i^2 < 1, \qquad |q_S| R_a R_b R_c R_d < 1. \end{gathered} \tag{XVII.5.56}$$

The character and coefficient obey the estimates

$$|\chi_n(a)| \le (n+1) R_a^n, \qquad |C_n(t)| \le \frac{|P(q_S)|\,|t|^n}{1 - |q_S|}. \tag{XVII.5.57}$$

The first follows by bounding each of the $n+1$ weights separately; the second uses $|1 - q_S^{n+1}| \ge 1 - |q_S|$. The remaining puncture factors are bounded on the compact gauge contour under the strict leg bounds. Thus the trinion and four-point sums have geometric majorants, up to finite constants,

$$\sum_{n \ge 0} (n+1)^3 (|t| R_i R_j)^n, \qquad \sum_{n \ge 0} (n+1)^4 (|q_S| R_a R_b R_c R_d)^n. \tag{XVII.5.58}$$

Each converges when its ratio is strictly less than one. The matter products have convergent geometric majorants under the same pair bounds.

The pair bounds control matter products and uniform trinion sums on the contour. The leg bounds control K; the last bound controls the four-point representation sum. In that neighborhood one may integrate term by term by dominated convergence. At external unit modulus every bound follows from $|t| < 1$. Beyond it, pole crossings and contour changes require separate analysis. Roots of unity and $q_S \to 1$ are excluded here. The rational flavor substitutions in the previous section remain legitimate finite polynomial evaluations even when these analytic bounds fail.

We have thus obtained both a direct finite gauge calculation and a diagonal organization of sewing. The protected trace, localization, class-S frame identification and full trinion identity provide the physical and analytic premises. The finite coefficient calculation tests their concrete consequences with labeled punctures. The next chapter changes the question again, identifying the Schur operators with states of a chiral algebra and supplying a new dictionary for the same series.

Exercises

The public problems below distinguish calculable algebra from written physical arguments. For benchmark submissions, see `benchmark/PROTOCOL.md`. Use exact rational expressions and coefficient arrays for the finite answers. Include the requested written arguments.

1. **Selecting letters.** For the four rows of (XVII.5.4) and the vector scalar $(1, 0, 0, 0, -1)$, calculate $(\delta_L, \delta_R, E - R)$ in that order. Expand the half-hyper and vector letters through t^5. Derive their rational forms by summing the derivative towers. Explain why adding the two kernel equations fixes E and why a signed index is not a degeneracy count. Submit the five charge triples and the two arrays in increasing degree starting at degree zero.

2. **Which singlets?** Compute the 6×6 matrix $\int d\mu\, \chi_n \chi_m$ for $0 \le n, m \le 5$ from full Haar constant terms. Separately compute the singlet multiplicities of $\mathbf{2}^{\otimes 4}$ and $\mathrm{Sym}^2(4\mathbf{2})$. Repeat the full and reduced projection on z^2 and explain their difference. Explain why a $U(1)$ projection fails on the adjoint. Submit the pairing matrix, the two counts, and the two values for z^2.

3. **A free trinion.** Derive (XVII.5.25) by exponentiating the logarithm. Recover the quadratic and cubic character decompositions with three independent flavor variables. Submit the dimensions through t^3, then the same coefficients at $(a, b, c) = (2, 3, 5)$ as exact rationals. Explain the derivative contribution at t^3 and translate the K/P leg convention to our normalization. Merely substituting one for every fugacity does not establish the character decomposition.

4. **Two labeled channels.** Construct both pairings in (XVII.5.35) through q_S^2 using letter weights and normalized Haar projection. Submit the coefficient of q_S as a Laurent expression in a, b, c, d, and the arrays of coefficients through q_S^2 at $(2, 3, 5, 7)$ and $(3/2, 4/3, 5/4, 6/5)$, separately for each channel. Keep the labels fixed. Explain why equal unflavored dimensions cannot detect a miswired flavor leg and what a finite match says about the sourced same-theory identification.

5. **Extracting the algebra.** Divide the direct T_2 expansion by three separately expanded K factors through t^4. Use (XVII.5.50) to determine all 27 triples with labels $0, 1, 2$. Submit their coefficient arrays and the metric matrix for labels $0, 1, 2, 3$ through t^4. Prove the valuation cutoff and give the maximum mode for $(p, L) = (1, 6), (2, 6), (2, 8)$. Identify a specific contribution lost by cutting the four-point sum one mode too early. Explain why $p = 0$ evades the argument.

6. **Where sewing converges.** Give sufficient bounds for uniform convergence of the matter factors, puncture factors and four-point representation sum on the unit gauge contour. Apply them first to unit-modulus flavor fugacities, then to $(2, 3, 5, 7)$ and a sufficiently small positive $|t|$. Explain why a formal substitution needs no such choice. Distinguish the protected-trace premise, the analytic trinion identity, the finite coefficient equality and the physical class-S interpretation. State what further work is needed to continue through a pole crossing. This exercise is wholly written.

Sources and scope

§1. The protected trace and deformation invariance are physical inputs `BPS:1/4|idx` under the unitary discrete radial-trace assumptions stated in the text. The fraction labels the protected sector, not the exact preserved fraction of every contributing state. The letter calculation `MATH` is conditional on the retained field content. The Cartan frame and charge tables are those of Gadde et al. 2011a, printed pp. 5–8, Tables 1–2, (2.2)–(2.11), and the Schur specialization on p. 14, (4.12)–(4.14). The variable called t there is u in our generic-letter formulas. The present $t^2 = q_S$ is independent of earlier instanton and plumbing parameters.

§2. The finite character and Haar calculation `MATH` includes labels zero through five. The gauging prescription is a physical localization premise `BPS:1/4|idx`. Its metric is given in Gadde et al. 2011b, printed pp. 1–2, (4)–(8), and Gadde et al. 2011a, pp. 9–11, (3.1)–(3.12). The compact $SU(2)$ group, liftable backgrounds and separately inserted vector factor are retained assumptions.

§3. The displayed series are finite expansions `MATH`. We use the cited derivation of the all-order A_1 identity `MATH`. The T_2 and q-dimension normalizations are in Gadde et al. 2011b, (9)–(12). The alternative leg convention and analytic pole/residue argument occur in Gadde et al. 2011a, (6.11) and Appendix E, printed pp. 50–51, (E.1)–(E.12). That appendix supplies an outlined analytic argument; no independent analytic uniqueness proof is added. The finite fully flavored trinion comparison stops at t^6.

§4. The finite coefficient calculations `MATH` assume the stated letters and gauging prescription. The two-channel comparison covers 820 nonzero Laurent monomials through q_S^3, and the unflavored series separately reaches q_S^5. Euler products and logarithmic recurrence differ, but share the weight generator and normalized projector. Their finite agreement is not an all-order crossing or S-duality proof. The physical two-frame premise is inherited from the A_1 class-S construction of XVI.3. The first coefficient supplies a Lie-algebra branching, without selecting a global flavor form.

§5. The metric, extracted-character and cutoff calculations `MATH` include the stated conditional convergence estimates. The finite comparison treats sixteen metric pairs and 64 extracted trinion triples through t^6. The zero-area q-Yang–Mills sewing prescription `BPS:1/4|idx` is given in Gadde et al. 2011b, (13); its four-dimensional interpretation retains the trace and class-S premises. Stable regular untwisted A_1 surfaces with $2g - 2 + s > 0$ are the scope of the valuation argument. No cap, unstable surface,

unpunctured-torus cutoff, root-of-unity or $q_S \to 1$ extension is supplied. The index is distinct from both the AGT conformal block and a Higgs-branch Hilbert series. The auxiliary discussion of trace scope in Pan and Peelaers 2021, introduction p. 2, imports no closed-form calculation.

The local conventions fix the Schur trace, charge frame, highest-weight labels, normalized Haar measure, half-hyper multiplicity and puncture normalization.

References

Gadde, A. et al. (2011a). “Gauge Theories and Macdonald Polynomials”. In: Inspected arXiv version3. arXiv: `1110.3740 [hep-th]`.

Gadde, A. et al. (2011b). “The 4d Superconformal Index from q-deformed 2d Yang-Mills”. In: Inspected arXiv version1. arXiv: `1104.3850 [hep-th]`.

Pan, Y. and W. Peelaers (2021). “The exact Schur index in closed form”. In: Inspected arXiv version2, introduction only. arXiv: `2112.09705 [hep-th]`.

Chapter XVII.6

Schur operators and vertex operator algebras

The Schur index records protected states, but a trace forgets how their local operators multiply. We now recover an operator product on a plane in four-dimensional spacetime. The mechanism is a twist by $SU(2)_R$: antiholomorphic motion becomes exact under a nilpotent supercharge, leaving meromorphic products of cohomology classes. Free hypermultiplets give symplectic bosons. Conformal gauging then leads to a concrete algebraic problem involving currents and ghosts.

We assume the four-dimensional $\mathcal{N} = 2$ superconformal algebra, radial operator–state correspondence and unitarity. From Volume XVI we need the T_2 half-hyper, conformal gauging, and the anomaly data of T_3. From the preceding chapter we need only the meaning of the signed Schur trace. Our main example is $SU(2)$ with four full fundamental hypermultiplets. We derive its flavor-current OPE and its grade-two affine vacuum quotient. The scalar stress state survives this quotient, although the corresponding classical Higgs-branch scalar vanishes. This difference will make the role of normal ordering concrete.

The final example compares the T_3 protected generators with E_6 currents. Throughout, finite graded computations and physical identifications have separate roles. In particular, agreement through a fixed power of the Schur variable is useful evidence for an identification, but it does not determine an entire vertex operator algebra. We normalize vacuum traces to have constant coefficient one and write the Schur variable as q_S.

XVII.6.1 Cohomology and a holomorphic plane

A protected operator should remain closed under the selected nilpotent supercharge when moved along the plane. Only antiholomorphic motion will be exact; holomorphic derivatives can give distinct cohomology classes. Ordinary translations do not provide this property in both directions. The useful choice combines a spacetime translation with an R-symmetry rotation. Let E be the scaling dimension, R the highest $SU(2)_R$

weight, r the abelian R-charge, and j_L, j_R the highest Lorentz weights. The supercharge and plane generators are

$$\mathbb{Q} = Q^1_- + \widetilde{S}^{2\dot{-}}, \qquad \mathbb{Q}^2 = 0, \qquad L_{-1} = P_{++}, \qquad \widehat{L}_{-1} = P_{--} + R_-. \tag{XVII.6.1}$$

A unit length is implicit when adding Poincare and conformal supercharges. The superconformal algebra gives the following exact charges and positive anticommutator:

$$\{\mathbb{Q}, \mathbb{Q}^\dagger\} = 2\widehat{L}_0, \qquad 2\widehat{L}_0 = E - j_L - j_R - 2R, \qquad Z = r + j_L - j_R = \{\mathbb{Q}, V_Z\}. \tag{XVII.6.2}$$

The twisted translation $\widehat{L}_{-1}$ is also $\mathbb{Q}$-exact. To see what exactness implies, let $A = \{\mathbb{Q}, V\}$ and let $\mathcal{O}$ be closed with eigenvalue a under A. If $a \neq 0$, then

$$A\mathcal{O} = a\mathcal{O}, \quad \mathbb{Q}\mathcal{O} = 0 \quad \Longrightarrow \quad \mathcal{O} = \mathbb{Q}\left(a^{-1} V \mathcal{O}\right). \tag{XVII.6.3}$$

Thus a nonzero class has zero eigenvalues under both exact charges. Positivity of the radial Hilbert space selects harmonic representatives, giving the Schur conditions

$$E - 2R - j_L - j_R = 0, \qquad r + j_L - j_R = 0. \tag{XVII.6.4}$$

This use of positivity is a physical premise. A pair of algebraic charge constraints, without a unitary radial space and the stated adjoint, would not establish the cohomology construction.

The Lorentz frame in the previous chapter used Cartan eigenvalues j_1, j_2. The change of frame is $j_1 = -j_L$, $j_2 = j_R$. Its two index anticommutators become

$$\delta_L = E - 2j_L - 2R - r, \qquad \delta_R = E - 2j_R - 2R + r, \qquad \delta_L = \delta_R = 0 \iff \text{(XVII.6.4)}. \tag{XVII.6.5}$$

The sign change belongs to a Lorentz Cartan; it is not a redefinition of r. Once the charges are fixed, translate a representative by

$$\mathcal{O}(z, \bar{z}) = e^{zL_{-1} + \bar{z}\widehat{L}_{-1}} \mathcal{O}(0), \qquad \partial_{\bar{z}} \mathcal{O}(z, \bar{z}) = \{\mathbb{Q}, \ldots\}. \tag{XVII.6.6}$$

The class is holomorphic even though the chosen representative depends on both coordinates. For an $SU(2)_R$ tensor the twist has an elementary realization:

$$\mathcal{O}(z, \bar{z}) = u_{I_1}(\bar{z}) \cdots u_{I_{2R}}(\bar{z}) \mathcal{O}^{I_1 \cdots I_{2R}}(z, \bar{z}), \qquad u = (1, \bar{z}). \tag{XVII.6.7}$$

The R-symmetry polarization moves as the insertion moves. Figure XVII.6.1 depicts the two motions that enter this formula. The holomorphic weight follows from the untwisted L_0 and the Schur constraint:

$$h = \frac{E + j_L + j_R}{2} = E - R = R + j_L + j_R, \qquad \bar{h} = \frac{E - j_L - j_R}{2} = R. \tag{XVII.6.8}$$

In an OPE channel, R-polarization supplies an antiholomorphic power $R_1 + R_2 - R_k$, while the original spacetime denominator supplies $\bar{h}_1 + \bar{h}_2 - \bar{h}_k$. Their difference vanishes. Channels with nonzero exact-charge eigenvalue disappear in cohomology. This explains why the meromorphic OPE requires the twist, rather than simply evaluating an untwisted correlator at $\bar{z} = 0$.

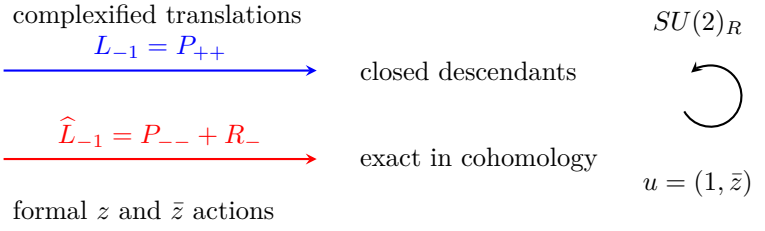


Figure XVII.6.1: The two formal lanes show complexified translation actions, rather than displacements along real coordinate axes. Holomorphic motion uses P_{++} and can create new closed descendants. Antiholomorphic motion combines P_{--} with R_{-} and is exact on closed operators. The separate rotation records the R-symmetry polarization u.

For a free hyper let $Q, \widetilde{Q}$ have the two equal scalar propagators $1/[(z-w)(\bar{z}-\bar{w})]$. The polarized combinations and their contraction are

$$X = Q + \bar{z}\widetilde{Q}^*, \quad Y = \widetilde{Q} - \bar{z}Q^*, \qquad X(z)Y(w) \sim \frac{\bar{z}-\bar{w}}{(z-w)(\bar{z}-\bar{w})} = \frac{1}{z-w}. \tag{XVII.6.9}$$

Reversing the fields reverses the numerator, so $Y(z)X(w) \sim -1/(z-w)$. The fields are bosonic, despite their half-integral holomorphic weight. For comparison, a moment map has $(E, R) = (2, 1)$ and $h = 1$. The R-current component $J_R^{11}{}_{++}$ has $(E, R, j_L, j_R) = (3, 1, \frac{1}{2}, \frac{1}{2})$ and $h = 2$. A Coulomb primary with $E = 2$ and all other displayed charges zero fails the first Schur condition.

The same twist explains the behavior of a product of highest-weight operators. Suppose the OPE has a Schur channel $\mathcal{O}_k$ of R-spin R_k. Contracting the R-indices with the two polarizations produces a factor determined by the invariant antisymmetric tensor:

$$\epsilon^{IJ} u_I(\bar{z}) u_J(\bar{w}) = \bar{w} - \bar{z}, \qquad n_{12k} = R_1 + R_2 - R_k. \tag{XVII.6.10}$$

There are n_{12k} contractions between the two insertions. The remaining indices form the polarization of the outgoing operator. The spacetime coefficient has the corresponding power

$$\frac{(\bar{z}-\bar{w})^{n_{12k}}}{(\bar{z}-\bar{w})^{\bar{h}_1+\bar{h}_2-\bar{h}_k}} = 1, \qquad \bar{h}_i = R_i. \tag{XVII.6.11}$$

Overall signs depend on the chosen epsilon convention, as the scalar example shows, but the cancellation of powers does not. This computation also clarifies the locality statement. We restrict insertion points to a plane, take cohomology classes of the twisted operators there, and use their ordinary four-dimensional OPE at separated points before passing to classes. We have not constructed a separate unitary two-dimensional Hilbert space by dimensional reduction. The antiholomorphic generator acts trivially in cohomology, while the holomorphic one still translates the surviving operators and creates their derivatives.

The trace therefore retains the physical fermion parity $(-1)^F$ inherited from four dimensions, with F denoting fermion number modulo two:

$$\chi_{\mathrm{vac}}(q_S) = \mathrm{Tr}_{H_{\mathbb{Q}}}(-1)^F q_S^{L_0}, \qquad \chi_{\mathrm{vac}}(0) = 1, \qquad (-1)^F \neq (-1)^{2h} \text{ in general.} \tag{XVII.6.12}$$

For a bosonic hyper scalar the two signs already differ. No factor $q_S^{-c/24}$ is included. Exercise 1 practices both the charge-frame translation and the propagator cancellation.

XVII.6.2 Stress tensors, currents and anomalies

Which four-dimensional operators become the two-dimensional stress tensor and flavor currents? The stress tensor comes from the R-current multiplet, rather than from restricting the four-dimensional stress tensor itself. Denote the twisted R-current component by $\mathcal{R}$, and a twisted flavor moment map by M^a. In the source normalization the central and quadratic poles of the first OPE are

$$\mathcal{R}(z)\mathcal{R}(0) \sim -\frac{3c_4}{2\pi^4 z^4} - \frac{\mathcal{R}(0)}{\pi^2 z^2} + \cdots . \tag{XVII.6.13}$$

Set $T = A\mathcal{R}$. Requiring the quadratic pole to be $2T$ determines A, and its fourth-order pole then determines the central charge:

$$-\frac{A}{\pi^2} = 2 \quad \Longrightarrow \quad A = -2\pi^2, \qquad A^2\left(-\frac{3c_4}{2\pi^4}\right) = -6c_4 = \frac{c_2}{2}. \tag{XVII.6.14}$$

Consequently the stress OPE and anomaly map are

$$T(z)T(0) \sim \frac{c_2}{2z^4} + \frac{2T(0)}{z^2} + \frac{\partial T(0)}{z}, \qquad T = -2\pi^2[\mathcal{R}], \qquad c_2 = -12c_4. \tag{XVII.6.15}$$

The derivative coefficient uses the source's conformal and Bose-symmetry argument. Rescaling the two displayed poles alone does not establish the action on every Schur class. The adopted source discusses the boundary of a universal proof; below we calculate the action explicitly for free fields.

For flavor currents use long roots of squared length two and structure constants in a Hermitian basis. The adjoint indices are a, b, c, and B^{ab} is the normalized invariant Lie-algebra bilinear form in that basis. The supplied moment-map OPE is

$$M^a(z)M^b(0) \sim -\frac{k_4 B^{ab}}{16\pi^4 z^2} + \frac{\sqrt{2}\, i f^{ab}{}_c M^c(0)}{4\pi^2 z}. \tag{XVII.6.16}$$

Writing $\mathcal{J}^a = CM^a$, the simple pole fixes C. Substitution into the double pole gives

$$\frac{C\sqrt{2}}{4\pi^2} = 1 \implies C = 2\sqrt{2}\pi^2, \qquad C^2\frac{-k_4}{16\pi^4} = -\frac{k_4}{2} = k_2. \tag{XVII.6.17}$$

Thus the local algebra has negative level when its unitary parent has positive flavor anomaly. This is consistent: the twisted two-dimensional adjoint is not the physical four-dimensional unitary adjoint. Figure XVII.6.2 records the two operator maps.

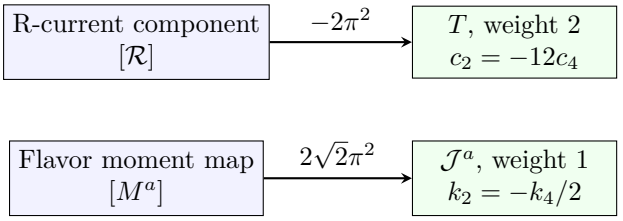


Figure XVII.6.2: Two different protected multiplets supply the stress tensor and flavor currents. The numerical rescalings fix their OPE conventions. The lower labels are anomaly maps, not equalities between four-dimensional anomaly coefficients and two-dimensional Hilbert-space norms.

The anomaly formula from Volume XVI provides a convenient first calculation. A free hyper has effective $(n_v, n_h) = (0, 1)$; the interacting T_3 has sourced effective data, rather than a literal collection of free multiplets. In either case the arithmetic is

$$c_4 = \frac{2n_v + n_h}{12}, \qquad c_2 = -(2n_v + n_h), \qquad k_2 = -\frac{k_4}{2}. \tag{XVII.6.18}$$

The relevant examples are

	n_v	n_h	c_4	c_2	$k_4 \longmapsto k_2$
H	0	1	1/12	-1	none
T_2	0	4	1/3	-4	$4 \longmapsto -2$ ($SU(2)$)
$SU(2)$, $N_f = 4$	3	8	7/6	-14	$4 \longmapsto -2$ ($\mathfrak{so}_8$)
T_3	5	16	13/6	-26	$6 \longmapsto -3$ ($\mathfrak{e}_6$)

(XVII.6.19)

Adding one neutral full hyper increases c_4 by 1/12 and lowers c_2 by one. It does not change a flavor level for a group under which the added hyper is neutral. This changed input tests why a central charge and a particular current level are independent data.

It is useful to test the rescaling directly on a correlator. With the normalizations just fixed, a flavor-current two-point function and the stress two-point function are

$$\langle \mathcal{J}^a(z)\mathcal{J}^b(0)\rangle = -\frac{k_4 B^{ab}}{2z^2}, \qquad \langle T(z)T(0)\rangle = -\frac{6c_4}{z^4}. \tag{XVII.6.20}$$

For $SU(2)$ with four flavors these have coefficients -2 in an orthonormal flavor basis and -7 for the stress tensor. The second coefficient will be an independent diagnostic of the retained scalar in the finite affine calculation. In particular, a scalar of negative norm can be nonzero: nonunitarity in the twisted algebra invalidates an argument that would identify vanishing norm with vanishing state without further hypotheses. Conversely, the stress state here has manifestly nonzero pairing, so no such subtlety is needed to prove its survival. Keeping the two-point normalization visible prevents a representation-dimension subtraction from being mistaken for an operator calculation.

A current algebra itself has a candidate stress tensor away from critical level. Write k for its affine level and $h^\vee$ for the dual Coxeter number of its Lie algebra $\mathfrak{g}$. With B_{ab}

inverse to B^{ab}, commuting the modes through its normal-ordered quadratic expression gives

$$T_{\mathrm{Sug}} = \frac{B_{ab} : \mathcal{J}^a \mathcal{J}^b :}{2(k + h^\vee)}, \qquad c_{\mathrm{Sug}} = \frac{k \dim \mathfrak{g}}{k + h^\vee}, \qquad k \neq -h^\vee. \tag{XVII.6.21}$$

The shift $h^\vee$ is the adjoint-contraction contribution to the single-current OPE; omitting it would give the wrong conformal weight for the currents. For our two comparators,

$$\frac{(-2)28}{-2+6} = -14, \qquad \frac{(-3)78}{-3+12} = -26. \tag{XVII.6.22}$$

These agree with the anomaly images. Equality of central charges alone does not identify stress classes in a nonunitary algebra. For the gauge example the adopted source makes the difference between the total and Sugawara stress tensors BRST-exact. For T_3 its protected unitarity-bound argument supplies the stress identification. These physical inputs supplement, rather than follow from, the arithmetic in (XVII.6.22). Exercise 2 asks the reader to separate the rescaling calculation from this operator statement.

XVII.6.3 Free fields and conformal gauging

We now construct the OPE rather than infer it from anomaly coefficients. A half-hyper in a pseudoreal complex representation $\mathcal{V}$ supplies $\dim_{\mathbb{C}} \mathcal{V}$ commuting fields with an antisymmetric pairing. For T_2, the representation is $(\mathbf{2}, \mathbf{2}, \mathbf{2})$, so

$$q^{abc}(z) q^{a'b'c'}(w) \sim \frac{\epsilon^{aa'} \epsilon^{bb'} \epsilon^{cc'}}{z - w}, \qquad \Omega = \epsilon \otimes \epsilon \otimes \epsilon, \quad \Omega^2 = -1. \tag{XVII.6.23}$$

There are eight fields and four symplectic pairs. Each pair has $XY \sim 1/(z-w)$ and $YX \sim -1/(z-w)$. Choose its stress tensor to be

$$T_{\mathrm{pair}} = \frac{1}{2}\big(: X\partial Y : - : \partial X Y :\big), \qquad \partial_z^a \partial_w^b \frac{1}{z-w} = \frac{(-1)^a (a+b)!}{(z-w)^{a+b+1}}. \tag{XVII.6.24}$$

The sign in the reversed OPE is needed even though the fields commute. Wick contraction in the first term of $T(z)X(w)$ gives $X(z)/[2(z-w)^2]$. The second term gives $\partial X(z)/[2(z-w)]$. Expanding the field at z about w yields

$$T(z)X(w) \sim \frac{X(w)}{2(z-w)^2} + \frac{\partial X(w)}{2(z-w)} + \frac{\partial X(w)}{2(z-w)} = \frac{X/2}{(z-w)^2} + \frac{\partial X}{z-w}. \tag{XVII.6.25}$$

The Taylor term supplies half the translation pole. For Y the reversed symplectic sign gives the same weight. To calculate the central charge, put $A =: X\partial Y :$ and $D =: \partial X Y :$. The four double contractions give respectively $1, 2, 2, 1$ in units of $(z-w)^{-4}$, hence

$$[T(z)T(w)]_{\mathrm{double}} = \frac{1 - 2 - 2 + 1}{4(z-w)^4} = -\frac{1}{2(z-w)^4}, \qquad c_{\mathrm{pair}} = -1. \tag{XVII.6.26}$$

The single contractions, with their Taylor expansions, recombine into $2T/(z-w)^2 + \partial T/(z-w)$. Thus four pairs reproduce $c(T_2) = -4$. For quadratic currents associated to matrices t, u on the symplectic representation, the two contractions similarly give

$$kB(t,u) = -\frac{1}{2}\,\mathrm{tr}_{\mathcal{V}}(tu). \tag{XVII.6.27}$$

At one T_2 puncture the other two doublets supply multiplicity four. In the Chevalley normalization $B(e,f) = 1$, $\mathrm{tr}_{\mathcal{V}}(ef) = 4$, so the puncture level is -2.

Gluing two T_2 blocks gauges a diagonal $SU(2)$. Equivalently, write eight half-doublets as X_i, Y_i, $i = 1, \dots, 8$. The gauge currents are

$$e = \frac{1}{2}\sum_i :Y_i^2:, \qquad f = -\frac{1}{2}\sum_i :X_i^2:, \qquad h = \sum_i :X_iY_i: . \tag{XVII.6.28}$$

For example, the two cross-contractions of Y_i^2 with X_i^2 give $-1/2$ per half-doublet after including the prefactors. The four single contractions give $:X_iY_i:/(z-w)$. Summing produces

$$\begin{aligned} e(z)f(w) &\sim -\frac{4}{(z-w)^2} + \frac{h}{z-w}, \\ h(z)h(w) \sim -\frac{8}{(z-w)^2}, \quad h(z)e(w) &\sim \frac{2e}{z-w}, \quad h(z)f(w) \sim -\frac{2f}{z-w}. \end{aligned} \tag{XVII.6.29}$$

Thus $k_{\mathrm{matter}} = -4$ with $B(h,h) = 2$. This is a gauge-current level; the surviving $\mathfrak{so}_8$ flavor level below is -2.

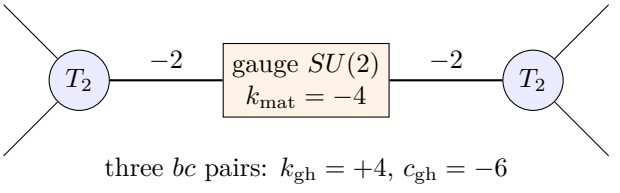


Figure XVII.6.3: Two T_2 systems contribute level -2 each at their shared $SU(2)$ puncture. Gauging introduces three fermionic bc pairs. Their adjoint contribution cancels the matter gauge anomaly. The four external punctures remain flavor data.

Introduce fermionic ghosts of weights $(1,0)$, one pair per gauge generator. Their stress tensor and central charge are

$$b_A(z)c^B(w) \sim \frac{\delta_A{}^B}{z-w}, \qquad T_{\mathrm{gh}} = -:b_A\partial c^A:, \qquad c_{\mathrm{gh}} = -2\dim\mathfrak{su}_2 = -6. \tag{XVII.6.30}$$

The small algebra is generated by b and ∂c. Unrestricted c_0 states are excluded; the relative complex further imposes $b_0^A = 0$ and total gauge invariance. These conditions matter both for the trace and for the cohomology problem.

The adjoint matrices obey the three Chevalley brackets. Explicitly, $[\operatorname{ad} h, \operatorname{ad} e] = 2 \operatorname{ad} e$ and $[\operatorname{ad} h, \operatorname{ad} f] = -2 \operatorname{ad} f$. The remaining bracket is $[\operatorname{ad} e, \operatorname{ad} f] = \operatorname{ad} h$. Their traces give

$$\operatorname{tr}_{\mathrm{adj}}(\operatorname{ad} e \operatorname{ad} f) = 4, \qquad \operatorname{tr}_{\mathrm{adj}}(\operatorname{ad} h)^2 = 8, \qquad k_{\mathrm{gh}} = 2h^\vee = 4. \tag{XVII.6.31}$$

The ghost trace can be checked with three small matrices rather than a general formula. In the ordered adjoint basis (e, h, f), the nonzero actions are

$$\operatorname{ad} e : h \mapsto -2e, \ f \mapsto h; \qquad \operatorname{ad} f : e \mapsto -h, \ h \mapsto 2f; \qquad \operatorname{ad} h = \operatorname{diag}(2, 0, -2). \tag{XVII.6.32}$$

The product $\operatorname{ad} e \operatorname{ad} f$ maps e to $2e$, h to $2h$ and f to zero. Its trace is four, while the square of the displayed diagonal matrix has trace eight. Their ratio reproduces $B(h,h)/B(e,f) = 2$. Checking the bracket on these matrices is necessary: a generic collection of matrices obeys an associative-matrix Jacobi identity even when it fails to represent the declared Lie algebra. Here the explicit actions verify the required representation before the ghost central term is used.

The BRST current includes half the ghost current. In its square the cubic-ghost terms cancel by Jacobi, while the double contractions leave

$$j_{\mathrm{B}} = c^A (J_A + \tfrac{1}{2} J_{\mathrm{gh},A}), \qquad Q_{\mathrm{B}}^2 = \frac{k_{\mathrm{matter}} + 2h^\vee}{2} \oint B(\partial c, c) = 0. \tag{XVII.6.33}$$

The contour denotes a residue. For m half-doublets the coefficient before the overall half is $4 - m/2$. Removing one full flavor gives $m = 6$, level -3 and obstruction $+1$. The four-dimensional comparison is

$$b_0 = 2h^\vee - \frac{k_{4,\mathrm{gauge}}}{2} = 4 - \frac{8}{2} = 0, \qquad c_{\mathrm{total}} = -8 - 6 = -14. \tag{XVII.6.34}$$

Algebraic nilpotence is established by this anomaly cancellation. The physical identification with all-order Schur cohomology additionally uses the adopted source's assumption that there is no further higher-order lifting. We use that physical prescription without turning the finite calculation into a computation of the complete relative cohomology. Exercise 3 tests the Wick and anomaly steps separately.

XVII.6.4 The so8 algebra of four-flavor SU2

The gauge-invariant bilinears already reveal the flavor algebra. Define $J_{ji} = -J_{ij}$ and use real antisymmetric matrices $M_{ij} = E_{ij} - E_{ji}$, where E_{ij} has its only nonzero entry, one, at row i and column j. Direct contraction gives

$$J_{ij} = -:X_i Y_j - Y_i X_j:, \qquad B(M_{ij}, M_{kl}) = \tfrac{1}{2} \operatorname{tr}(M_{ij} M_{kl}) = -(\delta_{ik}\delta_{jl} - \delta_{il}\delta_{jk}), \tag{XVII.6.35}$$

$$J_{ij}(z) J_{kl}(w) \sim \frac{2(\delta_{ik}\delta_{jl} - \delta_{il}\delta_{jk})}{(z-w)^2} + \frac{\delta_{jk} J_{il} - \delta_{ik} J_{jl} - \delta_{jl} J_{ik} + \delta_{il} J_{jk}}{z - w}. \tag{XVII.6.36}$$

For instance $J_{12}J_{12}$ has double pole $+2$, $J_{12}J_{23}$ has single pole J_{13}, and $J_{12}J_{34}$ is regular. Since the real metric is negative, the level is -2. Multiplying by i gives Hermitian

currents $\mathcal{J}_{ij} = iJ_{ij}$ with double pole -2. This basis change does not determine a global flavor-group quotient.

The classical Higgs quotient and the affine quotient have different scalar relations. Let x_i, y_i be the commuting classical scalar coordinates corresponding to X_i, Y_i. Set $m_{ij} = -(x_i y_j - y_i x_j)$. Decomposability gives seventy Pluecker components, and multiplication gives the symmetric contraction:

$$\begin{aligned} m_{ij}m_{kl} - m_{ik}m_{jl} + m_{il}m_{jk} &= 0, \\ \sum_l m_{il}m_{jl} = x_i x_j \sum_l y_l^2 + y_i y_j \sum_l x_l^2 - (x_i y_j + y_i x_j) \sum_l x_l y_l. & \end{aligned} \tag{XVII.6.37}$$

The three sums on the right are gauge moment maps. Setting them to zero removes the symmetric traceless 35 and its scalar trace. Thus the classical degree-four count is $406 - 70 - 35 - 1 = 300$. These identities explain the finite-degree count; they alone do not prove an arbitrary-degree ideal presentation.

Now perform the affine calculation. Its input is the mode commutator and vacuum condition

$$[J_m^a, J_n^b] = f^{ab}{}_c J_{m+n}^c + mkB^{ab}\delta_{m+n,0}, \qquad J_n^a|0\rangle = 0 \quad (n \geq 0). \tag{XVII.6.38}$$

At grade two choose the Poincare–Birkhoff–Witt basis

$$\mathcal{B}_2 = \{J_{-2}^a|0\rangle\}_{a=1}^{28} \cup \{J_{-1}^a J_{-1}^b|0\rangle\}_{a\leq b}, \qquad \dim \mathcal{B}_2 = 28 + \frac{28\cdot 29}{2} = 434. \tag{XVII.6.39}$$

Every matrix entry is obtainable by commuting positive modes to the right. To make the construction reproducible, put $C^{ab} = kB^{ab}$. The derivative block is $2C^{ab}$, the mixed block is $f^{ab}{}_e C^{ec}$, and the product block is

$$\langle 0|J_1^b J_1^a J_{-1}^c J_{-1}^d|0\rangle = C^{ac}C^{bd} + C^{ad}C^{bc} + f^{ac}{}_e f^{ed}{}_g C^{bg}. \tag{XVII.6.40}$$

For example J_1^a crossing J_{-1}^c supplies C^{ac} and $f^{ac}{}_e J_0^e$; the latter acts on the next current and produces the last term. This explains each summand. Row signs converting the real-basis pairing to the usual contravariant form do not alter its rank or right kernel.

Construct explicit relation columns using $A \odot B = A_{-1}B_{-1}|0\rangle + B_{-1}A_{-1}|0\rangle$:

$$W_{ijkl} = J_{ij} \odot J_{kl} - J_{ik} \odot J_{jl} + J_{il} \odot J_{jk}, \qquad S_{ij} = \sum_l J_{il} \odot J_{lj}. \tag{XVII.6.41}$$

Take all W for $i<j<k<l$, all S_{ij} for $i<j$, and $S_{ii} - S_{88}$ for $i = 1, \ldots, 7$. There are $70 + 28 + 7 = 105$ columns. Reordering a symmetrized product uses the commutator: for $a < b$, it is $2J_{-1}^a J_{-1}^b - f^{ab}{}_c J_{-2}^c$. Dropping the derivative correction changes the matrix problem.

One relation can be followed without handling all 434 rows. Disjoint current pairs commute, so

$$\begin{aligned} W_{1234} &= 2(J_{12,-1}J_{34,-1} - J_{13,-1}J_{24,-1} + J_{14,-1}J_{23,-1})|0\rangle, \\ \langle 0|J_{34,1}J_{12,1}W_{1234}\rangle &= 2k(k+2). \end{aligned} \tag{XVII.6.42}$$

Indeed, the first product contributes $2k^2$ and the two crossed products contribute $2k$ each, using (XVII.6.40). At $k=-2$ the result vanishes; at $k=-1$ it equals -2. Thus the relation depends on the level, rather than only on the classical representation decomposition.

Let G be the integer pairing matrix at $k=-2$ and R its 105-column relation matrix. Exact multiplication and finite-field row reduction give

$$GR=0 \text{ over } \mathbb{Z}, \qquad \operatorname{rank}_{\mathbb{F}_{1000003}} R=105, \qquad \operatorname{rank}_{\mathbb{F}_{1000003}} G=329. \tag{XVII.6.43}$$

To reproduce the reduction, scan columns for a nonzero pivot, multiply its row by the inverse of the pivot modulo the prime, and subtract multiples from all remaining rows. A nonzero minor modulo the prime is a nonzero integer minor. Hence the modular rank supplies a rational lower bound. The independent exact columns supply the upper bound:

$$329 \le \operatorname{rank}_{\mathbb{Q}} G \le 434-\operatorname{rank}_{\mathbb{Q}} R \le 434-105=329. \tag{XVII.6.44}$$

This closes an exact rank proof; modular rank alone would not. Grade one has nondegenerate central form, so there are no lower-grade nulls. The resulting grade-two null directions are the seventy four-forms and thirty-five symmetric traceless states. The four-forms split into two 35 representations upon choosing a Hodge orientation. The scalar is tested by a nonzero norm. In the Hermitian basis,

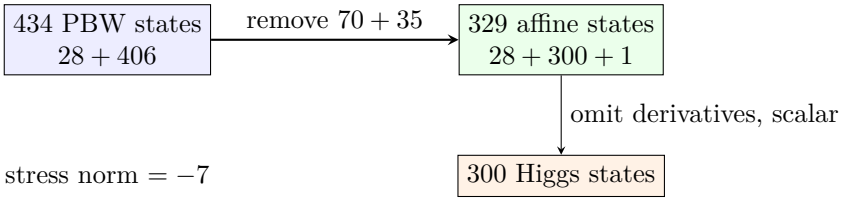


Figure XVII.6.4: The grade-two affine basis has 28 derivatives and 406 quadratic states. The exact kernel removes 105 quadratic directions and retains 300 nonsinglets plus the stress singlet. The classical Higgs quotient additionally removes that singlet and has no derivative contribution at this degree.

$$T_{\mathrm{Sug}}=\frac{1}{8}\sum_{i<j}:\mathcal{J}_{ij}\mathcal{J}_{ij}:, \qquad \langle T_{\mathrm{Sug}}|T_{\mathrm{Sug}}\rangle=\frac{c_2}{2}=-7, \qquad 434-105=28+300+1=329. \tag{XVII.6.45}$$

Deleting the classical scalar in the VOA would instead give 328. The source's BRST-exact stress relation identifies the retained class with the total stress tensor; the pairing itself proves its survival in this finite affine quotient.

There is a separate trace computation. Put $t^2=q_S$ and project the small-field Fock trace to $SU(2)$ singlets:

$$\begin{aligned}\mathrm{CT}_z(1-z^2)\prod_{n\ge 0,\ s=\pm 1}(1-t^{2n+1}z^s)^{-8}\prod_{n\ge 1,\ w=0,\pm 2}(1-t^{2n}z^w)^2 \\ =1+28q_S+329q_S^2+2632q_S^3+O(q_S^4).\end{aligned} \tag{XVII.6.46}$$

Here CT extracts the constant term. The Weyl factor is essential; the integrand's inversion symmetry allows this form of the $SU(2)$ Haar projection. It is not an unrestricted abelian projection. The final coefficient is an Euler trace, not an independently calculated affine grade-three dimension.

One can reproduce the first trace coefficient without multiplying the full infinite product. At order t^2, the bosonic letters supply $\mathrm{Sym}^2(\mathbf{2}\otimes\mathbf{8})$, whereas the two ghost towers start with two gauge adjoints and are removed by singlet projection. The elementary tensor identity is

$$\mathrm{Sym}^2(U\otimes V)=(\mathrm{Sym}^2 U\otimes \mathrm{Sym}^2 V)\oplus(\wedge^2 U\otimes\wedge^2 V). \tag{XVII.6.47}$$

For $U=\mathbf{2}$ of $SU(2)$ only $\wedge^2 U=\mathbf{1}$ is a singlet, leaving $\wedge^2\mathbf{8}=\mathbf{28}$. This recovers the currents at grade one directly from the gauge letters. At grade two the derivatives of those currents must be included as well as quadratic products. The affine pairing then supplies the relations among the latter. This separation explains the first A term in the flavored formula below: a calculation that keeps only symmetric current products misses all 28 derivative states even before it considers the scalar.

Retaining all four flavor Cartans strengthens the grade-two comparison. For vector character $V(\boldsymbol{x})=\sum_{i=1}^{4}(x_i+x_i^{-1})$, let $A=\wedge^2 V$ be the adjoint character. For a weight tuple $w=(w_1,\dots,w_4)$, write $\boldsymbol{x}^w=\prod_i x_i^{w_i}$ and denote its multiplicity by m_w. Let u be a formal variable recording the selected symmetric or exterior degree. Symmetric and exterior powers can be calculated by the generating functions $\prod_w(1-u\boldsymbol{x}^w)^{-m_w}$ and $\prod_w(1+u\boldsymbol{x}^w)^{m_w}$. The full result is

$$[q_S^2]\chi=A+\mathrm{Sym}^2 A-\wedge^4 V-\mathrm{Sym}^2 V+1,\qquad [q_S^2]\chi(1)=28+406-70-36+1=329. \tag{XVII.6.48}$$

The gauge product and this polynomial agree at every one of their 169 supported Laurent monomials, including the zero-weight monomial with multiplicity seventeen. This compares representations, rather than only dimensions. The independent affine result stops at grade two. The inspected source's all-grade $\widehat{\mathfrak{so}}_{8-2}$ identification is its Conjecture 1; neither the finite comparison nor the Euler trace resolves that stronger physical statement. Exercises 4 and 5 isolate the signs, scalar state and rank argument.

XVII.6.5 T3 and the E6 comparison

The T_3 theory supplies a useful non-Lagrangian comparison. Its effective anomaly data $(n_v,n_h)=(5,16)$ and enhanced E_6 flavor symmetry are physical inputs from Volume XVI. They yield

$$c_4=\frac{2\cdot 5+16}{12}=\frac{13}{6},\qquad c_2=-26,\qquad k_{4,E_6}=6,\qquad k_{2,E_6}=-3. \tag{XVII.6.49}$$

To test the Sugawara comparison we need the actual root data. Label the simple roots $\alpha_0,\dots,\alpha_5$, with edges 0–1–2–3–4 and 2–5, and squared lengths two. In this basis a root is an integer six-vector v, with Cartan matrix C. Write e_i for the ith coordinate unit vector and $\mathrm{ht}(v)=\sum_i v_i$ for its height in the simple-root basis. Reflection in the ith

simple root acts by

$$C_{ii} = 2, \quad C_{ij} = -1 \text{ on edges}, \quad C_{ij} = 0 \text{ otherwise}, \qquad s_i(v) = v - (Cv)_i e_i. \tag{XVII.6.50}$$

Starting with the six positive and six negative simple roots, repeatedly apply these six maps until the set closes. For example $s_1(e_0) = e_0 + e_1$, and $s_2(e_0 + e_1) = e_0 + e_1 + e_2$. The generated set contains 72 roots, 36 with nonnegative coefficients. Its highest positive root and consequences are

$$\begin{aligned} \theta = (1,2,3,2,1,2), \quad \operatorname{ht}\theta = 11, \quad h^\vee = 1 + \operatorname{ht}\theta = 12, \\ \dim E_6 = 72 + 6 = 78, \quad c_{\mathrm{Sug}} = \frac{-3 \cdot 78}{-3 + 12} = -26. \end{aligned} \tag{XVII.6.51}$$

The equality of dual Coxeter number and Coxeter number uses the simply laced root system. This method also detects an incorrect graph: changing an edge changes the reflection orbit and hence invalidates the root enumeration used in the comparator.

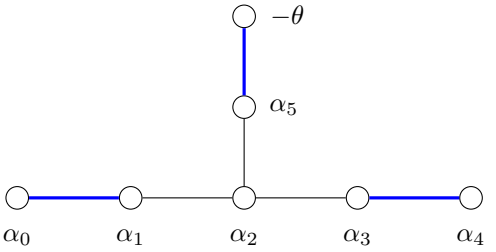


Figure XVII.6.5: The extended E_6 diagram makes three commuting A_2 pairs visible: (α_0, α_1), (α_3, α_4) and $(\alpha_5, -\theta)$. Each pair is an arm of the affine diagram; the central node α_2 joins them. The algebraic embedding uses the roots, rather than a count of nodes alone.

We can now test how the adjoint branches under the three puncture algebras. Choose the three pairs of simple roots indicated in the figure. The Dynkin labels of a root v in an A_2 factor are its inner products with that pair. Before an orientation change on the last two factors, the projection is

$$\lambda(v) = \big((Cv)_0, (Cv)_1;\ (Cv)_3, (Cv)_4; (Cv)_5, -v^T C\theta\big). \tag{XVII.6.52}$$

Project all 72 roots and include six zero weights for the Cartan. In A_2 Dynkin coordinates the fundamental weights form the multiset

$$\begin{aligned} F &= \{(1,0), (-1,1), (0,-1)\}, \qquad \overline{F} = -F, \\ \mathrm{wt}(\mathbf{8}) &= \{(2,-1), (-1,2), (1,1),\ \text{negatives}, 0, 0\}. \end{aligned} \tag{XVII.6.53}$$

These lists allow the branching to be reproduced by additions and Cartesian products of small sets. Reverse the fundamental orientation on the last two factors. The projection

is compared as a full multiset, with multiplicities retained at zero as well as at nonzero weights. The complete multiset identity is

$$\mathbf{78} = (\mathbf{8},\mathbf{1},\mathbf{1}) + (\mathbf{1},\mathbf{8},\mathbf{1}) + (\mathbf{1},\mathbf{1},\mathbf{8}) + (\mathbf{3},\mathbf{3},\mathbf{3}) + (\overline{\mathbf{3}},\overline{\mathbf{3}},\overline{\mathbf{3}}). \tag{XVII.6.54}$$

There are 73 distinct projected weights: 72 nonzero weights of multiplicity one, and the zero weight of multiplicity six. The three adjoints contribute their eighteen roots and six Cartan states; the two trifundamentals contribute 54 weights. Comparing these multisets tests the embedding more strongly than the dimension identity $24 + 27 + 27 = 78$.

For a concrete projection check, apply the formula to $v = \alpha_0$. Its labels are $(2, -1; 0, 0; 0, 0)$, one of the six nonzero weights of the first puncture adjoint. For $v = \alpha_2$, the unmodified labels are $(0, -1; -1, 0; -1, 0)$. Complex conjugating the final two factors changes the second and third pairs by $(a, b) \mapsto (-a, -b)$, giving

$$\lambda'(\alpha_2) = (0, -1; 1, 0; 1, 0) \in F \times F \times F. \tag{XVII.6.55}$$

Its negative belongs to the conjugate trifundamental. These two checks locate both an adjoint sector and a sector joining all three punctures. To perform the complete comparison, store each projected six-tuple together with its multiplicity, then form the three adjoint multisets and the two Cartesian products of F and $\overline{F}$. Equality means matching the multiplicity at each tuple, including the six copies at zero. A count of 78 without this comparison would not rule out a different embedding or an incorrect choice of fundamental orientation.

The physical assignment of these representations comes from the protected T_N generators. The three puncture moment maps give the adjoints. The additional generators $Q_{(r)}$, with label $r = 1, \ldots, N-1$ distinct from the earlier abelian R-charge, have the supplied quantum numbers

$$E[Q_{(r)}] = r(N-r), \qquad R[Q_{(r)}] = \frac{r(N-r)}{2}, \qquad h[Q_{(r)}] = \frac{r(N-r)}{2}. \tag{XVII.6.56}$$

At $N = 3$, both $r = 1, 2$ give $h = 1$, so the two trifundamentals can join the 24 puncture currents into the 78 enhanced currents. Changing the input to $N = 4$ instead gives

$$(h[Q_{(1)}], h[Q_{(2)}], h[Q_{(3)}]) = \left(\frac{3}{2}, 2, \frac{3}{2}\right). \tag{XVII.6.57}$$

They cannot be extra dimension-one currents. This comparison explains why the enhancement mechanism at T_3 does not follow merely from having three maximal punctures for general N.

Each puncture $SU(3)$ is at level -3, precisely its critical level. Its individual Sugawara tensor is therefore undefined:

$$k_{SU(3)} + h^\vee_{SU(3)} = -3 + 3 = 0, \qquad k_{E_6} + h^\vee_{E_6} = -3 + 12 = 9. \tag{XVII.6.58}$$

The full enhanced algebra is noncritical. Summing three puncture Sugawara expressions would miss this distinction and has no finite meaning. The valid comparator uses the full E_6 current algebra.

One further finite root calculation is possible. The Weyl dimension product for highest weight 2θ gives

$$\dim V(2\theta) = \prod_{\alpha>0} \frac{(2\theta,\alpha) + \operatorname{ht}\alpha}{\operatorname{ht}\alpha} = 2430, \qquad \text{(XVII.6.59)}$$

$$\operatorname{Sym}^2 \mathbf{78} \text{ has dimension } 3081 = 1 + 650 + 2430.$$

This does not construct 650 null vectors or an exceptional vacuum character. The adopted source presents the T_3 affine identification as Conjecture 4. That label describes the inspected source's claim; it is not a verdict on the status of every subsequent mathematical result.

Finally place this construction alongside the preceding two-dimensional descriptions. The Schur VOA lives on a plane in spacetime and organizes local OPEs. AGT Liouville or Toda theory is organized on the ultraviolet curve and computes Omega-background conformal blocks. The index gluing TQFT organizes the protected trace by representations on that curve. A VOA character can equal the Schur trace computed by gluing, while its local algebra remains a different object. Exercise 6 asks the reader to track both the root calculation and these different physical roles.

Exercises

For benchmark submissions, see `benchmark/PROTOCOL.md`. Use rational numbers or arithmetic strings for the finite answers. Include the written arguments below.

1. Translate the previous chapter's Lorentz Cartans into the highest-weight frame. For a hyper scalar, moment map, retained R-current, and $E = 2$ Coulomb primary, compute $E - 2R - j_L - j_R$ and $h = E - R$. Identify the rejected operator. Starting with the two scalar propagators, derive both ordered cross-contractions of X, Y. Explain why setting $\bar{z} = 0$ before twisting loses the cancellation, and identify where positivity entered the cohomological argument. Compare the hyper scalar's physical fermion parity with $(-1)^{2h}$. Submit the four defects and four weights, and the two OPE signs.

2. Starting from the unrescaled OPE coefficients in this chapter, solve for the stress and current rescalings and recover the central maps. Evaluate c_2 for $(n_v, n_h) = (3, 8)$ and $(3, 9)$, and evaluate k_2 for $k_4 = 4, 6$. Calculate the $\mathfrak{so}_8$ Sugawara central charge at levels -2 and -1. Explain why its agreement with the total central charge at the first level does not itself identify stress classes. Submit the two central charges, two levels, and two Sugawara values.

3. Reproduce $T(z)X(w)$ including the Taylor term, and the four double contractions of $T(z)T(w)$. For eight and six half-doublets compute the gauge level, the ef double pole, and $k_{\text{matter}} + 4$. Derive the adjoint trace giving the ghost contribution, and explain why unrestricted c_0 states are excluded. State the physical no-additional-lifting assumption separately from nilpotence. Submit the weight, translation-pole coefficient, pair central charge, and the two levels and obstructions.

4. Compute the OPEs $J_{12}J_{12}$, $J_{12}J_{23}$ and $J_{12}J_{34}$ in the real basis, then convert the repeated-pair double pole to the Hermitian basis. Derive the classical symmetric-contraction identity and explain what happens to its scalar after normal ordering. Submit the two repeated-pair double poles, the overlapping-current coefficient, the disjoint coefficient, the Sugawara norm and the erroneous state count obtained by deleting its scalar.

5. Build the grade-two basis and all relation columns in (XVII.6.41). Use the pairing formula to derive (XVII.6.42) at $k = -2, -1$. Explain how exact annihilation and modular independence yield the upper bound, and how modular rank yields the lower bound. Expand the character operations in (XVII.6.48), retaining four Cartans; specialize only at the end. Submit the basis size, relation count, lower and upper ranks, grade-two count, and the two sample pairings. Explain why neither the 169-weight equality nor the Euler coefficient at grade three proves an all-grade physical identification.

6. Generate the E_6 root orbit from the stated graph, project its weights onto the three A_2 pairs, and compare the complete multisets in (XVII.6.54). Determine $h^\vee$, the full Sugawara central charge, zero-weight multiplicity and number of distinct weights. Compute the T_4 generator weights and both critical-level denominators. Explain why a sum of three puncture Sugawara tensors fails, and distinguish the spacetime plane, AGT curve theory and gluing TQFT. State the historical status of Conjectures 1 and 4 in the adopted source and explain why these finite checks do not establish the all-grade identifications. Submit the root count, dual Coxeter number, central charge, zero multiplicity, distinct-weight count, three T_4 weights and two denominators.

Take-home result

Twisted translations turn Schur cohomology into a meromorphic local-operator problem. Symplectic bosons make the construction calculable, and conformal gauging cancels its BRST anomaly. In the four-flavor example the finite affine quotient has $1+28q_S+329q_S^2$; its grade-two stress singlet has nonzero norm -7 and survives the classical Higgs scalar relation. The T_3 root and generator data provide a corresponding E_6 comparison. Before proceeding, the reader should be able to derive the anomaly rescalings, track gauge and flavor levels separately, reproduce the two rank bounds, and explain the distinction between a finite character comparison and a physical VOA identification.

Sources and scope

§1. The unitary radial cohomology construction, exact superalgebra charges and protection map are adopted from Beem et al., *Infinite Chiral Symmetry in Four Dimensions*, arXiv:1312.5344v3, pp. 10–14, eqs. (2.19)–(2.31). The charge-frame conversion, exact-eigenvalue argument, weight and scalar contraction are derived here. The signed character convention uses their pp. 39–40, eqs. (4.22)–(4.23).

§2. The normalized R-current and moment-map OPEs, their conformal derivative argument and the universal stress-action boundary are from the same source, pp. 19–22, eqs. (3.10)–(3.23), especially the discussion after (3.17). The rescalings and anomaly arithmetic are explicit consequences. Physical T_3 anomaly data and enhancement are imported from XVI.6–7. The source's protected stress bound is on pp. 38–39, Table 4 and eqs. (4.20)–(4.21).
§3. The free-field protection map and relative BRST prescription are from pp. 23–29, eqs. (3.28)–(3.53). The absence of additional higher-order lifting is an assumption stated after (3.53). The symplectic signs, Taylor-expanded Wick products, adjoint traces and nilpotency obstruction are calculated here. They establish algebraic nilpotence, not a complete physical cohomology computation.
§4. The classical polynomial identities, 434-state pairing, exact 105-column kernel and modular lower bound establish the rational grade-two rank 329. The 169-weight comparison is finite; the grade-three coefficient 2632 is only a small-algebra Euler trace. The physical BRST-exact stress identification and nonsinglet relations are adopted from pp. 41–45, eqs. (5.1)–(5.19). The all-grade affine identification is Conjecture 1 of that inspected version, p. 45; Table 5 on pp. 46–47 is contextual comparison, not a coefficient input here. The finite classical identities do not establish the full Joseph ideal.
§5. The physical T_N generator assignments and T_3 enhancement use Volume XVI and Beem et al., pp. 59–61, eqs. (6.1)–(6.4). Root enumeration, the complete 73-weight branching, Sugawara data and changed-N weights are finite calculations. The T_3 affine identification is Conjecture 4 in the inspected source. No exceptional null ideal or all-grade vacuum character is derived here. These historical source labels do not survey the later literature. The AGT and gluing descriptions have the separate domains established in XVII.3–5.

Chapter XVII.7

Four supercharges from a wrapped curve

Wrapping an M5-brane on a curved surface rotates its spinors as they move around the surface. A partial twist compensates this rotation with a rotation of the normal directions. In XVI.2 one normal plane supplied the compensating connection and eight real supercharges survived. Here both normal planes participate. The extra freedom is geometric: the canonical bundle of the curve splits into two holomorphic normal lines. We will construct such a split, count the surviving spinors, and determine the geometric family of R generators.

Our parent is the six-dimensional $(2,0)$ theory. We use the interacting-parent versus free-center distinction of XVI.1, the Lorentzian four-dimensional spin decomposition of XVI.2, and its twist sign. The existence of the parent, a compatible supersymmetric background and a low-energy compactification regime are physical inputs. The explicit internal spin matrices below count supercharges within the supplied Lorentz representation and lift; they do not construct the full six-dimensional Lorentz action. An interacting six-dimensional adjoint-field Lagrangian is unnecessary.

The main example is the smooth compact completion of $y^2 = x^5 - 1$. Its two normal lines will both be $\mathcal{O}(\infty)$. We will establish their product as a holomorphic canonical bundle, rather than infer it from degrees. A second example changes the genus, and a flat line gives a useful obstruction to eight-supercharge enhancement. Finally, explicit complex Nahm poles introduce a local puncture color. Anomaly integration, gluing, extremization and infrared dynamics require the next chapter.

XVII.7.1 Rotations in the two normal planes

The normal rotation group acts on the supercharges through Spin(5), whose spinor has four complex components. To fix units, let σ_i be the Pauli matrices and construct

$$\Gamma_1 = \sigma_1 \otimes 1, \quad \Gamma_2 = \sigma_2 \otimes 1, \quad \Gamma_3 = \sigma_3 \otimes \sigma_1, \quad \Gamma_4 = \sigma_3 \otimes \sigma_2, \quad \Gamma_5 = \sigma_3 \otimes \sigma_3. \tag{XVII.7.1}$$

Each matrix squares to one. Pauli anticommutation makes distinct matrices anticommute, including pairs whose first factors coincide. Thus

$$\{\Gamma_i,\Gamma_j\}=2\delta_{ij}1_4,\qquad T_1=-\frac{i}{2}\Gamma_1\Gamma_2=\frac{1}{2}\sigma_3\otimes 1,\qquad T_2=-\frac{i}{2}\Gamma_3\Gamma_4=\frac{1}{2}1\otimes\sigma_3. \tag{XVII.7.2}$$

In the tensor-product basis e_0,e_1,e_2,e_3, the simultaneous weights are

$$(t_1,t_2)=\tfrac{1}{2}(1,1),\ \tfrac{1}{2}(1,-1),\ \tfrac{1}{2}(-1,1),\ \tfrac{1}{2}(-1,-1). \tag{XVII.7.3}$$

The factor of two between spinor and vector rotations matters for bundles. Define the complex normal vectors through the Clifford representatives $V_1=\Gamma_1+i\Gamma_2$ and $V_2=\Gamma_3+i\Gamma_4$. Direct multiplication gives

$$[T_1,V_1]=V_1,\quad [T_2,V_1]=0,\qquad [T_1,V_2]=0,\quad [T_2,V_2]=V_2. \tag{XVII.7.4}$$

Their vector weights are $(1,0)$ and $(0,1)$; conjugation supplies the negative weights and Γ_5 is neutral. A scalar associated to a complex normal direction therefore has unit normal charge, although a supercharge has half-unit charges.

Retain the six-dimensional Weyl decomposition under four-dimensional Lorentz rotations and rotations of the curve:

$$S_6^+=(\mathbf{2},\mathbf{1})_{s=1/2}\oplus(\mathbf{1},\mathbf{2})_{s=-1/2},\qquad S=\operatorname{diag}(\tfrac{1}{2},\tfrac{1}{2},-\tfrac{1}{2},-\tfrac{1}{2}). \tag{XVII.7.5}$$

Each value of s occurs twice because of its four-dimensional spinor components. If the normal connections locally obey $A_1=a\omega$, $A_2=b\omega$, with ω the curve spin connection, the compensated generator is

$$D=S\otimes 1_4+1_4\otimes(aT_1+bT_2),\qquad d(s,t_1,t_2)=s+at_1+bt_2. \tag{XVII.7.6}$$

For $a+b=1$, the weights $(s,t_1,t_2)=(-\frac{1}{2},\frac{1}{2},\frac{1}{2})$ and its negative are neutral. If both a,b are nonzero, the two mixed-sign normal weights cannot give additional zeros: their neutrality would require $a-b=\pm1$, which together with the sum condition forces an endpoint. Hence

$$\dim_{\mathbb{C}}\ker D=4\quad(ab\neq 0),\qquad \dim_{\mathbb{C}}\ker D=8\quad((a,b)=(1,0)\text{ or }(0,1)). \tag{XVII.7.7}$$

For example, at $(a,b)=(\frac{1}{4},\frac{3}{4})$ the four distinct normal contributions are $\frac{1}{2},-\frac{1}{4},\frac{1}{4},-\frac{1}{2}$. Only the first and last cancel a curve spin. In zero-based indices $k=4\ell+j$, with ℓ the Lorentz-basis index and j the normal index, the actual neutral entries are

$$\ker D=\operatorname{span}_{\mathbb{C}}\{e_3,e_7,e_8,e_{12}\}. \tag{XVII.7.8}$$

The same four entries survive at $(a,b)=(-\frac{1}{2},\frac{3}{2})$. This negative-coefficient example tests the weight method; it does not assert an infrared fixed point or assign fractional powers to arbitrary bundles.

The complex dimension must now be interpreted with the reality condition. In the supplied Lorentz basis take

$$B_6=\begin{pmatrix}0 & 1_2\\ -1_2 & 0\end{pmatrix},\qquad B_R=\Gamma_2\Gamma_4,\qquad B=B_6\otimes B_R,\qquad \rho(v)=B\overline{v}. \tag{XVII.7.9}$$

Here $B_6^2 = B_R^2 = -1$, the tensor product obeys $B\overline{B} = 1$, and ρ pairs opposite weights. It preserves the neutral subspace. Since these matrices are real, writing $v = x + iy$ reduces its fixed equation to two ordinary real linear equations:

$$\rho(v) = v \quad \Longleftrightarrow \quad (B-1)x = 0, \quad (B+1)y = 0. \tag{XVII.7.10}$$

On the four neutral entries, B has two $+1$ and two -1 eigenvalues. Each conjugate pair supplies two real parameters. At an endpoint there are four of each sign. Consequently

$$\dim_{\mathbb{R}}(\ker D)^{\rho} = 2 + 2 = 4, \qquad \dim_{\mathbb{R}}(\ker D_{1,0})^{\rho} = 4 + 4 = 8. \tag{XVII.7.11}$$

For clarity, in the ordered neutral basis (e_3, e_7, e_8, e_{12}) the restriction is

$$B_{\ker D} = \begin{pmatrix} 0 & 0 & -1 & 0 \\ 0 & 0 & 0 & -1 \\ -1 & 0 & 0 & 0 \\ 0 & -1 & 0 & 0 \end{pmatrix}, \qquad v = (z_1, z_2, -\overline{z}_1, -\overline{z}_2). \tag{XVII.7.12}$$

The two arbitrary complex numbers in this expression are four real parameters. This is a useful way to perform the count without choosing real eigenvectors individually. At $(a, b) = (1, 0)$ the neutral indices instead are $2, 3, 6, 7, 8, 9, 12, 13$. There are four conjugate pairs, with one arbitrary complex number per pair. One should first select the kernel and then impose reality inside it: counting a complex Lorentz component and its conjugate as independent would count the same real supersymmetry twice.

This compatible real involution removes the apparent complex doubling. Figure XVII.7.1 shows which corners participate. These are local curvature counts. A global supercharge must also return to itself after parallel transport, which will become decisive in the endpoint example.

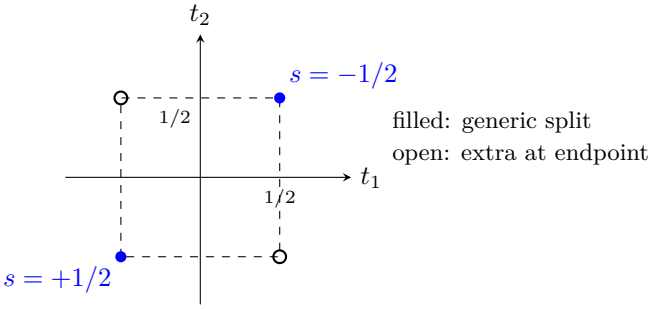


Figure XVII.7.1: Normal spinor weights. The filled opposite corners are neutral for a generic split with $a + b = 1$; their curve spins have opposite signs. At $a = 1, b = 0$, the two remaining corners also contribute, each with the curve spin fixed by t_1. Each corner carries a four-dimensional spinor multiplicity of two before reality.

XVII.7.2 Constructing the two holomorphic line bundles

The local rotation data acquire a global meaning when the two complex normal directions form holomorphic lines L_1, L_2 on a smooth curve C. The local ambient space is the total space of their direct sum. Let $\pi : X \to C$ denote the projection. Along every fiber, vertical tangent vectors transform in the pulled-back normal bundle, giving

$$0 \longrightarrow \pi^*(L_1 \oplus L_2) \longrightarrow TX \longrightarrow \pi^* TC \longrightarrow 0. \tag{XVII.7.13}$$

Taking determinants of the dual bundles yields

$$K_X = \pi^*\big(K_C \otimes (L_1 \otimes L_2)^{-1}\big)\,. \tag{XVII.7.14}$$

Thus a chosen holomorphic isomorphism $L_1 \otimes L_2 \simeq K_C$ trivializes the ambient canonical bundle. The zero section is the wrapped curve. This is the canonical-bundle part of the local Calabi–Yau construction; a Ricci-flat metric and a physical decoupling limit are additional inputs.

One can see precisely what glues by following coordinates. On overlapping patches write

$$z' = f(z), \qquad w_1' = u(z) w_1, \qquad w_2' = v(z) w_2. \tag{XVII.7.15}$$

We use fiber coordinates, rather than frames of sections. Their factors are inverse to the corresponding frame factors. The full Jacobian contains derivatives of the line transitions:

$$J = \frac{\partial(z', w_1', w_2')}{\partial(z, w_1, w_2)} = \begin{pmatrix} f' & 0 & 0 \\ u' w_1 & u & 0 \\ v' w_2 & 0 & v \end{pmatrix}, \qquad \det J = f' u v. \tag{XVII.7.16}$$

The off-diagonal terms are present even though triangularity removes them from the determinant. The volume form transforms by

$$dz' \wedge dw_1' \wedge dw_2' = f' u v \, dz \wedge dw_1 \wedge dw_2, \qquad u v = (f')^{-1}. \tag{XVII.7.17}$$

For a nonconstant check choose $z' = z^2$ and $w_1' = z^3 w_1$ on an overlap where $z \neq 0$. Then

$$w_2' = \frac{w_2}{2z^4}, \qquad J = \begin{pmatrix} 2z & 0 & 0 \\ 3z^2 w_1 & z^3 & 0 \\ -2z^{-5} w_2 & 0 & (2z^4)^{-1} \end{pmatrix}, \qquad \det J = 1. \tag{XVII.7.18}$$

The cancellation exhibits a holomorphic volume form directly. Omitting the base derivative $2z$ would instead give the wrong second fiber transition.

Degrees give a necessary topological condition. Let g be the genus of C, and write $p = \deg L_1$, $q = \deg L_2$. Additivity gives

$$p + q = \deg K_C = 2g - 2, \qquad a = \frac{p}{2g-2}, \quad b = \frac{q}{2g-2} \quad (g > 1) \tag{XVII.7.19}$$

for constant-curvature representatives in the chosen sign convention. Equal degrees do not specify a product isomorphism: a degree-zero factor can change the holomorphic bundle. We therefore construct the lines using an actual canonical divisor.

Consider the smooth compact completion of the squarefree odd-degree curve $y^2 = x^{2g+1} - 1$. At a finite branch point $x = a$, choose u with $x - a = u^2$. Since the polynomial has a simple zero, $y = cu + O(u^3)$ with $c \neq 0$, so

$$\frac{dx}{y} = \frac{2u\,du}{cu + O(u^3)} = \left(\frac{2}{c} + O(u^2)\right) du. \tag{XVII.7.20}$$

There is neither a zero nor a pole there. Away from branch points, x is a coordinate and $y \neq 0$, so the same differential is nonvanishing. There is a single point at infinity. In a local parameter t there,

$$x = t^{-2}, \qquad y = t^{-(2g+1)}\eta(t), \qquad \eta(t)^2 = 1 - t^{4g+2}, \quad \eta(0) \neq 0. \tag{XVII.7.21}$$

The differential consequently has the local form

$$\frac{dx}{y} = -2t^{2g-2}\eta(t)^{-1}dt, \qquad \operatorname{div}(dx/y) = (2g-2)\infty. \tag{XVII.7.22}$$

For a divisor D, $\mathcal{O}(D)$ denotes its associated holomorphic line bundle. Its canonical meromorphic section has zeros and poles prescribed by D; tensor products add these divisor orders.

This proves the holomorphic identification $K_C \simeq \mathcal{O}((2g-2)\infty)$, including its divisor, rather than just its degree.

A theta characteristic is a holomorphic line bundle whose square is K_C. For the central genus-two curve take $L = \mathcal{O}(\infty)$. Its square is canonical, and the split normal bundle is

$$y^2 = x^5 - 1: \qquad L_1 = L_2 = L, \quad L^{\otimes 2} \simeq K_C, \quad (p,q) = (1,1), \quad (a,b) = (\tfrac{1}{2}, \tfrac{1}{2}). \tag{XVII.7.23}$$

A compatible lift and background connections are understood. The generic local count in the preceding section is then four real supercharges. To transfer the method, change the curve to genus three:

$$y^2 = x^7 - 1: \qquad L_1 = \mathcal{O}(\infty), \quad L_2 = \mathcal{O}(3\infty), \quad (p,q) = (1,3), \quad (a,b) = (\tfrac{1}{4}, \tfrac{3}{4}). \tag{XVII.7.24}$$

The divisor product is again canonical, while the two normal lines are now different. Figure XVII.7.2 summarizes the local coordinate and global divisor descriptions. The differential dx/y supplies the representative for the canonical divisor. For genus two, the two order-one normal divisors add to its order-two zero at infinity. For genus three, orders one and three add to the order-four zero. No local choice at infinity needs to be extended by inventing zeros at finite branch points: the branch-coordinate computation has already ruled them out.

The product isomorphism also correlates the connections. In a local supersymmetric representative, the connection induced on L_1L_2 is identified with the canonical connection, with the twist sign already included in D. Their curvature contributions

consequently add to the curve contribution. The integral condition records this sum, whereas a flat tensor factor contributes no curvature. It can therefore survive every degree calculation and still alter parallel transport. The endpoint below will use exactly this freedom.

The arithmetic condition is useful for choosing candidates; the displayed divisor calculation is what realizes these two candidates as holomorphic backgrounds.

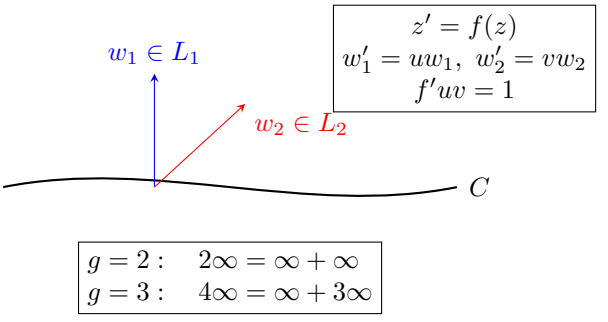


Figure XVII.7.2: The curve is the zero section of two normal lines. On an overlap, the base and two fiber Jacobian factors multiply to one. Below, the canonical divisor is split into two actual divisors at the unique infinity point; changing genus changes both the canonical order and the available split.

XVII.7.3 Choosing R symmetry and flavor

The preserved positive-R spinor has equal positive normal weights. Their sum therefore rotates it, while their difference leaves it invariant. This selects useful generators before any anomaly calculation:

$$R_0 = T_1 + T_2, \qquad F = T_1 - T_2, \qquad (R_0, F)_{(-1/2,1/2,1/2)} = (1, 0). \tag{XVII.7.25}$$

The conjugate spinor has charges $(-1, 0)$. Calling the first spinor positive-R fixes the R normalization without changing the inherited Lorentz labels for the supercharges. A generator that annihilates the preserved supersymmetry can act as a flavor generator. In the geometric abelian family this gives

$$R_{\text{trial}} = R_0 + \epsilon F = (1 + \epsilon)T_1 + (1 - \epsilon)T_2, \qquad R_{\text{trial}}(Q_+) = 1. \tag{XVII.7.26}$$

The last equality holds for every ϵ. It is a normalization condition, not a determination of the infrared R symmetry.

The two normal vectors have the unit weights derived from the Clifford commutators. Their complete geometric charge assignments are

	T_1	T_2	R_0	F	R_{trial}
w_1	1	0	1	1	$1 + \epsilon$
w_2	0	1	1	-1	$1 - \epsilon$
Q_+	1/2	1/2	1	0	1

(XVII.7.27)

The symbols w_i here label the normal complex directions and their rotations. Assigning a dimension to a particular interacting four-dimensional chiral operator requires an operator dictionary and the exact superconformal R generator. The geometric charge table alone supplies neither.

Relabeling the two lines is a useful consistency check. The transformation is

$$L_1 \leftrightarrow L_2 : \quad T_1 \leftrightarrow T_2, \quad R_0 \mapsto R_0, \quad F \mapsto -F, \quad \epsilon \mapsto -\epsilon. \tag{XVII.7.28}$$

Thus R_{trial} and the two charge assignments transform covariantly. Relabeling is available when writing the background; a physical exchange symmetry requires that it preserve the actual bundle, connection and other background data. In particular $p = q$ does not identify two holomorphic lines.

The genus-two example has more structure than degree equality. With identical connections and equal Hermitian fiber metrics, $L \oplus L \simeq L \otimes \mathbb{C}^2$ admits determinant-one unitary rotations of its multiplicity space. This gives a normal $SU(2)$ flavor symmetry. Its root can be seen directly in the spinor representation:

$$E = -\frac{1}{4}(\Gamma_1 + i\Gamma_2)(\Gamma_3 - i\Gamma_4), \qquad [F, E] = 2E, \qquad [E, E^\dagger] = F. \tag{XVII.7.29}$$

These commutators fix the Cartan normalization. Since the root changes (t_1, t_2) by $(1, -1)$, it commutes with their sum. Consequently

$$[R_0, E] = 0, \qquad [R_{\text{trial}}, E] = 2\epsilon E. \tag{XVII.7.30}$$

If this non-Abelian flavor symmetry survives in the physical infrared theory, its superconformal R generator must commute with it. Within the displayed geometric family this forces $\epsilon = 0$. The argument is a symmetry constraint conditional on the physical flavor symmetry, not an extremization or a proof of an infrared SCFT.

To see why the hypotheses matter, let P be a nontrivial degree-zero line and replace the pair by

$$L_1 = L \otimes P, \qquad L_2 = L \otimes P^{-1}, \qquad L_1 L_2 = L^2 = K_C, \qquad \deg L_1 = \deg L_2 = 1. \tag{XVII.7.31}$$

Their product and degrees agree with the central example. For a generic P they are not isomorphic and the multiplicity-space rotations are absent. An off-diagonal rotation would require a globally compatible map between the two lines, with the required connection behavior. Equality of the Chern numbers cannot provide that map. Figure XVII.7.3 shows how this distinction affects the R family.

There is another direct way to see the symmetry condition. In a trivialization of $L \otimes \mathbb{C}^2$, write a normal vector as $w = (w_1, w_2)^T$. Its common line transition multiplies both entries by the same scalar. A constant matrix $U \in SU(2)$ commutes with that scalar, so $w \mapsto Uw$ patches consistently. Equal fiber metrics make the transformation unitary, and identical connections make it parallel. For different transitions, an off-diagonal matrix generally fails this patching test. This gives a geometric explanation of the root commutator and identifies the particular background data that the extra symmetry needs.

Even in the symmetric background, the geometric $SU(2)$ is a statement about normal rotations. To use it as an infrared flavor group, one must establish its physical action and survival. Once that physical premise holds, a superconformal R generator cannot select a preferred direction inside a non-Abelian flavor multiplet. The commutator calculation makes this constraint quantitative within the family already constructed.

It is useful to translate two literature normalizations now, before combining this construction with building blocks. In the conventions used here, BBBW's geometric generator K is R_0. In the unrotated eight-supercharge frame let $r = 2T_1$ and $I_3 = T_2$. Then the GMTY block flavor generator is

$$J = r - 2I_3 = 2(T_1 - T_2) = 2F, \qquad R_0 + \epsilon F = R_0 + \frac{\epsilon}{2} J. \tag{XVII.7.32}$$

A colored collection of blocks carries additional signs in that block convention; the present formula fixes only the unrotated normalization. It does not specify a gluing superpotential.

For example $\epsilon = 1/3$ gives normal trial weights $(4/3, 2/3)$, while relabeling produces $\epsilon = -1/3$ and the reversed pair. Both choices give the same unit charge to the preserved positive-R spinor. A generic exact infrared value requires the available mixing symmetries, anomaly data and dynamical assumptions. Those ingredients enter XVII.8. Here we have determined which geometric generators can participate and how to compare their normalizations.

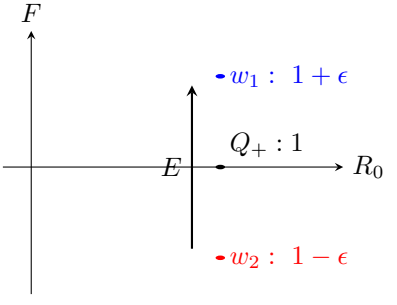


Figure XVII.7.3: The geometric charge plane. The two normal directions sit at $(R_0, F) = (1, \pm 1)$ and the preserved positive-R spinor at $(1, 0)$. A trial charge reads a point by $R_0 + \epsilon F$. The normal $SU(2)$ root connects the two normal directions only for identical lines with compatible identical backgrounds; commuting with that root selects $\epsilon = 0$ if the symmetry survives physically.

XVII.7.4 The eight-supercharge limit

The local endpoint $(a, b) = (1, 0)$ has eight real neutral spinors. To decide whether all eight survive globally, we must identify the line carried by each weight. With the

compatible spin/R lift, the weight line is written formally as

$$\mathcal{W}_{s,t_1,t_2} = K_C^s L_1^{t_1} L_2^{t_2}. \tag{XVII.7.33}$$

The half powers denote the chosen lift, not separate arbitrary square roots. Using the specified product isomorphism eliminates them in the sectors of interest:

$$L_2 = K_C L_1^{-1} \quad \Longrightarrow \quad \mathcal{W}_{s,t_1,t_2} = K_C^{s+t_2} L_1^{t_1-t_2}. \tag{XVII.7.34}$$

For $(-\frac{1}{2},\frac{1}{2},\frac{1}{2})$ both exponents vanish. Its conjugate also gives the trivial line. The compatible lift is chosen so these two sectors carry globally trivial transport. Each sector has its two Lorentz components, giving the four generic real charges already counted.

At $(a,b)=(1,0)$, neutrality says $s=-t_1$ and leaves t_2 free. The two new normal weights have opposite signs, giving

$$\begin{aligned} (s,t_1,t_2) = (-\tfrac{1}{2},\tfrac{1}{2},-\tfrac{1}{2}): &\quad \mathcal{W} = K_C^{-1} L_1 = L_2^{-1}, \\ (s,t_1,t_2) = (\tfrac{1}{2},-\tfrac{1}{2},\tfrac{1}{2}): &\quad \mathcal{W} = K_C L_1^{-1} = L_2. \end{aligned} \tag{XVII.7.35}$$

Thus the new spinors are sections of $L_2^{\pm 1}$ with the induced connection. Degree zero is necessary for these flat endpoint sectors but does not make their transport trivial.

The true product endpoint sets $L_2=\mathcal{O}$ with its trivial compatible connection and $L_1=K_C$. Then

$$X = \mathrm{Tot}(K_C \oplus \mathcal{O}) \simeq T^*C \times \mathbb{C}, \qquad N_Q = 8 \text{ real}. \tag{XVII.7.36}$$

The two extra sectors are globally parallel. The normal commutant has Lie algebra $\mathfrak{u}(1)_r \oplus \mathfrak{su}(2)_R$. The inherited eight-supercharge convention is

$$t = T_1, \qquad r = 2T_1, \qquad I_3 = T_2, \qquad I_3 \text{ doublet weights} = \pm\tfrac{1}{2}. \tag{XVII.7.37}$$

For a selected $\mathcal{N}=1$ subalgebra of an $\mathcal{N}=2$ superconformal theory, the standard generator becomes

$$R_{\mathcal{N}=1} = \frac{1}{3} r + \frac{4}{3} I_3 = \frac{2}{3} T_1 + \frac{4}{3} T_2 = R_0 - \frac{1}{3} F. \tag{XVII.7.38}$$

Both the preserved positive-R spinor and the original formula give charge one. The coefficient $-1/3$ is an endpoint normalization identity. It is not obtained by extremizing the generic geometric family.

Now change an input that degree arithmetic cannot see. On the genus-two curve choose a unitary flat line P with character

$$(\chi(a_1),\chi(b_1),\chi(a_2),\chi(b_2)) = (e^{2\pi i/3},1,1,1), \qquad \prod_{i=1}^{2} [\chi(a_i),\chi(b_i)] = 1. \tag{XVII.7.39}$$

The surface-group relation is automatic because the character is abelian. Set

$$L_2 = P, \qquad L_1 = K_C \otimes P^{-1}, \qquad (p,q)=(2,0), \qquad (a,b)=(1,0). \tag{XVII.7.40}$$

Curvature and the local kernel are unchanged. However, transport around a_1 multiplies the extra weight lines P and P^{-1} by $\zeta = e^{2\pi i/3}$ and ζ^{-1}. An invariant section would require

$$(\zeta - 1)v_+ = 0, \qquad (\zeta^{-1} - 1)v_- = 0, \qquad \zeta \neq 1 \quad \Longrightarrow \quad v_+ = v_- = 0. \quad \text{(XVII.7.41)}$$

Only four real charges survive. This is an actual degree-zero holonomy obstruction, drawn in Figure XVII.7.4. Replacing the character by $(-1, 1, 1, 1)$ gives the same loss of the extra sectors, while the identity character restores all eight.

Parallel transport provides a simple order of operations for such examples. First impose the curvature kernel $Dv = 0$ pointwise. Next regard the surviving components as fibers of their weight lines. Finally intersect the invariant subspaces of the holonomies of all generators of the surface group. For the present character, a single generator already removes both extra sectors. If the four holonomies are all one, this last intersection removes nothing. Thus the local eight-supercharge calculation remains correct in the counterexample; it is the subsequent invariant-space calculation that changes the answer.

One can equally perform the comparison in the real fixed space. The two extra complex sectors are paired by reality, so the phases are complex conjugates. A nontrivial phase acts as a real plane rotation on the corresponding real parameters. Such a rotation has no nonzero fixed vector when its angle is not an integer multiple of 2π. It removes a full conjugate pair rather than reducing a complex sector to one real component. This recovers the loss of four real charges without treating conjugate sectors independently.

The holomorphic version of the obstruction has a short proof. A nonzero holomorphic section of a degree-zero line P has an effective zero divisor D satisfying

$$\deg D = \deg P = 0 \quad \Longrightarrow \quad D = 0 \quad \Longrightarrow \quad P \simeq \mathcal{O}. \qquad \text{(XVII.7.42)}$$

It would be nowhere vanishing and trivialize the line, contradicting nontriviality. For the compatible unitary flat structure, holomorphic triviality and trivial holonomy coincide. An arbitrary connection on a holomorphically trivial line need not give parallel spinors. This explains why the endpoint requires the bundle and connection together. The discussion assumes $g > 1$ and the stated lift; special torus spin structures need a separate analysis.

XVII.7.5 Colored local boundary conditions

A puncture introduces local boundary data in addition to the closed-curve background. To see what a color can record, we use an auxiliary compactified/BPS description with two distinguished complex scalar directions. These matrices are not elementary adjoint fields of a six-dimensional interacting Lagrangian. We evaluate the complex Nahm equations on $r > 0$:

$$\frac{d\beta}{dr} + [\alpha, \beta] = 0, \qquad \frac{d\gamma}{dr} + [\alpha, \gamma] = 0, \qquad [\beta, \gamma] = 0. \qquad \text{(XVII.7.43)}$$

They provide a directly calculable local part of the proposed generalized boundary dictionary. The real moment-map equation and a global solution require additional work.

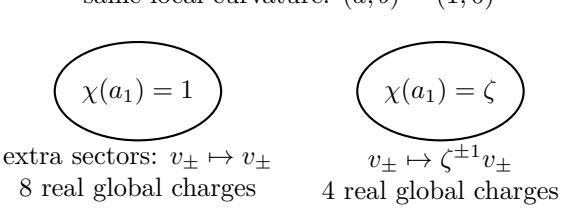


Figure XVII.7.4: The endpoint has eight local neutral spinors in either case. With the identity flat character the extra lines return unchanged. With $\chi(a_1) = \zeta$, the two extra sectors return with phases $\zeta^{\pm 1}$ and have no invariant vectors. The generic four real charges lie in the trivial weight lines and remain.

For an $\mathfrak{sl}_3$ example let E_{ij} be the elementary matrix. Choose

$$e = E_{12} = \begin{pmatrix} 0 & 1 & 0 \\ 0 & 0 & 0 \\ 0 & 0 & 0 \end{pmatrix}, \qquad h = \operatorname{diag}(\tfrac{1}{2}, -\tfrac{1}{2}, 0), \qquad [h, e] = e. \tag{XVII.7.44}$$

The conventional $\mathfrak{sl}_2$ Cartan is $H = 2h$. Use a pole in the first direction:

$$\alpha = \frac{h}{r}, \qquad \beta = \frac{e}{r}, \qquad \gamma = 0. \tag{XVII.7.45}$$

Differentiation fixes the coefficient of the Cartan residue. Explicitly,

$$\frac{d\beta}{dr} = -\frac{e}{r^2}, \qquad [\alpha, \beta] = \frac{[h, e]}{r^2} = \frac{e}{r^2}, \qquad \frac{d\beta}{dr} + [\alpha, \beta] = 0. \tag{XVII.7.46}$$

The other two residuals vanish because $\gamma = 0$. Exchanging the two slots gives a second local pole:

$$(\alpha, \beta, \gamma) = \left(\frac{h}{r}, 0, \frac{e}{r} \right). \tag{XVII.7.47}$$

The uncolored nilpotent matrix and partition are identical, but the selected normal/scalar direction differs. This is the single-color distinction, called the monochromatic D and D' types in the source proposal. A color is additional local data; it is not a sign of a line-bundle degree. An exchange of slots need not be a global symmetry of a given background.

The equation detects a wrong Cartan coefficient. Replacing α by $2h/r$ while keeping $\beta = e/r$ gives

$$\frac{d\beta}{dr} + [2h/r, \beta] = \frac{e}{r^2} \neq 0. \tag{XVII.7.48}$$

Likewise setting $\gamma = E_{21}/r$ produces $[\beta, \gamma] = (E_{11} - E_{22})/r^2 \neq 0$. Nilpotence of each residue separately is therefore insufficient to solve the two-direction equations.

We can determine the uncolored orbit without interpreting it as a four-dimensional moduli space. For a traceless matrix

$$X = \begin{pmatrix} a & b & c \\ d & f & g \\ j & k & -a-f \end{pmatrix}, \qquad [X,e] = \begin{pmatrix} -d & a-f & -g \\ 0 & d & 0 \\ 0 & j & 0 \end{pmatrix}. \tag{XVII.7.49}$$

The kernel imposes $d = g = j = 0$ and $f = a$, leaving a, b, c, k. Thus the nilpotent centralizer has complex dimension four and the orbit dimension is

$$\dim_{\mathbb{C}} \mathcal{O}_e = \dim \mathfrak{sl}_3 - \dim Z_{\mathfrak{sl}_3}(e) = 8 - 4 = 4, \qquad e^2 = 0, \quad \operatorname{rank} e = 1. \tag{XVII.7.50}$$

The last two conditions identify Jordan type $[2,1]$. The common commutant of the triple (e, h, e^T) is smaller. Commuting with h, whose eigenvalues are distinct, makes X diagonal, and commuting with e, e^T equates its first two entries. Hence

$$Z_{\mathfrak{sl}_3}(e, h, e^T) = \{\operatorname{diag}(a, a, -2a)\}, \qquad \dim_{\mathbb{C}} Z(e, h, e^T) = 1. \tag{XVII.7.51}$$

The orbit dimension four, nilpotent centralizer dimension four and triple-commutant dimension one answer different questions. The equal first two numbers here are accidental.

Change the residue to a principal pole:

$$e' = E_{12} + E_{23}, \qquad h' = \operatorname{diag}(1, 0, -1), \qquad [h', e'] = e', \quad (e')^3 = 0, \quad (e')^2 \neq 0. \tag{XVII.7.52}$$

The same differentiated pole solves the complex equations in either slot. Its partition is $[3]$. A matrix commuting with a single full Jordan block is a polynomial in that block; tracelessness leaves e' and $(e')^2$. The centralizer therefore has dimension two, the orbit dimension is six, and the triple commutant is zero. Commutation with h' first makes a matrix diagonal, after which the two adjacent links force all entries equal; tracelessness then removes the common scalar.

For repeated Jordan blocks, the triple commutant has a concrete multiplicity-space description. In the $[2,2]$ example the defining four-component space is a tensor product of the two-component irreducible block with a multiplicity space of dimension two. A commuting matrix acts as the identity on the irreducible factor and as an arbitrary matrix on the multiplicity factor. The traceless condition removes its scalar trace, leaving three complex parameters. In contrast, commuting only with e allows additional intertwiners that do not commute with h or e^T. This explains why its centralizer has dimension seven rather than three. The orbit removes that larger stabilizer from the fifteen-dimensional traceless matrix algebra and has dimension eight.

This example also explains what a partition forgets. Both choices of pole slot use the same nilpotent endomorphism and therefore the same stabilizer and orbit rank. The differential equations still know which scalar is singular. The color must be recorded alongside the partition before using the boundary as input to a compactification. Recovering it from the uncolored orbit dimension is impossible even in this elementary example.

A useful independent count for a partition λ of n uses its transpose, with column lengths c_j:

$$\dim \mathcal{O}_\lambda = n^2 - \sum_j c_j^2. \tag{XVII.7.53}$$

For $[2,1]$, the columns are $[2,1]$ and this gives $9-5=4$. For $[3]$ they are $[1,1,1]$ and it gives $9-3=6$. As changed-rank examples, $\mathfrak{sl}_4$ partitions $[2,2]$ and $[2,1,1]$ give $16-8=8$ and $16-10=6$. Their triple commutants have dimensions three and four: the repeated irreducible blocks admit multiplicity rotations, with the total trace removed. Figure XVII.7.5 keeps color and uncolored orbit data separate.

These finite local poles establish the complex differential equations and their algebraic counts. Their interpretation as physical punctures uses the proposed generalized boundary dictionary. They do not solve a global real BPS problem, classify all colored punctures, or identify an orbit dimension with a complete Higgs branch. The closed-curve bundle data and these local choices are the inputs from which the next chapter must build a four-supercharge field theory and test its anomaly and dynamical properties.

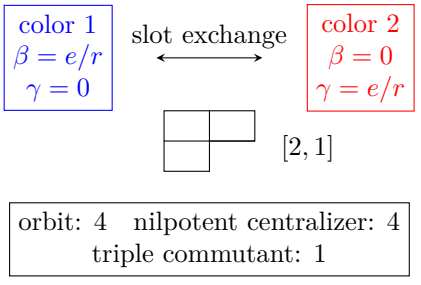


Figure XVII.7.5: Two colors of the same $[2,1]$ residue: the nilpotent matrix occupies the β slot or the γ slot. The Jordan diagram records only the uncolored partition. The three algebraic counts below it distinguish an adjoint orbit, a nilpotent centralizer and a common triple commutant; they are not assigned physical moduli-space dimensions here.

Exercises

The exercises use the matrices and compatible lift of the text. Give the written arguments as well as the numerical or symbolic entries. For benchmark submissions, see `benchmark/PROTOCOL.md`.

1. For $(a,b) = (1/4, 3/4)$, compute all four values of $aT_1 + bT_2$, list the zero-based neutral indices in the 16-component tensor basis, and determine the real fixed dimension. Explain why the complex kernel does not supply eight real supercharges after imposing the stated involution.

2. On $y^2 = x^7 - 1$, derive the order of dx/y at infinity and at every finite branch point. Construct normal lines of degrees one and three by divisors, and give (a, b). Explain what a degree sum alone would leave undetermined.

3. Let $z' = z^2$, $w_1' = z^3 w_1$, $w_2' = c z^m w_2$ on $z \neq 0$. Determine c, m for preservation of the holomorphic volume form. Write the entire Jacobian, including fiber-dependent off-diagonal entries, and explain which additional question a Ricci-flat metric would require.

4. Determine (R_0, F) for the two normal directions and the positive-R spinor. Translate $J = r - 2I_3$ to F, and determine ϵ in $R_0 + \epsilon F = r/3 + 4I_3/3$. Explain why the last answer does not select the exact R symmetry of a generic four-supercharge background.

5. On the genus-two curve take the flat character $(-1, 1, 1, 1)$ on (a_1, b_1, a_2, b_2) and $L_2 = P$, $L_1 = K_C P^{-1}$. Give the local and global real supercharge counts and the phases of the extra sectors around a_1. Prove that a nontrivial holomorphic degree-zero line has no nonzero holomorphic section.

6. In $\mathfrak{sl}_4$ use $e = E_{12} + E_{34}$ and $h = \mathrm{diag}(1/2, -1/2, 1/2, -1/2)$. Differentiate both single-color pole solutions. Compute the rank of ad_e, the nilpotent centralizer dimension and the triple-commutant dimension. Explain why neither color nor an orbit count proves existence of a global real BPS solution.

Take-home result

A four-supercharge curve background requires actual holomorphic normal lines with a specified product $L_1 L_2 \simeq K_C$, a compatible lift and supersymmetric connections. The genus-two pair $\mathcal{O}(\infty), \mathcal{O}(\infty)$ realizes this product explicitly. The local Clifford count gives four real supercharges and the geometric R family is $R_0 + \epsilon F$. Identical lines with identical backgrounds admit a normal $SU(2)$; equal degrees alone do not. Eight-supercharge enhancement requires trivial transport of the extra weight lines, as the flat counterexample demonstrates. Single-color complex poles add calculable local data, while anomaly matching, gluing and infrared existence remain separate physical tasks.

Sources and scope

§1. [MATH] The Clifford weights, vector normalization, neutral indices and compatible real fixed-space dimensions follow from the displayed matrices. They use the supplied Lorentz representation and spin/R lift. [GEO-E] Their supersymmetry interpretation assumes the $(2, 0)$ parent, a supersymmetric compactification background and its low-energy regime. Source anchors are Xie 2013, version 1, printed pp. 5–6, (2.1), (2.3), (2.5), and Bah et al. 2012, version 1, §2.1. The explicit commutators fix normal vector units; no assertion about a printed scalar-weight typo is needed.

§2. [MATH] The exact sequence, full Jacobian and hyperelliptic canonical-divisor calculation establish the stated holomorphic product examples. The geometric setup is Bah et al. 2012, printed pp. 3–4, (2.1)–(2.5). Canonical triviality alone supplies neither a Ricci-flat metric nor a decoupling theorem.
§3. [MATH] The charge assignments, exchange action, normal-root commutators and $J = 2F$ translation are explicit representation calculations. [GEO-E] The geometric R family and any surviving physical flavor symmetry use the compactification dictionary; exact infrared identification requires further assumptions. See Bah et al. 2012, (2.8), (2.14), (5.8)–(5.10), and Gadde et al. 2013, version 2, (2.2)–(2.3), (4.3), (5.3). The identical-line flavor constraint is conditional on survival of that symmetry.
§4. [MATH] The weight-line substitution, explicit flat character and degree-zero-section argument establish the global obstruction. [GEO-E] The true product endpoint and eight-supercharge interpretation assume compatible trivial transport and no extra breaking. See Bah et al. 2012, (2.3), printed p. 15 footnote 8 on Abelian Wilson lines, and (5.1)–(5.2) for the endpoint R normalization. The generic count assumes $g > 1$ and the stated lift.
§5. [MATH] The displayed poles solve the complex equations and have the stated orbit, centralizer and triple-commutant dimensions for the listed finite residues. [CONJ+] Their physical boundary interpretation uses the generalized dictionary of Xie 2013, printed pp. 10–13, (2.28)–(2.29) and the monochromatic D/D' discussion. [GEO-E] Color distinguishes the two normal/scalar slots; Gadde et al. 2013, printed p. 26, §5.2 provides related sign context. No full real/global solution, classification or orbit-to-physical-moduli identification is established. The scope throughout is the $(2, 0)$ parent.

References

Bah, I. et al. (2012). "Four-Dimensional SCFTs from M5-Branes". In: Version 1 inspected. arXiv: `1203.0303 [hep-th]`.

Gadde, A. et al. (2013). "New $\mathcal{N} = 1$ Dualities". In: Version 2 inspected. arXiv: `1303.0836 [hep-th]`.

Xie, D. (2013). "M5 brane and four dimensional $\mathcal{N} = 1$ theories I". In: Version 1 inspected. arXiv: `1307.5877 [hep-th]`.

Chapter XVII.8

Colored gluing, anomalies and mass deformations

A tube joining two class-S trinions gauges a common flavor symmetry. With eight supercharges, its vector multiplet includes an adjoint chiral field. With four supercharges, that adjoint is present only for one of the two possible color assignments. The colors record how the same $\mathcal{N} = 2$ block sits inside the preserved $\mathcal{N} = 1$ algebra. They therefore change both the coupling and the flavor current that can mix with the R-current.

We will construct a closed genus-two example from two T_3 sectors, gauge all three pairs of full punctures, and compute its anomalies in two ways. The first sums the block and gauge contributions. The second integrates the six-dimensional anomaly polynomial over the curve. Keeping both methods explicit makes finite-rank terms and mixed flavor anomalies visible. An adjoint mass deformation then supplies a concrete holomorphic relation to the familiar eight-supercharge graph. Its self-interaction terms will determine a tuning condition on the masses.

The reader needs the T_N building block and full-puncture level from XVI.6, anomaly traces and a-maximization from XVI.7 and Volume I, and the normal-bundle twist of XVII.7. We recall the conventions at each use. The parent is the interacting A_{N-1} six-dimensional $(2, 0)$ theory, with integer $N \geq 2$. The curve C is smooth, closed and of genus $g > 1$. Its normal lines L_1, L_2 obey $L_1 \otimes L_2 \simeq K_C$, with degrees $p, q \geq 0$ and $p + q = 2g - 2$. The colored-trinion construction and its infrared interpretation are physical inputs. Our calculations determine its anomaly data and the stated holomorphic mass elimination. Identifying a trial maximum with a superconformal current also requires an actual unitary fixed point and the complete set of currents that can mix.

XVII.8.1 Colored blocks and their couplings

Why should a color change remove an adjoint? Start with a single T_N sector. Use its abelian R-current r and Cartan I_3, normalized to $\pm\frac{1}{2}$ on a doublet. A color is a sign

$\sigma = \pm 1$. The two currents used in gluing are

$$R_0 = \frac{r}{2} + I_3, \qquad F = \sigma\left(\frac{r}{2} - I_3\right), \qquad R(\epsilon) = R_0 + \epsilon F. \tag{XVII.8.1}$$

Thus a color does not change the isolated block. It changes the sign with which that block contributes to the common flavor symmetry of the glued theory. In terms of the original currents,

$$R(\epsilon)\big|_{T_N^\sigma} = \frac{1+\sigma\epsilon}{2} r + (1-\sigma\epsilon) I_3. \tag{XVII.8.2}$$

This formula fixes a potential normalization ambiguity. If $J = r - 2I_3$ denotes the block current used by Gadde–Maruyoshi–Tachikawa–Yan, their colored flavor generator is $\sum_i \sigma_i J_i = 2F$ in our convention. Their mixing parameter must therefore be divided by two when attached to that generator to describe the same $R(\epsilon)$.

The operators needed below are the moment maps μ_e, one for each full leg e, the Higgs-branch tensors $Q^{(1)}, Q^{(N-1)}$, and Coulomb operators u_k. Their scalar charges follow from their $\mathcal{N} = 2$ multiplets:

operator	r	I_3	R_0	F
μ_e	0	1	1	$-\sigma$
$Q^{(1)}, Q^{(N-1)}$	0	$(N-1)/2$	$(N-1)/2$	$-\sigma(N-1)/2$
u_k	$2k$	0	k	σk

(XVII.8.3)

Here the indicated Q and moment maps are the highest-weight chiral operators for the chosen $\mathcal{N} = 1$ subalgebra. For T_3, the two Q tensors have $R_0 = 1$, while u_3 has $R_0 = 3$. These assignments describe operators of a non-Lagrangian block; they do not turn T_3 into elementary chiral matter.

Now gauge a common full-leg $SU(N)$ of blocks i, j. An $\mathcal{N} = 1$ vector has a gaugino of charges $(R_0, F) = (1, 0)$. If the colors agree, $\sigma_i = \sigma_j = \sigma$, add an adjoint chiral scalar ϕ with charges $(1, \sigma)$. The coupling is

$$W_{\text{same}} = \operatorname{Tr} \phi(\mu_i - \mu_j), \qquad (R_0, F)(\phi) = (1, \sigma). \tag{XVII.8.4}$$

The relative minus sign fixes a leg convention that we retain in the mass calculation. Each term has

$$R(\phi\mu_i) = (1+\sigma\epsilon) + (1-\sigma\epsilon) = 2, \qquad F(\phi\mu_i) = \sigma - \sigma = 0. \tag{XVII.8.5}$$

The vector and adjoint together have the field content of an $\mathcal{N} = 2$ vector, although a larger graph need only preserve four supercharges.

For opposite colors, take $\sigma_i = +1$, $\sigma_j = -1$. The gauge edge contains only the $\mathcal{N} = 1$ vector, and the allowed cross interaction is

$$W_{\text{opp}} = \lambda \operatorname{Tr}(\mu_i \mu_j), \qquad R(W_{\text{opp}}) = (1-\epsilon) + (1+\epsilon) = 2, \qquad F(W_{\text{opp}}) = 0. \tag{XVII.8.6}$$

The moment maps are adjoints of the gauged group, so their product can be traced without introducing an extra adjoint field. Figure XVII.8.1 summarizes the two constructions after their charges have been fixed.

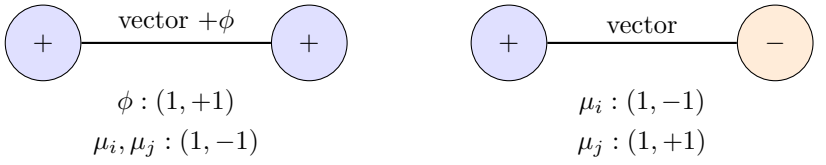


Figure XVII.8.1: Two ways to gauge a pair of full $SU(N)$ legs. A circle denotes a T_N block with the indicated color. The same-color edge includes a vector and adjoint ϕ; opposite colors require only a vector. The displayed scalar charges explain why the linear adjoint coupling and the moment-map cross coupling both preserve R_0 and F.

There is a dimensional issue hidden by the common R-charge. At a decoupled $\mathcal{N} = 2$ block, μ has scaling dimension two. The two candidate interactions consequently have ultraviolet dimensions

$$\Delta_{\mathrm{UV}}(\phi\mu) = 1 + 2 = 3, \qquad \Delta_{\mathrm{UV}}(\mu_i\mu_j) = 2 + 2 = 4, \qquad [\lambda]_{\mathrm{UV}} = -1. \tag{XVII.8.7}$$

The opposite-color interaction is irrelevant at that decoupled point. Its proposed marginal role belongs to an interacting infrared theory. If the product survives as a chiral primary at a superconformal point, $\Delta = 3R/2$ makes $R = 2$ the appropriate dimension-three condition. This is a conditional statement about that operator and fixed point. A charge assignment alone establishes neither their existence nor exact marginality: beta functions and possible recombination still matter.

The color assignment must be consistent across the whole graph. At a vertex all three moment maps inherit the same sign in F. One cannot flip the sign of a single moment map to repair one edge without also changing the block's current. The local edge rules then assemble a single conserved candidate flavor current. For a general closed graph, its two defining restrictions are

$$F(W_e) = 0 \quad \text{for every interaction,} \qquad \operatorname{Tr} F G_e^2 = 0 \quad \text{for every gauge factor.} \tag{XVII.8.8}$$

The first is a classical charge test; the second checks the quantum gauge anomaly that could destroy that current. We derive the second test in the next section. Distinguishing them is useful: an interaction with the correct charge cannot cancel an anomalous fermion measure, and a nonanomalous current can still be explicitly broken by an added coupling.

There is also a simple test of the normalization by changing the sign of both colors. The house flavor current changes sign while R_0 does not. Thus

$$(\sigma_i, \epsilon) \longmapsto (-\sigma_i, -\epsilon) \quad \Longrightarrow \quad R(\epsilon)\big|_{T_N^{\sigma_i}} \text{ is unchanged.} \tag{XVII.8.9}$$

A formula that changes a physical R-charge under this simultaneous relabeling has used an inconsistent flavor normalization. A sign change of only one vertex is physically different: the edge type and its adjoint content change. This is precisely the operation distinguishing the two panels of Figure XVII.8.1.

Changing the rank leaves the charge argument intact but changes its operator content. At $N = 2$, T_2 is a half-hypermultiplet in $(\mathbf{2}, \mathbf{2}, \mathbf{2})$; the chosen $\mathcal{N} = 1$ description has one chiral trifundamental per block. Its scalar has

$$R(Q_\sigma) = \frac{1 - \sigma\epsilon}{2}, \qquad F(Q_\sigma) = -\frac{\sigma}{2}, \qquad R(\mu_\sigma) = 1 - \sigma\epsilon. \tag{XVII.8.10}$$

The moment map is quadratic in that field, which recovers its row in (XVII.8.3). At $N = 3$ the same row is protected block data rather than an elementary quadratic expression. This distinction will let us use an elementary anomaly check without silently assuming a Lagrangian for every T_N.

XVII.8.2 A closed genus-two theory

Take two vertices T_3^+ and T_3^-. Join their corresponding full legs by three distinct edges $e = 1, 2, 3$. Denote their gauge groups by $G_e = SU(3)_e$, and their moment maps by $\mu_{\pm,e}$. There are no unglued punctures. The complete coupling data for this graph are three $\mathcal{N} = 1$ vectors and

$$W_\theta = \sum_{e=1}^{3} \lambda_e V_e, \qquad V_e = \mathrm{Tr}(\mu_{+,e}\mu_{-,e}). \tag{XVII.8.11}$$

We reserve V_e for the cross operator in this equation. A connected trivalent closed graph has $3v = 2E$, with v vertices and E edges. Its first Betti number is $E - v + 1$; for this graph it is $3 - 2 + 1 = 2$, the genus of the glued curve. The sourced elementary colored-trinion dictionary identifies p as the number of plus blocks and q as the number of minus blocks, corresponding to the two normal-line degrees. The two colors give $(p, q) = (1, 1)$.

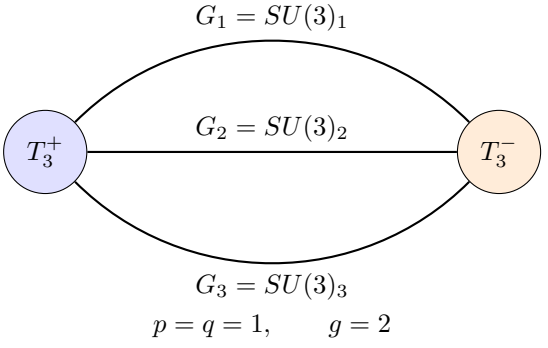


Figure XVII.8.2: The genus-two theta graph. Each of the three separately labeled edges gauges one pair of full $SU(3)$ punctures. All edges join opposite colors, so there are three $\mathcal{N} = 1$ vectors and no independent adjoint chirals. The three cross couplings in (XVII.8.11) can have different coefficients even though their anomaly calculations coincide.

Before computing abelian anomalies, test each gauge factor. Normalize $\mathrm{Tr}_{\mathbf{N}}\, T^a T^b = \frac{1}{2}\delta^{ab}$, so the adjoint Dynkin index is $T(\mathrm{adj}) = N$. A full T_N leg has flavor level $k = 2N$. The anomaly convention is

$$\mathrm{Tr}\, r T^a T^b = -\frac{k}{2}\delta^{ab}, \qquad \mathrm{Tr}\, I_3 T^a T^b = 0. \tag{XVII.8.12}$$

Every anomaly trace in this chapter runs over left-handed Weyl fermions. Using (XVII.8.1), a block of color σ contributes

$$\mathrm{Tr}_{T_N^\sigma}\, R_0 G^2 = -\frac{N}{2}, \qquad \mathrm{Tr}_{T_N^\sigma}\, F G^2 = -\frac{\sigma N}{2}. \tag{XVII.8.13}$$

A gaugino contributes N to the first trace and zero to the second. Thus an opposite-color edge gives, independently for every e,

$$\mathrm{Tr}\, R_0 G_e^2 = N - \frac{N}{2} - \frac{N}{2} = 0, \qquad \mathrm{Tr}\, F G_e^2 = -\frac{N}{2} + \frac{N}{2} = 0. \tag{XVII.8.14}$$

For the theta theory $N = 3$, each cancellation is $3 - 3/2 - 3/2 = 0$. Hence every member of the trial family also has $\mathrm{Tr}\, R(\epsilon) G_e^2 = 0$.

This test explains the adjoint on a same-color edge. Its scalar has $R_0 = 1$, so its Weyl fermion has $R_0 = 0$; its flavor charge remains σ. Consequently

$$\mathrm{Tr}\, R_0 G^2 = N - N = 0, \qquad \mathrm{Tr}\, F G^2 = -\sigma N + \sigma T(\mathrm{adj}) = 0. \tag{XVII.8.15}$$

Omitting that fermion would leave a flavor–gauge anomaly. Using its scalar R-charge in the trace would instead spoil the first cancellation. The shift by one between scalar and fermion is essential. The perturbative pure cubic $SU(N)$ flavor anomaly of the $\mathcal{N} = 2$ block vanishes as part of the block input; the added adjoint representation is real. These local checks do not determine an absolute global form of the resulting theory.

The weak-gauging beta coefficient tests a different question. A full leg contributes $k/2$ to the matter term. We use the convention $\beta(g) = -b_0 g^3/(16\pi^2) + \cdots$. With n_ϕ adjoint chirals on an edge,

$$b_0 = 3N - \frac{k_i}{2} - \frac{k_j}{2} - n_\phi N = \begin{cases} N, & \sigma_i = -\sigma_j, \\ 0, & \sigma_i = \sigma_j. \end{cases} \tag{XVII.8.16}$$

Opposite-color gauging is asymptotically free in this ultraviolet weak-gauging test, while both mixed gauge-current anomalies vanish. There is no contradiction: b_0 uses the ultraviolet matter response, whereas (XVII.8.14) tests the specified candidate R-current. Neither equation alone establishes an infrared zero of the exact beta function.

As a changed-color check, recolor just the minus vertex of the T_3 theta to plus. Each of the three edges now needs an adjoint. On each edge the two blocks contribute -3 to $\mathrm{Tr}\, F G_e^2$ and the added fermion contributes $+3$. Its ultraviolet beta coefficient changes from three to zero. In contrast, the R_0 cancellation is unchanged, since the new fermion has zero R_0. Introduce bookkeeping variables x, y for R_0, F. Summing over all three new adjoints changes the linear and cubic abelian traces by

$$\Delta\, \mathrm{Tr}(x R_0 + y F) = 24y, \qquad \Delta\, \mathrm{Tr}(x R_0 + y F)^3 = 24 y^3, \tag{XVII.8.17}$$

where the multiplicity is $3(3^2-1)=24$. The block whose color changed must also be recomputed. The adjoint shift alone is not the complete change in the theory. We will perform the full recoloring after deriving the anomaly formula.

For a direct changed-rank calculation, replace both blocks by T_2. There are two chiral trifundamentals, each with eight components, and three $SU(2)$ gaugini, each with three components. The matter fermion charges are the scalar charges minus one:

$$R(\psi_+)=-\frac{1+\epsilon}{2},\qquad R(\psi_-)=-\frac{1-\epsilon}{2},\qquad R(\lambda_e)=1. \tag{XVII.8.18}$$

The linear and cubic traces therefore follow without effective block coordinates:

$$\operatorname{Tr} R=9+8\left[-\frac{1+\epsilon}{2}-\frac{1-\epsilon}{2}\right]=1, \tag{XVII.8.19}$$

$$\operatorname{Tr} R^3=9-\left[(1+\epsilon)^3+(1-\epsilon)^3\right]=7-6\epsilon^2. \tag{XVII.8.20}$$

Each $SU(2)$ node sees four doublets from each trifundamental, hence eight Weyl doublets. Their number is even, as required by the ordinary $SU(2)$ Witten parity test. The parity calculation tests the ordinary Witten anomaly for this matter content. We will recover its central charges from the six-dimensional formula and return to the charged scalar's $R=1/2$ when discussing unitarity.

XVII.8.3 The same anomalies from six dimensions

The colored graph should remember the normal-bundle flux. To extract that memory, let η be the degree-two class on the fixed curve with $\int_C \eta = 1$. Since C has real dimension two, $\eta^2=0$ in this computation. Let x, y be four-dimensional background first Chern classes for R_0, F, and write $P=p_1(T_4)$. The two nonzero normal roots and the tangent class are

$$n_1=x+y+p\eta,\qquad n_2=x-y+q\eta,\qquad c_1(TC)=(2-2g)\eta. \tag{XVII.8.21}$$

The normal rank-five real bundle has roots $\pm n_1, \pm n_2, 0$, so $p_1(\mathcal{N})=n_1^2+n_2^2$ and $p_2(\mathcal{N})=n_1^2n_2^2$. Define $r_G=N-1$ and $H=N^3-N$. The interacting parent has

$$I_8=r_G I_8[1]+\frac{H}{24}p_2(\mathcal{N}),\quad I_8[1]=\frac{1}{48}\left[p_2(\mathcal{N})-p_2(T_6)+\frac{(p_1(T_6)-p_1(\mathcal{N}))^2}{4}\right]. \tag{XVII.8.22}$$

This includes the tangent terms of the free-tensor polynomial. For a fixed product tangent bundle, $p_1(T_6)=P+c_1(TC)^2=P$ to linear order in η. Also $p_2(T_6)=p_2(T_4)+Pc_1(TC)^2$ has no term linear in η. These observations remove only terms whose curve integral vanishes; the $Pp_1(\mathcal{N})$ term remains essential for the linear anomaly.

Set $A=x+y$, $B=x-y$, and $U=pA+qB$. Direct expansion gives

$$p_1(\mathcal{N})=A^2+B^2+2U\eta,\qquad [p_2(\mathcal{N})]_\eta=2pAB^2+2qBA^2. \tag{XVII.8.23}$$

The square in (XVII.8.22) contributes

$$\left[\frac{(P-p_1(\mathcal{N}))^2}{4}\right]_\eta = -(P-A^2-B^2)U. \tag{XVII.8.24}$$

Consequently the full pushforward, before converting to anomaly traces, is

$$I_6 = \frac{r_G}{48}\left[2pAB^2+2qBA^2+(A^2+B^2-P)U\right]+\frac{H}{12}(pAB^2+qBA^2). \tag{XVII.8.25}$$

Here $[\ ]_\eta$ means the coefficient of η. For $X = xR_0 + yF$, let $\mathcal{L}(x,y) = \operatorname{Tr} X$ and $\mathcal{C}(x,y) = \operatorname{Tr} X^3$. Figure XVII.8.3 displays the two separate computations whose outputs we will compare.

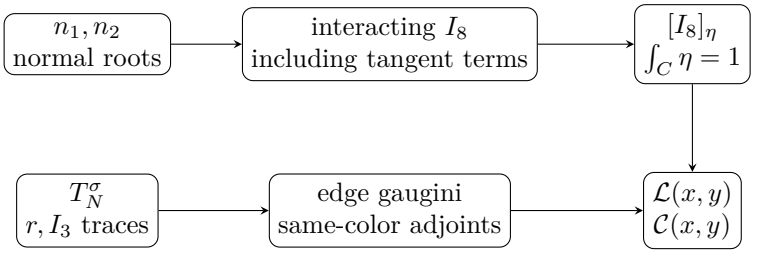


Figure XVII.8.3: Two routes to the abelian anomaly polynomial. The upper route expands the normal roots in the interacting six-dimensional I_8 and retains the coefficient of η. The lower route sums T_N block traces and actual edge fermions. Both retain the two linear and four cubic coefficients. They share physical compactification and block inputs; their different bookkeeping gives a consistency check of those inputs.

Define $S = p+q$ and $D = p-q$. The standard Weyl-fermion convention is

$$I_6 = \frac{\mathcal{C}}{6} - \frac{P\mathcal{L}}{24}. \tag{XVII.8.26}$$

Substituting A, B, U in (XVII.8.25) gives the complete answer

$$\mathcal{L} = \frac{r_G}{2}(Sx+Dy), \qquad \mathcal{C} = \frac{1}{2}\left[S\big((r_G+H)x^3 - Hxy^2\big) + D\big((r_G+H)y^3 - Hx^2y\big)\right]. \tag{XVII.8.27}$$

In particular, the six traces are

$$\begin{aligned} \operatorname{Tr} R_0 &= r_G S/2, & \operatorname{Tr} F &= r_G D/2, \\ \operatorname{Tr} R_0^3 &= (r_G+H)S/2, & \operatorname{Tr} F^3 &= (r_G+H)D/2, \\ \operatorname{Tr} R_0^2 F &= -HD/6, & \operatorname{Tr} R_0 F^2 &= -HS/6. \end{aligned} \tag{XVII.8.28}$$

The factor three relating mixed monomial coefficients to mixed traces follows from expanding X^3. Missing it would leave the pure cubic terms unchanged but give the wrong trial central charge.

We can reproduce this result from actual graph data. The anomaly coordinates of a T_N block are

$$n_v = \frac{4N^3 - 9N^2 - N + 6}{6}, \qquad n_h = \frac{2(N^3 - N)}{3}. \tag{XVII.8.29}$$

$$\operatorname{Tr} r = \operatorname{Tr} r^3 = 2(n_v - n_h), \qquad \operatorname{Tr} r I_3^2 = \frac{n_v}{2}. \tag{XVII.8.30}$$

These n_v, n_h parametrize anomalies; they count elementary fields only in a Lagrangian example. Put $\alpha_\sigma = (x + \sigma y)/2$, $\beta_\sigma = x - \sigma y$. Each block contributes

$$\mathcal{L}_\sigma = 2\alpha_\sigma(n_v - n_h), \qquad \mathcal{C}_\sigma = 2\alpha_\sigma^3(n_v - n_h) + \frac{3}{2}\alpha_\sigma \beta_\sigma^2 n_v. \tag{XVII.8.31}$$

Every edge adds $(N^2-1)x$ and $(N^2-1)x^3$ from its gaugino. Each same-color edge adds $(N^2-1)\sigma y$ and $(N^2-1)\sigma y^3$ from the adjoint fermion.

For completeness, the graph identities explain why the result depends on p, q. Let E_{++}, E_{--}, E_{+-} count the three edge types, with p plus vertices and q minus vertices. Trivalence implies

$$3p = 2E_{++} + E_{+-}, \qquad 3q = 2E_{--} + E_{+-}, \qquad E = \frac{3}{2}S, \quad E_{++} - E_{--} = \frac{3}{2}D. \tag{XVII.8.32}$$

To see the cancellation at general rank, define $A_r = 2(n_v - n_h)$ and $B_r = n_v/2$. Expanding a single block's cubic makes the two independent coefficients explicit:

$$\begin{aligned} \mathcal{C}_\sigma = &\left(\frac{A_r}{8} + \frac{3B_r}{2}\right)(x^3 + \sigma y^3) \\ &+ \left(\frac{3A_r}{8} - \frac{3B_r}{2}\right)(\sigma x^2 y + x y^2). \end{aligned} \tag{XVII.8.33}$$

The mixed coefficient is especially simple:

$$\frac{3A_r}{8} - \frac{3B_r}{2} = -\frac{3}{4}n_h = -\frac{H}{2}. \tag{XVII.8.34}$$

No edge fermion has both R_0 and F nonzero, so none contributes a mixed cubic term. Summing σ over the vertices gives D for $x^2 y$ and summing one gives S for xy^2, exactly as in the pushforward. For the pure terms the edge contributions do matter. Both the pure-cubic and linear combinations simplify as

$$n_v - \frac{n_h}{4} + \frac{3}{2}(N^2-1) = \frac{r_G + H}{2}, \qquad n_v - n_h + \frac{3}{2}(N^2-1) = \frac{r_G}{2}. \tag{XVII.8.35}$$

The x and x^3 edge counts multiply these expressions by S, while the same-color differences multiply the y and y^3 expressions by D. This recovers every coefficient of (XVII.8.27), rather than only its specialization to $y = 0$. This derivation uses no fictitious Lagrangian for T_N. Its agreement with the root expansion checks all six coefficients, including coefficients that vanish in a balanced graph. The two paths still share physical class-S premises and cannot establish that dictionary by themselves.

For the T_3 theta, $n_v = 5$, $n_h = 16$, $r_G = 2$, $H = 24$, and $S = 2, D = 0$. Thus

$$\mathcal{L} = 2x, \qquad \mathcal{C} = 26x^3 - 24xy^2, \qquad (\mathrm{Tr}\, R_0^3, \mathrm{Tr}\, R_0^2 F, \mathrm{Tr}\, R_0 F^2, \mathrm{Tr}\, F^3) = (26, 0, -8, 0). \tag{XVII.8.36}$$

We can see the individual cancellations directly in the four-dimensional route. For T_3, $2(n_v - n_h) = -22$ and $n_v/2 = 5/2$. Expanding (XVII.8.31) gives

$$\mathcal{L}_\sigma = -11(x + \sigma y), \qquad \mathcal{C}_\sigma = x^3 - 12\sigma x^2 y - 12xy^2 + \sigma y^3. \tag{XVII.8.37}$$

The opposite blocks add to $-22x$ and $2x^3 - 24xy^2$. The three actual edge gaugini add $3 \cdot 8x$ and $3 \cdot 8x^3$, so

$$\mathcal{L} = (-22 + 24)x = 2x, \qquad \mathcal{C} = (2 + 24)x^3 - 24xy^2. \tag{XVII.8.38}$$

The odd terms cancel between blocks, not within one block. The mixed even term survives entirely from the block sectors. This decomposition is a useful way to locate an error: a missing vector changes the pure x terms; a wrong color sign changes the mixed terms. At rank four, the analogous hypermultiplet coordinate is $n_h = 40$. The vector coordinate must be recomputed at that rank:

$$n_v(T_4) = \frac{256 - 144 - 4 + 6}{6} = 19, \qquad 2(n_v - n_h) = -42, \quad -42x + 45x = 3x. \tag{XVII.8.39}$$

This explicit finite-rank evaluation is preferable to extrapolating a block count from a lower rank. In particular the effective coordinates are polynomial anomaly data and need not count a proposed set of weakly coupled fields.

Set $x = 1, y = \epsilon$. The trial central functions and their extremum are

$$a(\epsilon) = \frac{3}{32}(3\mathcal{C} - \mathcal{L}) = \frac{57}{8} - \frac{27}{4}\epsilon^2, \quad c(\epsilon) = \frac{9\mathcal{C} - 5\mathcal{L}}{32} = 7 - \frac{27}{4}\epsilon^2, \quad \epsilon_* = 0, \quad a'' = -\frac{27}{2}. \tag{XVII.8.40}$$

The negative Hessian selects the local maximum in this one-current family. Under the fixed-point and complete-mixing assumptions it gives $a_* = 57/8, c_* = 7$. At changed rank $N = 4$, the same calculation has $\mathcal{L} = 3x$, $\mathcal{C} = 63x^3 - 60xy^2$, hence $a_* = 279/16, c_* = 69/4$ and $a'' = -135/4$. At $N = 2$ it gives (XVII.8.19)–(XVII.8.20), with $a_* = 15/8, c_* = 29/16$.

One finite-rank distinction survives even at balance. Restoring the free center tensor changes r_G to $r_G + 1$ without changing H. At $p = q = 1$ this adds

$$\Delta\mathcal{L} = x, \qquad \Delta\mathcal{C} = x^3, \qquad \Delta a\big|_{\epsilon=0} = \frac{3}{16}, \quad \Delta c\big|_{\epsilon=0} = \frac{1}{8}. \tag{XVII.8.41}$$

These are integrated anomaly differences. They do not determine the complete four-dimensional mode content of the compactified free tensor. The interacting comparison consistently excludes that tensor on the six-dimensional side.

XVII.8.4 An adjoint mass deformation

Can an eight-supercharge graph produce the opposite-color interaction? Begin with the ordinary T_3 theta and three $\mathcal{N} = 2$ vectors. The adjoint chirals are ϕ_e. Give

them nonzero masses m_e, allowing complex values. With the same leg convention as (XVII.8.4), take

$$W_{\mathrm{UV}} = \sum_{e=1}^{3} \operatorname{Tr}\left[\phi_e(\mu_{+,e} - \mu_{-,e}) + \frac{m_e}{2}\phi_e^2\right]. \tag{XVII.8.42}$$

The signs on the two block labels now name the proposed low-energy color assignment; they do not make its F an exact symmetry of this ultraviolet superpotential. The preserved current $R_0 = r/2 + I_3$ assigns one to every ϕ_e and $\mu_{\pm,e}$. It gives two to every term in (XVII.8.42) with uncharged masses.

Put $D_e = \mu_{+,e} - \mu_{-,e}$. Varying a traced matrix polynomial uses cyclicity, not commutativity. Since ϕ_e, D_e are traceless adjoint matrices, their variation stays in the adjoint and yields

$$\delta W_e = \operatorname{Tr}[\delta\phi_e(D_e + m_e\phi_e)], \qquad \phi_e = -\frac{D_e}{m_e}. \tag{XVII.8.43}$$

Substituting back gives the holomorphic Wilsonian superpotential below the adjoint masses:

$$W_{\mathrm{eff}} = -\sum_e \frac{1}{2m_e} \operatorname{Tr} D_e^2 = -\sum_e \frac{\operatorname{Tr}\mu_{+,e}^2 + \operatorname{Tr}\mu_{-,e}^2}{2m_e} + \sum_e \frac{V_e}{m_e}. \tag{XVII.8.44}$$

For noncommuting matrices the cross terms are $\operatorname{Tr}(\mu_+\mu_- + \mu_-\mu_+) = 2\operatorname{Tr}(\mu_+\mu_-)$ by cyclicity. Thus both self-square terms really occur. They cannot be removed by treating the two moment maps as independent variables in an ordinary matrix identity.

The additional input comes from the protected T_N operator algebra. Within each isolated block, the three full legs obey the equal-leg relation

$$U_\pm := \operatorname{Tr}\mu_{\pm,1}^2 = \operatorname{Tr}\mu_{\pm,2}^2 = \operatorname{Tr}\mu_{\pm,3}^2. \tag{XVII.8.45}$$

This sourced chiral-ring identity is not a property of arbitrary triples of traceless matrices. Applying it to the holomorphic deformation reorganizes the effective answer as

$$W_{\mathrm{eff}} = -\frac{1}{2}\left(\sum_e \frac{1}{m_e}\right)(U_+ + U_-) + \sum_e \frac{V_e}{m_e}. \tag{XVII.8.46}$$

The closed-graph simplification therefore requires a condition on all three masses:

$$\sum_e \frac{1}{m_e} = 0. \tag{XVII.8.47}$$

The relation in (XVII.8.45) is the operator input; (XVII.8.47) is the choice of deformation. They perform different jobs.

Take a nonzero common scale M and choose $m = (M, M, -M/2)$. The reciprocal sum is $(1 + 1 - 2)/M = 0$, so

$$W_{\mathrm{eff}} = \frac{1}{M}(V_1 + V_2 - 2V_3). \tag{XVII.8.48}$$

Changing the masses to $m = (2M, 3M, -6M/5)$ gives a second nontrivial point on the same tuning locus:

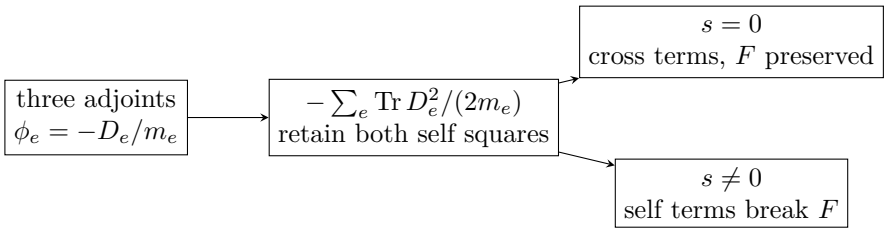
$$\frac{1}{2M} + \frac{1}{3M} - \frac{5}{6M} = 0, \qquad W_{\text{eff}} = \frac{1}{M}\left(\frac{1}{2}V_1 + \frac{1}{3}V_2 - \frac{5}{6}V_3\right). \tag{XVII.8.49}$$

The cross coefficients change while both self coefficients vanish. With three equal masses, in contrast, the answer is

$$W_{\text{eff}}^{\text{equal}} = -\frac{3}{2M}(U_+ + U_-) + \frac{1}{M}(V_1 + V_2 + V_3). \tag{XVII.8.50}$$

In the proposed colored assignment, $F(U_+) = -2$, $F(U_-) = +2$ and $F(V_e) = 0$. Generic self couplings thus break F. The tuned effective superpotential preserves it. This is how an emergent flavor current becomes available for infrared mixing, rather than a reason to match that current to the ultraviolet theory.

Writing $s = \sum_e 1/m_e$, we can summarize the two effective superpotentials in Figure XVII.8.4.



R_0 preserved throughout; $s = \sum_e 1/m_e$.

Figure XVII.8.4: The mass elimination keeps the full square of the moment-map difference. The equal-leg relation combines its self terms into the coefficient $s = \sum_e 1/m_e$. At $s = 0$ the effective interaction preserves the colored F; at generic s the two self terms break it. The preserved R_0 runs through both branches. The proposed infrared fixed point requires dynamical input beyond this holomorphic elimination.

The anomaly comparison can be done for the current that is actually preserved. Two T_3 blocks and three $\mathcal{N} = 2$ vectors have effective coordinates

$$n_v^{\text{UV}} = 2 \cdot 5 + 3 \cdot 8 = 34, \qquad n_h^{\text{UV}} = 2 \cdot 16 = 32. \tag{XVII.8.51}$$

The exact ultraviolet $\mathcal{N} = 2$ superconformal current, viewed as an $\mathcal{N} = 1$ current, is $R_{\text{UV}} = r/3 + 4I_3/3$. Its central charges are

$$a_{\text{UV}} = \frac{5n_v + n_h}{24} = \frac{101}{12}, \qquad c_{\text{UV}} = \frac{2n_v + n_h}{12} = \frac{25}{3}. \tag{XVII.8.52}$$

These formulas use the ultraviolet exact current, whereas anomaly matching along the mass deformation uses R_0. Each removed adjoint fermion has $R_0 = 0$ and therefore contributes neither its linear nor cubic trace. The matching statement is

$$(\operatorname{Tr} R_0, \operatorname{Tr} R_0^3)_{\text{UV}} = (2, 26) = (\operatorname{Tr} R_0, \operatorname{Tr} R_0^3)_{\text{target}}. \tag{XVII.8.53}$$

Conditional on reaching the proposed fixed point with no additional mixing, the candidate decrease is

$$a_{\mathrm{UV}} - a_{\mathrm{IR}} = \frac{101}{12} - \frac{57}{8} = \frac{31}{24} > 0. \tag{XVII.8.54}$$

The inequality is consistent with such a flow. It is not its construction or proof.

Below the mass scale ϕ_e ceases to be an independent field. For example $\operatorname{Tr}\phi_e^k$ is replaced holomorphically by $(-1/m_e)^k \operatorname{Tr} D_e^k$, subject to inherited relations. This explains what happens to these adjoint operators without asserting a complete isomorphism of deformed chiral rings. The source mass-deformation and marginal-retuning picture motivates the proposed endpoint. Our closed tuning follows algebraically from that picture and (XVII.8.45). Determining the endpoint, possible generated interactions and dangerously irrelevant effects requires its dynamics. In particular, there is no conserved ultraviolet colored F to which one could apply flavor anomaly matching.

XVII.8.5 Changed colors, unitarity and bundle data

The balanced theta cancels every term odd in F. A more asymmetric graph is needed to test whether the calculation retained them. Take four T_3 vertices labeled $1, 2, 3, 4$ and connect every pair, making the complete graph K_4. Color vertices $1, 2, 3$ plus and vertex 4 minus. There are three same-color edges in the plus triangle and three opposite-color edges to vertex 4. The curve has $g = 6 - 4 + 1 = 3$, with $(p, q) = (3, 1)$, so $S = 4, D = 2$.

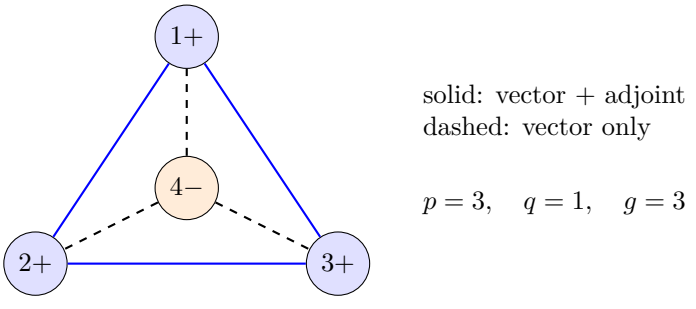


Figure XVII.8.5: The K_4 change of color balance. The plus triangle contains three adjoint chirals; its three connections to the minus vertex contain none. The six vectors and four T_3 blocks define a genus-three graph with $(p, q) = (3, 1)$. This example retains odd-flavor anomalies that cancel in the balanced theta.

Insert $r_G = 2, H = 24, S = 4, D = 2$ in (XVII.8.27). The separate linear and cubic polynomials are

$$\mathcal{L} = 4x + 2y, \qquad \mathcal{C} = 52x^3 - 24x^2y - 48xy^2 + 26y^3. \tag{XVII.8.55}$$

For example $\operatorname{Tr} R_0^2 F = -8$ and $\operatorname{Tr} F^3 = 26$. These coefficients distinguish a color reversal or a dropped adjoint contribution even when the balanced theta still agrees. The trial function is

$$a(\epsilon) = \frac{117}{16}\epsilon^3 - \frac{27}{2}\epsilon^2 - \frac{111}{16}\epsilon + \frac{57}{4}. \tag{XVII.8.56}$$

Its derivative is a quadratic, so both stationary branches must be examined:

$$16a' = 351\epsilon^2 - 432\epsilon - 111 = 0, \qquad \epsilon_\pm = \frac{24 \pm \sqrt{1057}}{39}. \tag{XVII.8.57}$$

The Hessian determines which is a local maximum:

$$a'' = \frac{351}{8}\epsilon - 27, \qquad a''(\epsilon_\pm) = \pm\frac{9}{8}\sqrt{1057}. \tag{XVII.8.58}$$

Thus $\epsilon_- \simeq -0.2183$ is the maximum branch. A cubic is not globally bounded above on the real line, so "maximum" here is explicitly local, as required in the physical extremization prescription. The plus branch is a local minimum and does not supply the candidate current.

A unitary four-dimensional chiral primary that is gauge invariant must satisfy $R \geq 2/3$. This bound follows from $\Delta = 3R/2$ and the scalar unitarity bound $\Delta \geq 1$. At equality a free chiral sector can bring an accidental current, changing the extremization problem. To apply this test, identify actual gauge-invariant candidates first. In the balanced T_3 theta the familiar list gives

candidate	$R(\epsilon = 0)$
$\operatorname{Tr}\mu_\pm^2$	2
$Q_+^{(1)}Q_-^{(N-1)}$ with all gauge indices contracted	$N-1=2$
u_3	3
$\operatorname{Tr} W_\alpha W^\alpha$	2

(XVII.8.59)

Here W_α is the gauge field-strength chiral superfield. The contraction of Q tensors uses conjugate representations on every gauged leg. Some listed candidates may vanish or become related after F-term constraints; their charge is not proof of a nonzero chiral-ring class. All the displayed charges exceed 2/3.

The changed-color extremum also permits a useful finite test. On a plus block the moment-map square and Coulomb operator have charges $2(1-\epsilon_-)$ and $3(1+\epsilon_-)$. On the minus block they have $2(1+\epsilon_-)$ and $3(1-\epsilon_-)$. Consequently

$$R(\operatorname{Tr}\mu_+^2) \simeq 2.437, \quad R(\operatorname{Tr}\mu_-^2) \simeq 1.563, \quad R(u_{3,+}) \simeq 2.345, \quad R(u_{3,-}) \simeq 3.655. \tag{XVII.8.60}$$

These surviving candidates would pass the bound. A complete operator analysis must establish which candidates survive, include other gauge-invariant primaries and identify all conserved currents. Our finite list does not exclude accidental symmetries or establish fixed-point existence. The K_4 maximum therefore remains a formal candidate subject to those extra conditions.

The elementary T_2 example clarifies why one cannot apply the bound to every symbol in a block. Its charged trifundamental has $R = 1/2$ at balance. It is not a gauge-invariant local operator of the glued theory. The contraction of the two trifundamentals is gauge invariant and has

$$R(Q_+Q_-) = \frac{1}{2} + \frac{1}{2} = 1 > \frac{2}{3}. \tag{XVII.8.61}$$

The bound concerns the gauge-invariant chiral primary, not the gauge-dependent field used to construct it.

One can also recolor the theta with two plus vertices. Its three same-color edges restore three adjoints, and $(p, q) = (2, 0)$. The resulting polynomial and trial function at $N = 3$ are

$$\mathcal{L} = 2x + 2y, \qquad \mathcal{C} = 26x^3 - 24x^2y - 24xy^2 + 26y^3, \tag{XVII.8.62}$$

$$a(\epsilon) = \frac{117}{16}\epsilon^3 - \frac{27}{4}\epsilon^2 - \frac{111}{16}\epsilon + \frac{57}{8}, \qquad \epsilon_* = -\frac{1}{3}, \quad a''(\epsilon_*) = -\frac{225}{8}. \tag{XVII.8.63}$$

Equation (XVII.8.2) then gives $R = r/3 + 4I_3/3$, and $a_* = 101/12, c_* = 25/3$, recovering the eight-supercharge values. Geometrically that endpoint requires the degree-zero line to be actually trivial, with a compatible trivial connection: $L_1 \simeq K_C, L_2 \simeq \mathcal{O}_C$. Its degree alone cannot supply an extra covariantly constant supercharge.

The balanced case has a similar geometric distinction. Let θ be a theta characteristic, meaning $\theta^{\otimes 2} \simeq K_C$, and let M be a nontrivial degree-zero flat line. Both pairs

$$(L_1, L_2) = (\theta, \theta), \qquad (L_1, L_2) = (\theta \otimes M, \theta \otimes M^{-1}) \tag{XVII.8.64}$$

have degrees $(g - 1, g - 1)$ and determinant K_C. The first, with identical connections, is $\theta \otimes \mathbb{C}^2$ and admits fiber $SU(2)$ rotations. In the second,

$$L_1 \otimes L_2^{-1} \simeq M^2. \tag{XVII.8.65}$$

For generic M with M^2 nontrivial, the two lines are not isomorphic; their holonomies obstruct those rotations. Even the first background requires four-dimensional couplings compatible with that symmetry before inferring flavor enhancement. There is a useful local way to see the obstruction. A rotation mixing the two normal directions contains an off-diagonal bundle map. For the second pair in (XVII.8.64), its two entries are sections of

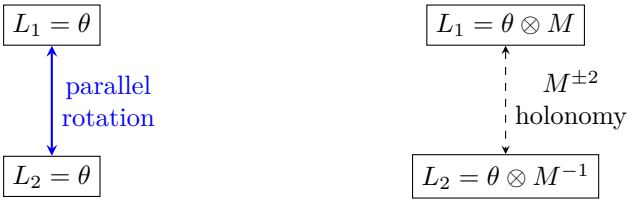
$$\mathrm{Hom}(L_2, L_1) = M^2, \qquad \mathrm{Hom}(L_1, L_2) = M^{-2}. \tag{XVII.8.66}$$

A fiberwise matrix written in one patch need not define the same transformation on an overlapping patch. For identical lines with identical connections, the off-diagonal constant matrices patch and are parallel. Generic flat holonomy in $M^{\pm 2}$ obstructs that parallel off-diagonal transformation. Figure XVII.8.6 separates the degree and connection data. This argument addresses symmetry of the background; invariance of the chosen interacting theory's couplings is still a separate requirement.

The integrated anomaly polynomial sees the degrees and misses these choices. It likewise cannot establish a discrete exchange symmetry of generic equal-degree lines. Negative degrees, punctures and genus one require constructions beyond the elementary nonnegative trinion counts used here.

Exercises

For benchmark submissions, see `benchmark/PROTOCOL.md`. Each problem has a bounded numerical or polynomial part and a written argument. Polynomial input uses



identical connections

generic flat twist

Figure XVII.8.6: Equal degrees with different connection data. In the left panel both copies of θ carry the same connection, allowing a parallel off-diagonal rotation. In the right panel the two flat twists have opposite holonomies; the off-diagonal maps take values in $M^{\pm 2}$. The degree and determinant seen by the integrated anomaly are identical in both panels.

e, N, p, q, x, y; `sqrt(1057)` is the only required radical. Include the requested written arguments.

1. Derive the same-color and opposite-color superpotential charges from (XVII.8.3). Submit `E1` with fields `same` and `opposite`, each the pair $[R(W), F(W)]$, and `GMTY_factor`, the factor multiplying house F to obtain the GMTY current. Explain why $R(W) = 2$ does not prove ultraviolet marginality of the cross interaction, distinguishing its ultraviolet dimension from a quantum chiral-primary dimension.

2. Build the rank-$N = 2$ theta from two chiral trifundamentals and three vectors. Submit `E2` with `linear`, `cubic`, `a`, `c`, and `doublets`: respectively $\operatorname{Tr} R(e)$, $\operatorname{Tr} R(e)^3$, the central charges at the local maximum, and the number of Weyl doublets seen by each node. Explain why the gauge-charged scalar with $R = 1/2$ does not violate the gauge-invariant chiral unitarity bound, and state the limited scope of the doublet parity test.

3. Repeat the coefficient-of-η extraction in (XVII.8.22) for symbolic N, p, q. Submit `E3` with `linear` and `cubic`, the full x, y polynomials, and `center_linear`, `center_cubic`, their balanced $p = q = 1$ differences on restoring one center tensor. In writing identify all six traces, explain the factor three for mixed terms and why shared physical premises limit what agreement with the block sum establishes. Explain why the center difference is not a full mode count.

4. Integrate out all three adjoints for $m = M(2, 3, -6/5)$, keeping both self terms before using the equal-leg relation. Submit `E4` with `cross`, the three coefficients in units of M^{-1}; `tuned_self`, the two combined self coefficients in those units; and `equal_self`, the corresponding two coefficients for $m = (M, M, M)$. Explain the sourced operator relation, which symmetry is preserved along the ultraviolet mass deformation, and why matching a conserved ultraviolet colored F would be invalid.

5. Construct the K_4 graph with colors $(+,+,+,-)$. Submit `E5` with `same_edges`, `opposite_edges`, `trial`, `maximum`, and `hessian`: the two edge counts, full trial $a(e)$, local-maximum branch and its Hessian. Show how the other branch is rejected. Explain what a complete analysis of operators and currents must establish before identifying the result with the exact superconformal R-current.

6. On a genus-two curve compare the two pairs in (XVII.8.64), with generic flat M such that M^2 is nontrivial. Submit `E6` with `degrees`, the common pair of degrees, and `determinant_degree`, the common determinant degree. Give a written line-isomorphism and connection argument for why identical anomaly polynomials cannot decide nonabelian flavor enhancement or a discrete exchange. State the additional condition on four-dimensional couplings even for the identical-line case.

Take-home result and exit check

The opposite-color T_3 theta has three $SU(3)$ gaugings, no adjoint chirals, and a complete abelian anomaly polynomial $\mathcal{L} = 2x$, $\mathcal{C} = 26x^3 - 24xy^2$. It has a unique local maximum in the displayed trial-current family at $\epsilon = 0$, giving candidate central charges $a = 57/8, c = 7$. The root pushforward and the separate block-plus-edge sum agree at finite rank. Integrating out the three adjoints of the eight-supercharge graph produces the opposite-color cross interaction only after the reciprocal-mass tuning removes both sourced self-square operators. The preserved R_0 anomalies match; the colored F is emergent in the tuned effective description.

A reader ready to continue should be able to reconstruct the charge of each edge coupling, include the adjoint fermion only where required, recover all six abelian coefficients, and derive the mass-tuning condition without deleting a self term. The K_4 example tests the terms that balance hides. The bundle comparison explains why identical degree data can describe different symmetry backgrounds. In the next chapter, replacing the compactification curve by a three-manifold changes both the twist and the low-dimensional observables.

Sources and scope

The colored construction and its proposed infrared interpretation follow Bah–Beem–Bobev–Wecht, especially §5 and Appendix E Bah, Beem, et al. 2012. The normal-root anomaly input is their §2 together with the interacting/free-tensor polynomial in Bah–Nardoni, equations (2.6)–(2.7) Bah and Nardoni 2018. The flavor normalization, mass deformation and equal-leg protected relation are from Gadde–Maruyoshi–Tachikawa–Yan, equations (2.2)–(2.4), (2.12) and the discussion following it, with block anomaly data in §3 Gadde et al. 2013. Their flavor generator is twice ours. We retain $I_3 = \pm 1/2$ on a doublet throughout.

The anomaly expansions and matrix elimination displayed here are finite algebraic consequences of those inputs. The equality of the two anomaly routes is a consistency test within the shared compactification framework. The actual infrared endpoint, completeness of the mixing currents and absence of accidental free sectors are additional

physical requirements. The finite candidate list neither classifies the chiral ring nor proves that its named candidates survive all relations. No all-order index identity, exact duality proof or absolute global gauge-group choice is established by these calculations.

Chapter XVII.9

M5-branes on three-manifolds

Wrapping M5-branes on a curved three-manifold changes the question posed by the compactification. The natural protected variables are now holonomies of a complex connection. For a manifold with a torus end, they retain a boundary position and a conjugate response. We will compute these variables for the figure-eight knot complement and compare a group representation with a local stationary equation. The calculation makes the boundary curve explicit. It also shows why a curve alone cannot count all interior connections or choose a physical integration cycle.

We use the interacting type-A_1 six-dimensional $(2,0)$ parent, with its free center removed, and assume an oriented spin three-manifold M with the compatible supersymmetric twist. The reader needs the parent and low-energy periodic-circle description of XVI.1, the distinction between a Lie algebra and an absolute global theory from XVI.11, and the four-real-supercharge meaning of three-dimensional $\mathcal{N}=2$ from Volume 0. The periodic-circle description is used only below the inverse circle radius. The supersymmetric background and the protected interpretation of the local chart are physical inputs. Matrix multiplication, branching of representations, and the finite eliminations below are calculations within those inputs.

XVII.9.1 A diagonal twist preserving four real supercharges

A spinor transported around a generic curved M is rotated by its $\mathrm{Spin}(3)_M$ holonomy. To retain a supersymmetry parameter, couple that rotation to a background $\mathrm{Spin}(3)_R$ inside $\mathrm{Spin}(5)_R$. The diagonal action must have a singlet. We can determine the singlets without writing a nonabelian six-dimensional tensor action.

Let σ_i be the Pauli matrices and $\epsilon = i\sigma_2 = \left(\begin{smallmatrix} 0 & 1 \\ -1 & 0 \end{smallmatrix}\right)$. A concrete Clifford representation on the four R-spinor components is

$$\Gamma_i = \sigma_i \otimes \sigma_1 \quad (i=1,2,3), \qquad \Gamma_4 = 1_2 \otimes \sigma_2, \qquad \Gamma_5 = 1_2 \otimes \sigma_3. \tag{XVII.9.1}$$

Multiplying the Pauli matrices gives the normalization and the chosen rotation genera-

tors,

$$\{\Gamma_a, \Gamma_b\} = 2\delta_{ab} 1_4, \qquad J_i = -\frac{i}{2}\Gamma_j \Gamma_k = \frac{\sigma_i}{2} \otimes 1_2 \quad (ijk \text{ cyclic}). \tag{XVII.9.2}$$

The commuting rotation in the last two scalar directions is normalized by

$$R = -i\Gamma_4 \Gamma_5 = 1_2 \otimes \sigma_1, \qquad \mathbf{4}_R = \mathbf{2}_{+1} \oplus \mathbf{2}_{-1}. \tag{XVII.9.3}$$

Thus each charge sector carries an R-doublet. Integer charges here are twice the half-integer Spin(2) weights. This convention will assign charges ± 2 to the two scalar singlets.

The parent Lorentz spinor restricts to $\mathbf{2}_{\text{ext}} \otimes \mathbf{2}_M$. Before reality is imposed, the parameter therefore lies in

$$Q_{\mathbb{C}} = \mathbb{C}^2_{\text{ext}} \otimes \mathbb{C}^2_M \otimes \mathbb{C}^2_R \otimes \mathbb{C}^2_{\text{charge}}, \qquad K_i = 1_{\text{ext}} \otimes \left(\frac{\sigma_i}{2} \otimes 1_4 + 1_2 \otimes J_i \right). \tag{XVII.9.4}$$

The twist selects $K_i q = 0$ for all three generators. To see the answer explicitly, regard a tensor in $\mathbf{2}_M \otimes \mathbf{2}_R$ as a matrix T. Its transformation is

$$K_i T = \frac{1}{2}(\sigma_i T + T\sigma_i^T), \qquad \sigma_i \epsilon + \epsilon \sigma_i^T = 0. \tag{XVII.9.5}$$

The antisymmetric matrix ϵ supplies one singlet. The three symmetric tensors form the triplet, so that

$$\mathbf{2}_M \otimes \mathbf{2}_R = \mathbf{1} \oplus \mathbf{3}, \qquad \dim_{\mathbb{C}} \bigcap_i \ker K_i = 2_{\text{ext}}\, 2_{\text{charge}} = 4. \tag{XVII.9.6}$$

The factor four is a complexified count. Doubling it to eight physical real supercharges would discard the reality inherited from the parent. In this finite restriction, take the compatible antilinear involution to be

$$q = B\bar{q}, \qquad B = 1_{\text{ext}} \otimes \epsilon_M \otimes \epsilon_R \otimes \sigma_3, \qquad B\bar{B} = 1, \quad K_i B = -B\bar{K}_i. \tag{XVII.9.7}$$

The last identity ensures that reality preserves the invariant subspace. For $q = a + ib$, with a, b real, the actual real equations are

$$(B-1)a = 0, \qquad (B+1)b = 0, \qquad (\Re K_i)a - (\Im K_i)b = 0, \quad (\Im K_i)a + (\Re K_i)b = 0. \tag{XVII.9.8}$$

Their kernel has real dimension four. Equivalently, an antilinear involution on the four-complex-dimensional invariant space fixes a real form of dimension four. This gives the ordinary three-dimensional $\mathcal{N} = 2$ count under the assumed parent reality and generic holonomy. It does not construct the full six-dimensional Lorentz algebra or exclude enhancement on special geometries.

The same embedding determines what becomes of the bosons. The R-vector consists of the five scalar directions represented by the five Γ_a. Their commutators with R give

$$[R, \Gamma_i] = 0, \qquad [R, \Gamma_4 \pm i\Gamma_5] = \pm 2(\Gamma_4 \pm i\Gamma_5), \qquad \mathbf{5}_R = \mathbf{3}_0 \oplus \mathbf{1}_{+2} \oplus \mathbf{1}_{-2}. \tag{XVII.9.9}$$

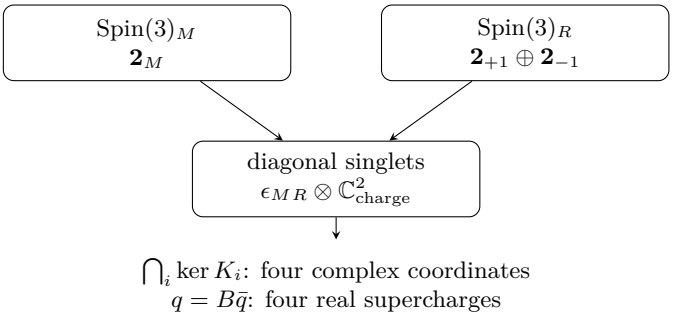


Figure XVII.9.1: The diagonal twist couples the two doublets. The antisymmetric tensor produces one singlet in each R-charge sector. The external spinor factor is retained, and the real involution reduces four complex invariant coordinates to four real supercharges.

After the diagonal identification, the triplet is an adjoint-valued one-form $\phi = \phi_m dy^m$ on M. The remaining two real scalar directions are scalar singlets. These are local field components, not five unconstrained scalar zero modes on an arbitrary M.

One can test how much of this answer depends on the chosen embedding. Reverse only the third R-generator in the singlet equations. A genuine singlet of the original embedding then obeys both $(\sigma_3 T + T\sigma_3^T) = 0$ and $(\sigma_3 T - T\sigma_3^T) = 0$. Together with the first two equations this forces $T = 0$. The changed triple also fails the original $su(2)$ commutator sign. Arbitrary sign choices therefore cannot replace a consistent twist. The surviving $U(1)_R$ labels this background construction; identifying an exact interacting infrared R-current requires additional dynamics.

For a more explicit count, choose the standard basis e_1, e_2 of each doublet. A normalized diagonal singlet and one triplet state are

$$S = \frac{e_1 \otimes e_2 - e_2 \otimes e_1}{\sqrt{2}}, \qquad T_+ = e_1 \otimes e_1, \qquad K_3 S = 0, \quad K_3 T_+ = T_+. \tag{XVII.9.10}$$

The other triplet components are $(e_1 \otimes e_2 + e_2 \otimes e_1)/\sqrt{2}$ and $e_2 \otimes e_2$. Acting with K_1, K_2 mixes these three states but annihilates S. A useful way to test the full decomposition, rather than one generator alone, is the diagonal quadratic Casimir,

$$\sum_i K_i^2\big|_{\mathbf{2}_M \otimes \mathbf{2}_R} = \frac{3}{2}\, 1_4 + \frac{1}{2} \sum_i \sigma_i \otimes \sigma_i, \qquad \operatorname{spec}\left(\sum_i K_i^2 \right) = \{0, 2, 2, 2\}. \tag{XVII.9.11}$$

A zero eigenvector of K_3 alone is insufficient because the middle triplet state also has weight zero. It is the common kernel, or equivalently the zero Casimir eigenspace in this unitary finite representation, that selects the invariant tensor.

Reality can also be seen on these coefficients. Use the σ_3 basis f_1, f_2 on the last

factor, in which $(\epsilon \otimes \epsilon)S = S$. Every invariant complex tensor is

$$q = \sum_{a=1}^{2} e_a^{\text{ext}} \otimes S \otimes (c_{a1} f_1 + c_{a2} f_2), \qquad q = B\bar{q} \iff c_{a1} = \bar{c}_{a1}, \quad c_{a2} = -\bar{c}_{a2}. \tag{XVII.9.12}$$

There are two real coefficients c_{a1} and two purely imaginary coefficients c_{a2}. Each latter coefficient supplies one real parameter, not two. The R-charge basis instead diagonalizes σ_1 and mixes f_1, f_2. Thus charge eigenvectors need not be individually real. The real algebra can have charge-conjugate complex supercharges while still containing only four real generators. This is precisely the count needed before attempting any vacuum interpretation.

XVII.9.2 Boundary holonomies and a polarization

What does the compactification hold fixed at a torus end? Let M now be the compact core of the figure-eight knot complement. Choose an oriented meridian μ and a preferred, null-homologous longitude λ on its boundary. Let $\rho : \pi_1(M) \to SL(2,\mathbb{C})$ be the chosen holonomy representation. Fix

$$\partial M = T^2, \qquad \mu \cdot \lambda = +1, \qquad [\rho(\mu), \rho(\lambda)] = 0. \tag{XVII.9.13}$$

We work with a local $SL(2,\mathbb{C})$ lift. On the generic semisimple locus the commuting matrices can be diagonalized simultaneously. Their eigenvalues define

$$\rho(\mu) \sim \operatorname{diag}(m, m^{-1}), \qquad \rho(\lambda) \sim \operatorname{diag}(\ell, \ell^{-1}), \qquad m, \ell \in \mathbb{C}^*. \tag{XVII.9.14}$$

The common eigenline ordering is immaterial. The Weyl operation acts on both eigenvalues at once,

$$(m, \ell) \longmapsto (m^{-1}, \ell^{-1}). \tag{XVII.9.15}$$

At a parabolic point, commuting matrices need only be triangular. Keeping only their eigenvalues then loses Jordan information. We will retain the actual upper-right longitude entry when that happens.

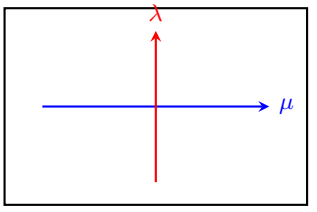
The squared meridian coordinate is useful in comparing with tetrahedron variables. Introduce local logarithms and retain their normalization,

$$u = \log m, \qquad U = 2u = \log x, \qquad x = m^2, \qquad v = \log(-\ell), \qquad \ell = -e^v. \tag{XVII.9.16}$$

In the boundary convention used here, the symplectic form and Poisson brackets are

$$\omega = \frac{1}{\hbar}\, dv \wedge dU, \qquad \{v, U\} = \hbar, \qquad \{v, u\} = \frac{\hbar}{2}. \tag{XVII.9.17}$$

We treat $\hbar$ as the deformation parameter. Choosing U as position fixes the type of response v that a generating function must produce. Replacing U by u without changing the bracket would change this normalization by a factor two. A boundary polarization is additional local information; it does not choose the absolute global M5 theory discussed in XVI.11.



$\mu \cdot \lambda = +1$; opposite sides identified

Figure XVII.9.2: An oriented square represents the marked boundary torus. The horizontal meridian and vertical preferred longitude have intersection $+1$. The right-hand variables are holonomy eigenvalues on a common eigenline and local logarithms in the chosen polarization. These boundary cycles are not integration cycles in field space.

For later matrix calculations, fix the actual group words. With meridian a, the source presentation and its preferred longitude are

$$\pi_1(M) = \langle a, b \mid wa = bw \rangle, \qquad w = a^{-1}bab^{-1}, \qquad \lambda = ba^{-1}b^{-1}a^2b^{-1}a^{-1}b. \tag{XVII.9.18}$$

Both a, b are meridians. Let r be a representation parameter, unrelated to u. A useful triangular normal form is

$$X = \rho(a) = \begin{pmatrix} m & m^{-1} \\ 0 & m^{-1} \end{pmatrix}, \qquad Y = \rho(b) = \begin{pmatrix} m & 0 \\ -mr & m^{-1} \end{pmatrix}, \qquad \det X = \det Y = 1. \tag{XVII.9.19}$$

The group relation will constrain r in Section XVII.9.4. In this gauge X selects the first eigenline generically, and the longitude response is the $(1,1)$ entry of its triangular matrix. Inverting the preferred longitude reverses v up to a logarithmic constant and gives the reciprocal version of the same peripheral equation. Our words fix which version is used throughout.

There is a separate representation family that needs no polynomial in r. Set both generators equal and diagonal,

$$\begin{aligned} \rho_{\mathrm{ab}}(a) = \rho_{\mathrm{ab}}(b) = D = \mathrm{diag}(m, m^{-1}), \\ \rho_{\mathrm{ab}}(w) = 1_2, \qquad \rho_{\mathrm{ab}}(\lambda) = D^{1-1-1+2-1-1+1} = 1_2. \end{aligned} \tag{XVII.9.20}$$

Hence the abelian family has $\ell = 1$ for every nonzero m. The preferred longitude is null-homologous, so this result has a direct topological meaning. A chart of nonabelian representations is not expected to contain it automatically.

The other meridian lift is obtained by twisting the knot representation by the nontrivial $\mathbb{Z}_2$ character of its abelianization. The total longitude exponent is zero, giving

$$(X, Y) \longmapsto (-X, -Y), \qquad m \longmapsto -m, \qquad L = \rho(\lambda) \longmapsto L, \qquad x = m^2 \longmapsto x. \tag{XVII.9.21}$$

For instance, $m = 2$ and $m = -2$ have the same $x = 4$ and the same longitude matrix at the same r, while their meridian eigenvalues differ. Weyl inversion instead takes

$x = 4$ to $x = 1/4$ and ℓ to ℓ^{-1}. These operations answer different questions. Squaring both peripheral eigenvalues would discard still more lift information. Neither operation by itself supplies a global spin refinement, a choice of line operators, or an absolute completion of the parent theory.

The logarithmic chart is local for two reasons. Both the logarithm and the choice of a common eigenline can change on continuation. If U is shifted by $2\pi i$, then x returns to itself, while $u = U/2$ can shift by πi and change the sign of m. Similarly v is defined only modulo $2\pi i$. The exponential coordinates therefore retain fewer choices than the logarithmic generating function:

$$(U, v) \longmapsto (U + 2\pi i n, v + 2\pi i k), \qquad (x, \ell) \longmapsto (x, \ell), \qquad n, k \in \mathbb{Z}. \tag{XVII.9.22}$$

To check the Poisson normalization directly, order the coordinates as (U, v). The antisymmetric matrix of the two-form and its inverse are

$$\omega_{ij} = \frac{1}{\hbar} \begin{pmatrix} 0 & -1 \\ 1 & 0 \end{pmatrix}, \qquad (\omega^{-1})^{ij} = \hbar \begin{pmatrix} 0 & 1 \\ -1 & 0 \end{pmatrix}. \tag{XVII.9.23}$$

Our bracket convention reads $\{f, g\} = -\partial_i f (\omega^{-1})^{ij} \partial_j g$, giving $\{v, U\} = \hbar$ as stated. This sign convention must be fixed along with the order in the two-form. It follows by the chain rule that $\{v, m\} = \hbar m/2$ and $\{v, x\} = \hbar x$. These relations let one recognize a missed factor two even after exponentiation.

There is also a useful direct check of the lift operation. Since every generator inverse changes by the same central sign as the generator, a word transforms by (-1) to its total number of letters. For the longitude, the exponent sum is zero and the word length is even. In contrast, a meridian word has odd parity. Thus the sign of a meridian eigenvalue survives in the $SL(2, \mathbb{C})$ representation even though it disappears from x. At the parabolic point $m = 1$, the matrix X in our gauge is $\left(\begin{smallmatrix} 1 & 1 \\ 0 & 1 \end{smallmatrix}\right)$; it cannot be diagonalized. This is why extending a generic diagonal boundary formula to that point must retain the triangular matrices, rather than assuming the limiting eigenvalues reconstruct them.

XVII.9.3 A complex connection and two different equations

The twist has converted three scalar components into a one-form, so they can join the gauge connection on M. Why does the resulting complex connection describe protected stationary data, and which equation does complex flatness omit? To use a controlled Lagrangian description, compactify an external spacetime direction on a periodic circle of radius R_c and take

$$E R_c \ll 1. \tag{XVII.9.24}$$

We import the low-energy maximal five-dimensional SYM description of the decoupled parent. The remaining two external directions admit an $\mathcal{N} = (2, 2)$ organization of fields that still depend on M. The three local chiral components are therefore an infinite-dimensional field problem, rather than a finite zero-mode reduction on a general knot complement.

Use anti-Hermitian A and ϕ, with $D = d + A$. In terms of Hermitian variables A_H, X_H often used in the five-dimensional description,

$$A = -iA_H, \qquad \phi = -iX_H, \qquad \mathcal{A} = A + i\phi = -i(A_H + iX_H). \tag{XVII.9.25}$$

This translation fixes the sign in the curvature. Expanding the wedge product gives

$$F_{\mathcal{A}} = d(A + i\phi) + (A + i\phi) \wedge (A + i\phi) = F_A - \phi \wedge \phi + i\, d_A\phi. \tag{XVII.9.26}$$

For example, the real component in two local directions is

$$(F_{\mathcal{A}})^{\text{real}}_{mn} = \partial_m A_n - \partial_n A_m + [A_m, A_n] - [\phi_m, \phi_n], \tag{XVII.9.27}$$

while its imaginary component is

$$(F_{\mathcal{A}})^{\text{imag}}_{mn} = D_m\phi_n - D_n\phi_m. \tag{XVII.9.28}$$

The minus sign in the quadratic term is $i^2 = -1$, not a consequence of a choice of contour. Reversing ϕ conjugates the complex connection in this real-form decomposition, reversing the imaginary term while leaving that minus sign intact.

The sourced supersymmetric organization has a holomorphic Chern–Simons superpotential. Its overall coefficient is unnecessary for locating critical points, so write

$$\mathcal{W}_{\text{CS}} = c \int_M \operatorname{Tr}\left(\mathcal{A} \wedge d\mathcal{A} + \frac{2}{3}\mathcal{A} \wedge \mathcal{A} \wedge \mathcal{A}\right), \qquad c \neq 0. \tag{XVII.9.29}$$

The variation follows by integration by parts. With the outward boundary orientation,

$$\delta\mathcal{W}_{\text{CS}} = 2c \int_M \operatorname{Tr}(\delta\mathcal{A} \wedge F_{\mathcal{A}}) - c \int_{\partial M} \operatorname{Tr}(\mathcal{A} \wedge \delta\mathcal{A}). \tag{XVII.9.30}$$

Fix the boundary polarization and the corresponding boundary term before setting the interior variation to zero. Its bulk critical equations are

$$F_A - \phi \wedge \phi = 0, \qquad d_A\phi = 0. \tag{XVII.9.31}$$

They are the real and imaginary parts of complex flatness. The real auxiliary-field equation supplies an additional condition,

$$d_A^*\phi = 0, \qquad \text{equivalently} \qquad D^m\phi_m = 0 \tag{XVII.9.32}$$

up to the harmless overall sign in the definition of d^*. It is a divergence equation, whereas the imaginary flatness equation is an antisymmetrized derivative. One cannot obtain one from the other by comparing real and imaginary parts again.

A local example makes the distinction visible without any noncommuting algebra. On Euclidean $\mathbb{R}^3$ with coordinates y^1, y^2, z, take

$$H = i\,\operatorname{diag}(1, -1), \quad H^\dagger = -H, \quad \operatorname{Tr} H = 0, \qquad A = 0, \qquad \phi = d(z^2)H = 2zH\, dz. \tag{XVII.9.33}$$

Since the one-form is exact and every component is proportional to H,

$$d\phi = 0, \qquad \phi \wedge \phi = 0, \qquad F_{\mathcal{A}} = 0, \qquad \partial^m \phi_m = 2H \neq 0. \tag{XVII.9.34}$$

The real-form condition matters. Replacing H by the Hermitian matrix $\mathrm{diag}(1, -1)$ would leave a formal polynomial calculation but leave our declared field space. Changing the scalar function instead, from z^2 to z, gives $\phi = H dz$ with zero divergence. This second configuration satisfies both local equations. Neither example is asserted to satisfy the knot-end conditions or finite-energy requirements of a global compactification.

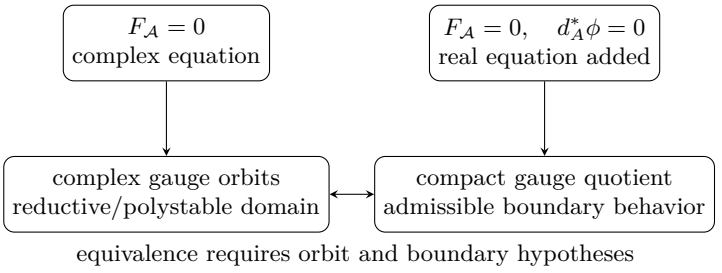


Figure XVII.9.3: Complex flatness and the real moment-map condition are different equations. Relating a complex-gauge quotient to the compact-gauge quotient of their joint solutions requires a suitable orbit and a well-posed boundary problem. The local exact one-form displayed below the diagram violates only the divergence condition.

This distinction also controls quotients. A complex flat connection gives a holonomy representation modulo complex gauge transformations preserving the boundary conditions. A real moment-map representative requires suitable reductivity or polystability and admissible boundary behavior. These hypotheses cannot be dropped on a noncompact manifold. We use the formal local flat equations and the representation algebra below, without asserting an unrestricted noncompact quotient theorem. The infinite-volume localization integral of the sourced five-dimensional construction has a semistable domain and a modified measure. Its whole integration domain is not the F-flat vacuum locus. Locating stationary points of the Chern–Simons functional is a different operation from specifying that integral.

One can verify the variational formula before using the supersymmetric interpretation. Write $a = \delta\mathcal{A}$. The quadratic variation is obtained from

$$\delta \operatorname{Tr}(\mathcal{A} \wedge d\mathcal{A}) = 2 \operatorname{Tr}(a \wedge d\mathcal{A}) - d \operatorname{Tr}(\mathcal{A} \wedge a), \tag{XVII.9.35}$$

where moving a two-form past a one-form produces no extra minus sign. Cyclicity in the cubic term gives three equal contributions, so

$$\delta \operatorname{Tr}\left(\frac{2}{3}\mathcal{A}^3\right) = 2 \operatorname{Tr}(a \wedge \mathcal{A} \wedge \mathcal{A}). \tag{XVII.9.36}$$

Adding these identities and applying Stokes' theorem yields the stated bulk and boundary terms. Only after the boundary variation is canceled or restricted does stationarity imply the flatness equations. This order matters on a knot complement, where a boundary position is part of the definition of the problem.

The local distinction between antisymmetric and contracted derivatives persists even in an abelian Cartan sector. With $\phi = df\,H$ and constant anti-Hermitian H, the two equations reduce to

$$d\phi = d^2 f\,H = 0, \qquad \operatorname{div}\phi = (\Delta f)H. \tag{XVII.9.37}$$

The first is an identity for any smooth f; the second is the harmonic equation. Our choices $f = z^2$ and $f = z$ simply compare a nonharmonic and harmonic function. They teach which operation the real moment map performs. Boundary values can forbid one or both choices, so this reduction is a diagnostic of the local equations, not a construction of global knot vacua. In the nonabelian problem the additional commutator term in $F_A - \phi \wedge \phi$ is essential and cannot be inferred from this abelian example.

XVII.9.4 A figure-eight vacuum chart computed in two ways

Can the protected stationary equations reproduce the boundary response of an actual group representation? Start with X, Y and the marked words already defined. Set $W = X^{-1}YXY^{-1}$. Multiplication gives

$$WX - YW = \begin{pmatrix} 0 & P/m \\ mrP & 0 \end{pmatrix}, \qquad P(r,m) = r^2 + (3 - m^2 - m^{-2})(r+1). \tag{XVII.9.38}$$

For example, $W_{11} = (r+1)^2 - r/m^2$, $W_{12} = r + 1 - m^{-2}$, and $W_{21} = -r(m^2 r + m^2 - 1)$. Substitution in the upper-right entry of $WX - YW$ produces P/m; the lower-left entry gives the same condition. Since $m \neq 0$, the relation is precisely $P = 0$.

Next multiply the longitude word,

$$L = YX^{-1}Y^{-1}X^2Y^{-1}X^{-1}Y. \tag{XVII.9.39}$$

Polynomial division by P means replacing every occurrence of r^2 with $-(3 - m^2 - m^{-2})(r + 1)$. The reduced entries are

$$L_{21} = 0, \quad L_{11} = \ell = -1 + m^{-2} - 2m^2 + m^4 + r(m^{-2} - m^2), \quad L_{22} = \ell^{-1}. \tag{XVII.9.40}$$

The remaining entry must also be retained,

$$L_{12} = -\frac{(m^2+1)(-m^4 + 2m^2 r + 3m^2 - 1)}{m^4}. \tag{XVII.9.41}$$

Thus one obtains both the eigenvalue curve and the Jordan information from the same word. To eliminate r, introduce $x = m^2$ and write $\ell = a + br$, where $a = x^2 - 2x - 1 + x^{-1}$ and $b = x^{-1} - x$. Multiplying the two values of $\ell - a - br$ over the roots of P gives

$$\operatorname{Res}_r(P, \ell - L_{11}) = \frac{A_{\mathrm{irr}}(x,\ell)}{x^2}, \quad A_{\mathrm{irr}} = x^2\ell^2 - (x^4 - x^3 - 2x^2 - x + 1)\ell + x^2. \tag{XVII.9.42}$$

This resultant formula remains meaningful at $b = 0$, where directly dividing by b would fail. Dividing by $x^2\ell$ on the allowed torus yields the reciprocal relation

$$\ell + \ell^{-1} = x^2 - x - 2 - x^{-1} + x^{-2}. \tag{XVII.9.43}$$

For the second route, label the first tetrahedron's three logarithmic shapes by Z, Z', Z''. For the second tetrahedron use $s = W_{\mathrm{tet}}$ and W''; primes label cyclic shapes, rather than derivatives. Set $Z' = U + s$ and call C the internal-edge logarithm. Their sourced local graphs and edge constraint are

$$\begin{aligned} Z &= \log(1 - e^{-U-s}), \qquad W'' = \log(1 - e^{-s}), \\ C &= 2Z + Z'' + 2s + W'' = 2\pi i, \qquad Z + Z' + Z'' = i\pi. \end{aligned} \tag{XVII.9.44}$$

The response is $v = Z - Z'$. Eliminating Z'' gives $C - 2\pi i = Z + W'' - U + s - i\pi$. A local generating family with precisely these two derivatives is

$$\mathcal{W}(U, s) = \mathrm{Li}_2(e^{-U-s}) + \mathrm{Li}_2(e^{-s}) - \frac{U^2}{2} - Us + \frac{s^2}{2} - i\pi s. \tag{XVII.9.45}$$

Since $d\,\mathrm{Li}_2(e^{-z})/dz = \log(1 - e^{-z})$, its actual gradients are

$$\partial_s \mathcal{W} = \log(1-e^{-U-s}) + \log(1-e^{-s}) - U + s - i\pi, \qquad \partial_U \mathcal{W} = \log(1-e^{-U-s}) - U - s = v. \tag{XVII.9.46}$$

All logarithms are on local sheets. Set $t = e^{-s}$, so $x, t \neq 0$, with $t \neq 1, x$ for the nonsingular logarithmic graph. Exponentiating the periodic stationary equation and the response gives

$$e^{\partial_s \mathcal{W}} = 1 \quad \Longrightarrow \quad B(t, x) = (x - t)(1 - t) + x^2 t = 0, \qquad \ell = -e^{\partial_U \mathcal{W}} = \frac{t(t - x)}{x^2}. \tag{XVII.9.47}$$

The minus sign in ℓ cancels the sign from $t - x$. Expanding $B = t^2 + (x^2 - x - 1)t + x$, then taking the resultant with $x^2\ell - t(t - x)$, yields

$$\mathrm{Res}_t\big(B, x^2\ell - t(t - x)\big) = x^2 A_{\mathrm{irr}}(x, \ell). \tag{XVII.9.48}$$

The prefactor is removable because $x \neq 0$. Also $B(0, x) = x$, $B(1, x) = x^2$, and $B(x, x) = x^3$, so no finite allowed stationary root lies on the excluded logarithmic divisors. This observation does not restore an omitted component.

At $m = 2$, a changed meridian gives $P = r^2 - 5r/4 - 5/4$, hence $r = (5 \pm \sqrt{105})/8$ and $\ell = 29/4 - 15r/4$. The other route has $x = 4$ and $B = t^2 + 11t + 4$. Its responses obey $16\ell^2 - 157\ell + 16 = 0$, exactly the matrix-word result. At $m = 3/2$, the same substitutions give $P = r^2 + 11(r + 1)/36$ and $B = t^2 + 29t/16 + 9/4$; the algebra is unchanged while the roots move. These comparisons test the response away from the cusp rather than assigning branches by their cusp eigenvalue.

The protected interpretation is that circle-compactified twisted-chiral stationary data of the intended $T[M]$ admit such a local chart. This remains a sourced physical identification. The naive two-tetrahedron theory lacks the required hard-edge operators and is not the complete figure-eight QFT. XVII.10 supplies the actual six-tetrahedron

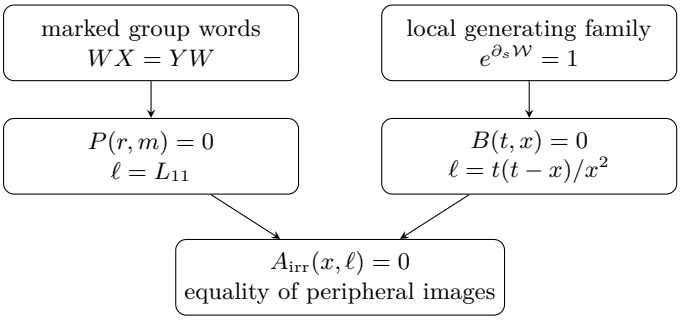


Figure XVII.9.4: Two finite eliminations produce the same peripheral image. The left route uses the marked group and longitude. The right uses the differentiated local dilogarithmic family. Equality at the bottom concerns eigenvalue curves; it supplies neither an interior-branch bijection nor a completed knot theory.

edge and contact-term construction. Our equality is an exact generating-chart identity, not a full partition-function computation.

The elimination can be reproduced without a resultant routine. Put $c = 3 - x - x^{-1}$ in the representation polynomial. Since $r_+ + r_- = -c$ and $r_+ r_- = c$, the two longitude responses satisfy

$$\ell_+ + \ell_- = 2a - bc, \qquad \ell_+ \ell_- = a^2 - abc + b^2 c = 1. \tag{XVII.9.49}$$

Substituting the displayed a, b gives $2a - bc = x^2 - x - 2 - x^{-1} + x^{-2}$. The monic quadratic with this sum and product is exactly A_{irr}/x^2. This derivation also explains why the peripheral polynomial is reciprocal in ℓ.

For the generating-family route, write $d = x^2 - x - 1$. Reduction by $B = t^2 + dt + x$ gives a linear response numerator,

$$t^2 = -dt - x, \qquad x^2 \ell = t^2 - xt = (1 - x^2)t - x. \tag{XVII.9.50}$$

At $x^2 \neq 1$, substitute $t = (x^2 \ell + x)/(1 - x^2)$ into B. Multiplying by $(1 - x^2)^2$ gives

$$(x^2 \ell + x)^2 + d(x^2 \ell + x)(1 - x^2) + x(1 - x^2)^2 = x^2 A_{\mathrm{irr}}(x, \ell). \tag{XVII.9.51}$$

The resultant preserves the formula at $x^2 = 1$, where this division is unavailable. In particular, the failure to solve linearly for t at $x = 1$ is already a warning that the boundary response can collapse two stationary points. It is not a failure of the stationary quadratic.

The changed-input example can be checked using only sums and products as well. For $x = 4$, the stationary roots have sum -11 and product 4. Their responses are $(-15t - 4)/16$. Hence their response sum is $157/16$ and their product is 1. The matrix roots give the same two symmetric functions via $\ell = 29/4 - 15r/4$, with $r_+ + r_- = 5/4$ and $r_+ r_- = -5/4$. This comparison checks both roots without assigning a root-to-root correspondence from a special limiting value.

XVII.9.5 Branches, singular limits and integration cycles

A peripheral curve has forgotten information twice. It projects an interior representation to boundary holonomies, then projects matrices to eigenvalues. Which branches and exceptional points survive those operations? Begin with the separately constructed diagonal family. Combining its image with the nonabelian-component image gives, up to multiplicity conventions,

$$(\ell - 1)A_{\mathrm{irr}}(x, \ell) = 0. \tag{XVII.9.52}$$

This equation describes the union of peripheral components in our calculation. It is not an assertion that this polynomial alone is the full character variety. In particular,

$$A_{\mathrm{irr}}(x, 1) = -(x + 1)^2(x^2 - 3x + 1). \tag{XVII.9.53}$$

The abelian family exists for every $x \neq 0$, whereas it lies on this nonabelian-component image only at the displayed intersection values.

To test reducibility of the actual triangular representation, ask for a common invariant line of X and Y. The first basis vector is an X eigenvector. It is also preserved by Y precisely when $r = 0$. For $m^2 \neq 1$, the other X eigenline is spanned by $(1, 1-m^2)^T$. Requiring Y to preserve it gives the alternative condition

$$r = (m - m^{-1})^2, \qquad P\big((m - m^{-1})^2, m\big) = 1. \tag{XVII.9.54}$$

Thus the alternative never solves the group relation. The reducible locus in this normal form is

$$r = 0, \qquad P(0, m) = 3 - m^2 - m^{-2} = 0, \qquad m^4 - 3m^2 + 1 = 0. \tag{XVII.9.55}$$

At these points the upper-triangular extension need not split. Its ordinary conjugacy orbit can be nonclosed. In the GIT character quotient, the character is identified with its diagonal semisimplification. A point of that quotient therefore records less information than an ordinary conjugacy class. Calling the polynomial component irreducible does not assert that every representation on it is irreducible. Moreover the peripheral intersection at $x = -1$ in $A_{\mathrm{irr}}(x, 1)$ does not satisfy this reducibility criterion and must not be reinterpreted as one.

The source of another exception is visible in a quadratic discriminant. Put $k = m^2 + m^{-2}$. The Riley polynomial and its discriminant are

$$P = r^2 + (3-k)r + (3-k), \qquad \Delta_r = (3-k)^2 - 4(3-k) = (k-3)(k+1). \tag{XVII.9.56}$$

For generic k the two roots are distinct. At $k = 3$ they coalesce at the reducible point; at $k = -1$ they coalesce for a different reason. An isolated nondegenerate saddle approximation cannot simply be continued through these loci.

The complete parabolic meridian value $m = 1$ behaves differently. There $k = 2$, so the representation roots remain distinct,

$$P(r, 1) = r^2 + r + 1, \qquad r_{\pm} = \frac{-1 \pm i\sqrt{3}}{2}, \qquad \Delta_r = -3. \tag{XVII.9.57}$$

Yet both give the same boundary eigenvalue,

$$L_{11} = -1, \qquad A_{\mathrm{irr}}(1,\ell) = (\ell+1)^2, \qquad L_{12}(r_\pm, 1) = \mp 2i\sqrt{3}. \tag{XVII.9.58}$$

The marked matrix still distinguishes Jordan extension information that the eigenvalue has lost. The stationary chart also retains two distinct roots,

$$B(t,1) = t^2 - t + 1, \qquad t_\pm = \frac{1 \pm i\sqrt{3}}{2}, \qquad t_\pm(t_\pm - 1) = -1. \tag{XVII.9.59}$$

Both responses are $\ell = -1$. Peripheral-image equality therefore does not determine a bijection between these interior roots. Nor does it label one as geometric and the other as conjugate without an oriented developing map. Changing the central meridian lift to $m = -1$ preserves the longitude and this eigenvalue statement.

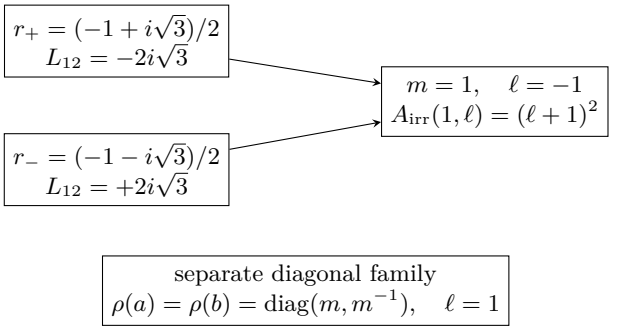


Figure XVII.9.5: At the parabolic meridian value the two representation roots have opposite nonzero longitude off-diagonal entries but project to the same eigenvalue. The diagonal abelian family is separate and has longitude eigenvalue $+1$. The arrows denote the boundary eigenvalue projection, not an identification of interior connections.

Finally a stationary root does not select an integration cycle. Fix x away from discriminants, a nonsingular logarithmic lift of $\mathcal{W}$, and a phase of $\hbar$. A root labelled α is nondegenerate when

$$B(t_\alpha, x) = 0, \qquad \partial_s^2 \mathcal{W}\big|_\alpha = \frac{t_\alpha}{x - t_\alpha} + \frac{t_\alpha}{1 - t_\alpha} + 1 \neq 0. \tag{XVII.9.60}$$

For example at $x = 1$, this Hessian is $(1 + t_\alpha)/(1 - t_\alpha)$, which is nonzero at both roots. A chosen local steepest-descent cycle $\mathcal{J}_\alpha$ for $\Re(\mathcal{W}/\hbar)$ defines a formal saddle sector. A physical relative integration cycle would instead require

$$\Gamma = \sum_\alpha n_\alpha \mathcal{J}_\alpha, \qquad n_\alpha = \langle \Gamma, \mathcal{K}_\alpha \rangle, \tag{XVII.9.61}$$

where $\mathcal{K}_\alpha$ is a dual upward cycle in a suitable relative homology problem. Intersection numbers, boundary conditions and a continuation path determine the coefficients. They cannot be set to one just by listing flat connections. At a Stokes wall the thimble

basis and its coefficients can jump while the specified cycle is continued consistently. No physical Γ, coefficient n_α, one-loop measure or full partition function has been constructed here. XVII.10 supplies the complete knot-theory gluing needed to compare an actual protected observable; XVII.11 addresses fillings and the boundary choices that enter integration cycles.

The common-eigenline test itself can be derived in coordinates. For a candidate vector $(1, z)^T$, the second component of the X eigenvalue equation is $m^{-1}z$. For the eigenvalue m^{-1}, the first component requires $z = 1 - m^2$. Applying Y to that vector gives

$$Y\begin{pmatrix} 1 \\ 1-m^2 \end{pmatrix} = \begin{pmatrix} m \\ -mr + m^{-1}(1-m^2) \end{pmatrix}. \tag{XVII.9.62}$$

Proportionality with the first component equal to m requires $-mr + m^{-1}(1-m^2) = m(1-m^2)$, or $r = (m - m^{-1})^2$. This is the excluded alternative found above. For the other eigenline, $z = 0$, the same calculation immediately gives $r = 0$. At $m^2 = 1$ the eigenlines merge, but the remaining line still requires $r = 0$, incompatible with $P = r^2 + r + 1$. This checks reducibility at the parabolic meridian without using a diagonalizing matrix that becomes singular there.

The stationary discriminant provides another comparison of what does and does not degenerate. From the displayed B,

$$\Delta_t = (x^2-x-1)^2-4x = (x^2-3x+1)(x^2+x+1), \qquad \Delta_r = \frac{(x^2-3x+1)(x^2+x+1)}{x^2}. \tag{XVII.9.63}$$

Their zeros agree for $x \neq 0$, but the cusp $x = 1$ is not among them. There the repeated root in the peripheral polynomial is a property of the projection. It is not a repeated interior Riley root or a vanishing stationary Hessian. This distinction is useful whenever a boundary polynomial appears to have a multiple solution.

For a steepest-descent calculation, a local critical value also has a logarithmic-lift ambiguity. Adding $2\pi i s$ to $\mathcal{W}$ leaves its exponential stationary equation invariant but changes the unexponentiated function along a path. Thus the algebraic stationary set and the analytic integration problem retain different amounts of information. A phase comparison between saddles requires actual lifted critical values and a specified continuation, not merely the polynomial roots. Even away from all discriminants, those choices must be made before a candidate sector can be interpreted as a contribution to an observable.

XVII.9.6 Exercises

For benchmark submissions, see `benchmark/PROTOCOL.md`. Give the polynomial expressions, intermediate derivations and explanations. Use the conventions of this chapter throughout; in particular $x = m^2$ and $\ell = -e^v$.

1. Construct the three K_i and the involution B from Section XVII.9.1. Find the complex invariant dimension, the real invariant dimension and the multiplicities of scalar R-charges $0, +2, -2$. Reverse only the third embedded R-generator and compute the invariant dimension again. Submit `E1.complex`, `real`,

`scalar_multiplicities` in that charge order, and `changed_kernel`. Explain why a compatible parent reality, rather than doubling a complex dimension, gives the physical supercharge count, and why the changed triple fails to define the original embedding.

2. At fixed Riley root, compare the central meridian lifts $m = 2, -2$ and the Weyl image of $m = 2$. Submit `E2.x_lifts` and `weyl_x`, together with the coefficients of $\hbar$ in $\{v, U\}$ and $\{v, u\}$ as `bracket_U`, `bracket_u`. Multiply the preferred longitude word to explain its invariance under the central twist. State why these choices do not determine the absolute global M5 theory and why a parabolic boundary matrix needs more than eigenvalues.

3. Expand $F_{A+i\phi}$ in the anti-Hermitian convention. For $A = 0$, $H = i\,\mathrm{diag}(1, -1)$ and $\phi = d(z^2)H$, submit the scalar coefficient multiplying H in the divergence as `E3.quadratic_divergence`; repeat for $\phi = d(z)H$ as `linear_divergence`. Submit the coefficient of $\phi \wedge \phi$ as `quadratic_sign`. Show both curvatures vanish and check $H^\dagger = -H$. Explain why the local example says nothing about admissibility at the knot end.

4. Multiply the group and longitude words at $m = 3/2$. Submit the monic polynomial P as `E4.riley`, the sum and product of its two roots as `root_sum`, `root_product`, the reduced L_{11} and L_{12} as `longitude`, `offdiagonal`, and $A_{\mathrm{irr}}(x, \ell)$ as `curve`. Derive the resultant normalization $\mathrm{Res}_r(P, \ell - L_{11}) = A_{\mathrm{irr}}/x^2$ and evaluate both L_{11} and L_{12} at each root in writing. Explain the loss of extension information at $m = 1$. Polynomial variables are `r,x,ell`.

5. Differentiate both dilogarithms and all polynomial terms in $\mathcal{W}$. At $x = 9$ submit the monic stationary polynomial in `t` as `E5.stationary`, the numerator $81\ell - t(t-9)$ as `response`, and the eliminated peripheral polynomial as `curve` with its normalization $A_{\mathrm{irr}}(9, \ell)$. Submit the multiplicative change in $e^{\partial_s \mathcal{W}}$ after adding $2\pi i s$ as `sheet_factor`. Show both logarithmic gradients and both stationary roots in writing, including the minus sign in ℓ. State the excluded divisors $t = 0, 1, x$ and $x = 0$, and explain why this chart is not the completed knot QFT.

6. Submit $A_{\mathrm{irr}}(x, 1)$, the Riley discriminant in `m`, and $A_{\mathrm{irr}}(1, \ell)$ as `E6.abelian_intersection`, `discriminant`, `cusp`. Explain separately the diagonal abelian family, the reducible nonabelian extension at $r = 0$, and its GIT semisimplification. Explain why the $x = -1$ boundary intersection need not be reducible and why two cusp roots cannot be labelled by orientation from the eigenvalue alone. Describe the extra information required to determine n_α, and the distinct next tasks of XVII.10 and XVII.11.

XVII.9.7 Take-home result and exit check

The diagonal twist preserves four real supercharges under the stated parent reality. It converts three scalar directions into a one-form, allowing $\mathcal{A} = A + i\phi$. Complex flatness supplies two equations; the real moment map remains a third condition with boundary

and stability hypotheses. For the marked figure-eight complement, matrix-word elimination and a differentiated local generating family yield the same nonabelian-component peripheral curve. The abelian component, reducible extensions, and parabolic Jordan matrices require separate attention.

Before continuing, recover the factor two between U and u, reconstruct the longitude from its word, and differentiate $\mathcal{W}$ without guessing the response sign. Then explain how two distinct roots can give $\ell = -1$ and why a saddle list cannot fix a physical contour. These are the ingredients needed to test the complete tetrahedron construction in the next chapter.

Sources and scope

§1. [DEC] The decoupled interacting parent and periodic low-energy five-dimensional SYM use are imported from XVI.1. [MATH] The explicit Clifford embedding, diagonal singlets, compatible finite real restriction and scalar branching are derived here using the parent representation of Yagi 2013, v2, (2.2)–(2.7). The supersymmetric background is assumed. The supersymmetry conventions are those specified for the parent theory in XVI.1.

§2. [MATH] The marked presentation, longitude and triangular normal form follow Andersen and Hansen 2003, pp. 23–25, (53)–(59). Boundary logarithms and the polarization use Dimofte et al. 2011, v1, (2.26)–(2.29), including its lift qualifications. The local $SL(2,\mathbb{C})$ model and squared meridian coordinate do not select an absolute M5 global theory.

§3. [MATH] Curvature expansion and the local anti-Hermitian counterexample are explicit calculations. The F/D-field organization and holomorphic Chern–Simons superpotential are physical inputs from Yagi 2013, (2.14)–(2.20), (4.11). [CONJ+] A vacuum/flat-connection quotient interpretation requires the stated stability and boundary assumptions. The localization domain in its (4.18)–(4.19) is not identified with the full flat locus.

§4. [MATH] Group-word multiplication reproduces the known Riley and peripheral equations from Andersen and Hansen 2003, (53)–(59), and Dimofte et al. 2011, (2.32). The local generating family is derived from the graph (2.29)–(2.32), rather than quoted as an independent source equation. [CONJ+] Its twisted-chiral protected interpretation uses (5.1)–(5.5). The hard-edge obstruction and six-tetrahedron completion appear on pp. 38–41. Equality here is of peripheral images, not interior branches or full QFTs.

§5. [MATH] Reducible and nonclosed-orbit qualifications use Andersen and Hansen 2003, Theorem 5.1 and Corollary 5.2, with the displayed finite calculations. The normal-form classification is imported, not newly proved. Formal sectors and intersection coefficients follow Witten 2010, v2, §§2.2–2.3, (2.14)–(2.16). Physical contours and their measures remain open here.

The algebraic comparisons share input data and establish identities only in the stated domain. The physical premises, a global quotient theorem, a one-loop measure and an absolute partition function require further input.

Chapter XVII.10

From tetrahedra to three-dimensional theories

An ideal triangulation replaces a three-manifold by tetrahedra whose vertices lie at its ends. Each tetrahedron carries a complex shape. Gluing imposes equations on those shapes and leaves boundary holonomies as external data. The field-theory construction follows the same operations: assign a chiral multiplet to a tetrahedron, gauge selected flavor symmetries, and add ordinary superpotential interactions for the internal edges. This gives a concrete way to ask which three-dimensional theory a polarized triangulation proposes.

We will carry out this construction for a six-tetrahedron chart of the figure-eight knot complement. The answer will include twelve abelian gauge factors, all contact terms, and six dressed monopole interactions. Eliminating the six shapes will recover its nonabelian boundary eigenvalue curve. A bipyramid will supply a smaller example in which the two-to-three move becomes the familiar SQED/XYZ mirror pair. Finally we will distinguish a formal quantum pentagon from a noncompact partition integral.

The prerequisites are three-dimensional $\mathcal{N} = 2$ chirals and vector multiplets, abelian Chern–Simons and BF couplings, and holomorphic symplectic reduction. We recall the conventions needed for monopoles and quantum products below. The connection to the type-A_1 six-dimensional $(2, 0)$ compactification is the tetrahedron/gluing proposal of Dimofte, Gaiotto and Gukov. We use their mirror identifications to transport easy-edge operators between presentations. These are physical inputs. The computations here establish the specified local geometry, charge and contact consistency, and protected identities in their stated domains; they do not derive the compactification from a six-dimensional action.

XVII.10.1 A chiral multiplet for an ideal tetrahedron

How can a shape become a field-theory mass? Begin with four distinct points on the Riemann sphere, and use a fractional linear transformation to put three at $0, 1, \infty$. The

fourth is a cross-ratio z. The three cyclic choices of opposite edges then carry

$$z' = \frac{1}{1-z}, \qquad z'' = 1 - \frac{1}{z}, \qquad zz'z'' = -1, \qquad z \in \mathbb{C} \setminus \{0, 1\}. \tag{XVII.10.1}$$

The excluded values collapse the tetrahedron. A cyclic relabeling sends $z \to z' \to z'' \to z$. It does not introduce three independent shape moduli. The first relation determines z' and the second determines z'' from z.

Choose local logarithms $Z = \log z$, $Z' = \log z'$, $Z'' = \log z''$, and set $h = i\pi$. The affine lift retained throughout this chapter is

$$Z + Z' + Z'' = h, \qquad q = Z, \quad p = Z'', \qquad \omega = \hbar^{-1} dp \wedge dq, \quad \{p, q\} = \hbar. \tag{XVII.10.2}$$

Changing logarithm branches changes this lift by integral multiples of $2\pi i$. We keep the displayed choice fixed when composing transformations. In these variables, one cyclic change is

$$\begin{pmatrix} q_{\text{new}} \\ p_{\text{new}} \end{pmatrix} = \begin{pmatrix} -1 & -1 \\ 1 & 0 \end{pmatrix} \begin{pmatrix} q \\ p \end{pmatrix} + \begin{pmatrix} h \\ 0 \end{pmatrix}. \tag{XVII.10.3}$$

The matrix has determinant one. The constant records the minus sign in $zz'z'' = -1$; dropping it would preserve the symplectic form but change the actual logarithmic gluing conditions.

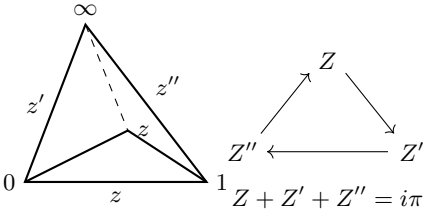


Figure XVII.10.1: An ideal tetrahedron with vertices normalized to $0, 1, \infty, z$. Opposite edges share a shape label. The cyclic diagram at right records the three choices of position coordinate. In logarithms their sum is $h = i\pi$, which produces the affine term in the polarization change.

The tetrahedron prescription assigns a single charge-one chiral multiplet Φ to the flavor symmetry whose complex mass is q. This is a regulated assignment: the chiral determinant comes together with a background Chern–Simons counterterm. Our convention for a symmetric level matrix is

$$S_{\text{CS}} = \frac{1}{4\pi} \int K_{AB} A_A \wedge dA_B, \qquad K_{AB} = K_{BA}. \tag{XVII.10.4}$$

Thus an off-diagonal entry k gives a BF coupling $k/(2\pi) \int A \wedge dB$, up to a boundary term. All electric charges and gauge fluxes used here are integral, and the three-dimensional spacetime is oriented and spin.

A massive charge-Q_e fermion shifts the level in the DGG convention by $Q_e^2\,\mathrm{sign}(M)/2$. The two massive chambers therefore have

$$k_{\mathrm{eff}}(M) = k + \frac{Q_e^2}{2}\,\mathrm{sign}(M), \qquad k + \frac{Q_e^2}{2} \in \mathbb{Z}. \tag{XVII.10.5}$$

For the tetrahedron choose $Q_e = 1$ and $k = -1/2$. This gives

$$k_{\mathrm{eff}}(M > 0) = 0, \qquad k_{\mathrm{eff}}(M < 0) = -1. \tag{XVII.10.6}$$

The regulator breaks parity while preserving gauge invariance. The half-level functional is not an arbitrary separately gauge-invariant ordinary CS action: its anomalous transformation cancels that of the determinant. Integer local counterterm shifts remain available on a spin manifold. In the contact convention of Closset et al., the effective coefficient is $\kappa = -k$; translating this sign is necessary before comparing massive chambers.

Compactify the physical theory on a circle of circumference β. If $m_{\mathbb{C}}$ is the complexified flavor mass, its dimensionless logarithm is $q = \beta m_{\mathbb{C}}$. In the chosen polarization and regulator, summing the Kaluza–Klein tower gives the local twisted superpotential

$$\widetilde{W}_\Delta(q) = \mathrm{Li}_2(e^{-q}), \qquad \frac{d}{dq}\widetilde{W}_\Delta(q) = \log(1 - e^{-q}). \tag{XVII.10.7}$$

One can verify the derivative directly from $d\,\mathrm{Li}_2(t)/dt = -\log(1-t)/t$. The circle response $p = \partial_q \widetilde{W}_\Delta$ thus obeys

$$e^p = 1 - e^{-q}, \qquad z'' + z^{-1} = 1. \tag{XVII.10.8}$$

The vacuum relation is exactly the shape Lagrangian. It is a local massive effective description: at $z = 1$ the derivative is singular because a chiral mode becomes massless. That singularity does not establish that the original three-dimensional theory disappears.

For an explicit change of shape, take $z = 2$. Then $z' = -1$, $z'' = 1/2$. For $z = 3$ the values become $-1/2$ and $2/3$. Both satisfy

$$z'z'' = -z^{-1}, \qquad d\widetilde{W}_\Delta/dq\Big|_{z=2} = \log\tfrac{1}{2}, \quad d\widetilde{W}_\Delta/dq\Big|_{z=3} = \log\tfrac{2}{3}. \tag{XVII.10.9}$$

The logarithms require compatible branches, but the exponentiated equations are unambiguous on this open set. These examples also separate a shape from an external holonomy: the letter z labels one building block, and it will not stand for the meridian eigenvalue of the glued manifold.

An ordinary superpotential is a different object from $\widetilde{W}_\Delta$. An ordinary chiral operator inserted into W must have vanishing real mass and R-charge two. A logarithmic internal-edge coordinate C therefore receives the condition

$$C = 2\pi i = 2h, \qquad e^C = 1. \tag{XVII.10.10}$$

The circle twisted superpotential instead generates a Lagrangian relation after massive fields have been integrated out. Confusing these two uses of superpotential would allow a vacuum equation to substitute for an ordinary local operator. The next section constructs the operators and contacts separately.

XVII.10.2 Gluing, gauging and edge interactions

The first gluing problem is a bipyramid. Take three tetrahedra with logarithmic positions (Z, W, Y) and momenta (Z'', W'', Y''). Let X_1, X_2 be two external positions and C the internal edge. A polarization adapted to that edge is

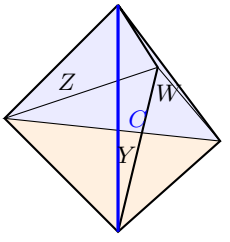
$$X_1 = Z, \quad X_2 = W, \quad C = Z + W + Y, \qquad P_1 = Z'' + Y', \quad P_2 = W'' + Y', \quad \Gamma = -Y'. \tag{XVII.10.11}$$

Because $Y' = h - Y - Y''$, the linear and affine parts are explicit:

$$g_3 = \begin{pmatrix} 1 & 0 & 0 & 0 & 0 & 0 \\ 0 & 1 & 0 & 0 & 0 & 0 \\ 1 & 1 & 1 & 0 & 0 & 0 \\ 0 & 0 & -1 & 1 & 0 & -1 \\ 0 & 0 & -1 & 0 & 1 & -1 \\ 0 & 0 & 1 & 0 & 0 & 1 \end{pmatrix}, \qquad \delta_3 = (0, 0, 0, h, h, -h)^t. \tag{XVII.10.12}$$

For $J_n = \left(\begin{smallmatrix} 0 & -I_n \\ I_n & 0 \end{smallmatrix}\right)$, direct multiplication gives $g_3 J_3 g_3^t = J_3$. This checks the conjugate variables as well as the external positions. At $C = 2h$, its exponential eliminates the third mass.

Call the resulting chiral fields X, Y, Z in the conventional name XYZ; these uppercase field symbols are separate from the logarithms in (XVII.10.11).



$C = Z + W + Y = 2h$
$X_1 = Z, \quad X_2 = W$

$Q_X = (1, 0)$, $Q_Y = (0, 1)$
$Q_Z = (-1, -1)$
$W_{\text{ordinary}} = XYZ$

Figure XVII.10.2: Three tetrahedra meeting along the central edge C. The equatorial sectors carry Z, W, Y and the external positions are $X_1 = Z, X_2 = W$. Setting $C = 2h$ fixes their sum. The resulting three chirals have the neutral product XYZ; the central edge is an ordinary-superpotential constraint.

In the flavor basis (X_1, X_2) their charge rows and ordinary superpotential are

$$Q_{XYZ} = \begin{pmatrix} 1 & 0 \\ 0 & 1 \\ -1 & -1 \end{pmatrix}, \qquad W_{XYZ} = XYZ, \qquad (1, 1, 1) Q_{XYZ} = 0. \tag{XVII.10.13}$$

Before changing flavor basis, add $+1$ to the third tetrahedron's background level. The bare levels become $(-1/2, -1/2, +1/2)$, so the final contact response is

$$K_{XYZ} = Q_{XYZ}^t \operatorname{diag}(-\tfrac{1}{2}, -\tfrac{1}{2}, \tfrac{1}{2}) Q_{XYZ} = \begin{pmatrix} 0 & 1/2 \\ 1/2 & 0 \end{pmatrix}. \tag{XVII.10.14}$$

The added integer shift matters even though it does not change the matter charges. Omitting it subtracts the all-ones 2×2 matrix from K_{XYZ}. It changes the background response and its partition-function phase.

For a larger example it is useful to realize the gauging without leaving an instruction to apply an unspecified symplectic transformation. Write a product polarization as $(\boldsymbol{q}, \boldsymbol{p})$ and desired positions as

$$\boldsymbol{x} = A\boldsymbol{q} + B\boldsymbol{p} + \boldsymbol{c}h, \qquad N = A^{-1}B = N^t, \qquad A \in GL(n, \mathbb{Z}). \tag{XVII.10.15}$$

Here $\boldsymbol{x}$ is a vector of logarithmic backgrounds, distinct from any single lowercase shape. The operations usually denoted S, T, GL have direct physical meanings: gauge a flavor and introduce its topological background, add an integral CS contact, and change the integral charge basis. A doubled BF presentation keeps both intermediate gauge fields. Introduce a_i, b_i and a chiral ϕ_i of charge $+1$ under a_i. Its bare gauge and background matrices are

$$Q_g = \begin{pmatrix} I_n \\ 0 \end{pmatrix}, \quad K_{gg} = \begin{pmatrix} -I_n/2 & I_n \\ I_n & -N \end{pmatrix}, \quad K_{ax} = 0, \quad K_{bx} = -A^{-1}, \quad K_{xx} = H = H^t. \tag{XVII.10.16}$$

The sequence is S, the shear $-N$, inverse S, basis change A, and the background shear H. Positive Maxwell terms can regulate the abelian gauge fields in the ultraviolet. They do not supply new protected infrared parameters. The parity-corrected matrix is

$$K_{gg} + \tfrac{1}{2} Q_g Q_g^t = \begin{pmatrix} 0 & I_n \\ I_n & -N \end{pmatrix} \in \mathrm{Mat}_{2n}(\mathbb{Z}). \tag{XVII.10.17}$$

This integral matrix is an anomaly test, not a replacement for the bare half-level matrix in the monopole Gauss law.

The signs and affine terms can be recovered from a generating function. Let $\boldsymbol{\eta}$ denote the complex scalars of the b_i multiplets, reserving b later for ellipsoid squashing. For an affine momentum shift $\boldsymbol{d}h$ use

$$\begin{aligned} F = {} & \sum_i \mathrm{Li}_2(e^{-q_i}) + \boldsymbol{q}^t\boldsymbol{\eta} - \tfrac{1}{2}\boldsymbol{\eta}^t N \boldsymbol{\eta} - \boldsymbol{\eta}^t A^{-1}(\boldsymbol{x} - \boldsymbol{c}h) \\ & + \tfrac{1}{2}\boldsymbol{x}^t H \boldsymbol{x} + \boldsymbol{d}^t \boldsymbol{x} h. \end{aligned} \tag{XVII.10.18}$$

Stationarity with respect to q_i, η_i gives

$$\boldsymbol{\eta} = -\boldsymbol{p}, \qquad \boldsymbol{q} - N\boldsymbol{\eta} = A^{-1}(\boldsymbol{x} - \boldsymbol{c}h), \qquad \partial_{\boldsymbol{x}} F = A^{-t}\boldsymbol{p} + H\boldsymbol{x} + \boldsymbol{d}h. \tag{XVII.10.19}$$

Thus (XVII.10.15) follows with $B = AN$. This is a local massive generating function, not a prescribed convergent multiple integral.

An easy internal edge uses at most one cyclic coordinate from each tetrahedron. A suitable mirror frame then represents it by a chiral operator. Different edges can require different frames; they need not all be elementary polynomials in one set of fields. To express their candidates in the doubled BF frame, write an edge as $C_i = \boldsymbol{\alpha}_i^t \boldsymbol{q} + \boldsymbol{\beta}_i^t \boldsymbol{p} + c_i h$. Use magnetic label $\boldsymbol{m} = (\boldsymbol{\beta}_i, \boldsymbol{\alpha}_i)$ and physical BCC flux $\mathcal{H} = -\boldsymbol{m}$. The imported

monopole zero-mode formula gives

$$Q_g(\mathcal{M}_{\boldsymbol{m}}) = -K_{gg}\boldsymbol{m} - \frac{1}{2}\begin{pmatrix}|\boldsymbol{\beta}_i|\\ 0\end{pmatrix}, \quad \boldsymbol{n}_i = \boldsymbol{\alpha}_i + \frac{|\boldsymbol{\beta}_i| - \boldsymbol{\beta}_i}{2}, \quad \mathcal{O}_i = \mathcal{M}_{\boldsymbol{m}} \prod_j \phi_j^{n_{ij}}. \tag{XVII.10.20}$$

Scalar dressing must have $n_{ij} \geq 0$ and $n_{ij}\beta_{ij} = 0$: a charged scalar in nonzero monopole flux has monopole harmonics rather than a spin-zero constant mode. Gauss-law neutrality alone therefore does not suffice. Nor does it prove that a candidate is a nonzero quantum chiral operator. In the application below that physical existence is conditional on the sourced easy-edge mirror transport, in addition to the displayed algebra.

XVII.10.3 The figure-eight complement in six tetrahedra

The six-tetrahedron chart resolves a concrete difficulty: the simpler two-tetrahedron presentation has hard edges for which its required ordinary chiral interactions are absent. We use the published six-edge rows, retaining multiplicities and logarithmic shifts. With tetrahedra X, Y, Z, W, R, S, they are

$$\begin{aligned} C_1 &= X + W + 2(R' + S' + Z''), & C_2 &= R + Y + 2(Z' + W' + S''),\\ C_3 &= S + W + 2(R'' + X'' + Y'), & C_4 &= R + Z + 2(Y'' + W'' + X'),\\ C_5 &= X + Y, & C_6 &= S + Z. \end{aligned} \tag{XVII.10.21}$$

The peripheral logarithms and their relation to eigenvalues are

$$U = S' + R' - X'' + Y'' - W' + Z'', \quad v = X + R' - S - R'', \quad a = e^U = m^2, \quad \ell = -e^v. \tag{XVII.10.22}$$

Here m is the $SL(2)$ meridian eigenvalue, and ℓ is the unsquared preferred longitude eigenvalue. Neither $a = m$ nor $\ell = e^v$ is our convention. The edge coordinates commute, $\{v, U\} = \hbar$, and $\sum_i C_i = 12h$; there are five independent constraints, but all six edge operators must be included.

The product polarization and the new positions are

$$\begin{gathered} \boldsymbol{q} = (X, Y, Z, W, R'', S'), \quad \boldsymbol{p} = (X'', Y'', Z'', W'', R', S),\\ \boldsymbol{x} = (U, C_1, \ldots, C_5). \end{gathered} \tag{XVII.10.23}$$

Substituting $T' = h - T - T''$ for each tetrahedron T gives (XVII.10.15) with

$$A = \begin{pmatrix} 0 & 0 & 0 & 1 & 0 & 1\\ 1 & 0 & 0 & 1 & 0 & 2\\ 0 & 1 & -2 & -2 & -1 & -2\\ 0 & -2 & 0 & 1 & 2 & 0\\ -2 & 0 & 1 & 0 & -1 & 0\\ 1 & 1 & 0 & 0 & 0 & 0 \end{pmatrix}, \quad B = \begin{pmatrix} -1 & 1 & 1 & 1 & 1 & 0\\ 0 & 0 & 2 & 0 & 2 & 0\\ 0 & 0 & -2 & -2 & -1 & -2\\ 2 & -2 & 0 & 0 & 0 & 1\\ -2 & 2 & 0 & 2 & -1 & 0\\ 0 & 0 & 0 & 0 & 0 & 0 \end{pmatrix},$$

$$\boldsymbol{c} = (-1, 0, 7, 2, 3, 0)^t. \tag{XVII.10.24}$$

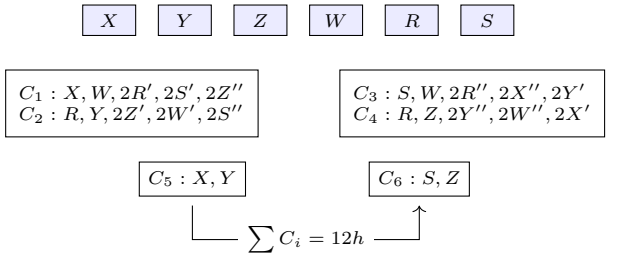


Figure XVII.10.3: Incidence diagram of the six published internal-edge rows. The six boxes denote tetrahedra; a list at an edge records its cyclic coordinates and multiplicities. The two simple rows are $C_5 = X + Y$ and $C_6 = S + Z$. This is a gluing-incidence diagram, not an additional face-pairing prescription; the peripheral paths are fixed by the explicit rows for U, v.

A is unimodular. The two symmetric matrices completing the polarization are

$$N = \begin{pmatrix} 0 & 0 & 0 & -2 & 2 & 1 \\ 0 & 0 & 0 & 2 & -2 & -1 \\ 0 & 0 & 0 & 0 & 0 & 1 \\ -2 & 2 & 0 & 0 & 2 & 1 \\ 2 & -2 & 0 & 2 & -3 & -1 \\ 1 & -1 & 1 & 1 & -1 & -1 \end{pmatrix}, \quad H = \begin{pmatrix} 6 & -8 & -5 & -8 & -10 & -11 \\ -8 & 0 & 0 & 0 & 0 & 0 \\ -5 & 0 & 0 & 0 & 0 & 0 \\ -8 & 0 & 0 & 0 & 0 & 0 \\ -10 & 0 & 0 & 0 & 0 & 0 \\ -11 & 0 & 0 & 0 & 0 & 0 \end{pmatrix}. \tag{XVII.10.25}$$

Specifically $N = A^{-1}B$ and the full new momenta are $A^{-t}\boldsymbol{p} + H\boldsymbol{x} + 87h\boldsymbol{e}_0$. Their first component is precisely v. On $C_i = 2h$ it becomes $(A^{-t}\boldsymbol{p})_0 + 6U + 3h$. The coefficient 87 is a consequence of this completion, not an arbitrary discarded contact. Equations (XVII.10.16) and (XVII.10.18), with $n = 6$ and $\boldsymbol{d} = 87\boldsymbol{e}_0$, now specify every gauge, background and affine coupling of a nonminimal $U(1)^{12}$ candidate.

The six magnetic labels and scalar exponents in that presentation are

	$\boldsymbol{m}_a$						$\boldsymbol{m}_b$						$\boldsymbol{n}$					
1	0	0	2	0	2	0	1	0	0	1	0	2	1	0	0	1	0	2
2	0	0	−2	−2	−1	−2	0	1	−2	−2	−1	−2	0	1	0	0	0	0
3	2	−2	0	0	0	1	0	−2	0	1	2	0	0	0	0	1	2	0
4	−2	2	0	2	−1	0	−2	0	1	0	−1	0	0	0	1	0	0	0
5	0	0	0	0	0	0	1	1	0	0	0	0	1	1	0	0	0	0
6	0	0	0	0	0	1	0	0	1	0	0	0	0	0	1	0	0	0

(XVII.10.26)

This table means six separate operators $\mathcal{O}_i$ defined by (XVII.10.20), with $W = \sum_{i=1}^{6} \lambda_i \mathcal{O}_i$ and nonzero λ_i. It is not one elementary polynomial in six fields. For a full row calculation take $i = 3$. Multiplying $N\boldsymbol{m}_b$ gives $(2, -2, 0, 0, 0, 1)^t = \boldsymbol{m}_a$, so

$$Q_g(\mathcal{M}_3) = \begin{pmatrix} \boldsymbol{m}_a/2 - \boldsymbol{m}_b - |\boldsymbol{m}_a|/2 \\ -\boldsymbol{m}_a + N\boldsymbol{m}_b \end{pmatrix} = \begin{pmatrix} (0,0,0,-1,-2,0)^t \\ 0 \end{pmatrix}, \qquad \mathcal{O}_3 = \mathcal{M}_3\phi_4\phi_5^2. \tag{XVII.10.27}$$

The dressing contributes $(0,0,0,1,2,0)$ to the first six charges. Both dressed fields have zero flux because $(m_a)_4 = (m_a)_5 = 0$. Thus all twelve charges vanish without using nonzero-flux scalar modes. Its flavor is $A^{-t}\boldsymbol{m}_b = \boldsymbol{e}_3$. For rows 1 through 5 these flavors are $\boldsymbol{e}_i$, and row 6 has flavor $(0,-1,-1,-1,-1,-1)$; every term is neutral under U.

A compatible trial assignment has $R(\phi_j) = 1/2$ and $K_{Ra_j} = 1/4$. The remaining mixed contacts are $K_{Rb} = (-3,1,-3,-3,3,3)/2$. For row three,

$$R(\mathcal{O}_3) = -\tfrac{1}{4}\sum m_a - K_{Rb}\cdot\boldsymbol{m}_b + \tfrac{1}{4}\sum |m_a| + \tfrac{1}{2}\sum n = -\tfrac{1}{4} - \tfrac{1}{2} + \tfrac{5}{4} + \tfrac{3}{2} = 2. \quad \text{(XVII.10.28)}$$

The same formula gives two for every row. This is a trial symmetry, not an exact infrared R-current. Nonvanishing of these chiral operators still uses the easy-edge mirror premise. In particular the simpler two-tetrahedron charge-$+1$ pair at level zero does not acquire missing hard-edge interactions by this charge test.

For the geometric vacuum calculation use lowercase unprimed shapes x, y, z, w, r, s. The six original monomials are

$$xw(r's'z'')^2 = 1, \quad ry(z'w's'')^2 = 1, \quad sw(r''x''y')^2 = 1, \quad rz(y''w''x')^2 = 1,$$
$$xy = 1, \qquad sz = 1. \quad \text{(XVII.10.29)}$$

Set $y = x^{-1}, z = s^{-1}$ and substitute the cyclic shape functions. The first four reduce to

$$wx = (r-1)^2, \quad r = x(w-1)^2, \quad sw(r-1)^2 = r^2, \quad r(w-1)^2 = sw^2. \quad \text{(XVII.10.30)}$$

The last follows from the first three in the nonzero chart. The peripheral rows give $a = -x(w-1)/(r-1)$ and $\ell = rx/[s(r-1)^2]$. Hence

$$a^2 = r/w, \quad \ell = wx/r, \quad x = \ell a^2, \quad r\ell = (r-1)^2, \quad a(r-1) + \ell(r - a^2) = 0. \quad \text{(XVII.10.31)}$$

Eliminating r, or using $r = (a + \ell a^2)/(a + \ell)$ when $a + \ell \neq 0$, yields

$$P(a,\ell) = \ell^2 - (a^2 - a - 2 - a^{-1} + a^{-2})\ell + 1 = 0. \quad \text{(XVII.10.32)}$$

The resultant of the two preceding r equations is $\ell a^2 P$. Nonzero monomial factors are removed only on the stated chart. At $a = 2$ the roots are $(-1 \pm i\sqrt{63})/8$; at $a = 3$ they are $(17 \pm 4\sqrt{13})/9$. For each root recover r above, $w = r/a^2$, $x = \ell a^2$, $s = a^2/\ell$, $y = 1/x, z = 1/s$. Substitution verifies all six original equations, providing four changed witnesses.

At the complete cusp $a = 1, \ell = -1$ the inverse has zero denominator. Directly choose $x = y = z = s = -1$ and $r = w = (1 + i\sqrt{3})/2$, or its conjugate. These satisfy (XVII.10.29) and the peripheral equations. Thus the exceptional inverse chart does not remove the cusp. The curve is the closure of this nondegenerate chart; it does not classify the full character variety, reducible components or integration sectors.

XVII.10.4 A two-to-three move and SQED/XYZ

The bipyramid can also be divided into two tetrahedra. To compare the decompositions, hold fixed the external positions and momenta, rather than matching only a count of

fields. For positions (R, S) and momenta (R'', S'') choose

$$X_1 = R + S'', \quad X_2 = R'' + S, \quad P_1 = R'', \quad P_2 = S'', \qquad g_2 = \begin{pmatrix} 1 & 0 & 0 & 1 \\ 0 & 1 & 1 & 0 \\ 0 & 0 & 1 & 0 \\ 0 & 0 & 0 & 1 \end{pmatrix}. \tag{XVII.10.33}$$

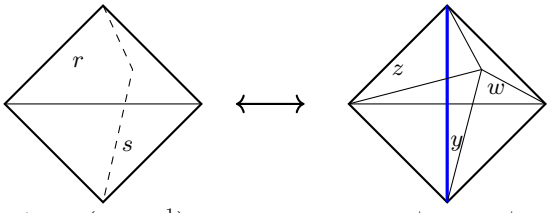
$g_2 J_2 g_2^t = J_2$, so these variables have the same canonical brackets as the three-tetrahedron variables of (XVII.10.12). Let $r = e^R$, $s = e^S$, and denote external positions by $\xi_i = e^{X_i}$ and momenta by $\pi_i = e^{P_i}$. The two-tetrahedron Lagrangian is

$$\xi_1 = r(1 - s^{-1}), \quad \xi_2 = s(1 - r^{-1}), \qquad \pi_1 = 1 - r^{-1}, \quad \pi_2 = 1 - s^{-1}. \tag{XVII.10.34}$$

In the other decomposition the external shapes are z, w, and the internal condition is $zwy = 1$. This determines the forward map

$$z = r(1 - s^{-1}), \quad w = s(1 - r^{-1}), \quad y = (zw)^{-1}, \qquad \pi_1 = \frac{1 - z^{-1}}{1 - y}, \quad \pi_2 = \frac{1 - w^{-1}}{1 - y}. \tag{XVII.10.35}$$

Substitution reduces these last two fractions exactly to $1 - r^{-1}$ and $1 - s^{-1}$. No limit or semiclassical approximation enters this local rational calculation.



$\xi_1 = r(1 - s^{-1})$
$\xi_2 = s(1 - r^{-1})$

$z = \xi_1,\ w = \xi_2$
$zwy = 1$

Figure XVII.10.4: Two decompositions of a bipyramid with the same external data $(\xi_1, \xi_2; \pi_1, \pi_2)$. The left decomposition uses two tetrahedra r, s sharing a face. The right uses three z, w, y meeting along an edge. The displayed rational map equates both positions and both momenta on the nondegenerate open set.

The reverse map can be read directly from the common boundary coordinates:

$$\pi_1 = \frac{1 - \xi_1^{-1}}{1 - (\xi_1 \xi_2)^{-1}}, \quad \pi_2 = \frac{1 - \xi_2^{-1}}{1 - (\xi_1 \xi_2)^{-1}}, \qquad r = \frac{1}{1 - \pi_1}, \quad s = \frac{1}{1 - \pi_2}. \tag{XVII.10.36}$$

Every denominator here must be nonzero, and all tetrahedron shapes must avoid zero and one. These restrictions are part of the birational statement. A boundary point outside this chart can require another triangulation; the local inverse does not establish that every such point is covered by some easy triangulation.

For $r = 2, s = 3$, the two external shapes and the new internal shape are

$$(z, w, y) = (4/3, 3/2, 1/2), \qquad (\pi_1, \pi_2) = (1/2, 2/3). \tag{XVII.10.37}$$

For $r = 3, s = 5$ the values change to

$$(z, w, y) = (12/5, 10/3, 1/8), \qquad (\pi_1, \pi_2) = (2/3, 4/5). \tag{XVII.10.38}$$

For example, $(1 - 5/12)/(1 - 1/8) = 2/3$ verifies the first momentum at the second point. The examples stay away from every excluded shape. Had $r = s = 2$ been used, $z = w = y = 1$ would have made the three-tetrahedron chart degenerate; agreement obtained by canceling its zero denominators would not be a valid witness.

Now construct the two-tetrahedron field theory in an integral charge basis. Let a_g denote the dynamical gauge field and retain X_1, X_2 as backgrounds. One-flavor SQED has chirals $q, \widetilde{q}$, no ordinary superpotential, and charge rows

$$Q_{\mathrm{SQED}} = \begin{pmatrix} 1 & 1 & 0 \\ -1 & 0 & 0 \end{pmatrix}_{(a_g, X_1, X_2)}, \qquad W_{\mathrm{SQED}} = 0. \tag{XVII.10.39}$$

The first column gives gauge charges $+1, -1$. In this basis the full bare gauge/flavor matrix is

$$K_{\mathrm{SQED}} = \begin{pmatrix} 0 & 1/2 & 1 \\ 1/2 & 1/2 & 1 \\ 1 & 1 & 0 \end{pmatrix}, \qquad K_{\mathrm{SQED}} + \tfrac{1}{2} Q_{\mathrm{SQED}}^t Q_{\mathrm{SQED}} = \begin{pmatrix} 1 & 1 & 1 \\ 1 & 1 & 1 \\ 1 & 1 & 0 \end{pmatrix}. \tag{XVII.10.40}$$

The dynamical CS level is zero, but the mixed contacts are not. DGG's source variable is $V_{\mathrm{source}} = a_g + X_1/2$ at the level of the complex scalar. Undoing that optional fractional shift gives precisely this integral matter basis. A half-axial shorthand does not define a quotient gauge group here.

The meson $M = q\widetilde{q}$ has flavor $(1, 0)$. For a monopole of physical gauge flux $\mathcal{H} = \pm 1$, the BCC formula is especially simple:

$$Q(\mathfrak{M}_{\mathcal{H}}) = K_{\mathrm{SQED}}(:, a_g)\, \mathcal{H} - \tfrac{1}{2}\big(Q_q + Q_{\widetilde{q}}\big)^t |\mathcal{H}|. \tag{XVII.10.41}$$

The sum of the two charge rows is $(0, 1, 0)$. Consequently the full gauge/flavor charges are

$$Q(\mathfrak{M}_+) = (0, 0, 1), \qquad Q(\mathfrak{M}_-) = (0, -1, -1), \qquad Q(M) = (0, 1, 0). \tag{XVII.10.42}$$

Both monopoles are gauge neutral without dressing. Their flavors match, in order, the three rows of Q_{XYZ}: $M \leftrightarrow X$, $\mathfrak{M}_+ \leftrightarrow Y$, $\mathfrak{M}_- \leftrightarrow Z$. This comparison tests contacts as well as a classical charge assignment: changing the mixed CS levels changes the monopole charges.

The identification as an infrared mirror pair is an imported physical result. It supplies the transport of chiral edge operators used earlier; matching the preceding charges is a consistency calculation, not its proof. On the XYZ side ordinary F-terms give

$$\begin{gathered} \partial_X W = YZ = 0, \quad \partial_Y W = XZ = 0, \quad \partial_Z W = XY = 0, \\ \mathcal{R}_{XYZ} = \mathbb{C}[X, Y, Z]/(XY, XZ, YZ). \end{gathered} \tag{XVII.10.43}$$

This ring is three coordinate axes meeting at the origin. Transporting it through the sourced mirror correspondence is a physical statement beyond deriving it from the

elementary XYZ potential. It should also not be confused with counting isolated massive circle vacua, where parameters and integration out have changed the problem.

The local move has therefore produced three different comparisons. The canonical maps identify an open holomorphic boundary Lagrangian. The matter and contact calculation realizes the prescribed SQED and XYZ pair. The sourced mirror statement supplies the quantum operator interpretation. Their roles remain distinct when composing local moves in a larger manifold: a finite calculation cannot supply a universal sequence of admissible triangulations or all global sectors.

XVII.10.5 Protected factors and their analytic domains

The classical shape relation has a simple quantum version, but its domain must be specified. Let q now denote a complex product parameter with $|q| < 1$, unrelated to the logarithmic position $q = Z$ used in the first section. Define the compact quantum dilogarithm in the Faddeev–Kashaev convention by

$$\Psi_q(t) = \prod_{n=1}^{\infty}(1 - q^n t), \qquad B_\Delta(z; q) = \Psi_q(z^{-1}). \tag{XVII.10.44}$$

Away from zeros, shifting the product index gives

$$B_\Delta(qz; q) = \prod_{n=0}^{\infty}(1 - q^n/z) = (1 - z^{-1})B_\Delta(z; q). \tag{XVII.10.45}$$

The factor $1 - z^{-1}$ reproduces the exponentiated momentum in (XVII.10.8). This is a local tetrahedron block equation, not a computed partition function of the figure-eight complement.

The finite product $B_M(z; q) = \prod_{n=1}^{M}(1 - q^n/z)$ makes the truncation error explicit:

$$\frac{B_M(qz; q)}{B_M(z; q)} = \frac{1 - z^{-1}}{1 - q^M/z}, \qquad B_M(qz) - (1 - z^{-1})B_M(z) = (1 - z^{-1})B_M(z)\frac{q^M/z}{1 - q^M/z}. \tag{XVII.10.46}$$

The denominator is essential. If $|q^M/z| < 1$, an immediate bound is

$$|\text{defect}| \le |(1 - z^{-1})B_M(z)|\frac{|q^M/z|}{1 - |q^M/z|}. \tag{XVII.10.47}$$

At $(q, z) = (0.4, 2+0.3i)$ and $(0.7, 3-0.2i)$, taking $M = 240$ makes $|q^M|$ about 3.1×10^{-96} and 6.6×10^{-38} respectively. Sixty-digit arithmetic resolves the latter defect and bounds the former by the numerical precision floor. The changed inputs test both the algebraic index shift and its analytic approximation; they do not replace the infinite-product derivation.

For the pentagon introduce formal generators U, V satisfying $\mathsf{U}\mathsf{V} = q\mathsf{V}\mathsf{U}$. These are not the boundary logarithm U in (XVII.10.22). In normal order $\mathsf{U}^i\mathsf{V}^j$, multiplication is

$$(\mathsf{U}^i\mathsf{V}^j)(\mathsf{U}^k\mathsf{V}^l) = q^{-jk}\mathsf{U}^{i+k}\mathsf{V}^{j+l}. \tag{XVII.10.48}$$

The coefficients of $\Psi_q(t) = \sum_{n\geq 0} c_n t^n$ obey

$$c_n = \frac{(-1)^n q^{n(n+1)/2}}{(q;q)_n}, \quad (q;q)_n = \prod_{j=1}^{n}(1-q^j), \quad c_1 = -\frac{q}{1-q}, \quad c_2 = \frac{q^3}{(1-q)(1-q^2)}. \tag{XVII.10.49}$$

The sourced quantum pentagon, in exactly this order and convention, is

$$\Psi_q(\mathsf{V})\Psi_q(\mathsf{U}) = \Psi_q(\mathsf{U})\Psi_q(-\mathsf{UV})\Psi_q(\mathsf{V}). \tag{XVII.10.50}$$

Its UV coefficient on the left is c_1^2/q; on the right it is $c_1^2 - c_1$. Both equal $q/(1-q)^2$. Changing the middle argument to $-q\mathsf{UV}$ instead gives

$$[\mathsf{UV}]_{\text{changed}} = c_1^2 - qc_1, \qquad [\mathsf{UV}]_{\text{changed}} - [\mathsf{UV}]_{\text{left}} = -q. \tag{XVII.10.51}$$

At $q = 2/3$, the correct coefficient is 6 and the changed coefficient is $16/3$. Ordering is observable already at degree two.

A higher check uses $\mathsf{U}^2\mathsf{V}$. On the left its coefficient is $c_2 c_1 q^{-2}$. On the right the two contributing choices of middle degree give

$$[\mathsf{U}^2\mathsf{V}]_{\text{right}} = c_2c_1 - c_1^2 = c_2c_1q^{-2}; \qquad [\mathsf{U}^2\mathsf{V}]\big|_{q=2/3} = -\frac{36}{5}. \tag{XVII.10.52}$$

The full identity is mathematical source input; coefficient checks through total degree eight at $q = 2/3, 3/7$, and degree four symbolically, test our implementation and its convention. They are finite tests of an infinite formal statement.

The noncompact mirror partition identity is a separate analytic object. Let $b > 0$ be real ellipsoid squashing and $Q = b + b^{-1}$. The meromorphic double sine in DGG's convention is defined by the regularized product

$$s_b(z) = \prod_{m,n\geq 0}^{\text{reg}} \frac{A_{mn} - iz}{A_{mn} + iz}, \qquad A_{mn} = mb + n/b + Q/2. \tag{XVII.10.53}$$

The superscript denotes the source's regularized product, rather than an absolutely convergent unregulated double product. Its poles are at $z = iA_{mn}$ and its zeros at $z = -iA_{mn}$, with multiplicities when lattice points coincide. These signs fix which side of the contour each translated family occupies. In this normalization, with overall constants suppressed as in that source, the mirror identity reads

$$\begin{aligned} &s_b(2y - iQ/2)s_b(iQ/2 - x - y)s_b(iQ/2 + x - y) \\ &\quad = \int_{\mathbb{R}} d\zeta\, e^{-2\pi i\zeta x} s_b(y-\zeta)s_b(y+\zeta). \end{aligned} \tag{XVII.10.54}$$

Here x is an external complex mass in this identity alone, not the earlier shape or vector $\boldsymbol{x}$. One safe initial strip takes x real and

$$y = y_{\mathbb{R}} + \frac{iQ}{2}r_y, \qquad 0 < r_y < 1. \tag{XVII.10.55}$$

The poles in the integration variable are

$$\begin{aligned} s_b(y+\zeta): &\quad \zeta = -\operatorname{Re} y + i(Q/2 - \operatorname{Im} y + mb + n/b), \\ s_b(y-\zeta): &\quad \zeta = \operatorname{Re} y - i(Q/2 - \operatorname{Im} y + mb + n/b), \end{aligned} \qquad m, n \geq 0. \tag{XVII.10.56}$$

Thus each family lies on a vertical line, with the displayed multiplicities, rather than on a horizontal row. The two pole families remain on opposite sides of the real contour, and the integrand decays as $\exp[-2\pi \operatorname{Im}(y)|\zeta|]$. More generally the decay condition is $|\operatorname{Im} x| < \operatorname{Im} y$ while the poles remain separated.

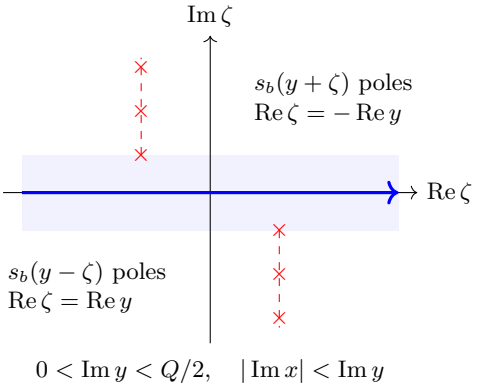


Figure XVII.10.5: The initial real ζ contour lies between the pole families of $s_b(y-\zeta)$ and $s_b(y+\zeta)$. Shown for $\operatorname{Re} y > 0$, the vertical families have real parts $-\operatorname{Re} y$ and $\operatorname{Re} y$; their nearest heights are $\pm(Q/2 - \operatorname{Im} y)$. The drawing schematically separates their first distinct heights; coincident lattice points contribute multiplicity. Increasing $\operatorname{Im} y$ to $Q/2$ closes the initial strip. Continuing through a pole requires a contour deformation or a residue contribution.

The strip has a physical R-charge interpretation. The two SQED chirals have $R = 1 - r_y$, while the XYZ multiplets have

$$R_{XYZ} = (2 - 2r_y, r_y, r_y), \quad \sum R_{XYZ} = 2, \qquad m_{XYZ} = (iQ - 2y, x + y, -x + y). \tag{XVII.10.57}$$

These parameters are compatible with the ordinary superpotential. They do not identify an exact infrared R-current. Contact phases must be retained when converting (XVII.10.54) to the background scheme of (XVII.10.14) and (XVII.10.40); DGG's contact-adjusted bipyramid formula performs that conversion. Setting all quadratic phases to one would change the scheme being compared.

For real b, the noncompact function is not certified by our absolutely convergent compact $|q| < 1$ product. Its full integral identity is an imported localization and special-function statement with the stated initial contour. A physical integration cycle for all twelve fields of the six-tetrahedron presentation, its global continuation, and absolute normalization have not been specified. The local construction determines explicit gauge data, edge candidates and a geometric vacuum chart. Completing the

full infrared and global-sector interpretation requires additional physical input beyond those results.

XVII.10.6 Exercises

1. **Parity and polarization.** Starting from (XVII.10.5), give one admissible bare k and the pair $(k_{\text{eff}}^{+}, k_{\text{eff}}^{-})$ for charges $Q_e = 1, 2$, choosing $k = -Q_e^2/2$. Check cancellation of the fractional parity anomaly. Apply (XVII.10.3) three times, retaining h, and determine the resulting affine transformation. Explain in writing why spin structure permits integer counterterm changes but does not make an isolated half-level ordinary CS functional arbitrary. Distinguish the determinant and its regulator.

2. **The central edge.** Reconstruct g_3 and δ_3 from (XVII.10.11), and verify $g_3 J_3 g_3^t = J_3$. Starting with three tetrahedron contacts, add the third $+1$ shift and derive Q_{XYZ} and K_{XYZ}. Give the changed contact matrix when that shift is deleted. Check $W = XYZ$ neutrality. Explain in writing why fixing $C = 2h$ by an ordinary superpotential is different from extremizing a circle twisted superpotential.

3. **A dressed monopole.** Using the bare K_{gg}, reconstruct the C_3 row in (XVII.10.26). Give its two six-component magnetic vectors, dressing, twelve bare gauge charges and final trial R-charge. Show every Gauss-law component, verify zero-flux dressing, and then change n_4 from one to zero and locate the nonvanishing gauge charge. Explain in writing why a scalar charged under nonzero magnetic flux cannot be silently used as spin-zero dressing. State the physical premise still required to interpret a neutral candidate as a nonzero chiral operator.

4. **Eliminating the knot shapes.** Starting with (XVII.10.29), derive the four reduced shape equations and the two equations in r, a, ℓ. Compute their resultant and give $P(a, \ell)$. At $a = 2$, give both longitude roots and reconstruct all six shapes; verify all six original monomials. Supply the direct complete-cusp witness at $a = 1, \ell = -1$. Explain in writing why the zero inverse denominator does not discard that point, and why this chart closure is not automatically the full character variety.

5. **A changed local move.** For $(r, s) = (2, 3)$ and $(3, 5)$ compute (z, w, y, π_1, π_2) using both descriptions, and reconstruct r, s by the reverse map. Diagnose the choice $(r, s) = (2, 2)$ before using it as a witness. Derive the full SQED monopole gauge/flavor charges at physical flux $+1, -1$ from (XVII.10.40); compare the meson and the XYZ charge rows. Explain in writing which step uses sourced mirror symmetry and why the rational map and charge comparison alone do not establish a full infrared equivalence.

6. **Quantum order and a contour.** Compute the UV and $\mathsf{U}^2\mathsf{V}$ coefficients in (XVII.10.50) at $q = 2/3$. Replace $-\mathsf{UV}$ by $-q\mathsf{UV}$ and give the changed degree-two coefficient. Derive the exact finite-product defect (XVII.10.46), including its

denominator. For $r_y = 1/3$, give the SQED and XYZ R-charges and verify the XYZ sum. Explain in writing the pole separation, the inequality on $\operatorname{Im} x$, what must change on crossing a pole, and why the compact product checks do not certify the real-b integral.

Take-home result and exit check

A tetrahedron supplies a regulated chiral and a local dilogarithm response. Integral gauging and contact changes assemble the polarization. Easy edges supply ordinary chiral interactions under the mirror dictionary. In the explicit figure-eight chart this yields a nonminimal $U(1)^{12}$ candidate with six interactions and five independent edge constraints. Its nondegenerate shape equations give $P(m^2, \ell) = 0$ with $\ell = -e^v$. The bipyramid exhibits the local canonical map and the contact-sensitive SQED/XYZ pair.

Before using the construction, the reader should be able to recover the affine polarization, distinguish bare and parity-corrected levels, dress the C_3 monopole using only zero-flux scalars, and reconstruct a generic point and the exceptional cusp from the original monomials. A quantum calculation should specify its normal order and analytic domain. A claim about a full compactification requires more than those local consistency tests.

Sources and scope

§1. The cross-ratio and affine symplectic relations are **MATH**. The tetrahedron assignment is **GEO-E**, used as a physical dictionary premise, and the half-level regulator is **ANOM**. Sources: Dimofte et al. 2014, inspected arXiv v1, (2.5)–(2.9), (4.1)–(4.3), (5.5)–(5.8), printed pp. 8–10, 29–30, 41–42; Closset et al. 2012, inspected v2, (1.5)–(1.7), (3.1)–(3.3), printed pp. 3, 9. The derivative in the local generating function is explicitly with respect to Z, the variable of the preceding potential; the derivative label in DGG (5.7) differs.

§2–3. The edge/peripheral rows, symplectic presentation and six-shape elimination are **MATH**, based on Dimofte et al. 2014, inspected v1, (4.21)–(4.22), printed p. 39, and (2.27)–(2.32). The doubled BF matrices, magnetic table and trial-R calculation are explicit algebra in the present polarization, rather than tables attributed to that source. The six chiral candidates are **BPS:**1/2|holo under the sourced easy-edge mirror construction and the monopole zero-mode formula of Benini et al. 2011, inspected v2, (2.3)–(2.4), printed pp. 6–7. Physical flux is $\mathcal{H} = -\boldsymbol{m}$ in our table. Their gauge neutrality and trial $R = 2$ do not prove nonvanishing in a quantum chiral ring. The interpretation of the abelian theory as the polarized type-A_1 compactification candidate is **CONJ+**, under DGG's construction and mirror premises, not an unconditional all-energy or global-sector identification.

§4. The two-to-three canonical maps are **MATH**; the SQED/XYZ protected operator identification is **BPS:**1/2|holo, imported from Dimofte et al. 2014, inspected v1, Table 2, (3.19), (4.7)–(4.14), printed pp. 25–26, 33–35. Its full infrared mirror statement is a

physical premise at the operator-transport step, not derived by matching charges. No universal triangulation theorem is inferred. The protected fraction refers to the chiral subalgebra of the three-dimensional four-real-supercharge theory.

§5. The compact product and pentagon are **MATH**: Faddeev and Kashaev 1994, inspected v1, (1.4), (2.1), (2.4), (2.14), printed pp. 1–3. Finite coefficients and truncation tests have the explicit degree and numerical domains stated in the text. The noncompact mirror integral is **BPS:**1/2|holo under the localization and special-function input of Dimofte et al. 2014, inspected v1, (6.6)–(6.20), particularly (6.18), printed pp. 46–49. We rename its integration variable consistently. Its normalization suppresses overall constants as in the source; contact phases are retained. Global analytic continuation, a six-tetrahedron physical contour and absolute normalization remain open here.

References

Benini, F., C. Closset, and S. Cremonesi (2011). "Quantum moduli space of Chern-Simons quivers, wrapped D6-branes and AdS4/CFT3". In: *JHEP* 09. Inspected arXiv version 2, 6 July 2011, p. 005. DOI: 10.1007/JHEP09(2011)005. arXiv: 1105.2299 [hep-th].

Closset, C. et al. (2012). "Comments on Chern-Simons Contact Terms in Three Dimensions". In: *JHEP* 09. Inspected arXiv version 2, 29 December 2012, p. 091. DOI: 10.1007/JHEP09(2012)091. arXiv: 1206.5218 [hep-th].

Dimofte, T., D. Gaiotto, and S. Gukov (2014). "Gauge Theories Labelled by Three-Manifolds". In: *Commun. Math. Phys.* 325. Inspected arXiv version 1, 22 August 2011, pp. 367–419. DOI: 10.1007/s00220-013-1863-2. arXiv: 1108.4389 [hep-th].

Faddeev, L. D. and R. M. Kashaev (1994). "Quantum Dilogarithm". In: *Mod. Phys. Lett. A* 9. Inspected arXiv version 1, 13 October 1993, pp. 427–434. DOI: 10.1142/S0217732394000447. arXiv: hep-th/9310070.

Chapter XVII.11

Boundaries, duality walls and filling

A torus boundary allows a three-manifold to be assembled in different ways. Choosing a meridian and longitude identifies which boundary variable is held fixed. Gluing in a solid torus then asks that one primitive cycle contract. In the protected description of wrapped M5-branes, these operations suggest changes of polarization, boundary states and integral kernels. The geometric operation is simple, but its translation must retain the full holonomy. A matrix can have eigenvalue one without being the identity.

We will follow this distinction through the figure-eight complement. Its meridian filling has trivial fundamental group, although an eigenvalue equation admits two nontrivial cusp representatives. Complementary cyclic examples retain all reducible sectors, and an entire Gaussian supplies an integral whose contour can actually be specified. These calculations explain which parts of gluing are controlled by a boundary chart and which require additional physical information.

The parent is the interacting type-A_1 six-dimensional $(2,0)$ theory. We use the marked boundary conventions of XVII.9, ordinary group representations and the global-choice warning of XVI.11. A proposed Lagrangian for a triangulated theory is not an input. The physical Abelian gauging prescription below assumes an oriented spin three-manifold and a gauge-invariant compact $U(1)$ background coupling. The reader should be able to multiply peripheral matrices, change a symplectic basis and distinguish an ordinary representation from its semisimplified character.

XVII.11.1 Polarization and boundary states

A boundary state describes a system with some boundary variables fixed. On a smooth semisimple torus chart, a choice of position coordinate determines which conjugate variable becomes a response. To use such a state in filling, first specify the peripheral marking and its lift. Let μ be the meridian and λ the preferred longitude. Their

commuting holonomies have simultaneous eigenvalues

$$M \sim \operatorname{diag}(m, m^{-1}), \qquad L \sim \operatorname{diag}(\ell, \ell^{-1}), \qquad m, \ell \in \mathbb{C}^*. \tag{XVII.11.1}$$

The simultaneous Weyl operation sends (m, ℓ) to (m^{-1}, ℓ^{-1}). It does not identify an arbitrary change of just one sign with this inversion. In the logarithmic chart inherited from XVII.9, write

$$u = \log m, \quad w = \log \ell = v + i\pi, \quad U = 2u, \qquad \ell = -e^{v}, \qquad \omega = \frac{2}{\hbar}\, dw \wedge du = \frac{1}{\hbar}\, dv \wedge dU. \tag{XVII.11.2}$$

The minus sign in the longitude is part of the chosen lift. A wavefunction $\Psi(U)$ uses U as position, but $e^{U} = m^2$ alone does not recover the sign of m. We therefore keep the marked logarithms along with the wavefunction. This factor of two and the longitude shift follow the boundary convention of Dimofte et al. 2011, printed p.16, equations (2.26)–(2.28).

Let a cycle change act on the column of logarithms. Its determinant-one condition expresses preservation of oriented intersection,

$$\begin{pmatrix} u' \\ w' \end{pmatrix} = g \begin{pmatrix} u \\ w \end{pmatrix}, \qquad g = \begin{pmatrix} a & b \\ c & d \end{pmatrix}, \qquad ad - bc = 1. \tag{XVII.11.3}$$

Substitute $u = U/2$ and $w = v + i\pi$ before subtracting the new longitude shift. This gives the full affine transformation,

$$\begin{pmatrix} U' \\ v' \end{pmatrix} = R_g \begin{pmatrix} U \\ v \end{pmatrix} + t_g, \qquad R_g = \begin{pmatrix} a & 2b \\ c/2 & d \end{pmatrix}, \qquad t_g = i\pi \begin{pmatrix} 2b \\ d - 1 \end{pmatrix}. \tag{XVII.11.4}$$

Only the constant term disappears under differentiation. Thus $dv' \wedge dU' = (ad - bc) dv \wedge dU$, while composition retains the translation. With $D = \operatorname{diag}(2, 1)$ and $z_0 = (0, i\pi)^t$, one can see both facts directly,

$$R_g = D g D^{-1}, \qquad t_g = D(g - 1) z_0, \qquad t_{gh} = R_g t_h + t_g. \tag{XVII.11.5}$$

The last identity prevents a sequence of changes from losing a central lift through omission of constant terms. A symplectic determinant check alone would miss that error.

For the lower-shear convention for the cycle twist, the generators and their converted linear parts are

$$S_c = \begin{pmatrix} 0 & -1 \\ 1 & 0 \end{pmatrix}, \quad T_c = \begin{pmatrix} 1 & 0 \\ 1 & 1 \end{pmatrix}, \qquad R_{S_c} = \begin{pmatrix} 0 & -2 \\ 1/2 & 0 \end{pmatrix}, \quad R_{T_c} = \begin{pmatrix} 1 & 0 \\ 1/2 & 1 \end{pmatrix}. \tag{XVII.11.6}$$

Their shifts are $t_{S_c} = (-2i\pi, -i\pi)^t$ and $t_{T_c} = 0$. In particular a single cycle twist gives $v' = v + U/2$. Applying it twice gives $v' = v + U$. A unit canonical shear of the Darboux pair (U, v) therefore corresponds to two such cycle twists, rather than one. The distinction matters when comparing a geometric marking with a contact-term operation.

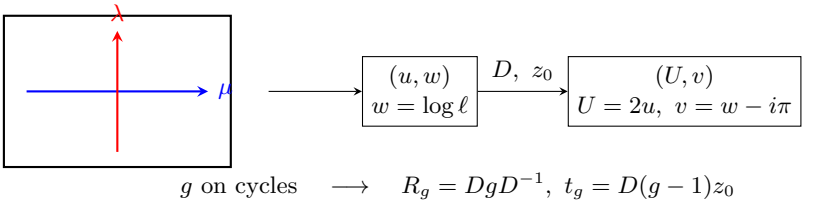


Figure XVII.11.1: A marked boundary torus and its logarithmic chart. The cycle transformation acts first on (u, w). Doubling u and shifting w produce the affine map of (U, v), including its constant lift. Opposite sides of the square are identified.

A slope is a row $s = (p, q)$ specifying $p\mu + q\lambda$. If the cycle column changes by g, the same geometric cycle must retain the same scalar logarithm. Consequently

$$s' = sg^{-1}, \qquad s'\begin{pmatrix} u' \\ w' \end{pmatrix} = s\begin{pmatrix} u \\ w \end{pmatrix}. \tag{XVII.11.7}$$

For a concrete changed marking, use

$$g = \begin{pmatrix} 2 & 1 \\ 1 & 1 \end{pmatrix}, \qquad g^{-1} = \begin{pmatrix} 1 & -1 \\ -1 & 2 \end{pmatrix}, \qquad (5,2)g^{-1} = (3,-1), \quad (7,3)g^{-1} = (4,-1). \tag{XVII.11.8}$$

This calculation transports a fixed attaching cycle, rather than choosing a new filling. It also illustrates why a row and a column cannot be transformed by the same rule. In section XVII.11.3, the invariant scalar will become a necessary filling equation. For a boundary state, the same change specifies which coordinate is fixed and which is integrated over. It still leaves the quantum normalization of that integration unspecified.

XVII.11.2 Mapping cylinders and Abelian wall operations

A mapping cylinder keeps the underlying boundary surface while changing how its two ends are identified. Composing cylinders composes changes of polarization. In a theory with an Abelian flavor current, the corresponding physical operations can be made concrete by following its background gauge field. Let $I[A]$ denote the original coupling to a compact background A. The prescriptions of Dimofte et al. 2011, printed pp.20–22, add the terms

$$T\colon I[A] \longmapsto I[A] + \frac{1}{4\pi}\int A \wedge dA, \qquad S\colon I[A] \longmapsto I[A] + \frac{1}{2\pi}\int B \wedge dA. \tag{XVII.11.9}$$

For S, A becomes dynamical and B is the new background. The path integral sums compact gauge fields and bundles with the gauge-invariant coupling understood. The displayed terms are action coefficients, with the usual factor i in the oscillatory weight. A kinetic term is absent in this infrared prescription. This is not a weakly coupled ultraviolet construction of a nonabelian wall.

An odd unit diagonal contact shift requires the stated spin choice. Witten 2003 uses the historical phrase level one-half for the displayed diagonal coefficient that Dimofte et al. 2011 calls level one. Comparing the coefficients in (XVII.11.9) avoids an apparent factor mismatch. It does not remove the spin or framing qualifications. We now compute the local quadratic couplings within that prescription.

For symmetric K, write the Abelian action modulo boundary terms as

$$I_K = \frac{1}{4\pi} \int \sum_{i,j} K_{ij} A_i \wedge dA_j. \tag{XVII.11.10}$$

The two off-diagonal entries produce twice the BF cross term. With ST meaning that T is performed first, the original field carries the contact term. In TS the new background carries it. In ordered fields (A, B),

$$K_{ST} = \begin{pmatrix} 1 & 1 \\ 1 & 0 \end{pmatrix}, \qquad K_{TS} = \begin{pmatrix} 0 & 1 \\ 1 & 1 \end{pmatrix}. \tag{XVII.11.11}$$

Their difference is physical information about which field has become dynamical. It cannot be erased by saying only that a shear has occurred. After two S operations, the ordered fields are (A, B, C), with C a spectator background, and

$$K_{SS} = \begin{pmatrix} 0 & 1 & 0 \\ 1 & 0 & 1 \\ 0 & 1 & 0 \end{pmatrix}, \qquad I_{SS} - I[A] = \frac{1}{2\pi} \int B \wedge d(A + C). \tag{XVII.11.12}$$

Variation with respect to B gives the local constraint $d(A + C) = 0$. The full compact BF integral, including its bundle sums, identifies A with $-C$ in the physical operation described in Witten 2003. Thus the sourced S^2 operation is charge conjugation. The finite matrix calculation by itself establishes only the local coupling and constraint.

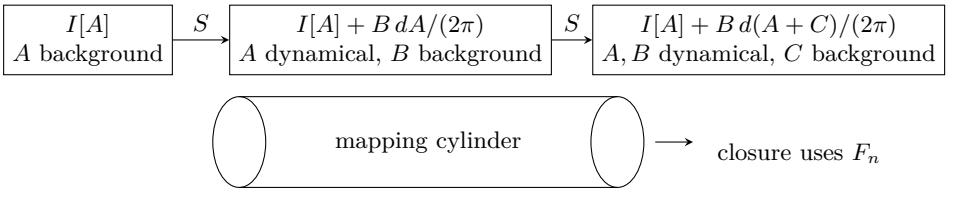


Figure XVII.11.2: Two successive Abelian gauging operations. The first makes A dynamical with background B; the second makes B dynamical with background C. The intermediate BF constraint relates the original field to the negative of the final background. A mapping-torus closure is a different operation, identifying the two torus ends with a specified monodromy.

On an abstract Darboux pair (X, P) one may use integral canonical matrices

$$S = \begin{pmatrix} 0 & -1 \\ 1 & 0 \end{pmatrix}, \quad T = \begin{pmatrix} 1 & 0 \\ 1 & 1 \end{pmatrix}, \qquad S^2 = -1_2, \quad (ST)^3 = 1_2. \tag{XVII.11.13}$$

These identities are classical. A quantum operator can carry an additional projective or gravitational factor, and Witten 2003 explicitly retains a decoupled gravitational contribution. The matrices also require the conversion of section XVII.11.1 before they can be interpreted as the marked cycle generators. Neither the matrix relations nor the K matrices fix an absolute framing phase.

A mapping torus supplies a separate example in which all Abelian flat sectors can be found. Let the fiber generators be the column $(a,b)^t$ and let the stable letter t implement

$$F_n=\begin{pmatrix} n & -1 \\ 1 & 0 \end{pmatrix}, \qquad \pi_1=\mathbb{Z}^2\rtimes_{F_n}\mathbb{Z}, \qquad H_1=\mathbb{Z}\langle t\rangle\oplus\operatorname{coker}(F_n-1). \quad \text{(XVII.11.14)}$$

Here F_n acts on the generator lattice, so the relations are the columns of F_n-1. Its entries have greatest common divisor one, and its determinant is $2-n$. Smith reduction therefore gives, for $n=4,5,7$,

$$F_n-1=\begin{pmatrix} n-1 & -1 \\ 1 & -1 \end{pmatrix}, \qquad \operatorname{SNF}(F_n-1)=\operatorname{diag}(1,n-2) \quad \text{up to signs.} \quad \text{(XVII.11.15)}$$

The second column imposes $b=-a$ in additive homology. The first then imposes $(n-2)a=0$. Every $U(1)$ character is consequently

$$\chi(t)=e^{i\theta}, \quad \chi(a)=e^{2\pi ij/(n-2)}, \quad \chi(b)=e^{-2\pi ij/(n-2)}, \qquad \theta\in\mathbb{R}/2\pi\mathbb{Z}, \quad 0\le j<n-2. \quad \text{(XVII.11.16)}$$

There are two, three and five circle components for $n=4,5,7$, respectively. Completeness follows because every map to the Abelian target $U(1)$ factors through H_1. This is stronger than listing a few stationary points, but concerns only Abelian characters. It neither classifies nonabelian connections nor evaluates the quantum trace associated with a closed cylinder. The filling calculation next will show how a further group relation can remove apparent boundary solutions.

XVII.11.3 Dehn filling conditions

Attaching a solid torus declares its meridian contractible. In a marked boundary this meridian is a primitive cycle $p\mu+q\lambda$, with $\gcd(p,q)=1$. Primitivity ensures that it can be completed to an oriented integral basis. For example,

$$\begin{pmatrix} 5 & 2 \\ 2 & 1 \end{pmatrix}, \qquad \begin{pmatrix} 7 & 3 \\ 2 & 1 \end{pmatrix}\in SL(2,\mathbb{Z}), \qquad 5\cdot 1-2\cdot 2=7\cdot 1-3\cdot 2=1. \quad \text{(XVII.11.17)}$$

The row $(10,4)$ is twice $(5,2)$. Its greatest common divisor is two, so it cannot itself be the meridian of a solid torus. The symbol $1/0$ is legitimate and denotes the meridian slope.

Van Kampen imposes the attaching relation on the whole knot group. Write $\mathcal{M}$ for the unfilled exterior and $\mathcal{M}_{p/q}$ for its filling. If M and L denote the actual peripheral matrices, extension of a representation is characterized by

$$\pi_1(\mathcal{M}_{p/q})=\pi_1(\mathcal{M})\big/\langle\!\langle \mu^p\lambda^q\rangle\!\rangle, \qquad M^pL^q=1_2 \quad \text{in } SL(2,\mathbb{C}). \quad \text{(XVII.11.18)}$$

On the simultaneous semisimple locus, this is equivalent to $m^p \ell^q = 1$. On a Jordan stratum it is only necessary. Keeping the marked logarithm of (XVII.11.2) gives

$$\frac{p}{2} U + q v = 2\pi i N - q i \pi, \qquad N \in \mathbb{Z}. \tag{XVII.11.19}$$

For $5/2$ the right side is $2\pi i N - 2i\pi$. For odd q the retained half-period is especially visible. Exponentiating twice would allow $m^p \ell^q = -1$ as well. Such a central matrix can become trivial in $PSL(2,\mathbb{C})$ but is rejected by (XVII.11.18). We fix $SL(2,\mathbb{C})$ throughout.

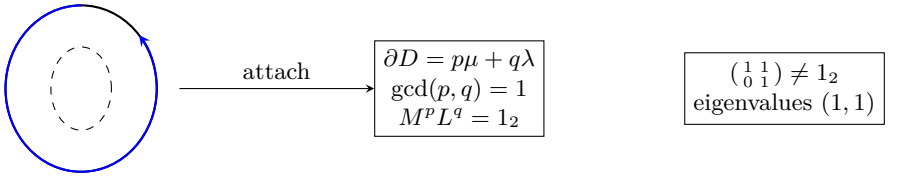


Figure XVII.11.3: The meridian disk of the attached solid torus has primitive boundary $p\mu + q\lambda$. A representation extends when its full holonomy is the identity. The right-hand example has both eigenvalues equal to one and a nonzero nilpotent entry, so the eigenvalue condition alone does not contract the cycle.

To compute the extension condition explicitly, use the figure-eight presentation and preferred longitude of Andersen and Hansen 2003, printed p.23, equation (53),

$$\pi_1 = \langle x, y \mid wx = yw \rangle, \quad w = x^{-1} y x y^{-1}, \quad \mu = x, \quad \lambda = y x^{-1} y^{-1} x^2 y^{-1} x^{-1} y. \tag{XVII.11.20}$$

Write the two generator matrices as

$$X = \begin{pmatrix} m & m^{-1} \\ 0 & m^{-1} \end{pmatrix}, \qquad Y = \begin{pmatrix} m & 0 \\ -mr & m^{-1} \end{pmatrix}, \qquad m \neq 0. \tag{XVII.11.21}$$

These are the source's $C_2(s)$ and $D_2(s,u)$ with $s = m$ and source polynomial variable $u = r$. This source u is unrelated to the logarithm u of section XVII.11.1. We use r only for the polynomial parameter in the present section and the next.

Multiplication of $W = X^{-1} Y X Y^{-1}$ gives

$$WX - YW = \begin{pmatrix} 0 & \phi/m \\ mr\phi & 0 \end{pmatrix}, \qquad \phi = r^2 + (3 - m^2 - m^{-2})(r+1). \tag{XVII.11.22}$$

Thus $\phi = 0$ imposes the knot relation in this normal form. Multiply the longitude word with the same matrices and reduce its entries modulo ϕ. The result is upper triangular, with

$$L_{11} = \ell = -1 + m^{-2} - 2m^2 + m^4 + r(m^{-2} - m^2), \qquad L_{22} = \ell^{-1}, \quad [L, X] = 0, \quad \det L = 1. \tag{XVII.11.23}$$

For example, the upper entry needed to diagnose the cusp is

$$L_{12} = -\frac{(m^2+1)(-m^4+2m^2r+3m^2-1)}{m^4} \pmod{\phi}. \tag{XVII.11.24}$$

Eliminating r between $\phi = 0$ and $\ell = L_{11}$ gives the irreducible peripheral equation

$$m^4\ell^2 - (m^8 - m^6 - 2m^4 - m^2 + 1)\ell + m^4 = 0. \tag{XVII.11.25}$$

This reproduces a boundary curve while retaining a route back to actual matrices. That route is essential at repeated eigenvalues. The Abelian branch $\ell = 1$ is separate and cannot be supplied by calling the normal form complete. In the next section we impose the meridian relation on the group itself, then compare what the curve and matrices report. This ordering determines which missing sectors must be restored before a physical filling construction can be discussed.

XVII.11.4 Flat sectors after filling

What survives the figure-eight 1/0 filling? Since its attaching relation is $x = 1$, the group presentation immediately yields

$$x = 1 \implies w = x^{-1}yxy^{-1} = 1 \implies wx = yw \implies y = 1. \tag{XVII.11.26}$$

The filled group is trivial. Geometrically, meridian filling replaces the removed knot neighborhood and gives S^3. There is exactly one $SL(2,\mathbb{C})$ representation of this group, the trivial representation. This is a complete group calculation. It is not a calculation of the quantum contribution of that representation to a triangulated integral.

The eigenvalue route appears to give a different answer. At $m = 1$, equations (XVII.11.22) and (XVII.11.25) become

$$r^2 + r + 1 = 0, \qquad r_\pm = \frac{-1 \pm i\sqrt{3}}{2}, \qquad (\ell+1)^2 = 0. \tag{XVII.11.27}$$

Both points satisfy the eigenvalue meridian condition $m = 1$. Let $N = \left(\begin{smallmatrix} 0 & 1 \\ 0 & 0 \end{smallmatrix}\right)$, so $N^2 = 0$ but $N \neq 0$. The actual matrices are

$$X = 1_2 + N, \qquad L = -1_2 + \beta N, \qquad \beta = -2(2r+1), \qquad \beta(r_\pm) = \mp 2i\sqrt{3}. \tag{XVII.11.28}$$

In particular $X \neq 1_2$, so neither representation extends over meridian filling. The discrepancy lies in the lost Jordan entry, not in the topology of the quotient. For arbitrary integer powers, nilpotence gives

$$X^pL^q = (-1)^q\big[1_2 + (p - q\beta)N\big]. \tag{XVII.11.29}$$

If this matrix is the identity, its off-diagonal entry forces $p = q\beta$. Since p, q are real integers and β is nonzero imaginary, it follows that $p = q = 0$. Thus these cusp matrices extend to no primitive integer filling. For the other meridian lift $X = -(1_2 + N)$, the central sign becomes $(-1)^{p+q}$; the off-diagonal obstruction remains. This is why the

source's eigenvalue extension criterion before equation (61) on printed p.25 of Andersen and Hansen 2003 restricts $s^2 \neq 1$.

There is a bounded sign issue on that same printed page. Keeping exactly the source's labels C_2, D_2, its longitude word and the translation $s = m, u = r$, equation (XVII.11.24) specializes to

$$L_{12} = 2r(r-1) = -2(2r+1) \pmod{r^2+r+1}. \tag{XVII.11.30}$$

The printed cusp expression is instead $2r(1-r)$. This reverses the sign at a fixed root label. To isolate the convention dependence, allow a free upper entry H by taking $X_{12} = H$ and $Y_{21} = -r/H$. Direct multiplication gives

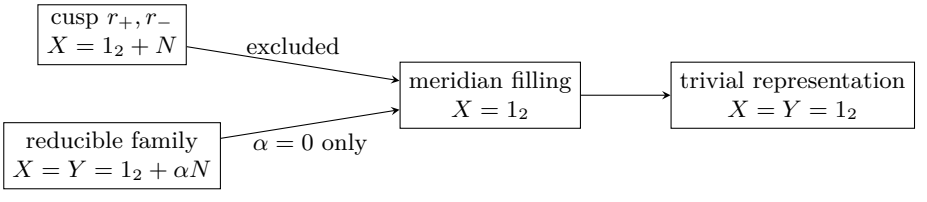
$$L = -1_2 - 2H(2r+1)N \quad (m = 1,\ r^2+r+1 = 0). \tag{XVII.11.31}$$

The source C_2 gauge is $H = m^{-1}$ and hence $H = 1$ at this cusp; its C_1 gauge has $H = 1$ already. Exchanging r_+ and r_- reverses β while preserving the unordered pair. Inverting the longitude also reverses β, but inverts the generic eigenvalue as well. These alternatives explain why the unordered cusp conclusion is unchanged. The comparison is a fixed-label discrepancy on this page, not a global erratum or a change to the preferred longitude used here.

The reducible sector makes a related loss of information visible without the non-abelian normal form. Set

$$X = Y = 1_2 + \alpha N, \qquad L = 1_2, \qquad \alpha \in \mathbb{C}. \tag{XVII.11.32}$$

The knot relation holds for all α. Every member has boundary eigenvalues $(m, \ell) = (1, 1)$, but full meridian filling requires $\alpha = 0$. Nonzero unipotents have the same semisimplified character as the identity. A character quotient can therefore collapse representation information needed to test extension. The trivial sector must be retained even when a chosen irreducible chart does not display it.



$p = 5 \quad \{0\}, \{1,4\}, \{2,3\}$
$p = 4 \quad \{0\}, \{1,3\}, \{2\}$
positive cyclic classes retain central orbits

Figure XVII.11.4: Meridian filling compares representations before quotienting to eigenvalues. The two irreducible cusp points and the reducible unipotent family all fail $X = 1_2$ except for $\alpha = 0$ in the latter. The resulting filled group has precisely the trivial representation. For the positive cyclic examples, the displayed orbits include the central sectors.

A second filling can be classified completely with elementary linear algebra. The unknot exterior is a solid torus, with knot meridian generating $\mathbb{Z}$ and preferred knot longitude already trivial. For $p > 0$ and $\gcd(p, q) = 1$,

$$\pi_1(\text{unknot } p/q \text{ filling}) = \langle a \mid a^p = 1 \rangle = \mathbb{Z}/p\mathbb{Z}. \tag{XVII.11.33}$$

We denote the oriented lens space by $L(p, q)$ in this surgery convention, but only its group is used. Over $\mathbb{C}$, the polynomial $z^p - 1$ has no repeated roots, since its derivative pz^{p-1} has no common zero with it. Hence a matrix satisfying $A^p = 1_2$ is diagonalizable, and all $SL(2, \mathbb{C})$ conjugacy classes are

$$A_j = \operatorname{diag}(e^{2\pi ij/p}, e^{-2\pi ij/p}), \qquad j \in \mathbb{Z}/p\mathbb{Z}, \qquad j \sim -j. \tag{XVII.11.34}$$

For $5/2$ the orbits are $\{0\}, \{1, 4\}, \{2, 3\}$. For $4/1$ they are $\{0\}, \{1, 3\}, \{2\}$. The last case retains both 1_2 and -1_2. All these representations are reducible. Central twists form $\operatorname{Hom}(\mathbb{Z}/p, \mathbb{Z}_2)$, of order one for odd p and two for even p. The group computation cannot distinguish different q with the same p, and does not classify $PSL(2, \mathbb{C})$ representations.

The hypothesis $p > 0$ changes the argument. The valid $0/1$ unknot filling imposes a relation on the already trivial longitude, leaving group $\mathbb{Z}$. Its meridian can be

$$A = 1_2 + N, \qquad A^0 L = 1_2, \qquad A^k = 1_2 + kN \quad (k \in \mathbb{Z}). \tag{XVII.11.35}$$

This is a genuine nonsemisimple representation of infinite order. Zero surgery is valid topology, but lies outside the finite-order theorem. The examples together separate a complete representation calculation from a chart calculation. Interpreting those representations as physical vacua still requires the protected compactification dictionary; their mere existence does not determine a partition function or its integration cycle.

XVII.11.5 Protected integrals and global limits

A boundary state becomes an observable only after an integration rule is chosen. To see exactly what that choice contributes, consider an entire one-variable model for which there is no uncertainty about convergence. Take $a, h > 0$, k, J, Y real, and define

$$\psi(X) = \exp\left[-\frac{aX^2}{2h} + \frac{JX}{h}\right], \qquad (T_k\psi)(X) = e^{ikX^2/(2h)}\psi(X). \tag{XVII.11.36}$$

The Fourier operation is defined by

$$(Sf)(Y) = \frac{1}{\sqrt{2\pi h}} \int_{\mathbb{R}} e^{iYX/h} f(X)\, dX. \tag{XVII.11.37}$$

The contour is the real line oriented from negative to positive infinity. The Fourier sign is fixed in this definition. Put $A = a - ik$, so $\Re A > 0$. Completing the square gives

$$-\frac{AX^2}{2h} + \frac{(J + iY)X}{h} = -\frac{A}{2h}(X - X_*)^2 + \frac{(J + iY)^2}{2hA}, \qquad X_* = \frac{J + iY}{A}. \tag{XVII.11.38}$$

The entire integrand allows translation to the saddle and rotation within the Gaussian decay sectors. With the principal square root on $\Re A > 0$, the exact answer is

$$(ST_k\psi)(Y) = A^{-1/2}\exp\left[\frac{(J+iY)^2}{2hA}\right]. \tag{XVII.11.39}$$

This is an actual convergent integral. A nonzero source J makes the sign of iY observable through its cross term. At $J = 0$, the even Gaussian would conceal that sign error.

Write $A = |A|e^{i\varphi}$, with $|\varphi| < \pi/2$. The descending and upward cycles through the unique saddle can be parameterized by real t as

$$\mathcal{J} = X_* + e^{-i\varphi/2}\mathbb{R}, \qquad \mathcal{K} = X_* + ie^{-i\varphi/2}\mathbb{R}. \tag{XVII.11.40}$$

On $\mathcal{J}$, the quadratic exponent is $-|A|t^2/(2h)$; on $\mathcal{K}$ its sign is reversed. Orient both by increasing real parameter, choosing the dual orientation so the ordered descending and upward tangent pair has the positive complex orientation. Then

$$\langle \mathbb{R}, \mathcal{K}\rangle = 1, \qquad \langle -\mathbb{R}, \mathcal{K}\rangle = -1. \tag{XVII.11.41}$$

The deformation uses an entire function and Gaussian decay at the ends. No poles are crossed. For $a = 2, k = 1, Y = 3, h = 1, J = 7/10$, one obtains

$$A = 2 - i, \qquad X_* = -\frac{8}{25} + \frac{67}{50}i, \qquad (ST_1\psi)(3) = (2-i)^{-1/2}\exp\left[\frac{(7/10+3i)^2}{2(2-i)}\right]. \tag{XVII.11.42}$$

This changed-input example specifies the critical point, the contour and its oriented coefficient. The Gaussian has none of the poles, reducible singularities or normalization choices of a knot state integral.

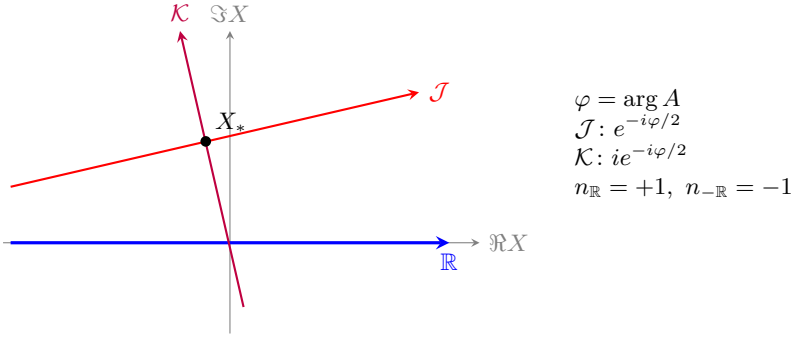


Figure XVII.11.5: Actual cycles of the entire Gaussian. The descending direction is $e^{-i\varphi/2}$, and the upward direction is rotated by $+\pi/2$. The real contour can be deformed to the descending cycle through X_* because the integrand is entire and its ends remain in decay sectors. Orientations determine the coefficient.

A finite protected knot observable provides a different controlled calculation. Let R now denote the positive integer level, to distinguish it from the polynomial parameter r

above. The reduced top-color figure-eight Jones sum in Andersen and Hansen 2003, printed p.3 before equation (1), has unknot normalization one and is

$$J_R = \sum_{k=0}^{R-1} \prod_{j=1}^{k} (1-q^j)(1-q^{-j}), \qquad q = e^{2\pi i/R}, \qquad (1-q^j)(1-q^{-j}) = 4\sin^2\frac{\pi j}{R}. \tag{XVII.11.43}$$

The empty product is one. At $R = 4$ the cumulative products are $1, 2, 8, 16$, giving $J_4 = 27$. At $R = 5$ they are

$$1, \quad \frac{5-\sqrt{5}}{2}, \quad 5, \quad \frac{5(5+\sqrt{5})}{2}, \quad 25, \qquad J_5 = 46 + 2\sqrt{5}. \tag{XVII.11.44}$$

The same sum gives $J_3 = 13$ and $J_6 = 89$. These exact finite sums reconstruct a normalized knot invariant. They do not evaluate a surgery partition function. In particular a reduced knot normalization cannot determine the absolute normalization or framing factor of a filled-manifold invariant.

The source integral representation also has specific contours. On printed p.4, equation (3) of Andersen and Hansen 2003 uses a contour in the strip $0 < \Re z < 1$ enclosing the half-grid $(k+1/2)/R$, $0 \le k < R$. The surgery double contour in equation (4) also encloses k/R, $1 \le k < R$. Figure XVII.11.6 distinguishes the two grids. Neither contour is an unrestricted real-line Gaussian, and neither integral is evaluated here.

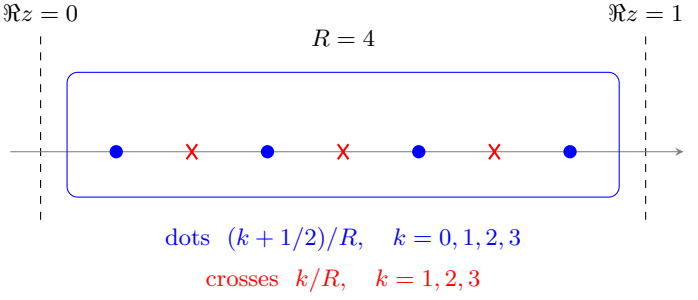


Figure XVII.11.6: The source strip and its two finite grids, illustrated at $R = 4$. Half-grid points occur in the knot contour representation, while the surgery double contour also encloses the interior integer grid. The drawing records domains and enclosed points; it does not prescribe a physical contour for the filled M5 theory.

For a holomorphic integral with isolated critical points, the framework of Witten 2010, printed pp.9–10, equations (2.15)–(2.16), organizes a specified cycle by

$$\Gamma = \sum_{\alpha} n_\alpha \mathcal{J}_\alpha, \qquad n_\alpha = \langle \Gamma, \mathcal{K}_\alpha \rangle. \tag{XVII.11.45}$$

The coefficients depend on the cycle and can change across Stokes walls. The Gaussian realizes this formula with one saddle and an explicitly chosen real contour. For the figure-eight filling, a physical Γ, its intersection coefficients and the one-loop measure

have not been determined. Reducible or degenerate sectors can also invalidate the isolated-critical-point setup. Assigning coefficient one to every flat connection would bypass precisely the missing information.

The physical task left by these calculations is concrete. A global filled M5 construction must specify the absolute lift and global choices, include the sectors omitted by an irreducible chart, and supply a contour, measure and quantum normalization compatible with gluing. Local Abelian gauging and the full matrix filling relation provide necessary structure. They do not by themselves establish that global theory or its complete protected partition function.

Sources and scope

Take-home message of this chapter

Filling contracts a primitive cycle through the full matrix relation $M^p L^q = 1_2$. The figure-eight meridian quotient is trivial, while cusp eigenvalues alone produce spurious solutions. Positive cyclic fillings retain all central and reducible classes; valid zero surgery can retain unipotents. A protected integral additionally needs an actual contour and normalization.

The exit calculation is to reproduce the affine marking map, identify which field carries the contact term in ST and TS, derive the meridian quotient before taking eigenvalues, and exhibit the failure of finite-order semisimplicity at $p = 0$. For an integral, the reader should be able to state the contour and its orientation separately from its critical equation.

The following exercises separate bounded calculation answers from written arguments. For benchmark submissions, see `benchmark/PROTOCOL.md`.

1. **Marked polarization and primitive slopes.** Derive (XVII.11.4) from (u, w), including both constant shifts, and verify preservation of the symplectic form. Give the converted S_c, transport $(7, 3)$ under $g = \left(\begin{smallmatrix} 2 & 1 \\ 1 & 1 \end{smallmatrix}\right)$, and complete the original slope to a determinant-one basis. In writing, explain the half shear and why $(14, 6)$ cannot be an attaching meridian.

2. **Gauging and contact terms.** Reconstruct K_{ST}, K_{TS} and K_{SS} from the displayed action coefficients. Give the local $A + C$ constraint. In writing, distinguish its local variation from the compact bundle sum and explain why no absolute framing phase follows.

3. **The meridian trap.** Multiply the preferred longitude word with $X_{12} = H, Y_{21} = -r/H$, $H \neq 0$, at $m = 1$ and reduce modulo $r^2 + r + 1$. Solve for both roots with their labels fixed. Give its upper entry as a polynomial in H, r. State how many of the two cusp representatives survive meridian filling. In writing, derive the group quotient and treat the family $X = Y = 1_2 + \alpha N$, including its semisimplified character.

4. **Complete cyclic filling sectors.** Classify the $SL(2,\mathbb{C})$ representations of unknot 5/2 filling and then 4/1 filling, listing the inversion orbits and the number of central twists. In writing, prove completeness using the squarefree polynomial, explain the lost q dependence, and verify the 0/1 unipotent counterexample and its powers.

5. **Changed mapping torsion.** Abelianize the mapping group for F_7 and compare F_5. Give the Smith invariants, all torsion angle fractions in increasing order and the number of circle components. In writing, recover the holonomies of a, b, t and explain why they neither classify nonabelian connections nor compute a quantum trace.

6. **Contour data and a finite sum.** For $a = 2, k = 1, Y = 3, h = 1, J = 7/10$, compute A, X_*, the exponent and squared prefactor in (XVII.11.39). Give the coefficients for the two orientations of the real line and calculate J_4, J_5 independently. In writing, justify the entire contour deformation and square-root branch, specify the two source grids, and identify the missing figure-eight integration data.

Section XVII.11.1 derives the affine symplectic conversion and slope transport [MATH]. Section XVII.11.2 uses a sourced protected interpretation [CONJ+] and calculates local K matrices and complete Abelian mapping-torus characters [MATH]. The canonical transformation alone leaves quantum normalization undetermined. Section XVII.11.3 derives the primitive relation, word algebra and Jordan-sensitive extension [MATH]. Section XVII.11.4 computes the complete meridian quotient and positive finite-order classification, with a fixed-label source comparison [MATH]. Section XVII.11.5 gives bounded Abelian, Gaussian and Jones calculations [MATH]. The physical relation to the global protected sector remains conjectural [CONJ+].

We retain the marked $SL(2,\mathbb{C})$ lift of XVII.9 and the displayed spin compact-$U(1)$ action coefficients. These conventions keep central holonomies, contact terms and integration-cycle choices distinct.

Primary anchors are Dimofte et al. 2011, v1, printed p.16 and pp.20–22; Andersen and Hansen 2003, the Maphysto 2003/28 report, printed pp.3–4 and pp.23–25; Witten 2003, v3, printed pp.4–5, pp.10–11 and pp.13–17; and Witten 2010, v2, printed pp.9–10. The physical coefficient prescriptions also have the supplied DGG source support. No full nonabelian wall, exact projective phase, figure-eight physical cycle or measure, surgery RT normalization, thimble completeness or global filled-theory existence is established.

References

Andersen, J. E. and S. K. Hansen (2003). *Asymptotics of the quantum invariants for surgeries on the figure 8 knot.* Maphysto report 2003/28. Unversioned report; inspected pp.3–4,23–25.

Dimofte, T., D. Gaiotto, and S. Gukov (2011). *Gauge Theories Labelled by Three-Manifolds.* Version 1 inspected. arXiv: `1108.4389 [hep-th]`.

Witten, E. (2003). *SL(2,Z) Action On Three-Dimensional Conformal Field Theories With Abelian Symmetry*. Inspected version v3; browser PDF text access. arXiv: `hep-th/0307041`.

Witten, E. (2010). *Analytic Continuation of Chern–Simons Theory*. Version 2 inspected. arXiv: `1001.2933 [hep-th]`.

Chapter XVII.12

Strings from M5-branes on divisors

A brane wrapped on a compact cycle leaves a quantum field theory on its unwrapped directions. For an M5-brane wrapped on a complex surface in a Calabi–Yau threefold, those directions form a string worldsheet. The surface determines how many massless fields propagate along the string. Its intersection numbers also determine anomalies, so we can compare a direct field count with a calculation that survives the renormalization-group flow.

We will carry out this comparison for one smooth wrapped M5-brane, including its universal translation and fermion modes. The hyperplane surface in the quintic provides a concrete example throughout. Changing the divisor from H to a smooth $2H$ will teach us why the answer is sensitive to the geometry of one connected surface. We then introduce the modified elliptic genus and identify which further information is needed to turn an anomaly calculation into an asymptotic statement about states.

The reader needs the single tensor multiplet of XVI.1, complex surfaces and adjunction, and the basic meaning of a chiral boson and a Ramond trace. We recall the characteristic classes and anomaly normalization locally. The divisor restriction used in Section XIII.2.2 is the same geometric operation, but the present surface is compact and ample. Its spectrum cannot be imported from a noncompact local surface. By the end, the reader should be able to compute the topology, integrate the tensor anomaly, count the zero modes, and follow one flux orbit without identifying these operations with a computation of the complete genus.

XVII.12.1 A smooth divisor becomes a string

Consider M-theory on a smooth compact projective Calabi–Yau threefold X of full $SU(3)$ holonomy. Its noncompact spacetime has five dimensions. An M5-brane on a smooth connected ample divisor $P \subset X$ occupies a string in that spacetime. We write

its worldvolume and the two relevant bundles as

$$W_6 = \Sigma \times P, \qquad TW_6 = T\Sigma \oplus TP, \qquad NW_6 = N_{P/X,\mathbb{R}} \oplus E_3. \tag{XVII.12.1}$$

Here E_3 describes the three transverse noncompact directions. The complex normal line $N_{P/X}$ uses the remaining two real transverse directions. The holomorphic embedding preserves four right-moving supercharges. The resulting low-energy wrapped-string construction has $(0,4)$ supersymmetry, under the physical assumption of a suitable decoupling limit and infrared conformal theory. Energies are taken below the internal Kaluza–Klein scale.

The five real scalar fields of the single tensor multiplet have a geometric interpretation in this splitting. Three translate the string in noncompact space. The other two describe motion normal to P inside X and therefore become sections of its normal line. Introduce the integral divisor class and its two intersection numbers,

$$\begin{aligned} p = [P] \in H^2(X,\mathbb{Z}), \qquad x = p|_P = c_1(N_{P/X}), \\ A = \int_X p^3 = \int_P x^2, \qquad B = \int_X c_2(X) p. \end{aligned} \tag{XVII.12.2}$$

No factorial is included in A. The conventional MSW symbol D would be $A/6$.

We first compute the topology needed by the reduction. The exact tangent sequence and the vanishing of $c_1(X)$ give

$$c(TP) = \frac{c(TX)|_P}{1+x} = (1 + c_2(X)|_P + \cdots)(1 - x + x^2 + \cdots). \tag{XVII.12.3}$$

Comparing degrees two and four produces

$$c_1(P) = -x, \qquad c_2(P) = c_2(X)|_P + x^2, \qquad K_P = N_{P/X}. \tag{XVII.12.4}$$

The last equality is adjunction for the canonical bundle. It means that a holomorphic normal deformation is a holomorphic two-form on P.

The Euler number, signature and holomorphic Euler characteristic of a smooth complex surface follow from Gauss–Bonnet, the signature theorem and Hirzebruch–Riemann–Roch. Substituting the classes just derived yields

$$\begin{aligned} e(P) &= \int_P c_2(P) = A + B, \\ \sigma(P) &= \frac{1}{3}\int_P \big(c_1(P)^2 - 2c_2(P)\big) = -\frac{A+2B}{3}, \\ \chi(\mathcal{O}_P) &= \frac{1}{12}\int_P \big(c_1(P)^2 + c_2(P)\big) = \frac{2A+B}{12}. \end{aligned} \tag{XVII.12.5}$$

These theorem inputs apply to the smooth projective surface with its complex orientation. We now need an additional vanishing statement to extract individual Hodge numbers from the indices.

Weak Lefschetz identifies $H^1(P)$ with $H^1(X)$ for an ample smooth divisor in a threefold. Full $SU(3)$ holonomy implies $h^{0,1}(X) = 0$. Thus

$$h^{0,1}(P) = 0, \qquad \chi(\mathcal{O}_P) = 1 - h^{0,1}(P) + h^{2,0}(P), \qquad p_g \equiv h^{2,0}(P) = \frac{2A+B}{12} - 1. \tag{XVII.12.6}$$

This is where the hypotheses on the ambient holonomy and ampleness enter the field count. An irregular surface would have $h^{0,1} \neq 0$ and a different fermion inventory.

For a Kähler surface, the Kähler form and the real and imaginary parts of the holomorphic two-forms are selfdual. Primitive real $(1,1)$ forms are antiselfdual. Consequently

$$b_2^+ = 1 + 2p_g = \frac{2A+B}{6} - 1, \qquad b_2^- = h^{1,1} - 1 = \frac{4A+5B}{6} - 1. \tag{XVII.12.7}$$

The second expression can be obtained without any further Hodge calculation. Since $b_1 = b_3 = 0$, $e(P) = 2 + b_2^+ + b_2^-$; inserting the first expression gives the second. Equivalently $b_2^\pm = (e - 2 \pm \sigma)/2$. Their difference recovers the signature in (XVII.12.5).

A normal deformation is counted by $h^0(N_{P/X}) = h^0(K_P) = p_g$. Each complex deformation gives two real nonchiral scalar fields. Hence the scalar fields apart from the tensor reduction are

$$n_{\text{def}} = 2p_g = \frac{2A+B}{6} - 2, \qquad n_{\text{ordinary}} = 2p_g + 3. \tag{XVII.12.8}$$

The equality also follows from the linear system of divisors. In the sequence

$$0 \longrightarrow \mathcal{O}_X \longrightarrow \mathcal{O}_X(P) \longrightarrow N_{P/X} \longrightarrow 0, \qquad h^0(N_{P/X}) = h^0(\mathcal{O}_X(P)) - 1, \tag{XVII.12.9}$$

we used $H^1(X, \mathcal{O}_X) = 0$. Kodaira vanishing for the ample line bundle on X, together with threefold Riemann–Roch, gives $h^0(\mathcal{O}_X(P)) = A/6 + B/12$. Thus the deformation count agrees with the surface index.

The tensor field provides the chiral scalar fields. Expanding its two-form potential in harmonic two-forms on P gives

$$B_2(\sigma, y) = \sum_{i=1}^{b_2(P)} \phi_i(\sigma)\omega_i(y) + \cdots, \qquad *_P\omega_i = \epsilon_i\omega_i, \quad \epsilon_i = \pm 1. \tag{XVII.12.10}$$

The six-dimensional selfduality equation relates the derivative of ϕ_i to its worldsheet dual. We call the supersymmetric side right-moving, so $\epsilon_i = +1$ gives a right chiral boson and $\epsilon_i = -1$ gives a left chiral boson. This fixes the chirality convention for the entire chapter.

For the quintic hyperplane surface, $A = 5$ and $B = 50$. The above steps give

$$\chi(\mathcal{O}_P) = 5, \quad p_g = 4, \quad n_{\text{def}} = 8, \quad b_2^+ = 9, \quad b_2^- = 44. \tag{XVII.12.11}$$

The tensor therefore gives nine right chiral bosons and forty-four left chiral bosons. Three translations and eight real deformations contribute on both sides. We will derive A and B directly from the quintic in Section XVII.12.4; first we compute the anomaly without resolving any individual mode.

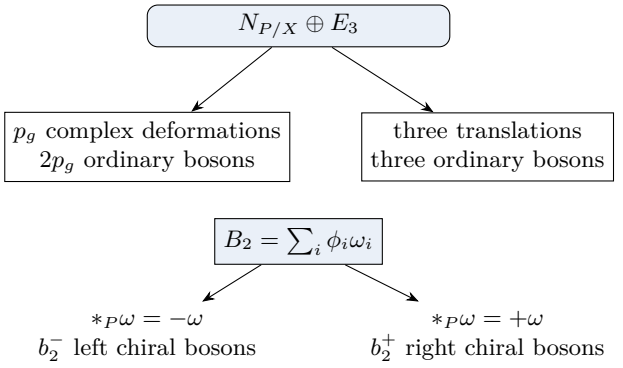


Figure XVII.12.1: Reduction of one wrapped tensor multiplet. The two internal normal directions become p_g complex surface deformations, while E_3 gives three translations. Harmonic two-forms split the tensor scalars by their Hodge-star eigenvalue. The right-moving fermion count uses $h^{0,1}(P) = 0$.

XVII.12.2 Integrating the M5 anomaly

An anomaly polynomial records the response to background transformations. For a chiral theory it contains products of background curvatures whose descent gives the anomalous variation. Compactification on P integrates the six-dimensional eight-form to a worldsheet four-form. The mixed terms are essential because the retained term must contain four internal form degrees and four external form degrees.

For one full M5 tensor multiplet the input polynomial is

$$I_8 = \frac{1}{48}\left[p_2(N) - p_2(T) + \frac{1}{4}\big(p_1(T) - p_1(N)\big)^2\right]. \tag{XVII.12.12}$$

Here $T = TW_6$ and $N = NW_6$. These are integral Pontryagin classes. This worldvolume polynomial is different from the similarly named bulk curvature coupling. In particular we retain the single tensor multiplet in full; a center subtraction for a nonabelian stack would erase the very field system being reduced.

To perform the integral, abbreviate the formal four-forms by

$$t = p_1(T\Sigma), \qquad a = p_1(TP) = -x^2 - 2c, \qquad r = p_1(E_3), \qquad c = c_2(X)|_P. \tag{XVII.12.13}$$

The class t is an external background class in the anomaly calculation, even though a literal four-form vanishes on a two-dimensional manifold. Anomaly polynomials use the corresponding formal curvature expressions before descent. The classes a, x^2, c carry internal degree four. Multiplicativity of the total Pontryagin class gives

$$\begin{aligned} p_1(T) &= t + a, \qquad [p_2(T)]_{4,4} = ta, \\ p_1(N) &= x^2 + r, \quad [p_2(N)]_{4,4} = x^2 r. \end{aligned} \tag{XVII.12.14}$$

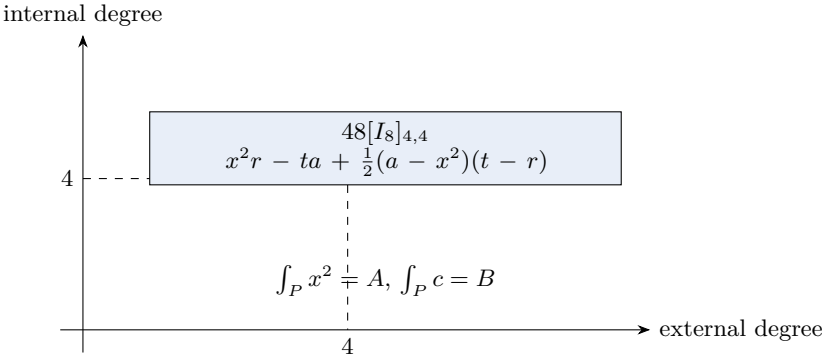


Figure XVII.12.2: Terms retained by fiber integration. Every displayed product lies at internal degree four and external degree four. The pure degree-eight parts of the square lie outside this cell. The x^2r term originates in $p_2(N)$ and cannot be dropped.

The notation $[\,]_{4,4}$ specifies internal degree four and external degree four. Purely internal degree-eight terms integrate to zero on the real four-manifold P. Purely external terms have no internal volume degree and also do not contribute.

The square in (XVII.12.12) has its own mixed term. It is useful to extract it before substituting the surface classes,

$$\left[\frac{1}{4}\big((a-x^2)+(t-r)\big)^2\right]_{4,4} = \frac{1}{2}(a-x^2)(t-r). \tag{XVII.12.15}$$

The factor two comes from the cross term; its omission would change both anomalies. Together the three retained terms give

$$48[I_8]_{4,4} = x^2r - ta + \frac{1}{2}(a-x^2)(t-r). \tag{XVII.12.16}$$

We can now do the algebra in two visible steps. Since $a = -x^2 - 2c$,

$$\begin{aligned} -ta + \tfrac{1}{2}(a-x^2)t &= \tfrac{1}{2}(-a-x^2)t = ct, \\ x^2r - \tfrac{1}{2}(a-x^2)r &= \tfrac{1}{2}(3x^2-a)r = (2x^2+c)r. \end{aligned} \tag{XVII.12.17}$$

Integration therefore depends only on A and B,

$$I_4 = \int_P I_8 = \frac{B}{48}t + \left(\frac{A}{24} + \frac{B}{48}\right)r. \tag{XVII.12.18}$$

The cancellation of the A term multiplying t is meaningful. The cubic intersection enters the R anomaly, while the gravitational anomaly is linear in the ambient c_2 pairing.

To translate r to an $SU(2)$ class, let the fundamental representation have formal Chern roots $\pm z$. The associated oriented rank-three bundle has complex weights $0, \pm 2z$. Thus

$$c_2(R) = -z^2, \qquad p_1(E_3) = (2z)^2 = -4c_2(R), \qquad I_4 = \frac{B}{48}p_1(T\Sigma) - \left(\frac{A}{6} + \frac{B}{12}\right)c_2(R). \tag{XVII.12.19}$$

The four in this conversion follows from the adjoint weight. Replacing it by one would divide the inferred R level by four.

Our chirality convention is fixed by writing the worldsheet anomaly as

$$I_4 = \frac{c_L - c_R}{24} p_1(T\Sigma) - k_R c_2(R). \tag{XVII.12.20}$$

For example, a complex right-moving Weyl fermion contributes $-p_1/24$ from $\widehat{A}$, consistent with $c_R = 1$. For an $SU(2)$ fundamental, $\mathrm{ch}_2 = -c_2(R)$ fixes the displayed gauge sign. These checks choose the whole polynomial's convention; reversing chirality reverses the anomaly as a whole.

The hyperplane values provide a numerical check on every coefficient,

$$I_4(H) = \frac{25}{24} t + \frac{5}{4} r = \frac{25}{24} p_1(T\Sigma) - 5c_2(R). \tag{XVII.12.21}$$

If $p_2(N)$ were deleted from (XVII.12.12), the error would be $-Ar/48$. For H the coefficient of r would be $55/48$ instead of $60/48$, and the inferred level would be $55/12$ instead of 5. The surface topology has not changed, so the mismatch diagnoses an error in the reduction, rather than a new choice of physical sector.

XVII.12.3 Two ways to compute the central charges

The integrated anomaly measures two protected coefficients. Translating the R anomaly into a central charge also needs supersymmetry and an infrared identification. Suppose that the wrapped theory reaches a $(0,4)$ conformal theory and the transverse $SU(2)$ is its superconformal R symmetry. The small $(0,4)$ algebra then gives

$$k_R = \frac{2A + B}{12}, \qquad c_R = 6k_R = A + \frac{B}{2}, \qquad c_L - c_R = \frac{B}{2}. \tag{XVII.12.22}$$

It follows that

$$c_L = A + B, \qquad c_R = A + \frac{B}{2}. \tag{XVII.12.23}$$

The anomaly coefficient itself is defined without an assumption about the infrared fixed point. The extra identification in the preceding paragraph is needed precisely at the step $c_R = 6k_R$.

We can compare this answer with the massless fields. Each ordinary real boson contributes one unit on each side; a real chiral boson contributes one on its own side; a real chiral fermion contributes one-half. The twisted fermion zero modes of the wrapped tensor multiplet are counted by the surface Dolbeault groups,

$$n_F^R = 4\big(h^{0,0} + h^{2,0}\big) = 4(p_g + 1), \qquad n_F^L = 4h^{0,1} = 0. \tag{XVII.12.24}$$

The tensor and scalar reductions of Section XVII.12.1 give

$$n_B^L = 2p_g + 3 + b_2^-, \qquad n_B^R = 2p_g + 3 + b_2^+. \tag{XVII.12.25}$$

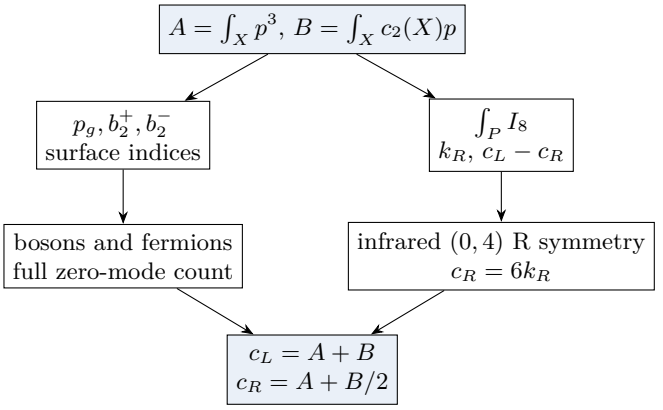


Figure XVII.12.3: Two computations of the central charges. Surface topology determines the massless field inventory. The fiber integral determines the gravitational anomaly and $SU(2)$ level. The second branch needs the displayed infrared R-symmetry assumption before it determines c_R. Both branches refer to one full wrapped M5-brane.

This decomposition makes the three translations explicit. They are physical massless fields even when an infinite spatial volume is later removed from a partition function.

Inserting $p_g = (2A + B)/12 - 1$ in the left count gives

$$n_B^L = \left(\frac{2A+B}{6} - 2\right) + 3 + \left(\frac{4A+5B}{6} - 1\right) = A + B. \tag{XVII.12.26}$$

The constants cancel, rather than being discarded. The right-moving count and fermion contribution are

$$n_B^R = 4(p_g + 1) = \frac{2A+B}{3}, \qquad \frac{1}{2}n_F^R = 2(p_g + 1) = \frac{2A+B}{6}. \tag{XVII.12.27}$$

Consequently the massless inventory reproduces both central charges,

$$c_L = n_B^L + \tfrac{1}{2}n_F^L = A + B, \qquad c_R = n_B^R + \tfrac{1}{2}n_F^R = A + \tfrac{B}{2}. \tag{XVII.12.28}$$

The equality compares two calculations with the same wrapped-brane premises. It explains the topological answer at the level of fields, without establishing a second independent construction of the full conformal theory.

For $P = H$, one can see every summand numerically,

$$(n_B^L, n_B^R, n_F^L, n_F^R) = (8{+}3{+}44,\ 8{+}3{+}9,\ 0,\ 20) = (55, 20, 0, 20), \qquad (c_L, c_R) = (55, 30). \tag{XVII.12.29}$$

The right-moving fermions account for the difference between twenty bosons and thirty units of c_R. Swapping the tensor chiralities or dropping the translations would fail this comparison in a different way.

A universal set of local oscillators accompanies the string. It consists of the three translation bosons, one right chiral tensor boson and four real right-moving goldstinos.

Its central-charge contribution is

$$(c_L, c_R)_{\mathrm{univ}} = (3, 3 + 1 + 4/2) = (3, 6). \tag{XVII.12.30}$$

The chiral tensor boson has no left partner in this contribution. Removing a nonchiral four-boson hypermultiplet would instead subtract $(4, 6)$ and give the wrong left count. Subtracting the stated local oscillators produces

$$(c_L, c_R)_{\mathrm{remainder}} = (A + B - 3, A + B/2 - 6), \qquad H \longmapsto (52, 24). \tag{XVII.12.31}$$

We call this an oscillator remainder. A decomposition of a local inventory does not by itself factor the full Hilbert space or its charge lattice. In particular the distinguished selfdual tensor direction can be coupled to other directions by lattice identifications. Equations (XVII.12.23) and (XVII.12.29) continue to denote the full theory, including these universal modes.

There is a useful link with the linear system already counted. Since $k_R = \chi(\mathcal{O}_P) = p_g + 1$, the number of right-moving bosons is $4k_R$ and that of right-moving real fermions is also $4k_R$. Their combined central charge is $6k_R$. This explains how the scalar, tensor and fermion modes assemble into the $(0, 4)$ counting while leaving the left chiral excess measured by $B/2$.

XVII.12.4 The quintic and its first two divisor degrees

We now generate the topological inputs from an explicit complete intersection. Let X be a smooth degree-five hypersurface in $\mathbb{CP}^4$, and let H denote the restricted hyperplane class. The ambient Euler sequence and the hypersurface normal sequence give

$$c(T\mathbb{CP}^4) = (1 + H)^5, \qquad 0 \longrightarrow TX \longrightarrow T\mathbb{CP}^4|_X \longrightarrow \mathcal{O}_X(5) \longrightarrow 0. \tag{XVII.12.32}$$

Multiplying by $(1 + 5H)^{-1}$ through degree six yields

$$\begin{aligned} c(TX) &= (1 + 5H + 10H^2 + 10H^3 + \cdots)(1 - 5H + 25H^2 - 125H^3 + \cdots) \\ &= 1 + 10H^2 - 40H^3, \qquad \int_X H^3 = 5. \end{aligned} \tag{XVII.12.33}$$

For example, the cubic coefficient is $10 - 50 + 125 - 125 = -40$. We therefore find $c_1(X) = 0$ and $e(X) = \int_X c_3(X) = -200$. The two intersection inputs for a divisor in $|nH|$ follow immediately,

$$p = nH, \qquad A_n = 5n^3, \qquad B_n = 50n. \tag{XVII.12.34}$$

We choose a smooth connected member of this linear system for every positive degree considered below. A generic member has this property; an arbitrary singular polynomial does not satisfy the assumptions of the reduction.

For $n = 1$, the surface can also be viewed as a smooth quintic in $\mathbb{CP}^3$. Writing $h = H|_P$, its own normal sequence gives a separate surface computation,

$$c(TP) = \frac{(1+h)^4}{1+5h} = 1 + (4-5)h + (6-20+25)h^2 = 1 - h + 11h^2, \qquad \int_P h^2 = 5. \tag{XVII.12.35}$$

Thus $e(P) = 55$ and $\sigma(P) = 5(1-22)/3 = -35$. The holomorphic Euler characteristic is $5(1+11)/12 = 5$. Using $h^{0,1} = 0$ and $e = 2 + 2p_g + h^{1,1}$, we obtain

$$(p_g, h^{1,1}, b_2^+, b_2^-) = (4, 45, 9, 44), \qquad b_2 = 53. \tag{XVII.12.36}$$

This supplies the topology used in the earlier example. In particular the rank-one ambient class h is only one direction in a rank-fifty-three surface lattice.

The deformation count has an elementary polynomial interpretation. A hyperplane in $\mathbb{CP}^4$ is specified by five coefficients, modulo overall scaling. Its projective parameter space has complex dimension four,

$$h^0(X, \mathcal{O}_X(H)) = 5, \qquad \dim_{\mathbb{C}} |H| = 5 - 1 = 4 = p_g(H). \tag{XVII.12.37}$$

This agrees with the four complex normal deformations. It is a useful independent way to see why the eight real deformation fields must be retained.

Now replace P by a smooth quadratic section $P_2 \in |2H|$. It is a complete intersection of degrees five and two in $\mathbb{CP}^4$. The Chern-class expansion changes to

$$c(TP_2) = \frac{(1+h)^5}{(1+5h)(1+2h)} = (1 + 10h^2 + \cdots)(1 - 2h + 4h^2 + \cdots) = 1 - 2h + 14h^2. \tag{XVII.12.38}$$

Since $\int_{P_2} h^2 = 10$, this gives

$$e(P_2) = 140, \quad \sigma(P_2) = \frac{10}{3}(4-28) = -80, \quad \chi(\mathcal{O}_{P_2}) = \frac{10}{12}(4+14) = 15. \tag{XVII.12.39}$$

The Hodge and mode counts follow with the same steps as before,

$$\begin{aligned} (p_g, h^{1,1}, b_2^+, b_2^-) &= (14, 110, 29, 109), \\ (n_B^L, n_B^R, n_F^R) &= (28 + 3 + 109, 28 + 3 + 29, 60) = (140, 60, 60), \\ (c_L, c_R) &= (140, 90). \end{aligned} \tag{XVII.12.40}$$

There are fifteen independent quadrics in five homogeneous coordinates, so the projective linear system has dimension fourteen, again agreeing with p_g. The anomaly comparison also gives $k_R = 15$ and $c_L - c_R = 50$.

The exact sequence of the quintic hypersurface explains the section count at higher degree,

$$0 \longrightarrow \mathcal{O}_{\mathbb{CP}^4}(n-5) \xrightarrow{\cdot F_5} \mathcal{O}_{\mathbb{CP}^4}(n) \longrightarrow \mathcal{O}_X(n) \longrightarrow 0. \tag{XVII.12.41}$$

For $n > 0$, the resulting dimension is

$$h^0(X, \mathcal{O}_X(nH)) = \binom{n+4}{4} - \begin{cases} \binom{n-1}{4}, & n \geq 5, \\ 0, & 1 \leq n < 5 \end{cases} = \frac{5n^3 + 25n}{6}. \tag{XVII.12.42}$$

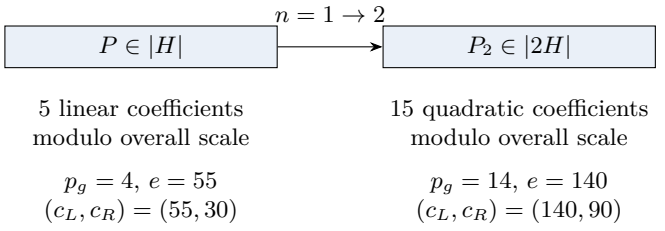


Figure XVII.12.4: A smooth divisor is a member of a projective linear system. For H, five linear coefficients modulo scale give four complex deformations; for $2H$, fifteen quadratic coefficients modulo scale give fourteen. The corresponding surface and central-charge numbers change through both the cubic and linear intersection terms.

At $n = 5$, the defining quintic itself becomes a relation among the degree-five polynomials. Thus $h^0 = 126-1 = 125$, rather than 126. The final cubic is also $\chi(\mathcal{O}_P) = (2A_n+B_n)/12$, as required by (XVII.12.9).

The change from H to $2H$ is not multiplication of a Hilbert space by two. A single smooth surface in class $2H$ has cubic intersection $A_2 = 40$, whereas twice the numerical contribution of H has cubic term 10. Explicitly,

$$(c_L, c_R)_{\text{smooth } 2H} = (140, 90), \qquad 2(c_L, c_R)_H = (110, 60). \tag{XVII.12.43}$$

The latter is an additive comparison for separate wrapped objects, not the spectrum of the smooth quadratic divisor. A reducible representative such as a union of hyperplanes has intersection regions and lies outside the smooth calculation. Smoothing changes the deformation and tensor modes. The n^3 term measures this geometry, while the ambient c_2 pairing scales only linearly with n.

XVII.12.5 The modified genus, spectral flow and the Cardy window

The central charges constrain a conformal theory but do not determine its protected spectrum. To see the missing information, start with the right-moving goldstino zero modes. Four real zero modes form two fermionic creation operators. Their quartet has fermion-number offsets $0, 1, 1, 2$, so an ordinary signed trace vanishes,

$$\mathrm{Tr}_{\text{quartet}}(-1)^F = 1 - 2 + 1 = 0, \qquad \mathrm{Tr}_{\text{quartet}}\, \frac{F^2}{2}(-1)^F = 0 - \frac{1}{2} - \frac{1}{2} + 2 = 1. \tag{XVII.12.44}$$

The same result follows from $Z_0(s) = (1-e^s)^2$ by taking $Z_0''(0)/2$. A common offset in F does not change the second derivative at zero, apart from the overall parity convention.

This finite calculation explains the quadratic insertion, rather than evaluating the trace over all excited states.

Let J_R^3 be the Cartan generator of the transverse $SU(2)$, identified with the superconformal R symmetry under the assumption above. The operators Q_A measure ambient charges, and y^A are their chemical potentials. The operators L_0 and $\bar{L}_0$ are the left and right Virasoro zero modes, and Tr_R denotes the trace over the Ramond Hilbert space. With $q = e^{2\pi i\tau}$ and $\bar{q} = e^{-2\pi i\bar{\tau}}$, the modified trace is formally

$$Z_P(\tau,\bar{\tau},y) = \mathrm{Tr}_R\left[\frac{F^2}{2}(-1)^F q^{L_0-c_L/24}\bar{q}^{\bar{L}_0-c_R/24}e^{2\pi i y\cdot Q}\right], \qquad F = 2J_R^3 + p\cdot Q. \tag{XVII.12.45}$$

We divide out the infinite volume of the three translational coordinates and specify zero translational momentum in oscillator expressions. Their oscillators still contribute to the full central charges. The trace is a protected, signed quantity in the smooth single-string MSW sector. Its relation to a complete four-dimensional multicenter spectrum would need additional physical information.

We need to distinguish the surface flux lattice from the ambient charges visible to the lower-dimensional gauge fields. Choose an integral ambient basis ω_A and write $p = p^A\omega_A$. Thus $p\cdot Q = p^A Q_A$ and $p\cdot\kappa p = p^A\kappa_{AB}p^B$. The eigenvalues of Q_A are q_A, and the intersection form and flux charges are

$$\kappa_{AB} = \int_X p\,\omega_A\omega_B = \int_P \omega_A|_P\,\omega_B|_P, \qquad q_A = \int_P \omega_A|_P\, f. \tag{XVII.12.46}$$

We work on the free, nondegenerate ambient lattice. The full free $H^2(P,\mathbb{Z})$ contains more directions. On the quintic hyperplane its rank is 53 and its signature is $(9,44)$, while the ambient form has rank one with $\kappa = 5$. Thus ambient theta sectors do not replace the tensor's entire flux lattice.

The flux obeys a characteristic shift. In the convention adopted here,

$$f \in H^2(P,\mathbb{Z}) + \frac{x}{2}, \qquad q_0 = -\frac{e(P)}{24} - \frac{1}{2}\int_P f^2 \quad \text{for the pure-flux representative.} \tag{XVII.12.47}$$

For the quintic H example, $x = h$. Taking $f = h/2$ gives the explicit charges

$$q = \int_P h\frac{h}{2} = \frac{5}{2}, \qquad q_0 = -\frac{55}{24} - \frac{1}{2}\frac{5}{4} = -\frac{35}{12}. \tag{XVII.12.48}$$

The sign of q_0 is the MSW charge convention used here. A source calling an oppositely signed quantity a D0 number must first translate that sign before its excitation formula is compared with ours.

An integral ambient flux shift $f \mapsto f + \lambda^A\omega_A|_P$ acts by spectral flow,

$$q'_A = q_A + \kappa_{AB}\lambda^B, \qquad q'_0 = q_0 - \lambda^A q_A - \frac{1}{2}\kappa_{AB}\lambda^A\lambda^B. \tag{XVII.12.49}$$

The first formula is linear in the flux; the second follows by expanding its square. Its invariant is

$$\widehat{q}_0 = q_0 + \frac{1}{2}q_A(\kappa^{-1})^{AB}q_B. \tag{XVII.12.50}$$

Indeed direct substitution gives the cancellation

$$\widehat{q}_0' - \widehat{q}_0 = -\lambda\cdot q - \tfrac{1}{2}\lambda\cdot\kappa\lambda + \tfrac{1}{2}\left(2\lambda\cdot q + \lambda\cdot\kappa\lambda\right) = 0. \tag{XVII.12.51}$$

For the half-flux example,

$$\left(\frac{5}{2}, -\frac{35}{12}\right) \xrightarrow{\lambda=1} \left(\frac{15}{2}, -\frac{95}{12}\right), \qquad \widehat{q}_0 = -\frac{35}{12} + \frac{(5/2)^2}{10} = -\frac{55}{24}. \tag{XVII.12.52}$$

The negative invariant labels a polar vacuum representative, not a positive excitation to which a high-energy estimate can be applied.

The ambient-flux family has $q = 5(k + 1/2)$ with $k \in \mathbb{Z}$. The combined ambient charge cosets can be written

$$q = 5\left(k + \frac{1}{2}\right) + \delta, \qquad k \in \mathbb{Z}, \quad \delta = 0, 1, 2, 3, 4. \tag{XVII.12.53}$$

Spectral flow changes k and preserves δ. The five labels reflect the discriminant group of $\kappa = 5$, not five tensor fields. General surface fluxes and their ambient projections require the full lattice description; the pure ambient family alone occupies $\delta = 0$.

For the charged right-energy formula, impose a further geometric condition that has not been needed for anomalies. The restricted Kähler class is proportional to $x = p|_P$. More generally, the projection of an ambient charge onto a positive Kähler direction j has squared energy

$$E_R(j) = \frac{(j\cdot q)^2}{2\, j\cdot\kappa j}. \tag{XVII.12.54}$$

When j is proportional to p, $p\cdot\kappa p = A$ and the sourced charged BPS condition becomes

$$\bar{L}_0 - \frac{c_R}{24} = \frac{(p\cdot Q)^2}{2A}. \tag{XVII.12.55}$$

The rank-one quintic examples satisfy this alignment automatically. On H, the right-energy factor of a charge-q term is therefore

$$\bar{q}^{q^2/10} e^{2\pi i y q}, \qquad q = 5(k + 1/2) + \delta. \tag{XVII.12.56}$$

Summing these Gaussian charge factors along the flow orbit is the origin of the theta functions. Their characteristics, other lattice directions and left-moving coefficient functions belong to the full protected-trace construction. The Gaussian alone does not determine those coefficients or imply a product decomposition of the theory. A charged state need not have zero right-moving energy after vacuum subtraction, so this theta presentation retains $\bar{\tau}$ dependence.

The alignment condition changes an actual number when more than one Kähler direction is available. As a projection calculation, take

$$\kappa = \begin{pmatrix} 3 & 6 \\ 6 & 3 \end{pmatrix}, \quad p = \begin{pmatrix} 1 \\ 1 \end{pmatrix}, \quad q = \frac{1}{2}\kappa p = \begin{pmatrix} 9/2 \\ 9/2 \end{pmatrix}. \tag{XVII.12.57}$$

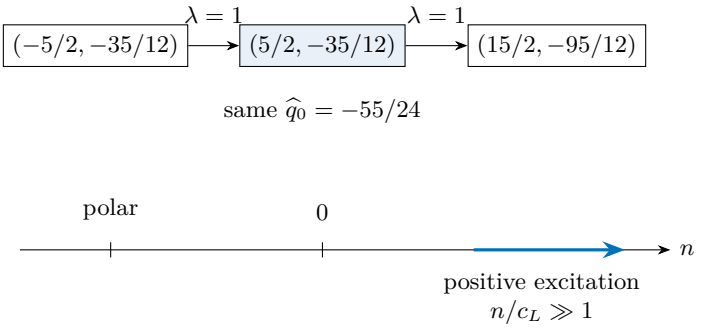


Figure XVII.12.5: The upper row shows one spectral-flow orbit for the quintic half-flux representative. The invariant remains $-55/24$ while both charges change. The lower row distinguishes this polar representative from the positive left excitation n used in an asymptotic saddle. The displayed hierarchy is a regime condition, not a state-count formula at finite charge.

Then $E_R(p) = 81/36 = 9/4$, whereas $j = (1, 2)$ gives $E_R(j) = (27/2)^2/78 = 243/104$. This example concerns the projection, without asserting occupation of any proposed BPS state. It shows why (XVII.12.55) cannot be used unchanged at an arbitrary Kähler direction. The topological anomaly calculation is independent of this choice.

We finish by deriving the conditional Cardy estimate. Let $n > 0$ denote the available left oscillator excitation after the appropriate charge and vacuum subtraction in a fixed sector. Suppose first that modular and infrared assumptions give a high-temperature canonical function with

$$\log Z(\beta) \simeq \frac{\pi^2 c_L}{6\beta}, \qquad d(n) \sim \int d\beta \, \exp\left[\beta n + \frac{\pi^2 c_L}{6\beta}\right]. \tag{XVII.12.58}$$

The stationary point of the exponent satisfies

$$0 = n - \frac{\pi^2 c_L}{6\beta_*^2}, \qquad \beta_* = \pi\sqrt{\frac{c_L}{6n}}, \qquad S_* = 2\pi\sqrt{\frac{c_L n}{6}}. \tag{XVII.12.59}$$

The approximation demands that the saddle sample the assumed high-temperature regime. A conservative sufficient asymptotic condition at fixed geometry is

$$\frac{n}{c_L} \longrightarrow \infty. \tag{XVII.12.60}$$

For a signed index, one must further determine the dominant polar contribution and its effective central charge, and establish that leading terms do not cancel. The trace insertion and anomaly coefficients alone establish none of those ingredients. The saddle above is thus a conditional asymptotic derivation, rather than an evaluation of the modified genus.

The change of divisor makes the scale issue concrete. As a numerical hierarchy test,

demand $n/c_L \geq 100$. Then

$$\frac{5500}{c_L(H)} = 100, \qquad \frac{5500}{c_L(2H)} = \frac{275}{7} < 100, \qquad \frac{14000}{c_L(2H)} = 100. \tag{XVII.12.61}$$

For the first and third ratios the formal saddle is $\beta_* = \pi/\sqrt{600}$. At the first excitation of H, it would instead be $\pi\sqrt{55/6}$, outside a high-temperature approximation. The chosen value 100 only illustrates a scale separation. It neither certifies finite-charge growth nor supplies the missing polar coefficients. The explicit geometry has given two central charges, a charge orbit and a trace structure; an exact spectrum requires further dynamical or enumerative input.

Take-home message

One smooth connected ample divisor of a compact full-$SU(3)$ Calabi–Yau threefold supplies a wrapped single-M5 string whose topology fixes the integrated tensor anomaly. With the stated infrared R-symmetry assumption, the full central charges are $c_L = P^3 + c_2(X)P$ and $c_R = P^3 + \frac{1}{2}c_2(X)P$. Direct zero modes reproduce them, including the universal $(3, 6)$ oscillators. A smooth quintic hyperplane gives $(55, 30)$; a smooth quadratic divisor gives $(140, 90)$. The modified trace, shifted charge sectors and conditional Cardy saddle organize the next spectral questions, while keeping the full surface lattice and the charge-dependent right energy visible.

Exercises

1. Starting from adjunction, derive e, σ, $\chi(\mathcal{O}_P)$ and $b_2^{\pm}$ for $h^{0,1} = 0$. Evaluate them at $A = 40, B = 100$. As a separate check, take an irregular surface with $h^{0,1} = 1, p_g = 1, h^{1,1} = 4$ and find its actual Euler number and the value incorrectly inferred by setting $h^{0,1} = 0$. Explain which geometric hypotheses justified that vanishing in our construction.

2. Reproduce the internal-degree-four, external-degree-four part of I_8. At $A = 5, B = 50$, submit the coefficients of t and r in I_4 and the coefficient of r after deleting $p_2(N)$. Derive the symbolic error and explain why a purely internal $p_2(TP)$ cannot contribute to this integral.

3. Give the full boson and fermion counts for H, its two central charges, the universal oscillator contribution and the oscillator remainder. Explain why the universal tensor boson is chiral and why these subtractions alone do not factor the full Hilbert space.

4. Derive the complete-intersection Chern classes of a smooth $2H$ surface. Submit $\chi(\mathcal{O})$, p_g, $h^{1,1}$ and both central charges. Also find $h^0(\mathcal{O}_X(5H))$ from the hypersurface exact sequence. Explain the degree-five relation and why a smooth $2H$ surface differs from two independent wrapped hyperplanes.

5. Starting with $(q, q_0) = (5/2, -35/12)$ and $\kappa = 5$, compute both charges for $\lambda = -1$ and $\lambda = 1$ and their invariant. Derive its invariance for arbitrary ambient λ. Explain the half-flux shift, the five residue labels and the distinction between the ambient lattice rank and $b_2(P)$.

6. Compute the ordinary and modified quartet traces. Derive the inverse-Laplace saddle and evaluate β_* at $c_L = 55, n = 5500$. Submit the ratios n/c_L for H and $2H$ at $n = 5500$, and the excitation on $2H$ needed to attain ratio 100. Explain what a signed index needs in addition to modularity before its leading growth can be inferred from this saddle.

For benchmark submissions, see `benchmark/PROTOCOL.md`. Include the derivations, geometric arguments and physical interpretations.

Sources and scope

Section 12.1. The smooth single-M5 wrapped-string interpretation is [GEO-E], with decoupling and infrared-CFT assumptions, following Maldacena et al. 1997, arXiv v1, pp. 5–6, §3 and Gaiotto et al. 2007, arXiv v1, pp. 3–4, §2.1. Adjunction, surface indices, weak Lefschetz and the ample line-bundle vanishing are [MATH] theorem inputs under their stated hypotheses. Their explicit local consequences, including $h^{0,1} = 0$, the Hodge numbers and section counts, are derived here. No irregular or singular-divisor spectrum is inferred.

Section 12.2. The single-tensor polynomial is the input of Harvey et al. 1998, arXiv v1, eq. (2.6). The bidegree expansion and fiber integral are explicit [ANOM] calculations, compared with its eq. (2.11). The calculation uses integral characteristic classes, $p_1(E_3) = -4c_2(R)$, right-moving supersymmetry and the full single-tensor polynomial displayed above. The result concerns the displayed gravitational and R backgrounds; it does not compute global anomalies.

Section 12.3. The two central charges are [ANOM], using $c_R = 6k_R$ conditional on the transverse $SU(2)$ being the infrared superconformal R symmetry. The explicit zero-mode arithmetic follows Maldacena et al. 1997, arXiv v1, eqs. (3.10)–(3.15); Harvey et al. 1998, arXiv v1, eqs. (2.13)–(2.16) gives the anomaly relation. The universal chiral sector is sourced in Gaiotto et al. 2007, arXiv v1, §2.1. Oscillator subtraction supplies no global factorization assertion.

Section 12.4. Chern expansions, complete-intersection indices and the quintic Hilbert polynomial are [MATH]. Their H comparison agrees with Gaiotto et al. 2007, arXiv v1, p. 7, §3.1. Central charges for these surfaces use the conditional physical identification of Section 12.3, rather than following from topology alone.

Section 12.5. The modified trace and charged BPS/theta structure are sourced [BPS:1/2|idx] statements for the smooth single-string sector, following Gaiotto et al. 2007, arXiv v1, pp. 3–6, eqs. (2.1)–(2.9). The fraction refers to eight bulk supercharges. The charged-energy formula assumes the Kähler alignment stated on that source's p. 3; it is independent of the anomaly calculation. Quartet saturation, the flux-orbit algebra and the conditional saddle are finite explicit calculations. The conservative high-excitation regime is discussed in Maldacena et al. 1997, arXiv v1, p. 6, eq. (3.4) and surrounding discussion. No complete genus, unsigned BPS count, multicenter spectrum or exact finite-charge degeneracy is determined.

References

Gaiotto, D., A. Strominger, and X. Yin (2007). "The M5-brane elliptic genus: Modularity and BPS states". In: *JHEP* 08, p. 070. DOI: 10.1088/1126-6708/2007/08/070. arXiv: hep-th/0607010.

Harvey, J. A., R. Minasian, and G. W. Moore (1998). "NonAbelian tensor multiplet anomalies". In: *JHEP* 09, p. 004. DOI: 10.1088/1126-6708/1998/09/004. arXiv: hep-th/9808060.

Maldacena, J. M., A. Strominger, and E. Witten (1997). "Black hole entropy in M-theory". In: *JHEP* 12, p. 002. DOI: 10.1088/1126-6708/1997/12/002. arXiv: hep-th/9711053.

Chapter XVII.13

An atlas of wrapped-M5 constructions

An M5-brane construction answers different questions depending on what we keep after compactification. A period can measure a particle's central charge. An instanton sum can become a chiral conformal block. A signed trace can retain a local operator algebra. Each operation discards information, so a useful comparison must say which observable survives and which additional physical data it needs.

This chapter develops a selection method through the examples of XVII.1–12. The four-flavor $SU(2)$ theory lets us compare several protected structures within one theory. Changing the compactification geometry then exposes different missing inputs: a flat connection on a curve, a stability condition on a character variety, or an infrared R symmetry for a wrapped string. We will recompute small witnesses that make these distinctions visible. The twelve examples form a finite atlas, rather than a classification of all wrapped-M5 theories.

The reader should know the $(2,0)$ parent and global-choice discipline of Volume XVI, together with the constructions of XVII.1–12. We recall the finite algebra used in each comparison. The example descriptions specify sources, orders, domains and the physical completions not determined here. A missing completion means that it has not been determined. It is never a zero partition function or an absent theory.

XVII.13.1 Choose the protected question before the tool

Suppose we are given a compactification and asked for its spectrum. Before calculating, we must specify what kind of state or operator is meant. A chamber-dependent particle spectrum, a local-operator trace and an eigenvalue variety have different inputs and different outputs. We organize a request as

$$\mathcal{R} = (\mathcal{T}_6, G, d, \mathcal{O}; \mathcal{D}), \qquad \mathcal{T}_6 = (2,0), \tag{XVII.13.1}$$

where G is the compactification geometry, d the remaining spacetime dimension, $\mathcal{O}$ the observable and $\mathcal{D}$ its chamber, domain, background and global choices. Matching d alone cannot select a calculation. For example the AD particle problem and four-flavor Schur problem both have $d = 4$, but their observables and theories differ.

Take the deformed (A_1, A_2) curve from XVII.1. Its differential is the physical starting point for scaling,

$$x^2 = z^3 - 3\Lambda^2 z + u, \qquad \lambda = x\,dz, \qquad [\lambda] = 1. \tag{XVII.13.2}$$

Quasihomogeneity of the conformal curve and the differential impose two equations,

$$2[x] = 3[z], \qquad [x] + [z] = 1. \tag{XVII.13.3}$$

Solving them, and assigning the same dimension to each curve term, gives

$$[x] = \frac{3}{5}, \qquad [z] = \frac{2}{5}, \qquad [u] = \frac{6}{5}, \qquad [\Lambda] = \frac{2}{5}. \tag{XVII.13.4}$$

These weights follow from the local scaling geometry. An absolute normalization of the central charge needs an additional calibration. In a chosen oriented cycle basis,

$$Z_\gamma = c_{\mathrm{SW}} \oint_\gamma \lambda, \qquad \langle \gamma_1, \gamma_2 \rangle = 1, \qquad Z_{\gamma_1+\gamma_2} = Z_{\gamma_1} + Z_{\gamma_2}. \tag{XVII.13.5}$$

The pairing here is the selected upstream oriented-cycle convention. We have not reconstructed the intersection basis from a new geometric drawing. Linearity gives a candidate composite charge and central charge; stability determines whether that charge is occupied by a particle.

The sourced half-plane chambers illustrate the distinction. At the two-state point $u = 0$ and across the specified alignment segment, respectively, their charge lists are

$$\mathcal{S}_2 = \{(1,0), (0,1)\}, \qquad \mathcal{S}_3 = \{(1,0), (1,1), (0,1)\}. \tag{XVII.13.6}$$

The lattice contains $(1, 1)$ in both chambers. Its appearance in the second list is physical stability information, not a new lattice generator. The calibrated M2 lift and the completeness of these particular chamber lists remain sourced inputs.

We can nevertheless test the classical wall-crossing arithmetic directly. Let x, y now denote torus coordinates, unrelated to the curve coordinate above, and use the upstream ordering of the classical KS transformations. Both compositions reduce to

$$(x, y) \longmapsto \left(x(1+y), \frac{y}{1+x+xy} \right). \tag{XVII.13.7}$$

The equality is an identity of rational maps on their common domain, with the displayed denominator nonzero. For a concrete point it gives

$$(x, y) = (2, 3) \longmapsto \left(8, \frac{1}{3} \right). \tag{XVII.13.8}$$

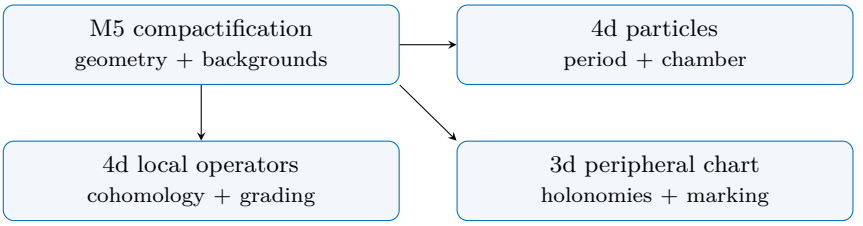


Figure XVII.13.1: Selecting an observable after compactification. The particle route keeps a half-plane and a chamber. The local-operator route keeps a cohomology and radial grading. A peripheral chart retains boundary holonomies and a polarization. The arrows organize requests; they do not identify their endpoint objects.

This tests the coordinate transformation, while the chamber lists specify which factors describe the physical particles. The rational identity alone does not select the stability chamber.

A Schur operator instead belongs to a local-operator cohomology in radial quantization. Its graded contribution is not indexed by an electromagnetic charge cycle with the above stability condition. Thus even a nonzero period, a valid KS identity and a sourced BPS particle list do not construct a map to Schur operators. This distinction will let us compare several structures in one four-flavor theory without merging them with the AD example. When using the atlas, the first useful operation is therefore to retain $\mathcal{O}$ and $\mathcal{D}$ in every proposed match.

XVII.13.2 One four-dimensional theory, several protected structures

The $\mathcal{N} = 2$ four-flavor $SU(2)$ theory provides a common physical system with two different kinds of protected calculation. Localization in an Omega background depends on the instanton coupling and equivariant masses. The Schur trace grades local operators by $E - R$. We first make the finite localization/block comparison explicit, then identify how much of the local-operator comparison has actually been computed.

Fix the asymmetric fixture used in the atlas. Asymmetry prevents an accidental equality forced by equal external weights:

$$(\epsilon_1, \epsilon_2) = (2, 3), \quad a = \frac{7}{3}, \quad (m_1, m_2, m_3, m_4) = \left(\frac{1}{3}, \frac{2}{5}, -\frac{4}{7}, \frac{3}{2}\right). \tag{XVII.13.9}$$

The centered mass convention is essential. Setting $E = \epsilon_1 + \epsilon_2 = 5$ gives

$$\mu_i = m_i + \frac{E}{2}, \qquad (\mu_1, \mu_2, \mu_3, \mu_4) = \left(\frac{17}{6}, \frac{29}{10}, \frac{27}{14}, 4\right). \tag{XVII.13.10}$$

The auxiliary $U(2)$ fixed points at instanton numbers $0, 1, 2$ are pairs of Young diagrams. Their counts are $1, 2, 5$: at two boxes either one diagram has one of its two two-box

shapes, or both diagrams have one box. To reconstruct the weights, take Coulomb parameters $(a_1, a_2) = (a, -a)$. For a box $s = (i, j)$ of Y_u, define its arm $A_{Y_u}(s) = Y_{u,i} - j$ and relative leg $L_{Y_v}(s) = Y^t_{v,j} - i$, where Y^t denotes the transposed diagram. The relative leg may be negative. Set

$$\phi_{u,s} = a_u + \epsilon_1(i-1) + \epsilon_2(j-1), \qquad w_{uv}(s) = a_u - a_v - \epsilon_1 L_{Y_v}(s) + \epsilon_2(A_{Y_u}(s)+1). \tag{XVII.13.11}$$

In the two-fundamental/two-antifundamental convention the contribution is

$$Z_{\boldsymbol{Y}} = \frac{\displaystyle\prod_{u=1}^{2}\prod_{s\in Y_u}(\phi_{u,s}+\mu_1)(\phi_{u,s}+\mu_2)(\phi_{u,s}-\mu_3+E)(\phi_{u,s}-\mu_4+E)}{\displaystyle\prod_{u,v=1}^{2}\prod_{s\in Y_u} w_{uv}(s)(E-w_{uv}(s))}, \tag{XVII.13.12}$$

$$Z_k = \sum_{|Y_1|+|Y_2|=k} Z_{\boldsymbol{Y}}.$$

For example, direct substitution for the two one-box fixed points gives

$$Z_{(\varnothing,\square)} = -\frac{527}{17640}, \qquad Z_{(\square,\varnothing)} = -\frac{1104809}{613872}, \qquad Z_1 = -\frac{114607}{62640}. \tag{XVII.13.13}$$

The same summand applied to the five two-box pairs determines Z_2. Summing the corresponding weights yields

$$Z_{U(2)} = 1 - \frac{114607}{62640}q_{\text{inst}} + \frac{95920869631}{116021808000}q_{\text{inst}}^2 + O(q_{\text{inst}}^3). \tag{XVII.13.14}$$

Let $m_0 = (\mu_1+\mu_2)/2$ and $m_0' = (\mu_3+\mu_4)/2$. In this prescription the abelian exponent and the reduced coefficients follow by convolution,

$$\begin{aligned} \eta &= \frac{2m_0(E-m_0')}{\epsilon_1\epsilon_2} = \frac{817}{420}, \\ (1-q)^{-\eta}Z_{U(2)} &= 1 + (Z_1+\eta)q + \left(Z_2 + \eta Z_1 + \frac{\eta(\eta+1)}{2}\right)q^2 + O(q^3). \end{aligned} \tag{XVII.13.15}$$

For example the first coefficient is $-114607/62640 + 817/420 = 50699/438480$. Removing the mass shift or the abelian factor changes this numerical comparison.

On the Liouville side put $b^2 = \epsilon_1/\epsilon_2$, $Q = b + b^{-1}$. The internal weight, central charge and four external weights at the same fixture are

$$\begin{aligned} h &= \frac{Q^2}{4} - \frac{a^2}{\epsilon_1\epsilon_2} = \frac{29}{216}, \quad c = 1 + 6Q^2 = 26, \\ (d_1,d_2,d_3,d_4) &= \left(\frac{703}{675}, \frac{688}{675}, \frac{1577}{1568}, \frac{1353}{1568}\right). \end{aligned} \tag{XVII.13.16}$$

The external-weight dictionary in this centered convention is

$$\begin{aligned} d_1 &= \frac{E^2-(\mu_1-\mu_2)^2}{4\epsilon_1\epsilon_2}, \qquad d_2 = \frac{m_0(E-m_0)}{\epsilon_1\epsilon_2}, \\ d_3 &= \frac{m_0'(E-m_0')}{\epsilon_1\epsilon_2}, \qquad d_4 = \frac{E^2-(\mu_3-\mu_4)^2}{4\epsilon_1\epsilon_2}. \end{aligned} \tag{XVII.13.17}$$

At level two use descendants $(L_{-2}|h\rangle, L_{-1}^2|h\rangle)$. Commuting positive modes to the right gives the Gram matrix and the two Ward-identity vertex vectors,

$$G_2 = \begin{pmatrix} 4h + c/2 & 6h \\ 6h & 4h(2h+1) \end{pmatrix}, \qquad v(d,e) = \begin{pmatrix} h + 2d - e \\ (h+d-e)(h+d-e+1) \end{pmatrix}. \tag{XVII.13.18}$$

The level-one coefficient is $(h + d_2 - d_1)(h + d_3 - d_4)/(2h)$. At level two we contract the left and right vectors with G_2^{-1}. Substitution gives the finite join

$$\mathcal{B} = 1 + \frac{50699}{438480} q_{\text{inst}} + \frac{15350739781}{116021808000} q_{\text{inst}}^2 + O(q_{\text{inst}}^3) = (1 - q_{\text{inst}})^{-\eta} Z_{U(2)} + O(q_{\text{inst}}^3). \tag{XVII.13.19}$$

This uses two algebraic implementations under the same physical dictionary. It computes neither the DOZZ measure nor its integration contour, principal spectrum or crossing kernel. Those ingredients enter a complete correlator rather than a single block.

For the Schur trace write $t^2 = q_{\text{Schur}}$ and let z be the $SU(2)$ torus coordinate. Eight half-hyper weights occur at each of z, z^{-1}; the vector has adjoint weights $z^2, 1, z^{-2}$. The direct Haar calculation is the constant term

$$\mathcal{I}(t^2) = \mathrm{CT}_z (1 - z^2) \prod_{n \geq 0} \frac{(1 - t^{2n+2} z^2)^2 (1 - t^{2n+2})^2 (1 - t^{2n+2} z^{-2})^2}{(1 - t^{2n+1} z)^8 (1 - t^{2n+1} z^{-1})^8}. \tag{XVII.13.20}$$

The Weyl-symmetric integrand permits this normalized Haar factor. To compute through q^3 retain powers through t^6. For each inverse factor use $(1 - w)^{-8} = \sum_{j \geq 0} \binom{7+j}{j} w^j$; then subtract the coefficient of z^2 from that of z^0 at each even t degree. This gives the same finite unflavored coefficients as the auxiliary zero-area qYM sewing, extending further than the independent affine comparison:

$$\mathcal{I}(q_{\text{Schur}}) = 1 + 28 q_{\text{Schur}} + 329 q_{\text{Schur}}^2 + 2632 q_{\text{Schur}}^3 + 16380 q_{\text{Schur}}^4 + 85764 q_{\text{Schur}}^5 + O(q_{\text{Schur}}^6). \tag{XVII.13.21}$$

The fully flavored upstream trace reaches order three. For the VOA comparator, $c_{4d} = 7/6$, $k_{4d} = 4$ give $c_{2d} = -14$, $k_{2d} = -2$. The $\mathfrak{so}(8)$ Sugawara calculation and the reused grade-two null inventory give

$$\frac{k_{2d} \dim \mathfrak{so}(8)}{k_{2d} + h^\vee} = \frac{-2 \cdot 28}{-2 + 6} = -14, \qquad 28 + \frac{28 \cdot 29}{2} - 105 = 329. \tag{XVII.13.22}$$

The null-space dimension 105 comes from the affine calculation in XVII.6. The independently reached character is $1 + 28q + 329q^2$ only. Higgs degree four has dimension 300, a different object from VOA grade two; their difference is 29.

The three parameters must also retain their physical meaning: q_{inst} is a UV coupling/cross-ratio chart, q_{Schur} grades $E - R$, and the q_{quantum} of a three-dimensional Weyl algebra will quantize a boundary phase space. The NS limit $\epsilon_2 \to 0$ keeps $\epsilon_1 = \hbar$ fixed and assumes differentiable block factorization. A later $\hbar \to 0$ limit is a second operation. For the sourced endpoint model, the pole weight $1/4 - m^2/\hbar^2$ gives exponents $1/2 \pm m/\hbar$; holomorphy is imposed on the factored Gauss function at both endpoints. This does not specify a physical gauge-theory Hilbert space.

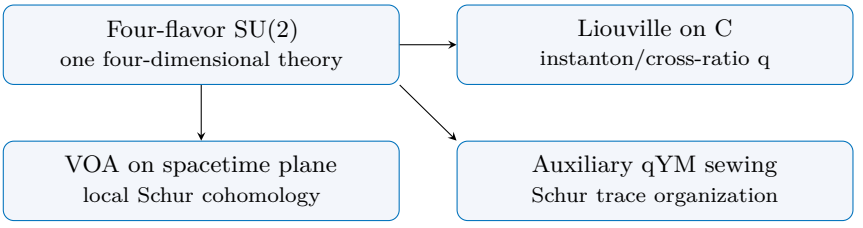


Figure XVII.13.2: Three two-dimensional spaces organizing one four-dimensional theory. Liouville lives on the ultraviolet compactification curve C. The Schur VOA lives on a plane in physical four-dimensional spacetime. qYM organizes an auxiliary sewing problem on the curve. Sharing a curve or a coefficient does not identify their chiral algebras or central charges.

XVII.13.3 Change the geometry and retain its premises

Changing the internal geometry changes what data survive reduction. For a curve in a local Calabi–Yau threefold, the normal bundle determines the twist. For a three-manifold, boundary holonomies provide a local chart. A compact divisor instead gives a two-dimensional string whose anomalies depend on surface topology. We compare one concrete diagnostic in each case, keeping the physical interpretation attached to its own construction.

For the $\mathcal{N} = 1$ curve construction the local geometry and determinant constraint are

$$G = \mathrm{Tot}(L_1 \oplus L_2 \to C), \qquad L_1 \otimes L_2 \simeq K_C, \qquad \deg L_1 + \deg L_2 = 2g-2. \tag{XVII.13.23}$$

At genus two, degrees $(1,1)$ satisfy the constraint. With $R_0 = T_1 + T_2$ and $F = T_1 - T_2$, a spin-weight calculation tests the twist locally. Writing spin and two normal weights as $s, t_1, t_2 \in \{\pm 1/2\}$, the neutrality equation is

$$s + \alpha t_1 + \beta t_2 = 0, \qquad \alpha + \beta = 1. \tag{XVII.13.24}$$

At $\alpha = \beta = 1/2$ only equal normal signs solve it. At $(\alpha, \beta) = (1, 0)$ the second normal sign becomes free. Including the remaining spin multiplicity, the local real counts are

$$N_Q^{\mathrm{generic}} = 4, \qquad N_Q^{\mathrm{endpoint,local}} = 8. \tag{XVII.13.25}$$

Local neutrality must still descend around all cycles. At an endpoint with a degree-zero normal line, trivial transport on four genus-two generators retains eight charges, whereas one nontrivial sign removes the extra four:

$$(1,1,1,1) \Rightarrow N_Q = 8, \qquad (-1,1,1,1) \Rightarrow N_Q = 4. \tag{XVII.13.26}$$

Thus a degree-zero line must be holomorphically trivial with a compatible connection for the enhanced global spinors. Equal degrees also do not establish an enhanced flavor group. The background, spin lift and infrared existence remain physical inputs.

For the balanced theta graph of two T_3 blocks and three gauged edges, the sourced T_3 anomaly inventory is $n_v = 5, n_h = 16$. To perform the sum explicitly set $A_T =$

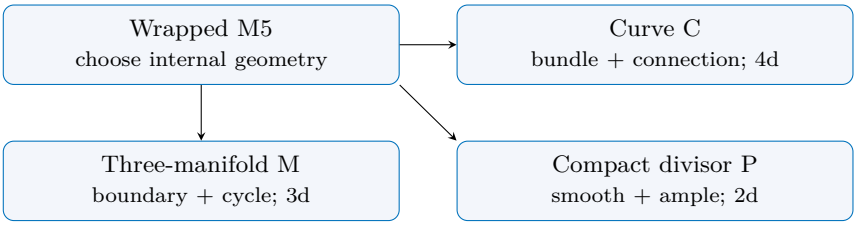


Figure XVII.13.3: Three compactification geometries and their surviving data. Curve twisting tests global spinors, a marked boundary torus records peripheral holonomies, and a smooth compact divisor determines a wrapped string's anomaly. The hypotheses below each geometry belong to that route; they cannot be imported by matching a numerical invariant.

$2(5-16) = -22$, $B_T = 5/2$, $\alpha_\sigma = (x+\sigma y)/2$ and $\beta_\sigma = x - \sigma y$ for the two colors $\sigma = \pm 1$. A block contributes $A_T \alpha_\sigma$ to the linear trace and $A_T \alpha_\sigma^3 + 3B_T \alpha_\sigma \beta_\sigma^2$ to the cubic trace. The three adjoint-eight vectors add $24x$ and $24x^3$. Summing these terms gives

$$\mathrm{Tr}(xR_0 + yF) = 2x, \qquad \mathrm{Tr}(xR_0 + yF)^3 = 2x(13x^2 - 12y^2). \tag{XVII.13.27}$$

Set $x = 1, y = \epsilon$ to evaluate $R_{\mathrm{trial}} = R_0 + \epsilon F$. The standard trial functions then become

$$a(\epsilon) = \frac{3}{32}\left(3\,\mathrm{Tr}\,R_{\mathrm{trial}}^3 - \mathrm{Tr}\,R_{\mathrm{trial}}\right) = \frac{57}{8} - \frac{27}{4}\epsilon^2, \qquad c(\epsilon) = 7 - \frac{27}{4}\epsilon^2. \tag{XVII.13.28}$$

Differentiating gives $a'(\epsilon) = -27\epsilon/2$ and $a'' = -27/2$, hence a local maximum at $\epsilon = 0$ with $(a, c) = (57/8, 7)$. To interpret it as the exact infrared R symmetry requires the interacting parent, the proposed conserved currents and no missing accidental mixing. A negative Hessian by itself constructs no SCFT.

In the three-dimensional route let m be the unsquared meridian eigenvalue, $x = m^2$ and ℓ the preferred unsquared longitude. The irreducible peripheral polynomial is

$$A_{\mathrm{irr}}(x, \ell) = x^2\ell^2 - \ell(x^4 - x^3 - 2x^2 - x + 1) + x^2. \tag{XVII.13.29}$$

At $x = 1$ it becomes $(\ell + 1)^2$, whereas $A_{\mathrm{irr}}(2, 1) = 9$. The latter computation demonstrates that the abelian branch $\ell = 1$ is not contained in this local irreducible image. Real quotient and stability data, reducible sectors and physical integration cycles must still be supplied. This chart cannot be handed to the next engine as a complete three-dimensional QFT.

For the string route, retain the full single M5 tensor on a smooth connected ample divisor P in a compact full-$SU(3)$ Calabi–Yau threefold. Put $A = P^3$ and $B = c_2(X)P$. Adjunction and weak Lefschetz give

$$e(P) = A + B, \quad \sigma(P) = -\frac{A + 2B}{3}, \quad p_g = \frac{2A + B}{12} - 1, \quad h^{0,1} = 0. \tag{XVII.13.30}$$

The full anomaly yields $c_L = A + B$, $c_R = A + B/2$, with the latter interpretation conditional on the transverse $SU(2)$ being the exact infrared R symmetry. On the

quintic, smooth H has $(A, B) = (5, 50)$ and smooth $2H$ has $(40, 100)$. Their central charges are respectively $(55, 30)$ and $(140, 90)$, whereas doubling the first pair gives $(110, 60)$. The cubic term measures the geometry of a connected smooth surface. A disconnected sum, or an intersecting reducible surface, is a different problem. These anomaly formulas require no alignment of the Kähler class; that additional condition will enter charged energies below.

XVII.13.4 Recompute a witness and expose what it forgets

A useful comparison should survive an equivalent rewrite and fail when an essential physical sign or contribution changes. We illustrate this with peripheral elimination and filling. The calculation also separates an independently executed algebraic operation from an independent derivation of its starting objects. Here the Riley polynomial and longitude formula are supplied from XVII.9; we eliminate them without claiming to reconstruct the knot word.

Use $a = m^2$, longitude ℓ and Riley variable r. The supplied equations are

$$\phi(r) = r^2 + (3 - a - a^{-1})r + (3 - a - a^{-1}) = 0, \tag{XVII.13.31}$$

$$\ell = -1 + a^{-1} - 2a + a^2 + r(a^{-1} - a), \qquad a \neq 0. \tag{XVII.13.32}$$

Multiplying the first equation by a and clearing the longitude denominator, their resultant is $aA_{\mathrm{irr}}(a, \ell)$. Thus eliminating r recovers the peripheral image of the preceding section on the specified open set. This agreement tests the supplied polynomial and longitude normalization together; it is not a new knot-group derivation.

The six-tetrahedron candidate of XVII.10 has a stored normalized peripheral witness. A smaller pair of compact equations can be eliminated against it:

$$r\ell - (r - 1)^2 = 0, \qquad r(a + \ell) - a - \ell a^2 = 0. \tag{XVII.13.33}$$

Their resultant divided by ℓa^2 agrees with $A_{\mathrm{irr}}(a, \ell)/a^2$, in the chart where the divisions are allowed. This elimination compares two equations with the six-shape result of XVII.10. The candidate theory retains four source assumptions from XVII.10: the proposed tetrahedron/gluing assignment to the type-A_1 parent; SQED/XYZ and tetrahedron-triality mirror identifications that transport easy-edge operators; the BPS monopole zero-mode charge formula with its translated flux and Chern–Simons sign; and the noncompact ellipsoid localization formula and contact scheme. Numerical charge neutrality and trial R charge two alone do not establish quantum existence of the dressed monopoles. No global analytic continuation or six-tetrahedron physical contour follows from this resultant.

Contact terms already show why a local classical curve cannot supply the entire theory. A charge-one chiral in the chosen parity scheme has

$$k_{\mathrm{bare}} = -\frac{1}{2}, \qquad k_{\mathrm{eff}} = k_{\mathrm{bare}} + \frac{1}{2}\operatorname{sign} M = \begin{cases} 0, & M > 0, \\ -1, & M < 0. \end{cases} \tag{XVII.13.34}$$

Only the parity-corrected massive level is integral. The compact product used for the local difference equation is

$$\Psi_q(z) = \prod_{n\geq 1}(1-q^n z) = 1 - \frac{q}{1-q}z + O(z^2), \qquad |q| < 1. \tag{XVII.13.35}$$

For $q = 1/2$ the coefficient is -1. Reversing its sign fails this elementary product check. Here $q = q_{\text{quantum}}$ controls $UV = qVU$, with normal order U^iV^j. The compact product is not the noncompact real-b integral, and neither its convergence domain nor its finite coefficients choose a physical integration cycle.

A change of boundary cycles also carries more than the linear matrix visible in an unmarked curve. Here m is the unsquared $SL(2,\mathbb{C})$ meridian eigenvalue, $a = m^2$, and $u = \log m$ is a chosen logarithmic branch, unrelated to the AD Coulomb modulus of Section 13.1. Fix the longitude lift $\log \ell = v + i\pi$, equivalently $v = \log \ell - i\pi$. For the example $g = \left(\begin{smallmatrix} 2 & 1 \\ 1 & 1 \end{smallmatrix}\right)$ acting on $(u, \log \ell)$, take $U = 2u$, $v = \log(-\ell)$ and $D = \operatorname{diag}(2,1)$. Then

$$\begin{pmatrix} U' \\ v' \end{pmatrix} = DgD^{-1}\begin{pmatrix} U \\ v \end{pmatrix} + \begin{pmatrix} 2\pi i \\ 0 \end{pmatrix}, \qquad DgD^{-1} = \begin{pmatrix} 2 & 2 \\ 1/2 & 1 \end{pmatrix}. \tag{XVII.13.36}$$

The affine shift comes from the longitude sign and logarithm choice. Dropping it preserves a derivative calculation but changes the lift. A filling slope transforms contragrediently:

$$\begin{pmatrix} p' \\ q' \end{pmatrix} = g^{-t}\begin{pmatrix} 5 \\ 2 \end{pmatrix} = \begin{pmatrix} 3 \\ -1 \end{pmatrix}, \qquad (p', q')g = (5, 2). \tag{XVII.13.37}$$

This verifies that the original filling word is unchanged by reexpressing the cycles.

The decisive changed-input test uses a cusp meridian matrix rather than its eigenvalues:

$$M = \begin{pmatrix} 1 & 1 \\ 0 & 1 \end{pmatrix} = I + N, \qquad N^2 = 0, \qquad M^p = I + pN \neq I \quad (p > 0). \tag{XVII.13.38}$$

Both eigenvalues equal one, so an eigenvalue-only filling test accepts every p. The full matrix test rejects this nontrivial unipotent for positive finite cyclic order. For a $p = 5$ cyclic model the eigenvalue labels modulo Weyl inversion are $\{0\}$, $\{1, 4\}$ and $\{2, 3\}$, three classes. The legitimate $0/1$ surgery instead leaves an infinite $\mathbb{Z}$ group and can allow unipotents. It must not be forced into the positive-finite-order classification.

A useful recomputation changes a sign or contribution that affects the observable, then tests the same mathematical relation. An equivalent row ordering or symbolic rewrite should preserve the result. Such checks constrain the calculation under its stated premises; they do not establish the physical premises or complete the theory.

XVII.13.5 Carry the observable into the next construction

A construction can be useful to another engine without supplying its entire physical completion. The wrapped-string example makes a concrete transfer possible: topology

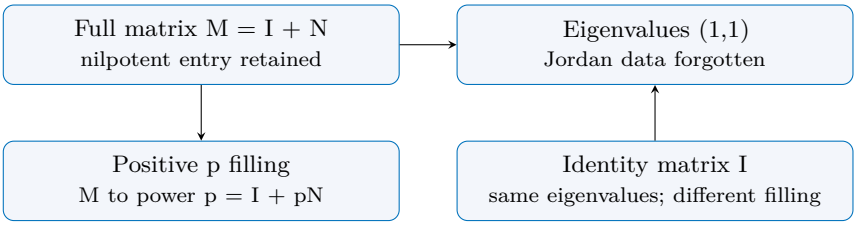


Figure XVII.13.4: Information lost in passing to a peripheral eigenvalue chart. The full matrix retains its nilpotent entry, whereas the eigenvalues of $I + N$ agree with those of I. The positive-order filling equation distinguishes the matrices. A reused six-shape answer and a fresh compact resultant are two algebraic inputs to a comparison, with the shared physical premises retained.

gives an anomaly, anomalies constrain a candidate conformal theory, and a charge orbit organizes a trace. Each step requires data that the previous invariant alone does not contain. We now calculate the orbit and isolate the additional geometric and infrared hypotheses that must travel with it.

For the quintic hyperplane use $A = 5$, $B = 50$ and $p_g = 4$. The harmonic forms and full tensor multiplet give

$$(b_2^+, b_2^-) = (9, 44), \quad (n_B^L, n_B^R, n_F^L, n_F^R) = (55, 20, 0, 20). \tag{XVII.13.39}$$

The real mode counts reproduce the full central charges, including universal fields,

$$c_L = 55 + \tfrac{1}{2}(0) = 55, \qquad c_R = 20 + \tfrac{1}{2}(20) = 30. \tag{XVII.13.40}$$

For smooth $2H$, $p_g = 14$ and $(b_2^+, b_2^-) = (29, 109)$ instead give $(n_B^L, n_B^R, n_F^R) = (140, 60, 60)$. These numbers make the nonadditivity of the smooth surface explicit. The anomaly and mode routes share the wrapped-brane and infrared assumptions; their agreement does not independently prove those premises.

The full surface lattice for H has rank 53, while the ambient quintic charge lattice has rank one with $\kappa = 5$. Write $h = H|_P$ for the hyperplane class restricted to the surface, so $\int_P h^2 = 5$ for $P = H$. This h is a cohomology class, distinct from the conformal weight used earlier. A half-shifted flux $f = h/2$ gives the ambient charges

$$q = \int_P hf = \frac{5}{2}, \qquad q_0 = -\frac{e(P)}{24} - \frac{1}{2}\int_P f^2 = -\frac{35}{12}. \tag{XVII.13.41}$$

An integral ambient flux change by λ has the spectral-flow action

$$q' = q + \kappa\lambda, \qquad q_0' = q_0 - \lambda q - \frac{1}{2}\kappa\lambda^2, \qquad \widehat{q}_0 = q_0 + \frac{q^2}{2\kappa}. \tag{XVII.13.42}$$

The invariant follows by expanding the square: the extra terms $\lambda q + \kappa\lambda^2/2$ cancel the change of q_0. At $\lambda = 1$,

$$(q', q_0') = \left(\frac{15}{2}, -\frac{95}{12}\right), \qquad \widehat{q}_0' = \widehat{q}_0 = -\frac{55}{24}. \tag{XVII.13.43}$$

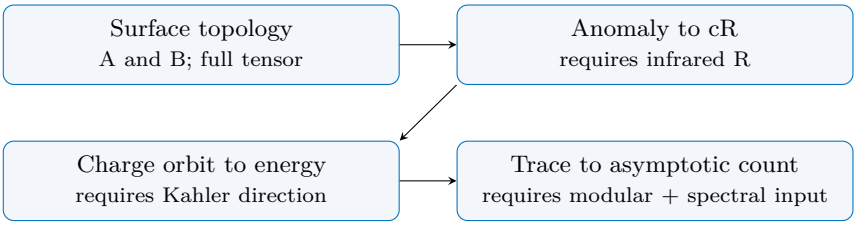


Figure XVII.13.5: The wrapped-string transfer keeps different kinds of information at successive steps. Topological numbers determine the anomaly. The R-symmetry assumption translates its coefficient into c_R. A charge sector and a Kähler direction enter the theta energy. Modular and spectral input is needed for an asymptotic count. Each lower annotation names an additional input.

This negative polar anchor is not a positive Cardy excitation. Ambient spectral flow also does not enumerate all fluxes on the rank-fifty-three surface lattice.

To interpret the charge factor as a right-moving energy, specify a positive Kähler direction j. Choose ambient divisor classes D_a and write $P = p^a D_a$. On the surface set $\kappa_{ab} = \int_P D_a \wedge D_b$, $p = [P]|_P = p^a D_a|_P$, and $j = j^a D_a|_P$. The repeated ambient index is summed. Let Q be the full surface charge class and $q_a = \int_P D_a \wedge Q$ its ambient charge covector. Thus $p \cdot Q = p^a q_a$ and $A = p^a \kappa_{ab} p^b = P^3$. In the rank-one flux sector here $p = h$, $Q = f$, $p^1 = 1$ and $q_1 = q$. These local charge symbols are distinct from the Liouville background charge. The projection formula is

$$E_R(j) = \frac{(j^a q_a)^2}{2 j^a \kappa_{ab} j^b}, \qquad j \parallel p \;\Rightarrow\; \bar{L}_0 - \frac{c_R}{24} = \frac{(p \cdot Q)^2}{2A}. \tag{XVII.13.44}$$

The divisor-ray alignment belongs to this energy/theta interpretation, not to the topological anomaly. For rank-one H it gives $E_R = q^2/10$. A charged term therefore carries $\bar{q}^{q^2/10}$; its right-moving vacuum-subtracted energy is not identically zero.

An entropy estimate would require still more information. Assuming a high-temperature function with vacuum-dominated logarithm, its inverse-Laplace saddle gives

$$\log Z(\beta) \simeq \frac{\pi^2 c_L}{6\beta}, \qquad \beta_* = \pi\sqrt{\frac{c_L}{6n}}, \qquad S_* = 2\pi\sqrt{\frac{c_L n}{6}}, \quad n > 0. \tag{XVII.13.45}$$

A conservative asymptotic regime has $n/c_L \to \infty$ at fixed geometry. A signed index additionally needs the dominant polar contribution, its effective central charge and control of leading cancellations. The anomaly and the single polar charge above give none of those spectral coefficients.

We can express a proposed transfer as a pair of an available result and a requested completion,

$$\begin{aligned}\mathcal{H} = (&\mathcal{T}_6, G, \mathcal{O}, \text{normalization}, \text{domain}, \text{global data};\\ &\text{physical premises}, \text{uncomputed target}).\end{aligned} \tag{XVII.13.46}$$

For the present example, $\mathcal{O}$ includes the full tensor anomaly and the ambient spectral-flow orbit. Its domain contains a smooth connected ample divisor, a suitable decoupling limit and the specified infrared R identification. The charged-energy use also contains $j \parallel p$. A request for the full elliptic genus remains an uncomputed target. For a peripheral curve the corresponding missing entries include reducible and Jordan sectors, stability, physical cycles, measure and contact/framing data. For a trial a maximum they include the actual infrared theory and full mixing-current spectrum.

A transfer to a six-dimensional $(1, 0)$ parent or a composite construction belongs to Volume XIII. It needs its own parent, decoupling regime, backgrounds, global choices and observable calculation. Sharing a central charge, a polynomial or a supersymmetry count cannot fill those entries. The atlas supplies concrete starting results and the conditions under which they were obtained. This is the useful information to carry across engines.

The twelve examples and their domains

The numerical summary below is inseparable from the adjacent example descriptions. Each description specifies the physical observable, finite order or chart, source, premises and exclusions. The source assumptions for the coefficients in this summary retain the qualifications stated in XVII.1–12.

Chapter	Selected witness	Scope
XVII.1	1	cycle pairing
XVII.2	[1, 2, 5]	fixed-point counts
XVII.3	$\frac{50699}{438480}$	first block coefficient
XVII.4	152	Toda central term, b=2
XVII.5	[1, 28, 329, 2632, 16380, 85764]	Schur orders 0–5
XVII.6	[1, 28, 329]	affine orders 0–2
XVII.7	4	generic real supercharges
XVII.8	$\frac{57}{8}$	trial a maximum
XVII.9	$(\ell + 1)^2$	cusp polynomial
XVII.10	$-\frac{1}{2}$	bare contact level
XVII.11	3	p=5 Weyl classes
XVII.12	[55, 30]	full H central charges

XVII.1: particles in an AD chamber. The deformed (A_1, A_2) example uses Seiberg–Witten cover cycles, a chosen half-plane and the sourced two-state or three-state chamber. Its pairing is the selected oriented-cycle convention. The scaling weights and classical KS maps are recomputed from the upstream functions; the chamber occupancy lists are sourced stability information. Their interpretation needs the calibrated M2 lift and the stated completeness of the chamber spectrum; the geometric c_{SW} remains uncalibrated. A nonzero period does not establish an occupied particle, and these particles are distinct from local Schur operators. The source is Gaiotto, Moore, et al. 2013, v2, §9.4.4, eqs. (9.29)–(9.32).

XVII.2: localization through two instantons. The four-flavor $SU(2)$ calculation uses auxiliary $U(2)$ fixed points on Omega-deformed $\mathbb{R}^4$. It retains the UV instanton-coupling chart, the asymmetric fixture, the half-epsilon centered-mass lift and the specified abelian factor. The actual one- and two-box sums produce the coefficients in Section 13.2. Resolved framed moduli and localization are physical inputs. The finite sums establish neither an all-instanton identity nor a full correlator, and they do not calibrate c_{SW}. The convention and formulas follow Alday, Gaiotto, and Tachikawa 2010, v2, App. B, eqs. (B.3)–(B.13), (B.27)–(B.28), (C.1).

XVII.3: a Liouville block on the UV curve. For the same four-flavor theory and mass dictionary, Gram and Ward sewing computes a chiral block through level two. Its variable is the same named UV cross-ratio chart q_{inst}, and its two-dimensional space is the compactification curve C. This is a second algebraic implementation of the finite coefficient comparison under shared AGT premises. The AGT identification, DOZZ structure constants and principal spectrum are sourced inputs, with the masses and external powers of q retained. A single block is not a complete correlator: its measure, contour and crossing kernel remain additional information. See Alday, Gaiotto, and Tachikawa 2010, v2, App. A, eqs. (A.1)–(A.5) and Teschner 2001, v3, §17.1.

XVII.4: higher rank and a specified endpoint model. The rank-three Toda central term is $c = 2 + 24Q^2$; at $b = 2$ it gives 152. The special defect/NS comparison uses a degenerate conformal block and fixes $\epsilon_1 = \hbar$ as $\epsilon_2 \to 0$. Differentiable NS block factorization and the physical gauge/Bethe identification are conditional source premises. The endpoint model requires the factored Gauss function to be holomorphic at both zero and one. Its displayed eigenvalues begin $0, 41/15, 112/15, 71/5$. This analytic domain is not a physical gauge Hilbert-space prescription, and neither a four-heavy accessory nor that physical spectrum is computed. The source chain is Wyllard 2009, v2, eqs. (3.2)–(3.19), Alday, Gaiotto, Gukov, et al. 2009, v2, App. B.1 and Nekrasov and Shatashvili 2009, v1, eqs. (3.5)–(3.8).

XVII.5: the Schur trace and auxiliary sewing. The signed radial trace of the four-flavor $SU(2)$ theory grades local operators by $E - R$, with $t^2 = q_{\mathrm{Schur}}$. The regenerated unflavored trace and zero-area qYM representation sum reach order five; the fully flavored upstream trace reaches order three. Their use assumes shortening, cancellation and localization, while the diagonal A_1 sewing identity and puncture normalization are sourced. Finite coefficients do not prove full crossing or equality of complete QFTs. The auxiliary sewing space organizes the trace rather than supplying the spacetime VOA plane. See Gadde, Rastelli, et al. 2011b, v1, eqs. (10)–(13) and Gadde, Rastelli, et al. 2011a, v3, §6 and App. E.

XVII.6: currents and the finite VOA character. The Schur VOA is constructed by cohomology and OPE on a chosen plane in physical four-dimensional spacetime. The anomaly and Sugawara comparators use $c_{2d} = -12c_{4d}$, $k_{2d} = -k_{4d}/2$, long roots squared two and $h^\vee = 6$. The independent affine reach is order two, with unshifted signed character $1 + 28q + 329q^2$ and no vacuum Casimir factor. The grade-two null dimension

105 comes from the affine calculation in XVII.6. The physical inputs include unitary $\mathcal{N} = 2$ cohomology/OPE, BRST no-additional-lifting premises and the sourced historical affine identification. A trace coefficient at order three is not an independently computed affine coefficient. Equal dimensions do not prove an all-grade VOA isomorphism. See Beem et al. 2015, v3, eqs. (3.15), (3.23), (5.20)–(5.21), Conjecture 1.

XVII.7: global spinors on a curve. The four-dimensional $\mathcal{N} = 1$ curve construction uses actual holomorphic bundles L_1, L_2 with $L_1 L_2 = K_C$, their connections, a spin lift and a compatible background. Neutral-weight enumeration and the flat-transport obstruction are evaluated from the upstream twist functions. The local endpoint count of eight only survives globally when the additional degree-zero line is holomorphically trivial with compatible connection; nontrivial flat transport can leave four. Degree zero alone does not imply triviality, equal degrees do not prove flavor enhancement, and an infrared theory's existence is a separate premise. See Bah et al. 2012, v1, eqs. (2.1)–(2.8), p. 15 fn. 8 and Xie 2013, v1, eqs. (2.28)–(2.29).

XVII.8: a conditional trial R maximum. The balanced theta graph uses two T_3 blocks of the interacting A_2 parent and three gauged edges, with colors $(p, q) = (1, 1)$. Its sourced block anomalies and explicit vector contributions give the full cubic and linear traces in Section 13.3. The finite maximization has negative Hessian and the trial values $(a, c) = (57/8, 7)$. Interpreting the candidate current as the exact infrared R symmetry requires a complete mixing-current spectrum and no accidental symmetry. The local maximum proves neither SCFT existence nor that current completeness. See Bah et al. 2012, v1, §5 and App. E and Gadde, Maruyoshi, et al. 2013, v2, §2.2.4.

XVII.9: the irreducible peripheral image. The type-A_1 figure-eight construction uses a marked boundary torus with unsquared meridian m, $x = m^2$, $U = 2 \log m$ and $v = \log(-\ell)$. The polynomial is the local irreducible peripheral image; the fresh resultant eliminates the supplied Riley and longitude expressions, without reconstructing knot words. A decoupled low-energy parent, real quotient/stability and protected-chart dictionary remain physical premises. The abelian component $\ell = 1$ and Jordan data are not recovered from this image, and no physical cycle Γ or thimble coefficients n_α are computed. See Andersen and Hansen 2003, 2003 report, §5.1, eqs. (53)–(59) and Dimofte et al. 2011, v1, eqs. (2.26)–(2.32).

XVII.10: the polarized tetrahedron candidate. The six-tetrahedron figure-eight candidate is restricted to nondegenerate open shape charts, fixed contact conventions and the four source assumptions stated in Section 13.4. The two-equation resultant provides an algebraic comparison with the normalized six-shape polynomial of XVII.10. Easy-edge mirror transport and physical dressed-monopole existence remain source-dependent. The parity scheme has bare level $-1/2$. The local compact product uses the quantum parameter of $UV = q_{\text{quantum}} VU$, distinct from the Schur grading. These results give neither global triangulation invariance nor a physical noncompact integral and contour. See Dimofte et al. 2014, v1, eqs. (4.21)–(4.22) and Faddeev and Kashaev 1994, v1, eqs. (1.1)–(1.5).

XVII.11: marked filling and polarization models. Affine logarithmic conversion, contragredient slopes and cyclic classes are finite models retaining the full $SL(2,\mathbb{C})$ matrix filling equation. Finite cyclic order requires $p > 0$; the valid $0/1$ surgery instead has infinite $\mathbb{Z}$ and can retain unipotents. The displayed $p = 5$ model has three Weyl classes. Physical compact BF, spin and framing conventions, choices of cycles and measure remain separate inputs. An eigenvalue condition cannot replace the matrix equation, and no filled M5 partition function or physical knot cycle is computed. See Dimofte et al. 2011, v1, eqs. (2.26)–(2.28), §3.1 and Andersen and Hansen 2003, 2003 report, §5.1.

XVII.12: the full smooth-divisor string. One full tensor is retained on a smooth connected ample divisor in a compact full-$SU(3)$ Calabi–Yau threefold; in this setting $h^{0,1} = 0$. The topology and zero-mode inventory for H and smooth $2H$ are reconstructed and compared with the full anomaly and charge flow. A suitable decoupling limit and infrared CFT remain physical inputs, and c_R requires the transverse $SU(2)$ to be the exact infrared R symmetry. The modified trace retains charged right energy; its displayed theta formula separately assumes the divisor Kähler ray. Smooth $2H$ is not two disconnected H components. No full elliptic genus is computed, and the polar vacuum anchor is not a positive Cardy excitation. Vacuum dominance and cancellation control are further spectral assumptions. See Maldacena et al. 1997, v1, eqs. (3.1)–(3.15), Harvey et al. 1998, v1, eqs. (2.6), (2.11) and Gaiotto, Strominger, et al. 2007, v1, eqs. (2.6)–(2.9), §3.1.

Take-home message

A protected observable is useful across constructions when its geometry, normalization, domain and physical premises travel with it. Finite block coefficients, a Schur trace, a local peripheral curve and a wrapped-string anomaly retain different information. Explicit witnesses make these differences calculable: chamber occupancy can change without changing a lattice, a flat line can remove extra spinors, a Jordan entry can obstruct a filling, and a smooth doubled divisor can change a cubic anomaly term. These are starting points for further construction, with their uncomputed physical completions visible.

Exercises

1. Derive the AD scaling dimensions from the curve and differential in Section 13.1. Evaluate the common rational KS map at $(2, 3)$ and give the sizes of the two sourced chamber lists. Explain why neither a nonzero composite period nor the rational-map identity proves an occupied particle or a Schur operator.

2. Recompute the shifted masses at the asymmetric fixture, the abelian exponent and the first two reduced instanton coefficients. Construct G_2 and the Ward vectors and recover the same coefficients by sewing. Submit the masses, exponent

and two coefficients. Explain which measure, contour and spectrum data are missing from a complete crossing-symmetric correlator.

3. Compute the Schur coefficients through order three and independently check the affine grade-two inventory, Sugawara central charge and Higgs/VOA difference. Submit the three trace coefficients, c_{2d}, k_{2d}, affine grade two and that difference. Locate the Liouville curve, VOA plane and qYM sewing problem, distinguish all three q parameters, and explain why the affine comparison stops at order two.

4. Enumerate neutral spin weights at the generic and endpoint twists. Apply trivial and one-sign flat transport. Differentiate the balanced T_3 trial polynomial and find its stationary point, Hessian and trial central charges. Explain the holomorphic-bundle, connection and current-spectrum assumptions needed for enhancement and an exact infrared R interpretation.

5. Eliminate the supplied Riley variable and compare the compact equations against the stored six-shape witness. Evaluate the irreducible polynomial at $(a, \ell) = (2, 1)$. Transform slope $(5, 2)$ by the specified g, compute the affine shift in units of $i\pi$, and find the upper-right entry of M^5. Explain the missing abelian and Jordan data, the zero-surgery exception and the absence of a physical filled-QFT contour.

6. Recompute the full H and smooth $2H$ central charges and mode counts. Flow the half-flux charges by $\lambda = 1$ and compute the invariant. Submit both central-charge pairs, both right-fermion counts, the flowed charges and invariant. Explain smoothness, ampleness, the full single tensor, the infrared R assumption, the separate Kähler-ray condition for charged energy and the polar-versus-Cardy distinction. State what a transfer to a $(1, 0)$ parent would still need.

For benchmark submissions, see `benchmark/PROTOCOL.md`. Include the derivations, domain choices and physical explanations.

Sources and scope

Sections 13.1–13.5 compare the bounded results of XVII.1–12. The examples state the orders of the expansions and the assumptions on which the comparisons depend. Classical KS arithmetic, finite Gram sewing, anomaly sums, resultants and spectral-flow arithmetic are explicit computations. The particle interpretation, protected dictionaries, infrared identifications and physical contour prescriptions remain sourced with their stated conditions. These comparisons leave open full duality or geometric equivalence, all-order protected identities, complete spectra, SCFT existence and global three-dimensional QFT constructions.

The atlas reuses the upstream grade-two affine null dimension and the stored six-shape peripheral witness. A new algebraic comparison using these inputs is not a second independent physical derivation. Agreement under shared physical assumptions is not a new proof of those assumptions. The three-dimensional historical discussion uses the cited web-text version of Witten's 2003 work. The compact BF and spin contact conventions are those already fixed in XVII.11. Physical cycles, thimble coefficients and a framed quantum wall remain outside the computed objects.

References

Alday, L. F., D. Gaiotto, S. Gukov, et al. (2009). "Loop and surface operators in N=2 gauge theory and Liouville modular geometry". In: Version 2; equation 2.12, section 3.1 and appendix B.1. arXiv: 0909.0945 [hep-th].

Alday, L. F., D. Gaiotto, and Y. Tachikawa (2010). "Liouville Correlation Functions from Four-dimensional Gauge Theories". In: *Lett. Math. Phys.* 91. Version 2, 9 February 2010, pp. 167–197. DOI: 10.1007/s11005-010-0369-5. arXiv: 0906.3219 [hep-th].

Andersen, J. E. and S. K. Hansen (2003). *Asymptotics of the Quantum Invariants for Surgeries on the Figure 8 Knot*. Tech. rep. 2003/28. Maphysto.

Bah, I. et al. (2012). "Four-Dimensional SCFTs from M5-Branes". In: Version 1 inspected. arXiv: 1203.0303 [hep-th].

Beem, C. et al. (2015). "Infinite Chiral Symmetry in Four Dimensions". In: *Commun. Math. Phys.* 336.3. Inspected arXiv v3, 29 September 2015, pp. 1359–1433. DOI: 10.1007/s00220-014-2272-x. arXiv: 1312.5344 [hep-th].

Dimofte, T., D. Gaiotto, and S. Gukov (2011). *Gauge Theories Labelled by Three-Manifolds*. Version 1 inspected. arXiv: 1108.4389 [hep-th].

Dimofte, T., D. Gaiotto, and S. Gukov (2014). "Gauge Theories Labelled by Three-Manifolds". In: *Commun. Math. Phys.* 325. Inspected arXiv version 1, 22 August 2011, pp. 367–419. DOI: 10.1007/s00220-013-1863-2. arXiv: 1108.4389 [hep-th].

Faddeev, L. D. and R. M. Kashaev (1994). "Quantum Dilogarithm". In: *Mod. Phys. Lett. A* 9. Inspected arXiv version 1, 13 October 1993, pp. 427–434. DOI: 10.1142/S0217732394000447. arXiv: hep-th/9310070.

Gadde, A., K. Maruyoshi, et al. (2013). "New N=1 Dualities". In: Version 2 inspected. arXiv: 1303.0836 [hep-th].

Gadde, A., L. Rastelli, et al. (2011a). "Gauge Theories and Macdonald Polynomials". In: Inspected arXiv version3. arXiv: 1110.3740 [hep-th].

Gadde, A., L. Rastelli, et al. (2011b). "The 4d Superconformal Index from q-deformed 2d Yang-Mills". In: Inspected arXiv version1. arXiv: 1104.3850 [hep-th].

Gaiotto, D., G. W. Moore, and A. Neitzke (2013). "Wall-crossing, Hitchin Systems, and the WKB Approximation". In: *Adv. Math.* 234, pp. 239–403. DOI: 10.1016/j.aim.2012.09.027. arXiv: 0907.3987 [hep-th].

Gaiotto, D., A. Strominger, and X. Yin (2007). "The M5-brane elliptic genus: Modularity and BPS states". In: *JHEP* 08, p. 070. DOI: 10.1088/1126-6708/2007/08/070. arXiv: hep-th/0607010.

Harvey, J. A., R. Minasian, and G. W. Moore (1998). "NonAbelian tensor multiplet anomalies". In: *JHEP* 09, p. 004. DOI: 10.1088/1126-6708/1998/09/004. arXiv: hep-th/9808060.

Maldacena, J. M., A. Strominger, and E. Witten (1997). "Black hole entropy in M-theory". In: *JHEP* 12, p. 002. DOI: 10.1088/1126-6708/1997/12/002. arXiv: hep-th/9711053.

Nekrasov, N. A. and S. L. Shatashvili (2009). "Quantization of Integrable Systems and Four Dimensional Gauge Theories". In: Version 1; equations 2.17–2.19 and 3.5–3.8. arXiv: 0908.4052 [hep-th].

Teschner, J. (2001). “Liouville theory revisited”. In: Version 3, 9 November 2001; inspected version. arXiv: hep-th/0104158.

Wyllard, N. (2009). “A_{N-1} conformal Toda field theory correlation functions from conformal N=2 SU(N) quiver gauge theories”. In: Version 2; source equations 3.2–3.19 and 3.21–3.24. arXiv: 0907.2189 [hep-th].

Xie, D. (2013). “M5 brane and four dimensional $\mathcal{N} = 1$ theories I”. In: Version 1 inspected. arXiv: 1307.5877 [hep-th].